Synthesis and coordination of multifunctional ligands: Functionalised phosphinoamines, isonicotinic acid and silasesquioxanes

Palmer, Mark Thomas

Award date:
2000

Awarding institution:
University of Bath

Synthesis and Coordination of Multifunctional Ligands

Functionalised Phosphinoamines, Isonicotinic acid and Silasesquioxanes

submitted by Mark Thomas Palmer

for the degree of PhD

of the University of Bath

2000

M. T. Palmer

ProQuest LLC
789 East Eisenhower Parkway
P.O. Box 1346
Ann Arbor, MI 48106-1346

Abstract

The ether- and amine-functionalised phosphinoamines Ph_2PNHR [R = $CH_2CH_2OCH_3$ ($\mathbf{L^1}$), $CH_2CH_2CH_2OCH_3$ ($\mathbf{L^2}$), $CH_2CH(OCH_3)_2$ ($\mathbf{L^3}$), $C_6H_4OCH_3$-2 ($\mathbf{L^4}$) and $CH_2CH_2N(CH_3)_2$ ($\mathbf{L^8}$)] and $Ph_2PN(CH_3)CH_2CH_2N(CH_3)_2$ ($\mathbf{L^7}$) were prepared from the reaction of Ph_2PCl and the appropriate amine in the presence of a base. The keto-functionalised *N*-pyrrolyl phosphine $Ph_2PNC_4H_3C(O)CH_3$-2 ($\mathbf{L^{10}}$) was synthesised in an analogous manner from 2-acetylpyrrole.

X-ray crystallographic and multinuclear NMR spectroscopic studies demonstrated that the ligands can coordinate in either a unidentate manner through the phosphorus or in a bidentate manner to give *P,O*- or *P,N*-chelate rings. Displacement of the coordinated ether and keto oxygens was observed for a number of cases on the addition of CO, xylyl isocyanide and acetonitrile. X-ray crystallographic analysis of the complexes $[PdCl_2(\mathbf{L^1})_2]$ (**1**), $[PdCl_2(\mathbf{L^3})_2]$ (**3**), $[PtBr(NO_2)(\mathbf{L^1})_2]$ (**16**) and $[Pd(dmba)Cl(\mathbf{L^1})]$ (**18**) showed the presence of bifurcated hydrogen bonds between the NH protons and both the halide ligands and the ether oxygen atoms, though N-H···O interactions were absent in the structure of $[Pd(dmba)Cl(\mathbf{L^2})]$ (**19**).

The complexes $[PtCl_2(\mathbf{L^7})_2]$ (**43**) and $[PtCl_2(\mathbf{L^8})_2]$ (**44**) were shown to be fluxional in solution and abstraction of one of the chlorides from **44** gave $[PtCl(\mathbf{L^8}\text{-}P,N)(\mathbf{L^8}\text{-}P)]^+$. The reaction of **43** with $CoCl_2$ gave the bimetallic complex $[Pt(\mathbf{L^7}\text{-}P,N)(\mu\text{-}\mathbf{L^7})CoCl_3]$ (**52**) in which one $\mathbf{L^7}$ is bridging between the metal centres.

$\mathbf{L^{10}}$ was shown to coordinate to rhodium(I) as a uni- or bi-dentate ligand. However when $[RhCl(CO)(\mathbf{L^{10}})_2]$ was dissolved in wet dichloromethane it gave the dinuclear species $[RhCl(CO)(\mu\text{-}PPh_2OPPh_2)]_2$ (**69**) in high yield.

The crystallographically characterised late transition metal silasesquioxane complex $[(c\text{-}C_5H_9)_7Si_7O_9(OSiMe_3)O_2Pt(dppe)]$ was prepared from the reaction of $(c\text{-}C_5H_9)_7Si_7O_9(OSiMe_3)(OH)_2]$ with $[Pt(CO_3)(dppe)]$ or $[PtCl_2(dppe)]/Ag_2O$.

In an attempt to build molecular squares using self assembly through coordination and hydrogen bonds, the compound $[Pd(dppe)(NC_5H_4CO_2H\text{-}4)_2]^{2+}$ was prepared. During these studies, the complex $[Ag_3(isonic)_2]BF_4$ (**75**) was isolated and shown to have a polymeric structure consisting of Ag_3 triangles linked together by two isonicotinate ligands.

Acknowledgements

I would like to thank my supervisor, Dr Andrew Burrows for his help, advice and guidance during the course of my work. The members past and present, of the research group are thanked for their help and friendship during the last three years.

I would like to thank Dr Mary Mahon for collecting the X-ray data and solving the crystal structures. I would also like to thank the technical staff for all their help during the last three years.

I wish to acknowledge the use of the EPSRC's Chemical Database Service at Daresbury.

Financial assistance from the University of Bath is gratefully acknowledged.

Most of all I would like to thank my parents for their love and support throughout my studies.

Contents

Abbreviations 11

Chapter One **Review of Phosphine and Phosphinoamine Chemistry** 13

1.0 Introduction 14

1.1 Historical Background 14

1.2 Transition Metal Phosphine Chemistry 15

1.3 Phosphine Syntheses 17

1.3.1 Preparation of Tertiary Phosphines 17

1.3.1.1 Grignard Method 18

1.3.1.2 Organolithium and Alkali-Organic Methods 22

1.3.1.3 Organosilyl Method 24

1.3.1.4 Organozinc Method 24

1.3.1.5 Using Other Organometallics 25

1.3.1.6 Metal Phosphide Method 27

1.3.1.7 Radical Addition 28

1.3.1.8 Reduction of Phosphine Oxides and Sulphides 29

1.4 Functionalised Phosphines 31

1.4.1 Phosphorus-Oxygen Containing Ligands 32

1.4.1.1 Ether-Functionalised Phosphines 33

1.4.1.2 Ketone- and Ester-Functionalised Phosphines 36

1.5 Hemilability 37

1.6 Phosphinoamines 39

1.7 *N*-Pyrrolyl Phosphines 46

1.8 Phosphorus-31 NMR 47

1.8.1 Chemical Shifts 47

1.8.2 Metal-Phosphorus Coupling Constants $^{1}J(P,M)$ 48

1.9 References 51

Chapter Two **Ether-Functionalised Phosphinoamines** 60

2.0 Introduction 61

2.1 Results and Discussion 62

2.1.1 Synthesis of Ether-Functionalised Phosphinoamines 62

2.1.2 Complexes of the Ether-Functionalised Phosphinoamines 66

2.1.2.1 Synthesis of $[MCl_2L_2]$ (M = Pd and Pt) 66

2.1.2.1.1 Characterisation of $[PdCl_2L_2]$ (L = $\mathbf{L^1}$-$\mathbf{L^4}$) 66

2.1.2.1.2 Characterisation of *cis*-$[PtCl_2L_2]$ (L = $\mathbf{L^1}$, $\mathbf{L^3}$ and $\mathbf{L^4}$) and *cis*-$[PtBr_2(\mathbf{L^1})_2]$ 68

2.1.2.1.3 X-ray Crystal Structure of *trans*-$[PdCl_2(\mathbf{L^1})_2]$ (**1**) and *trans*-$[PdCl_2(\mathbf{L^3})_2]$ (**3**) 69

2.1.2.1.4 Reactions of $[MCl_2L_2]$ (M = Pd and Pt) 73

2.1.2.1.4.1 Abstraction of Chloride from *cis*-$[PtCl_2L_2]$ (L = $\mathbf{L^1}$ and $\mathbf{L^4}$) and *trans*-$[PdCl_2(\mathbf{L^1})_2]$ 73

2.1.2.1.4.2 Lability of Coordinated Ether Oxygen 77

2.1.2.1.4.3 Methanolysis of the P-N Bonds of Coordinated Phosphinoamines 78

2.1.2.1.4.4 Synthesis of *cis*-$[PtX(NO_2)(\mathbf{L^1})_2]$ [X = Cl and Br] and *cis*-$[Pt(NO_2)_2(\mathbf{L^1})_2]$ 78

2.1.2.1.4.4.1 X-ray Crystal Structure of *cis*-$[PtBr(NO_2)(\mathbf{L^1})_2]$ (**16**) 81

2.1.2.2 Synthesis of [Pd(dmba)Cl(L)] (L = $\mathbf{L^1}$-$\mathbf{L^4}$) and [Pt(dmba)Cl(L)] (L = $\mathbf{L^1}$, $\mathbf{L^3}$ and $\mathbf{L^4}$) 83

2.1.2.2.1 Characterisation of [Pd(dmba)Cl(L)] (L = $\mathbf{L^1}$-$\mathbf{L^4}$) 84

2.1.2.2.2 Characterisation of [Pt(dmba)Cl(L)] (L = $\mathbf{L^1}$, $\mathbf{L^3}$ and $\mathbf{L^4}$) 85

2.1.2.2.3 X-ray Crystal Structures of [Pd(dmba)Cl($\mathbf{L^1}$)] (**18**) and [Pd(dmba)Cl($\mathbf{L^2}$)] (**19**) 86

2.1.2.2.4 Reactions of [M(dmba)Cl(L)] (M = Pd and Pt) 90

2.1.2.2.4.1 Abstraction of Chloride from [Pt(dmba)Cl(L)] (L = $\mathbf{L^1}$ and $\mathbf{L^4}$) and [Pd(dmba)Cl($\mathbf{L^1}$)] 90

2.1.2.2.4.2 Lability of the Coordinated Ether Oxygen 93

2.1.2.2.4.3 Formation of [Pt(dmba)(μ-PPh_2O)]$_2$ 96

2.1.2.2.4.3.1 X-ray Crystal Structure of [Pt(dmba)(μ-PPh_2O)]$_2$ (**35**) 96

2.1.2.3 Complexes of Molybdenum 98

2.1.2.3.1 Synthesis of [$Mo(CO)_4L_2$] (L = $\mathbf{L^1}$, $\mathbf{L^3}$ and $\mathbf{L^4}$) 99

2.1.2.3.2 Characterisation of [$Mo(CO)_4L_2$] (L = $\mathbf{L^1}$, $\mathbf{L^3}$ and $\mathbf{L^4}$) 99

2.1.2.3.3 X-ray Crystal Structure of *cis*-[$Mo(CO)_4$($\mathbf{L^4}$)$_2$] (**38**) 100

2.1.2.3.4 Synthesis of [$Mo(CO)_3$($\mathbf{L^3}$)$_3$] 103

2.1.2.4 Complexes of Rhodium 103

2.1.2.4.1 Synthesis of [RhCl(CO)L_2] (L = $\mathbf{L^1}$, $\mathbf{L^3}$ and $\mathbf{L^4}$) 103

2.1.2.4.2 Characterisation of [RhCl(CO)L_2] (L = $\mathbf{L^1}$, $\mathbf{L^3}$ and $\mathbf{L^4}$) 104

2.2 Conclusion 108

2.3 References 109

Chapter Three **Amine-Functionalised Phosphinoamines** 112

3.0 Introduction 113

3.1 Results and Discussion 114

3.1.1 Ligand Synthesis 114

3.1.2 Complexes of the Amine-Functionalised Phosphinoamines 116

3.1.2.1 Synthesis of $[PtCl_2L_2]$ (L = $\mathbf{L^7}$ and $\mathbf{L^8}$) 116

3.1.2.1.1 Abstraction of Chloride from *cis*-$[PtCl_2(\mathbf{L^8})_2]$ 122

3.1.2.2 Synthesis of the [M(dmba)Cl($\mathbf{L^7}$)] (M = Pd and Pt) 125

3.1.2.2.1 Abstraction of Chloride from [Pt(dmba)Cl($\mathbf{L^7}$)] 127

3.1.2.3 Formation of *cis*-[Pt($\mathbf{L^7}$-*P,N*)(μ-$\mathbf{L^7}$)$CoCl_3$] 127

3.1.2.3.1 X-ray Crystal Structure of *cis*-[Pt($\mathbf{L^7}$-*P,N*)(μ-$\mathbf{L^7}$)$CoCl_3$] (**52**) .. 129

3.1.2.4 Synthesis of $[Pt(O_2C_6H_3{}^tBu)(\mathbf{L^7})_2]$ 131

3.1.2.5 Synthesis of [RhCl(CO)($\mathbf{L^8}$-*P,N*)] and $[RhCl(CO)(\mathbf{L^8})_2]$ 134

3.2 Conclusion 136

3.3 References 137

Chapter Four **Keto-Functionalised *N*-Pyrrolyl Phosphines** 139

4.0 Introduction 140

4.1 Results and Discussion 141

4.1.1 Ligand Synthesis 141

4.1.2 Complexes of 2-Acetyl *N*-Pyrrolyl Phosphine 143

4.1.2.1 Synthesis of $[MCl_2(\mathbf{L^{10}})_2]$ (M = Pd and Pt) 143

4.1.2.2 Synthesis of [M(dmba)Cl($\mathbf{L^{10}}$)] (M = Pd and Pt) 144

4.1.2.2.1 Abstraction of Chloride from [M(dmba)Cl($\mathbf{L^{10}}$)] (M = Pd and Pt) 145

4.1.2.2.1.1 X-ray Crystal Structure of [Pt(dmba)($\mathbf{L^{10}}$-*P,O*)]PF_6 (**63**) 147

4.1.2.2.2 Lability of Coordinated Ketone Oxygen 150

4.1.2.3 Rhodium(I) Complexes 151

4.1.2.3.1 Synthesis of [RhCl(CO)($\mathbf{L^{10}}$-*P,O*)] 151

4.1.2.3.2 Synthesis of *trans*-[RhCl(CO)($\mathbf{L^{10}}$)$_2$] 153

4.1.2.3.3 Formation of [RhCl(CO)(μ-PPh_2OPPh_2)]$_2$ 154

4.1.2.3.3.1 X-ray Crystal Structure of [RhCl(CO)(μ-PPh_2OPPh_2)]$_2$ (**66**) .. 155

4.1.2.3.4 Synthesis of [Rh($\mathbf{L^{10}}$-*P,O*)$_2$]X (X = Cl and PF_6) 159

4.2 Conclusion 161

4.3 References 163

Chapter Five **Late Transition Metal Complexes of Silasesquioxanes** 165

5.0 Introduction 166

5.1 Results and Discussion 169

5.1.1 Introduction 169

5.1.2 Synthesis of the Palladium(II) and Platinum(II) Complexes of Silasesquioxanes 169

5.1.2.1 X-ray Crystal Structure of *cis*-[(c-C_5H_9)$_7Si_7O_9$($OSiMe_3$)O_2Pt(dppe) (**69**) 173

5.2 Conclusion 175

5.3 References 176

Chapter Six **Self Assembly and Silver Isonicotinate Structure** 177

6.0 Introduction 178

6.1 Results and Discussion 182

6.1.1 Synthesis of *cis*-[M(dppe)(isonicH)$_2$](BF$_4$)$_2$ (M = Pd and Pt).. 182

6.1.2 Formation of [Ag$_3$(isonic)$_2$]BF$_4$ 184

6.1.2.1 X-ray Crystal Structure of [Ag$_3$(isonic)$_2$]BF$_4$ (**75**) 184

6.2 Conclusion 190

6.3 References 191

Chapter Seven **Experimental Section** 193

7.0 General Experimental 194

7.1 Safety 195

7.2 Syntheses 195

7.3 References 231

Appendix 1 **Crystallography** 232

Appendix 2 **Crystallographic Data** 234

Abbreviations

χ	electronic parameter
δ	chemical shift (NMR)
ν	frequency (infra-red)
$\{^1H\}$	proton decoupled (NMR)
Bu	butyl group
br	broad (NMR and infra-red)
cod	1,5-cyclooctadiene
Cp*	C_5Me_5
Cy	cyclohexyl group
d	doublet (NMR)
Dbu	1,8-diazabicyclo[5.4.0]undec-7-ene
dppe	$Ph_2PCH_2CH_2PPh_2$
dppm	$Ph_2PCH_2PPh_2$
dppp	$Ph_2PCH_2CH_2CH_2PPh_2$
dq	doublet of quartets
Et	ethyl group
fac	facial (stereochemistry)
FAB	fast atom bombardment
FTIR	fourier transform infra-red spectroscopy
Hdmba	*N,N*-dimethylbenzylamine
isonicH	isonicotinic acid $[NC_5H_4(CO_2H)\text{-}4]$
IR	infra-red
J	nuclear spin-spin coupling constant (NMR)

L	generalised ligand
L_nM	generalised metal fragment with n ligands
m	multiplet (NMR) and medium (infra-red)
Me	methyl group
MS	mass spectroscopy
m/z	mass to charge ratio (mass spectroscopy)
NMR	nuclear magnetic resonance
Ph	phenyl group
Pr	propyl group
qui	quintet (NMR)
r.t.	room temperature
S	sinister (stereochemistry)
s	singlet (NMR) and strong (infra-red)
S^1	$(c\text{-}C_5H_9)_7Si_7O_9(OH)_2OSiMe_3$
S^2	$(c\text{-}C_6H_{11})_7Si_7O_9(OH)_2OSiMe_3$
S^3	$(c\text{-}C_5H_9)_7Si_7O_9(OH)_3$
sep	septet (NMR)
t	triplet (NMR)
THF	tetrahydrofuran
vs	very strong (infra-red)
w	weak (infra-red)
Xyl	$C_6H_3(Me)_2$-2,4

Chapter One

Review of Phosphine and Phosphinoamine Chemistry

1.0 Introduction

The immense interest in phosphine ligands in both organometallic and coordination chemistry has spanned many decades. Research into the transition metal complexes of phosphines has been driven by their importance as homogeneous catalysts for a range of industrially important processes such as hydrogenation and hydroformylation. Phosphines, unlike many other classes of ligands, offer great versatility in their coordination properties due to the ease and the systematic ways in which their steric and electronic properties can be altered. Numerous methods have been developed to synthesise new phosphines containing a wide range of substituent groups, some of which are outlined below.

1.1 Historical Background[1]

Trimethylphosphine was first synthesised by Thénard[2] in 1847, from the reaction of methyl chloride with impure calcium phosphide at 180-300°C. Following this work Bérle[3] synthesised triethylphosphine from the reaction of ethyl iodide and impure sodium phosphide in 1855.

It was the discovery of aliphatic amines and their relation to phosphines, which resulted in the revival of interest in the chemistry of tertiary phosphines. During the period 1857-1871, Hofmann and Cahours[4] were responsible for much of the early development of organic phosphorus chemistry. The difficulties that had to be overcome with these early syntheses of tertiary phosphines were immense, with the risk of fires and explosions, as well as difficulties in separating the desired product from the complex mixture produced from these reactions.

The development of aromatic phosphines occurred in the last quarter of the nineteenth century, and much of this work was carried out by Michaelis and co-workers.[5] He synthesised dichlorophenylphosphine by passing a mixture of benzene and trichlorophosphine vapours through a red-hot porcelain tube. From this work phenylphosphine, diphenylphosphine and triphenylphosphine were synthesised.

The development of aliphatic phosphorus chemistry was significantly slower than that of the aromatic phosphines due to their difficult syntheses. It was not until the application of Grignard reagents that their study really developed.

1.2 Transition Metal Phosphine Chemistry

The early synthesis of tertiary phosphines was quickly followed by the synthesis of their metal complexes. Hofmann, during work to characterise the phosphines,[6] synthesised the platinum(II) complexes, now known to be $[PtCl_2(PMe_3)_2]$ and $[PtCl_2(PEt_3)_2]$. The start of serious investigation into phosphine complexes began when Cahours and Gal[7] in the 1870s obtained two different forms of $[PtCl_2(PEt_3)_2]$ from the reaction of triethylphosphine and a boiling solution of platinum(IV) chloride. They and other workers also prepared gold(I), copper(I) and palladium(II) phosphine complexes, but little interest was shown in these except for the isomeric platinum species.

It was not until the 1930s and the work by Mann[8] and Jensen[9] that the interest in transition metal phosphine chemistry really developed. As a result of these extensive studies of the chemistry of organo-phosphine complexes, the number of known complexes containing tertiary phosphine ligands increased considerably. Other key figures in the development of the coordination chemistry of transition metal phosphine complexes were Dwyer,[10] Chatt,[8] and Nyholm.[11]

Reppe and co-workers published the first work applying phosphine complexes to catalysis in 1948.[12] They showed that triphenylphosphine complexes of nickel were effective catalysts for the polymerisation of olefinic and acetylenic substances. This work resulted in considerable industrial interest in the potential catalytic properties of phosphine complexes soluble in organic media. From this work the development of phosphine complexes in homogeneous catalysis began.

The volume of chemicals produced from homogeneous catalytic systems is still relatively small when compared to heterogeneous systems,[13] but their improved reactivity and selectivity means that the importance of homogeneous catalysts in both the petrochemical and pharmaceutical industries is immense.

There is a considerable range of chemical processes which have been catalysed using homogeneous catalysts containing tertiary phosphines, including hydrogenation, isomerisation and hydroformylation.

Hydrogenation is the addition of hydrogen to an unsaturated compound (e.g. olefins and acetylenes). A simple hydrogenation catalyst precursor is the complex $[RhCl(PPh_3)_3]$, this was shown by two groups in 1965[14] to hydrogenate alkenes and alkynes at 25°C and 1 atm of H_2. Asymmetric hydrogenation in which an achiral unit is converted into a chiral entity is of particular importance in the pharmaceutical industry, for example the synthesis of L-DOPA, which is used in treating Parkinson's disease. Here a soluble rhodium catalyst containing an optically active tertiary phosphine has been used to give the desired product with an optical purity of over 90%.

In isomerisation the chemical formula of a compound is unchanged but the molecular structure is altered. For example, in alkene isomerisation, the double bond of an alkene migrates via the metal mediated transfer of hydrogen atoms. Most

commonly the alkyl and allyl mechanisms for alkene isomerisation are observed - these differ in that the alkyl route involves a 1,2 shift of hydrogen whereas the allyl route involves a 1,3 shift. A typical catalyst precursor for alkene isomerisation is $[RhH(CO)(PPh_3)_3]$.[15]

In hydroformylation, the addition of the units CHO and H to a double bond gives either a 'normal' or 'iso' aldehyde. A number of rhodium complexes containing tertiary phosphines have been shown to be effective precursors to hydroformylation catalysts e.g. $[RhCl(CO)L_2]$ (L = PBu_3 or PPh_3), $[RhH(CO)(PPh_3)_3]$ and $[RhCl(PPh_3)_3]$.[16]

1.3 Phosphine Syntheses

Since the first synthetic methods for tertiary phosphines were developed over 150 years ago, a vast array of preparative methods has been developed. The initial raw materials, which are used to synthesise most organophosphorus compounds, are derived from elemental phosphorus. Phosphorus is converted into either phosphorus trichloride (PCl_3) by direct reaction with excess chlorine, or phosphoryl chloride ($POCl_3$) by exposing phosphorus trichloride to air. From these starting materials most organophosphorus compounds may be prepared.

1.3.1 Preparation of Tertiary Phosphines[17,18]

On considering the possible disconnections of the phosphorus-carbon bond, three synthetic routes become apparent:

$P\text{-}C \Rightarrow P^{+} + C^{-}$, equivalent to P-X + M-C (1)

$P\text{-}C \Rightarrow P^{-} + C^{+}$, equivalent to P-M + X-C (2)

$P\text{-}C \Rightarrow P^{\cdot} + C^{\cdot}$ (3)

Disconnection **1** may be considered as the reaction of electrophilic phosphorus with a nucleophilic carbon, for example the reaction of a halophosphine with an organometallic reagent such as a Grignard or organolithium reagent. This is one of the most commonly used synthetic routes as the starting materials required are readily available.

Disconnection **2** represents the reaction of nucleophilic phosphorus with a suitable carbon electrophile, for example the reaction of a metal phosphide with an organohalogen compound. This is also a popular synthetic route, though the synthetic steps are somewhat more complex than with the previous case.

Disconnection **3** shows the radical-based reaction of phosphorus and carbon. This is a much less common synthetic route than the previous two examples, though it can be useful with multiple bonds as acceptors.

Another very useful route to the synthesis of tertiary phosphines uses the reduction of phosphorus(V) compounds to phosphorus(III) compounds, an outline of this procedure is given later.

1.3.1.1 Grignard Method

This is one of the most commonly used laboratory methods for synthesising tertiary phosphines. This route may be used to give tertiary phosphines with either identical or different components depending on the starting materials used e.g. R_3P or RR'R"P. The starting materials may be the halophosphines (PX_3, RPX_2 or RR'PX) -

these are added to the Grignard reagent usually in ether, and refluxed to complete the reaction. Heating the reaction mixture to reflux is particularly necessary in the case of bulky alkyl groups otherwise mono- or di- substituted products result. Separation of the product can be achieved by treating the reaction mixture with an ammonium chloride solution, followed by separation and distillation of or crystallisation from the organic layer. The hydrolysis step is sometimes omitted and vacuum distillation used to extract the product, though this is only useful for phosphines with low boiling points.

The Grignard derivatives of primary alkyl and aryl halides give the best yields whilst branched chain halides, secondary alkyl halides and *t*-butyl halides give little, if at all any of the desired product. This occurs even when the optimal conditions are used: an excess of the Grignard reagent, which is added to the phosphorus halide keeping the initial reaction temperature as low as possible. Steric hindrance is believed to be responsible for the difficulty in synthesising tri-substituted phosphine containing these bulky alkyl groups, since products are often isolated in which full substitution has not occurred.[19]

$$PCl_3 + Bu^tMgX_{(xs)} \rightarrow Bu^t_2PCl$$

The synthesis of unsymmetrical and asymmetric tertiary phosphines may be achieved using the Grignard route with careful selection of the starting materials. Examples of phosphines synthesised via the Grignard route (Figure 1): (i) the synthesis of [4-{bis(2-diethylaminoethyl)aminomethyl}diphenyl]phosphine[20] (**1**); (ii) the reaction of chlorodiphenylphosphine and the Grignard derived from 1-bromo-8-dimethylaminonaphthalene to yield (8-dimethylaminonaphthyl)-

diphenylphosphine[21] (**2**); and (iii) the synthesis of (2,5-dimethoxybenzyl)diphenylphosphine which was prepared from the Grignard derived from 2,5-dimethoxybenzylbromide and chlorodiphenylphosphine[22] (**3**).

Figure 1 Preparation of unsymmetrical tertiary phosphines

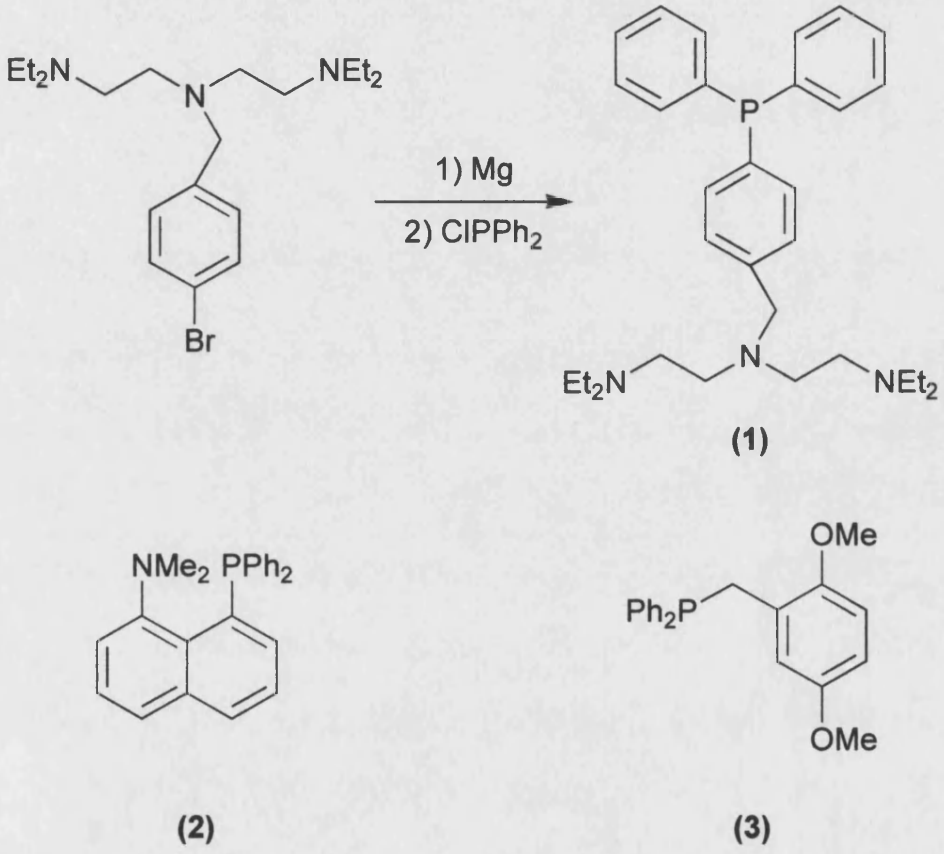

One drawback to the Grignard route is that occasionally it is necessary to protect functional groups, which are sensitive to organometallic reagents. Such a case is the synthesis of triarylphosphines containing formyl or acetyl groups as aryl substituents, where the ethylene keto derivative is used as a protecting group for the carbonyl group during the Grignard reaction. The protecting group from the resulting phosphine can then be removed to give the desired product (Scheme 1).[23]

Scheme 1

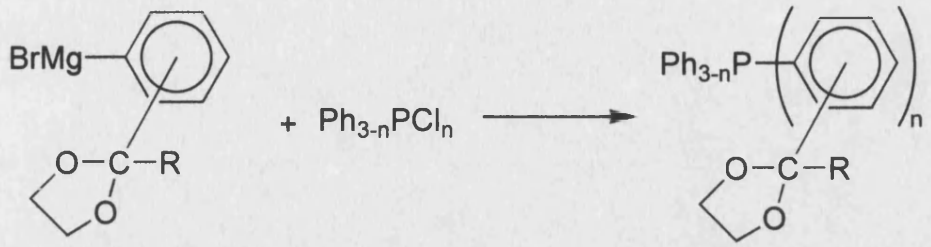

The incorporation of three different groups to give asymmetric phosphines may be achieved by either reacting the Grignard reagent R"MgX with the phosphinous chloride of the type RR'PCl or from phosphonous dihalide RPX_2 and a mixture of different Grignard reagents R'MgX and R"MgX (Scheme 2). In the latter case the two Grignard reagents must be significantly different to allow separation of the different tertiary phosphines produced.[24]

Scheme 2

$PhPCl_2$ + EtMgBr + $PhCH_2MgCl$ ⟶ $PhEt_2P$ (24%) + $EtPh(PhCH_2)P$ (41%) + $Ph(PhCH_2)_2P$ (18%)

An unusual example of the formation of a phosphorus-nitrogen bond is found when the magnesium compounds derived from indole and its derivatives are reacted with phosphorus trichloride. Due to the tautomeric nature of the magnesium indole species a mixture of the normal tertiary phosphine as well as some phosphorus-nitrogen bound derivatives is produced (Figure 2).[25]

Figure 2

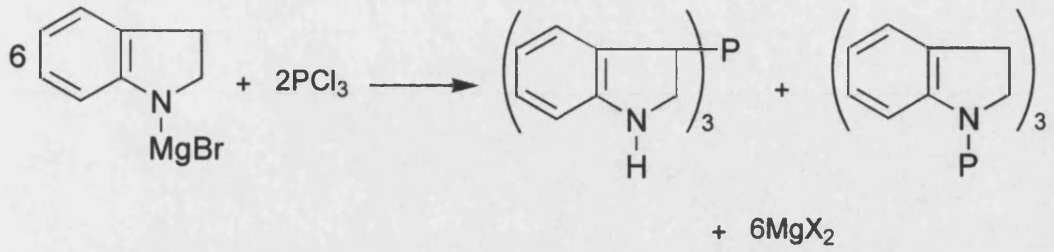

1.3.1.2 Organolithium and Alkali-Organic Methods[17]

Organolithium reagents resemble Grignard reagents except that they are more reactive due to the C-Li bond being more ionic than C-Mg. The synthesis of tertiary phosphines using organolithium reagents is similar to the Grignard route giving comparable yields.[26] An exception to this is in the synthesis of tertiary phosphines containing bulky alkyl groups e.g. tri-*tert*-butylphosphine, which are not accessible via the Grignard route (Figure 3).[27]

Figure 3

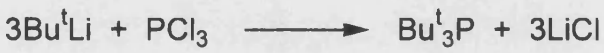

The aryllithium reagents are often used in preference to the Grignard reagents, as the aryllithium reagents are easier to prepare. A wide range of tertiary phosphines have been synthesised using the organolithium route, examples (Figure 4) of which are: (i) the reaction of chlorodiphenylphosphine and the organolithium reagent 5,5'-dilithium bis(pyrazol-1-yl)methane to yield the bis(5-diphenylphosinopyrazol-1-yl)methane[28] (**1**), (ii) the synthesis of 2-(2'-diphenylphosphinophenyl)-1,3-dioxolane[29] (**2**), and (iii) the synthesis of

1,2-bis[bis(2,6-difluorophenyl)phosphino]ethane[30] from the 2,6-difluorophenyllithium reagent with bis(dichlorophosphino)ethane in diethyl ether at -78°C (**3**).

Figure 4 Examples of tertiary phosphines synthesised via the organolithium route

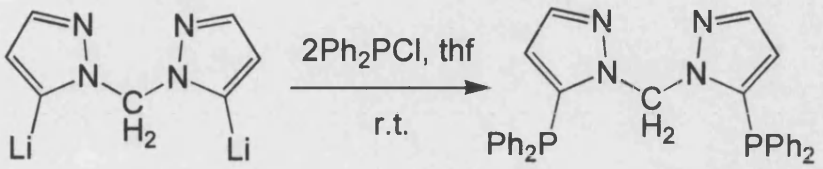

(1)

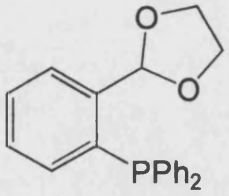

(2)

(3)

The reaction of phosphorus trichloride with organo-sodium and potassium compounds also yields tertiary phosphines in a similar fashion. The reaction conditions are similar to those used in the Grignard route, with either the alkali organic compounds being synthesised *in situ* from the alkali metal and organic halide, or via an exchange reaction at low temperature. Both give comparable yields to that of the Grignard route, for example tribenzylphosphine has been synthesised from benzylsodium and phosphorus trichloride in 84% yield.[31]

1.3.1.3 Organosilyl Method

In a number of cases the synthesis of heterocyclic substituted phosphines via addition of chlorophosphine to organometallic reagents such as organolithium, resulted in poor yields due to the formation of unwanted side products.[32,33,34] In order to avoid such side reactions trimethylsilyl-substituted derivatives were used instead of the corresponding organometallic reagents. The silyl-substituted derivatives can be synthesised by the addition of Me_3SiCl to the deprotonated heterocycle at -78 °C; addition of chlorophosphine to this mixture then gives the desired phosphine. For example bis(2-oxazolin-2-ylmethyl)phenylphosphine[33] (**1**) and 2-(diphenylphosphinomethyl)-1-methylimidazole[32] (**2**) were synthesised via this route (Figure 5).

Figure 5

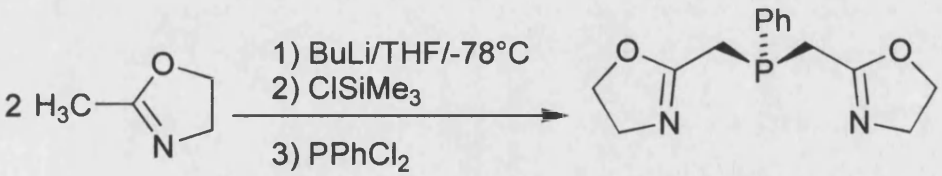

(1)

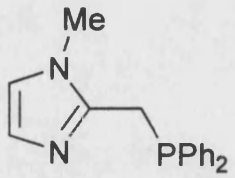

(2)

1.3.1.4 Organozinc Method

The Grignard/organolithium routes can be extended using softer organometallics such as organozinc reagents. The reaction of functionalised organozinc reagents with chlorophosphines has been shown[35] to allow the direct

incorporation of a number of functional groups (Figure 6), which are not directly accessible using the equivalent Grignard or organolithium reagents. This reduced reactivity of organozinc reagents compared with that of the corresponding Grignard/organolithium regents is due to the significantly less polar metal-carbon bond. Examples of an ester-functionalised (**1**) and chloro-functionalised (**2**) phosphines synthesised using the organozinc route are shown in Figure 6.

Figure 6

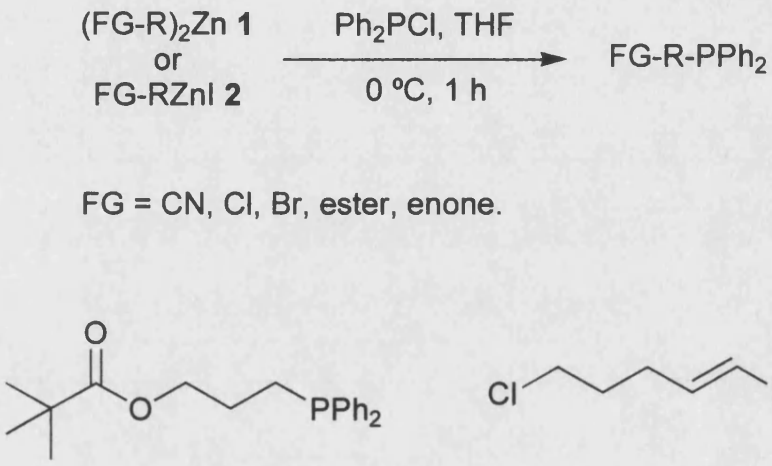

1.3.1.5 Using Other Organometallics

A sizeable number of alternative routes have been developed to the synthesis of phosphines using a variety of organometallic reagents such as, organo-aluminium,[36] -mercury[37] and -tin[38] compounds. A number of these routes have been developed to synthesise novel phosphines, which are not generally accessible via the standard synthetic routes, for example, organo-zirconium[39,40,41] reagents react with dichlorophosphine to give a range of heterocyclic phosphorus compounds (Figure 7) such as 1-phenyl-1,4-diphosphaindene[41] (**1**) and 2,5-di(2-pyridyl)phospholes[40] (**2**).

Figure 7

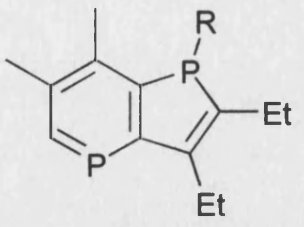

R = CH_2CH_2CN, Me, $SiMe_3$

(1)

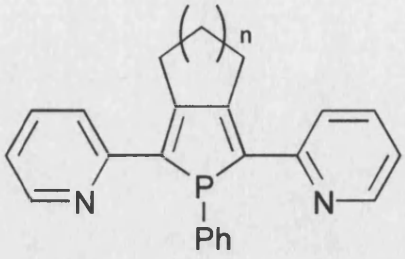

n = 1 or 2

(2)

Recent reports have shown that functionalised phosphines containing amino acids and ester functional groups can be synthesised using palladium[42] and platinum[43] catalysts respectively. For example, the palladium catalysed synthesis of amino acid functionalised phosphine[42] (Figure 8).

Figure 8

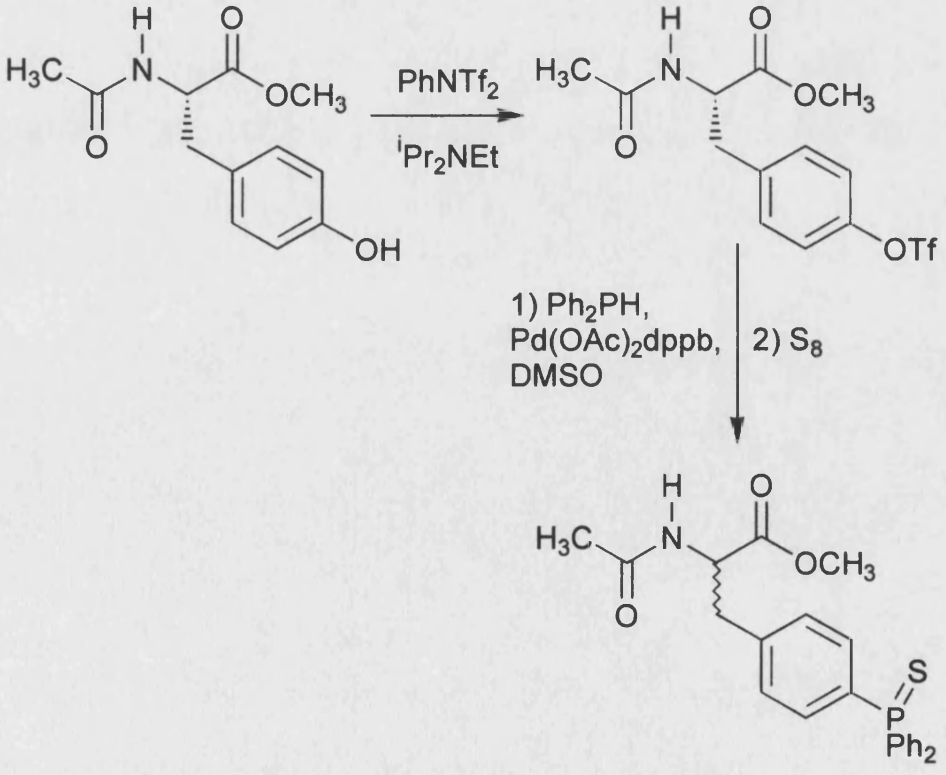

1.3.1.6 Metal Phosphide Method[17]

In this method the phosphorus acts as a nucleophile attacking an electrophilic carbon, which is the reverse of Disconnection **1** (Section 1.3.1). The alkali metal derivatives of phosphines PM_3, RPM_2 and R_2PM readily react with alkylhalides or other suitable electrophiles to give tertiary phosphines in good yield, examples of typical reactions are shown:

$$PM_3 + 3RX \rightarrow R_3P + 3MX$$

$$RPM_2 + 2R'X \rightarrow R_2R'P + 2MX$$

$$RR'PM + R''X \rightarrow RR'R''P + MX$$

The reaction conditions require stoichiometric amounts of the alkylhalide to be added with care to a suspension or solution of the alkali phosphide in an inert solvent, this stoichiometry is required so as to avoid the formation of unwanted by-products. Heating the reaction mixture to reflux is usually carried out to complete the reaction, with the metal halide removed by filtration. The phosphine is then purified by distillation. The chloride, bromide and iodide alkyl and aryl halides may be used in these reactions.

It is unusual to make symmetrical tertiary phosphines via this route, due to the ease and availability of the starting materials required for the electrophilic (e.g. Grignard) route. This method only becomes comparable to the electrophilic phosphorus routes when synthesising unsymmetrical and asymmetric tertiary phosphines, as the availability and ease of synthesising the starting materials is about the same for both methods. A wide range of tertiary phosphines have been synthesised using the metal phosphide route, examples of which are (Figure 9): (i) the synthesis of

2,5-bis[(diphenylphosphino)methyl]thiophene[44] (**1**), (ii) the synthesis of (2-tetrahydrofurylmethyl)diphenylphosphine[45] (**2**), and (iii) the reaction of metal phosphides with spiroheptadiene,[46] in which the cyclopentadienyl acts as a stabilising unit (**3**).

Figure 9 Examples of tertiary phosphines synthesised from metal phosphides

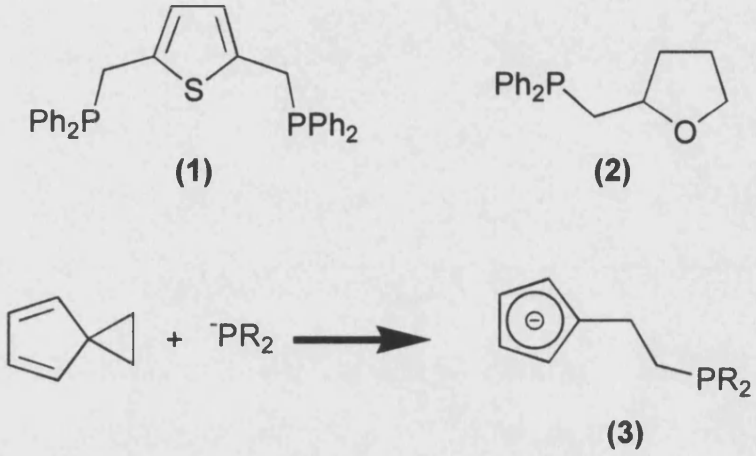

1.3.1.7 Radical Addition[18]

The use of radical addition of phosphines to alkenes and alkynes has provided a useful high yielding route to the synthesis of a limited number of tertiary phosphines. Limited control of the reaction products can be achieved by varying the reagent ratios; this is of particular use when using sterically bulky alkenes.

The reaction may be initiated by the usual radical initiators for example ultraviolet light, peroxides and α,α'-azobisisobutyronitrile. The reaction proceeds via a chain mechanism as shown:

$$R_2PH + \text{initiator} \rightarrow R_2P^{\cdot}$$

$$R_2P^{\cdot} + RCH{=}CH_2 \rightarrow R_2PCH_2C^{\cdot}HR$$

$$R_2PCH_2C^{\cdot}HR + R_2PH \rightarrow R_2PCH_2CH_2R + R_2P^{\cdot}$$

Examples where the radical route has been used (Figure 10): (i) the addition of simple alkenes to bis(trifluoromethyl)phosphine using ultraviolet light as an initiator at a temperature of 40°C to give the alkylbis(trifluoromethyl)phosphine[47] (**1**), and (ii) the sequential addition of silanes and secondary phosphines to α,ω-dienes using ultraviolet light as initiator to give silylalkylphosphines[48] (**2**).

Figure 10 Examples of tertiary phosphines synthesised via radical addition

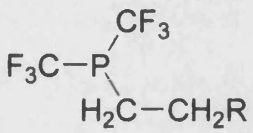

(1)

$R_2P(CH_2)_2(CH_2)_n(CH_2)_2SiR_2$ (n = 1 - 4)

(2)

1.3.1.8 Reduction of Phosphine Oxides and Sulphides[17]

The route is particularly useful in the synthesis of chiral phosphines, as it is easier to resolve phosphonium salts and phosphine oxides than the parent tertiary phosphine; these species can then be reduced to the corresponding tertiary phosphine with retention or inversion of configuration.

Many phosphines can only be made via the phosphine oxide so methods of reducing these to give the tertiary phosphine are of great importance. A wide range of reducing agents may be used for example $LiAlH_4$, CaH_2, silanes, and boranes. One of the most commonly used reductants for phosphine oxides and sulphides are silanes (e.g. $SiHCl_3$ and $R_{4-x}SiH_x$) as they are easy to use, effective for a wide range of

phosphines, give clean stereochemistry and high yields. The reduction is carried out by mixing the oxide with an excess of silane, in an inert solvent under nitrogen, a weak base is often added such as a tertiary amine to remove any HCl formed (Figure 11). Heating the reaction mixture to reflux is then used to complete the reaction and the phosphine is extracted by distillation.

Figure 11

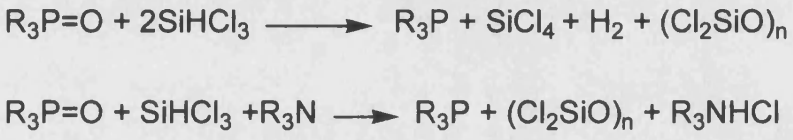

A major advantage of silanes is that reduction may be carried out in the presence of a wide range functional groups for example carbonyls, nitriles and amines.[49] By careful control of the reaction conditions and the silane used great control of the stereochemistry of the tertiary phosphine produced can be achieved, to give either retention or inversion of configuration. An example where trichlorosilane has been used in the presence of other functional groups is shown below (Figure 12).

Figure 12

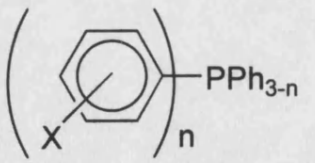

X = CN, CO_2H, CO_2Me

Lithium aluminium hydride may also be used as a reducing agent though its use is limited compared to silanes due to the sensitivity of many more functional

groups to reduction by it. As with silanes reduction may occur with retention of configuration though racemisation often occurs, for example (Figure 13) the reduction of the optically active phosphine oxide (**1**) by lithium aluminium hydride gave a racemic mixture of (**2**).[50]

Figure 13

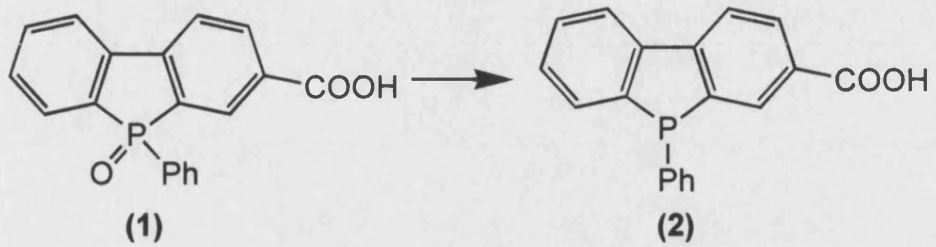

(1) **(2)**

1.4 Functionalised Phosphines

Tertiary phosphines may be used as substitutionally inert ligands to which additional ligating groups such as oxygen, nitrogen, carbon or sulfur containing functional groups may be attached (Figure 14).

Figure 14

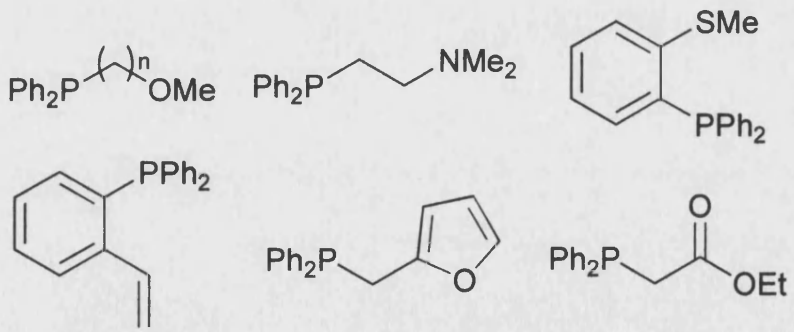

The combination of a phosphorus atom which forms a strong substitutionally inert bond to a late transition metal centre, with a labile ligating group provides the potential combination required for hemilability. The labile donor groups within the

functionalised side chain of the phosphine allows the phosphine to weakly coordinate to the transition metal through these labile donor groups in the absence of coordinating ligands or solvents (e.g. CO, $NCCH_3$ etc.), so forming bidentate or polydentate ligands. However when coordinating ligands or solvents are present, the labile portion of the ligand may be displaced, so forming the metal-ligand/solvent complex (Figure 15). The presence of the substitutionally inert metal-phosphorus bond maintains the labile group in close proximity to the metal centre, so allowing recoordination of the labile group once the bonded small molecule has been lost. This mixing of donor atoms to give hemilabile ligands is of particular interest in the synthesis of complexes suitable for homogeneous transition metal catalysis,[51,52] chemical sensing[53] and stabilisation of reactive unsaturated transition metal complexes.[54]

Figure 15

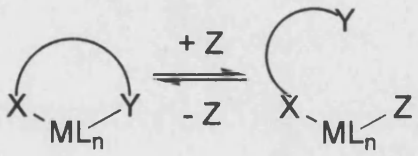

X = substitutionally inert group
Y = substitutionally labile group
Z = ligand or solvent

1.4.1 Phosphorus-Oxygen Containing Ligands

Hemilabile ligands which contain both phosphorus and oxygen donor groups are one of the most extensively studied groups of hemilabile ligands.[55,56] In these systems the phosphorus forms substitutionally inert bonds to the transition metal centre, while the oxygen incorporated in the side chain can form weak metal-oxygen

bonds, which may be cleaved reversibly. There is a considerable range of labile oxygen groups that have been incorporated into hemilabile phosphorus-oxygen ligands for example, ethers,[55] ketones,[57] esters,[58,59] alcohols,[60,61] amides[62] and phosphine oxides.[63,64] Of these the ether- and keto-functionalised phosphines are the two main classes of phosphorus oxygen containing ligands.

1.4.1.1 Ether-Functionalised Phosphines

The chemistry of ether-functionalised phosphines has received considerable attention most notably from Lindner and co-workers.[55] The oxygen donor atom of the ether group may be incorporated into the phosphine as either a simple acyclic or cyclic ether, or as part of a more complex macrocycle or polyether chain in which two or more oxygen donor atoms are incorporated (Figure 16).

Figure 16

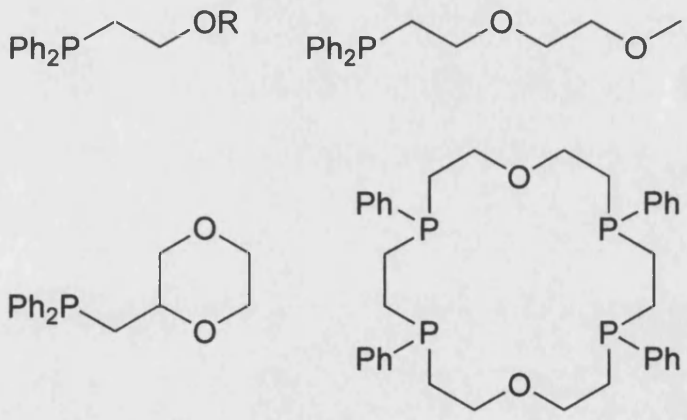

Fluxional intramolecular ligand exchange of ether-functionalised phosphines has been observed in a number of complexes in which the labile ether groups dissociate and recoordinate on a single transition metal centre. For example,

[RhCl(PCy$_2$CH$_2$CH$_2$OCH$_3$-*P,O*)(PCy$_2$CH$_2$CH$_2$OCH$_3$-*P*)][65] undergoes rapid exchange of the labile ether groups at room temperature.

Many transition metal complexes of ether-functionalised phosphines have been shown to be useful for various catalytic processes. For example, rhodium[29,66] and palladium[67] complexes of ether-functionalised phosphines have proved effective hydrogenation catalysts, and cobalt[68] and rhodium[69] (Figure 17) complexes have been used for the carbonylation of methanol.

Figure 17 Catalytic cycle for the carbonylation of methyl iodide by a cationic ether-phosphine rhodium complex

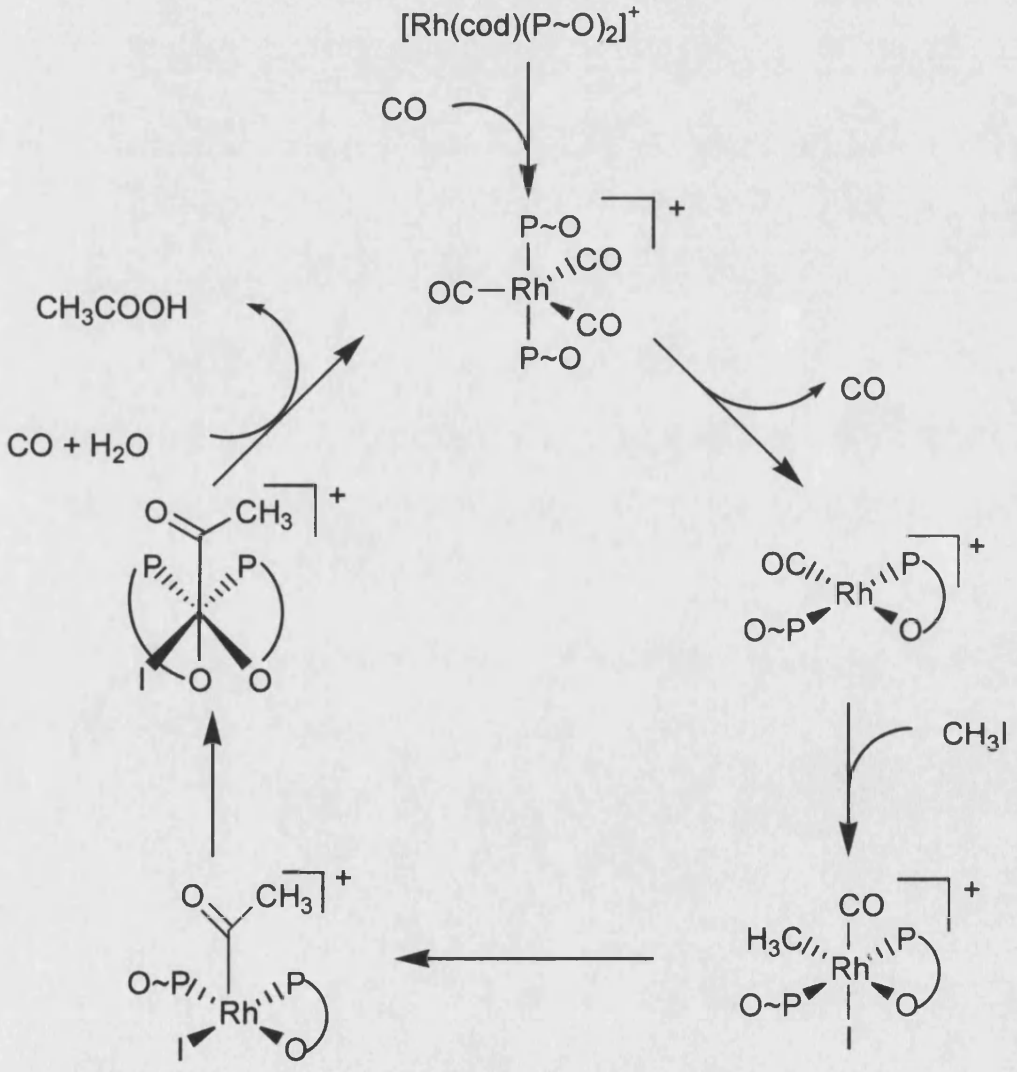

Recent work has examined the properties of supported complexes containing hemilabile ether-functionalised phosphines.[70] These complexes have been shown to exhibit dynamic behaviour, for example the palladium(II) complex[71] was shown to reversibly coordinate acetonitrile (Figure 18). This supported Pd(II) complex was also found to be an effective catalyst for the copolymerisation of CO and ethylene in the absence of solvent.

Figure 18

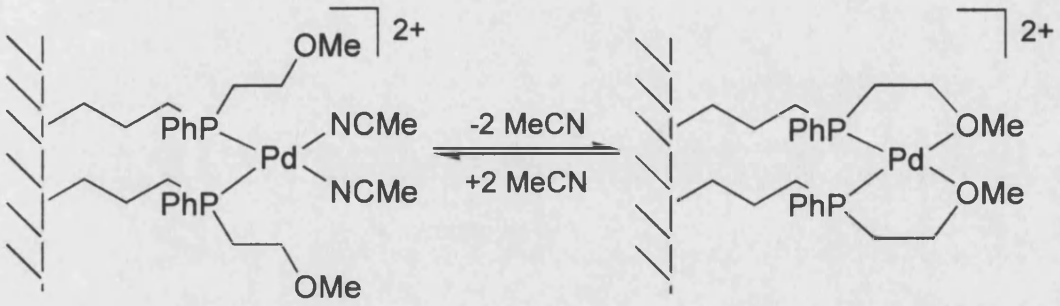

The study of polyether-functionalised phosphines has concentrated on two main properties, their ability to stabilise multiple coordination sites at metal centres[72] and to impart phase-transfer properties to homogeneous catalysts.[73] For example $[RuCl_2\{PPh[(C_3H_6CHMe_2](C_2H_4OC_2H_4OMe\text{-}P,O,O)]$[72] was shown to exhibit an η^3-P-O-O bonding mode of the polyether-functionalised phosphine (Figure 19).

Figure 19

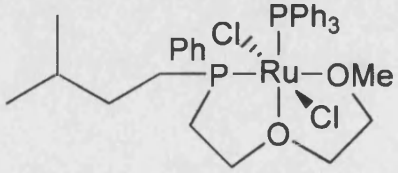

1.4.1.2 Ketone- and Ester-Functionalised Phosphines

An oxygen donor may be incorporated into a phosphine in the form of a carbonyl functionality such as a ketone,[74] aldehyde[75] or ester[58] (Figure 20). These

Figure 20

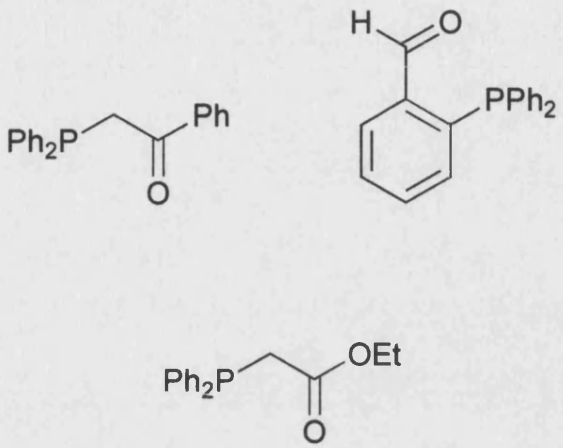

have been found to coordinate in either a unidentate fashion through the phosphorus atoms or in a bidentate fashion to give the *P,O*-chelate (Figure 21).

Figure 21

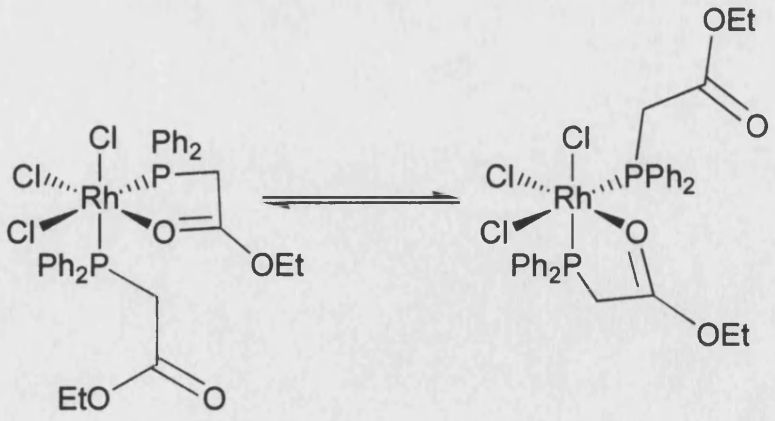

Braunstein et al[76] has shown that the carbonyl group of ketone- and ester-functionalised phosphines generally coordinates more strongly to late transition metal centres than the corresponding ether group of ether-functionalised phosphines. This results in complexes containing ketone- and ester-functionalised phosphines exhibiting increased stability and static nature compared to equivalent ether-functionalised phosphine complexes. For example, $[Rh\{PPh_2CH_2C(O)Ph\text{-}P,O\}_2]PF_6$[76] is stable at room temperature whereas the analogous ether-functionalised complex $[Rh(PPh_2CH_2CH_2OCH_3\text{-}P,O)_2]BPh_4$[55] is unstable above -30°C. This increased bond strength of carbonyl oxygen-metal bond has been observed to result in a number of ketone- and ester-functionalised phosphine complexes being static structures at room temperature, in contrast to the equivalent ether-functionalised phosphine complexes many of which exhibit fluxionality under similar conditions. For example, the *P,O*-chelate ring in $[RhCl\{PPh_2CH_2C(O)Ph\text{-}P,O\}\{PPh_2CH_2C(O)Ph\text{-}P\}]$[76] is static at room temperature whereas $[RhClH_2(PCy_2CH_2CH_2OCH_3\text{-}P,O)(PCy_2CH_2CH_2OCH_3\text{-}P)]$[77] is fluxional under comparable conditions.

The ease of forming *P,O*-chelates is affected by the chelate ring size, 5- and 6-membered chelate rings are the most common as the ring strain is minimised as the rings conformation is such that the steric strain is reduced. In contrast 4- and 7-membered chelate rings are considerably rarer due to unfavourable steric strain.

1.5 Hemilability

Within complexes the hemilabile behaviour of ligands has been observed to occur via a number of different processes. Variable temperature ^1H and ^{31}P NMR

spectroscopy may be utilised to demonstrate the presence of hemilabile ligand exchange involving the labile oxygen groups.

One of the most common of these processes is the fluxional dissociation and recoordination of the weakly bonding groups on a single transition metal centre via intramolecular ligand exchange processes. For example the ester groups in *cis*-[$RhCl_3(PPh_2CH_2CO_2Et$-*P,O*)($PPh_2CH_2CO_2Et$-*P*)][58] undergo intramolecular ligand exchange (Figure 21).

The next type of hemilabile behaviour involves ligand interchange in which an equilibrium exists between the weakly coordinating groups of the hemilabile ligands and the coordinating counter ions. For example, *trans*-[$Fe\{P(CH_2Ph)(CH_2CH_2OEt)_2\}_2](O_3SCF_3)_2$[78] was observed to undergo ligand interchange between the polydentate ether-functionalised phosphine ligands and the two triflate counter ions (Figure 22).

Figure 22

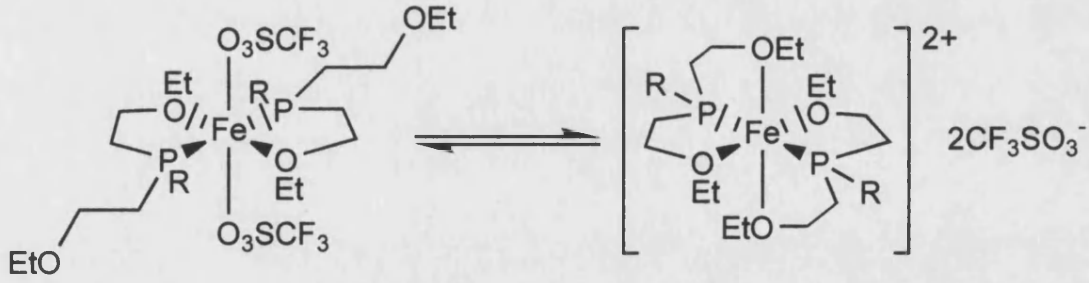

In contrast to the hemilabile properties based on fluxional ligand exchange processes, the hemilabile behaviour of bifunctional ligands is also observed in the displacement of the labile metal bound group of the bifunctional ligand by coordinating ligands and solvents such as CO, nitriles, phosphines and amines. For, example, [$Cu\{PPh_2CH_2C(O)NPh_2$-*P,O*$\}\{PPh_2CH_2C(O)NPh_2$-*P*$\}]BF_4$[62] undergoes

reversible coordination of small molecules such as acetonitrile and SMe_2, which is accompanied by the opening and closing of the *P,O*-chelate (Figure 23).

Figure 23

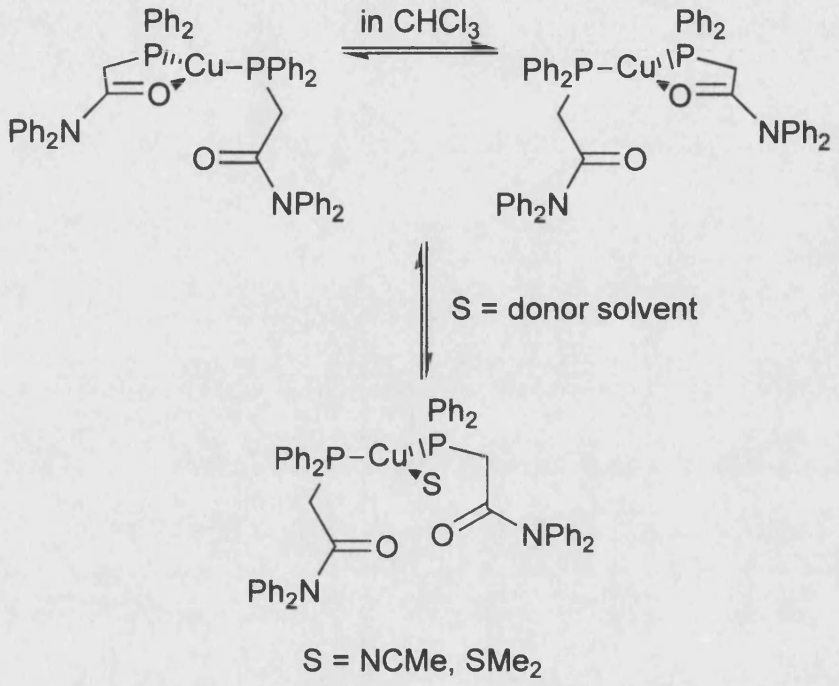

1.6 Phosphinoamines

Compared with the vast body of data accumulated on phosphines and phosphites, phosphinoamines (or aminophosphines) containing P-N bonds have received relatively little interest. The probable reason for this lack of interest is the perceived ease of P-N bond cleavage,[79] though from the number of stable phosphinoamines reported, this factor does not appear to be as important as originally thought. Phosphinoamines can be readily synthesised via the deprotonation of an amine with base such as triethylamine (NEt_3), followed by addition of chlorophosphine (Figure 24). The mild reaction conditions required for the synthesis

of phosphinoamines allows ready incorporation of a range of additional functionalities. Over the past few years a number of diphosphinoamines and functionalised phosphinoamines have been prepared and studied, in which ketones,[80,81,82] phosphinites,[83,84] pyridines,[85,86] phosphines[87] and additional phosphinoamines[88,89,90,91,92] have been incorporated. Complexes containing functionalised phosphinoamines have been utilised in a number of catalytic applications. For example, rhodium(I)[93] and platinum(II)[83] complexes of chiral phosphinoamines have been shown to be efficient catalysts for asymmetric hydrogenation and hydroformylation reactions respectively.

Figure 24

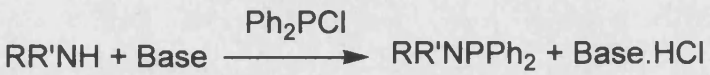

R and R' = alkyl, aryl or H

The diphosphine bis(diphenylphosphino)amine $Ph_2PNHPPh_2$ and its derivatives have received considerable attention most notably from Woollins and co-workers.[94] These ligands are of particular interest due to the range of bonding modes that they exhibit on coordination to metal centres. For example, they may coordinate in monodentate, chelating or bridging modes (Figure 25).[95] These bonding modes are similar to those observed for the isoelectronic methylene compound bis(diphenylphosphino)methane (dppm). In contrast to the methylene group of bis(diphenylphosphino)methane, the acidic amine proton of bis(diphenylphosphino)amine can readily be deprotonated to give the anionic ligand $[Ph_2PNPPh_2]^-$.

Figure 25

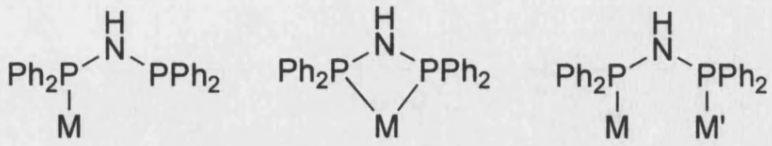

Bis(diphenylphosphino)amine is synthesised in good yield from the condensation reaction between hexamethyldisilane and chlorodiphenylphosphine (Figure 26). It is possible to incorporate a range of substituents at the nitrogen atom using the reaction of primary amines (RNH_2) with either PCl_3 or Ph_2PCl, for example the chiral bidentate phosphines *S*-$(Ph_2P)_2NC(H)(Me)(Ph)$ and *S*-$(Ph_2P)_2NC(H)(CH_3)C(O)OC_2H_5$.[96]

Figure 26

$$2Ph_2PCl + NH(SiMe_3)_2 \longrightarrow Ph_2PNHPPh_2 + 2Me_3SiCl$$

$$2PCl_3 + RNH_2 \longrightarrow RN(PCl_2)_2 + 2HCl$$

$$2Ph_2PCl + RNH_2 \longrightarrow RN(PPh_2)_2 + 2HCl$$

The mono-oxidised derivatives of diphosphines $Ph_2PNHP(E)Ph_2$ (E = oxygen, sulfur or selenium) may be synthesised by direct oxidation of one of the two phosphorus(III) groups with hydrogen peroxide, elemental sulfur and grey selenium respectively. On coordination to metal centres these ligands have been shown to exhibit both *P,E*-chelation and monodenate coordination,[97,98,99] for example *cis*-$[PtCl_2\{PPh_2PNHP(O)Ph_2\text{-}P\}_2]$ has been shown to form the 5-membered *P,O*-chelate on reaction with $AgBF_4$, which is reversible on addition of LiCl (Figure 27).

Figure 27

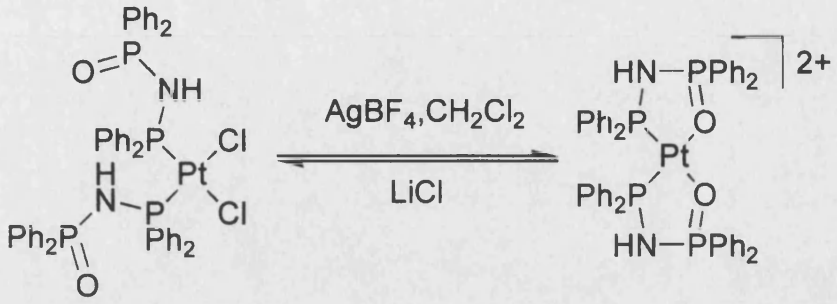

A number of bidentate ligands have been synthesised and studied in which two phosphinoamines are separated by a carbon backbone (Figure 28).[88,91,100] Some of these have been shown to have potential catalytic properties, for example, the rhodium complexes containing the chiral bisphosphinoamines *S*-$R'_2PNC_4H_7(CH_2N\{PR'_2\}\{C_6H_5R\text{-}2\}\text{-}2)$[88] (R = H, Me, OMe and R' = Ph) and 2,2'-bis(diphenylphosphinoamino)-1,1'-binaphthyl[91] have been shown to be effective

Figure 28

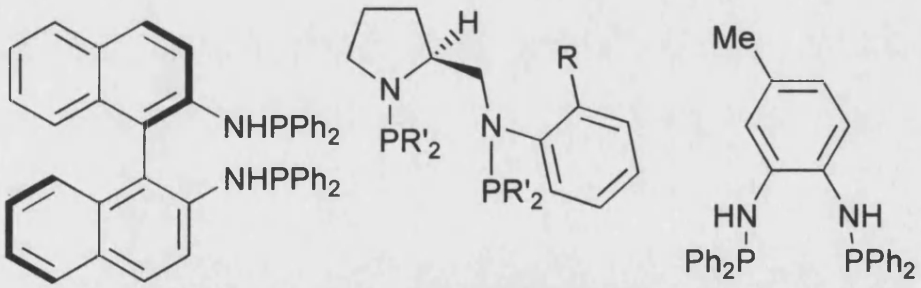

R = H, Me, OMe; R' = Ph

catalysts for the enantioselective hydrogenation of olefins and derivatives of α-phenylenamide (Scheme 3) respectively.

Scheme 3

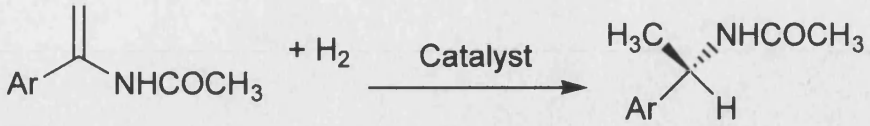

The incorporation of phosphines and phosphites into phosphinoamines to give unsymmetrical diphosphines has produced a range of ligands, which exhibit interesting coordination modes and catalytic properties.

Examination of the coordination chemistry of the unsymmetric diphosphine $Ph_2PNC_6H_4PPh_2$-2,[87] showed that the phosphine could coordinate either in a bidentate or a monodenate fashion in which the ligand is coordinated via the N-PPh_2 moiety only (Figure 29).

Figure 29

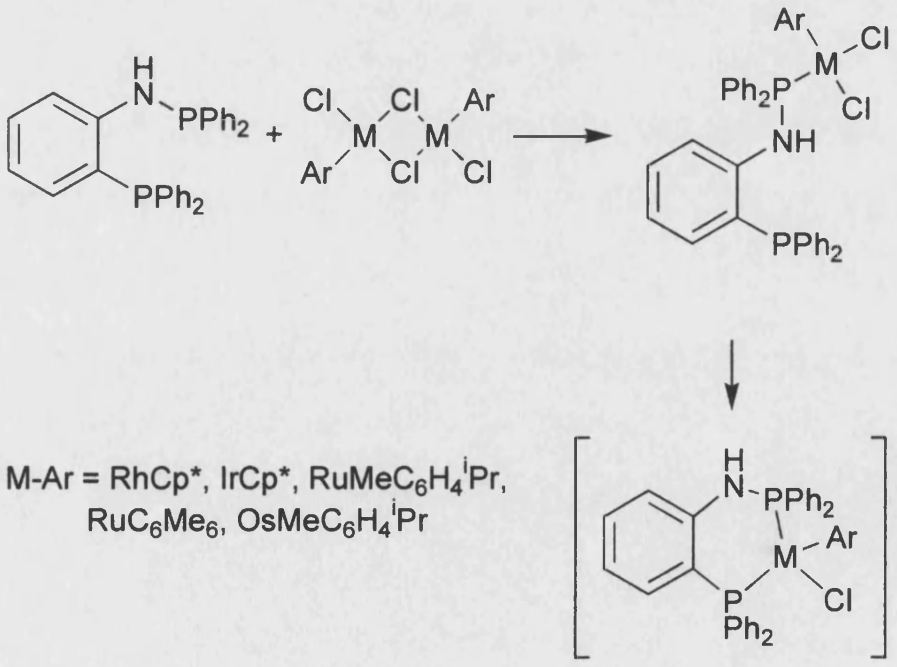

Chiral phosphinoamine-phosphinite ligands have been shown to be easily prepared via the reaction of the chiral amino-alcohol with chlorophosphine in the presence of tertiary amine (Figure 30).

Figure 30

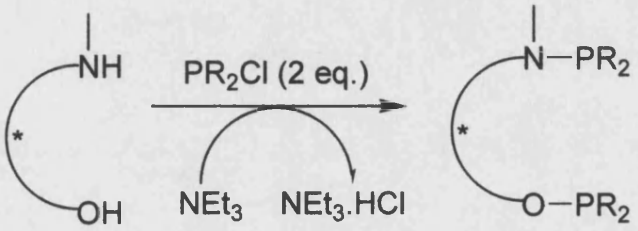

The catalytic properties of chiral phosphinoamine-phosphinite ligands have been extensively studied, in particular their application to enantioselective catalysis.[101] For example, rhodium complexes of chiral phosphinoamines-phosphinites have proved effective catalysts for asymmetric hydroformylation,[102] hydrosilylation[103,104] and hydrogenation,[105,106] and nickel complexes have been employed[107] in enantioselective C-C bond formation.

A number of functionalised phosphinoamine ligands have been prepared and studied, in which additional functional groups such as ketones[81] and pyridines[85] have been incorporated (Figure 31).

Figure 31

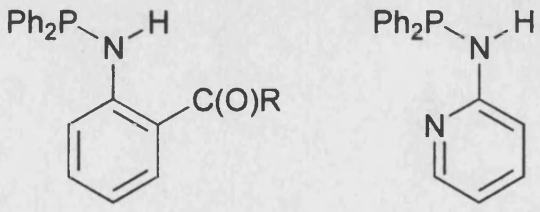

R = Me, Ph

The combination of both a hard (e.g. nitrogen, oxygen) and a soft (e.g. phosphorus) donor atoms within the phosphinoamine provides the donor combination in which coordination may occur through either or both of the donor atoms, resulting in a number of potential coordination modes (Figure 32).

Figure 32

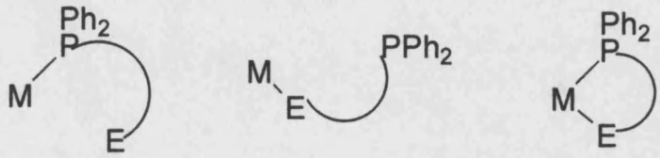

Examination of the coordination chemistry of pyridylphosphinoamine with a range of transition metals showed that it could coordinate in a monodentate fashion through the phosphorus or in a bidentate fashion through the phosphorus and nitrogen to give a 5-membered *P,N*-chelate ring (Figure 33). In contrast the ketone functionalised phosphinoamine undergoes C-H bond activation to give a 5-membered M-P-N-C-C metallacycle (Figure 33), as coordination of the ketone oxygen to give the *P,O*-chelate is unfavourable as it would require the formation of a 7-membered ring.

Figure 33

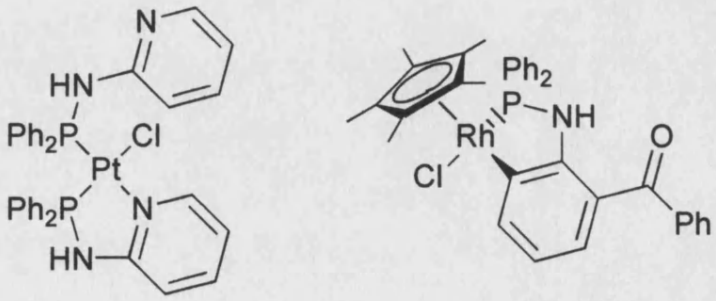

1.7 *N*-Pyrrolyl Phosphines

The chemistry of *N*-pyrrolyl substituted phosphines has currently received interest due to their exceptional π-acceptor properties, which can exceed those of phosphites such as $P(OPh)_3$.[108,109] Delocalization of the nitrogen lone pair into the 5-membered ring (Figure 34) contributes to the *N*-pyrrolyl groups strong electron withdrawing properties, which result in the phosphines acting as relatively poor σ donors and as good π acceptors.

Figure 34

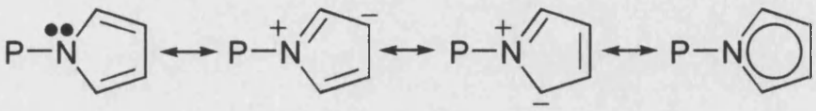

The synthesis of *N*-pyrrolyl phosphines is similar to that of phosphinoamines in which pyrrole is directly reacted with a chlorophosphine in the presence of triethylamine (Figure 35). These mild reaction conditions allow the incorporation of additional functional groups for example, the ester groups in 3,4-dicarboethoxy-*N*-pyrrolyl phosphine $[R_2P\text{-}NC_4H_2(CO_2Et)_2]$.[110]

Figure 35

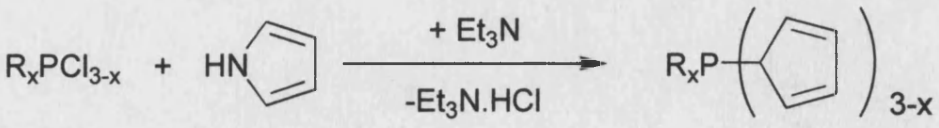

Complexes containing *N*-pyrrolyl substituted phosphines have been shown to be of catalytic relevance. For example, the rhodium(I) complexes of *N*-pyrrolyl

substituted phosphines have been used to catalyse the hydroformylation of hex-1-ene[111] and the hydrogenation of olefins and arenes.[112]

1.8 Phosphorus-31 NMR

^{31}P NMR spectroscopy has been shown to be of immense importance in the study of phosphorus containing compounds, allowing detailed analysis of the type of substituents at the phosphorus atom and its coordination modes.

1.8.1 Chemical Shifts

^{31}P chemical shifts normally fall within the range ± 250 ppm relative to 85% H_3PO_4, though a number of notable exceptions have been observed, for example chemical shifts as low as -460 and as high as +1362 ppm have been recorded for P_4 and [^{t}BuP{Cr(CO)$_5$}$_2$] respectively.

A number of empirical observations have been made in which the range of factors affecting the ^{31}P chemical shifts of the free phosphine (PX_3) have been reviewed.[113] These showed that the X-P-X bond angle, the nature of the substituent group X and the electronegativity of X were some of the major factors affecting the value of ^{31}P chemical shifts. Increasing the steric bulk of the substituents, such that the X-P-X (where X = C) bond angle increases, was observed to result in the chemical shift moving to lower field. For example, $P(CH_3)_3$ δ(P) -62 ppm and P^tBu_3 δ(P) +61.9 ppm. The effects of changing the substituent X [X= $C(CH_3)_3$, $Si(CH_3)_3$, $Ge(CH_3)_3$ and $Sn(CH_3)_3$] has also been shown to result in marked changes to the ^{31}P chemical shifts, with the chemical shift moving to higher field with increasing atomic number of X.

Other factors have also been shown to effect the value of the phosphorus chemical shift on coordination of the phosphine to a transition metal. The value of the

phosphorus chemical shift has been observed to be dependent on the oxidation state of the metal and on the *trans* influence of the remaining ligands in the complex. The formation of chelate rings has also been shown to have a significant effect on the value of the ^{31}P chemical shifts.[114] Formation of a 5-membered ring resulted in deshielding of the phosphorus resonance by 21 to 33 ppm, whereas on formation of a 4- or 6-membered chelate rings the phosphorus resonance was shifted to higher field by between 2 to 25 ppm. This effect has been suggested[115] to be due to changing hybridisation of the phosphorus, on changing the bond angles at the phosphorus in different ways depending on the size of the ring formed.

1.8.2 Metal-Phosphorus Coupling Constants $^{1}J(P,M)$

The coupling constant term is made up of three components that arise from nucleus-electron interactions.[116] These three terms are due to: (1) the interaction of the magnetic moment of one nucleus with the field produced by the orbital motion of the electrons, which in turn interacts with the second nuclear moment, (2) dipole interaction involving the electron spin magnetic moments and the final contribution (3) which is known as the Fermi contact term is due to the spins of the electrons in orbitals (derived from *s* atomic orbitals). In cases where the orbital and dipolar terms are of little importance, the one-bond coupling constant can be approximated such that it is dependent on the amount of *s* orbital character in the internuclear bond. This means that the hybridisation of the atoms involved plays a significant role in the actual value of the one-bond coupling constant.[113] This approximation is only useful as a rough guide, as the errors introduced by this simplification for metal-phosphorus coupling constants can be significant.

General trends in metal-phosphorus coupling constants have shown the presence of a relationship between the chemical environment of the metal and the value of $^{1}J(P,M)$. In particular $^{1}J(P,M)$ is dependent on the oxidation state of the metal, the *trans* influence of the remaining ligands in the complex, the size of the chelate ring formed and the type of phosphorus ligand.

Changes in the oxidation state of the metal have been observed to result in large differences in $^{1}J(P,M)$, for example the $^{1}J(P,Pt)$ values for Pt(IV) are smaller than for those of Pt(II) and Pt(0) complexes containing comparable ligands (Figure 36).

Figure 36

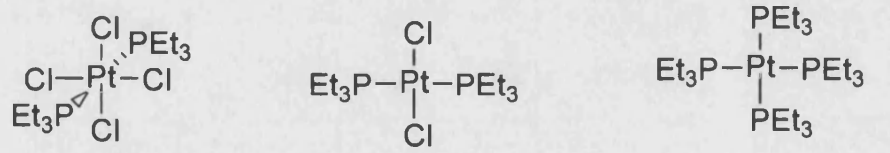

$^{1}J(P,Pt) = 1455$ Hz $^{1}J(P,Pt) = 2397$ Hz $^{1}J(P,Pt) = 3740$ Hz

The metal-phosphorus coupling constant *trans* to a ligand with a small *trans* influence such as a halogen or oxygen ligands, has been observed to be significantly larger than the equivalent phosphine *trans* to a ligand with a much larger *trans* influence, such as a phosphine or an alkyl group. For example, this trend is observed in the complex *cis*-$[PtClMe(PEt_3)_2]$[113] in which there are two different metal-phosphorus $^{1}J(P,Pt)$ coupling constants, 4179 Hz (phosphorus *trans* to chloride), and 1719 Hz (phosphorus *trans* to methyl).

The size of the chelate ring has been observed to have an effect on the metal-phosphorus coupling constant, though the size of these changes is often small.

The general trend appears to be that the value of $^1J(P,M)$ increases in the order 5-membered > 6-membered > 4-membered chelate rings. For example, the complexes *cis*-$[PtCl_2L]$ (L = dppm, dppe and dppp)[114] (Figure 37).

Figure 37

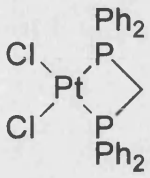

$^1J(P,Pt) = 3078$ Hz

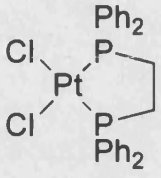

$^1J(P,Pt) = 3618$ Hz

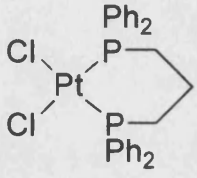

$^1J(P,Pt) = 3420$ Hz

The effect of substituting a more electronegative group for carbon on phosphorus has been observed to generally result in an increase in the metal-phosphorus coupling constant. Such a trend is observed for the complex $[W(CO)_5(PX_3)]$ (X = F, Cl, Br and Bu^n) for which increasing the electronegativity of the substituent X resulted in an increase in the value of $^1J(P,W)$ (Table 1).[113]

Table 1 Values of $^1J(P,W)$ for the complexes $[W(CO)_5PX_3]$

X =	F	Cl	Br	Bu^n
$^1J(P,W)$/Hz	485	426	398	227

1.9 References

1 J. Chatt, *'Homogeneous Catalysis with Metal Phosphine Complexes'*, ed. L. H. Pignolet, Plenum Press, New York and London, 1983, 1.

2 P. E. Thénard, *Jahresber.*, 1847-1848, 645; *C. R. Acad. Sci. Paris,* 1847, **25**, 892.

3 F. Bérle, *Jahresber.*, 1855, 590; *J. Prakt. Chem.,* 1855, **66**, 73; *Annalen,* 1856, **97**, 334.

4 A. Cahours and A. W. Hofmann, *Annalen,* 1857, **104**, 1; A. W. Hofmann and A. Cahours, *Quart. J. Chem. Soc.,* 1859, **11**, 56; A. W. Hofmann, *Phil. Trans.,* 1860, **150**, 409.

5 A. Michaelis, *Ber.,* 1873, **6**, 601; *Annalen,* 1876, **181**, 265; A. Michaelis and L. Gleichman, *Ber.,* 1882, **15**, 801.

6 A. W. Hofmann, *Annalen,* 1857, **103**, 357.

7 A. Cahours and H. Gal, *C. R. Acad. Sci. Paris,* 1870, **70**, 897; *Jahresber.,* 1870, 808.

8 J. Chatt and F. G. Mann, *J. Chem. Soc.,* 1938, 1949.

9 K. A. Jensen, *Z. Anorg. Allg. Chem.*, 1936, **229**, 225.

10 F. P. Dwyer and D. M. Stewart, *J. Proc. R. Soc. NSW*, 1949, **83**, 177.

11 D. P. Craig, 'Ronald Sydney Nyholm', *Biogr. Mem. R. Soc*, 1972, **18**, 445.

12 W. Reppe and W. J. Schweckendick, *Annalen.,* 1948, **560**, 104.

13 C. Masters, *'Homogeneous Transition Metal Catalsts'*, Chapman & Hall, London and New York, 1981.

14 J. F. Young, J. A. Osborn, F. H. Jardine and G. Wilkinson, *J. Chem. Commun.*, 1965, 131; R. S. Coffey and Imperial Chemical Industries, *Brit. Pat. 1*, 1965, **121**, 642.

15 D. Evans, J. A. Osborn and G. Wilkinson, *J. Chem. Soc. A*, 1968, 3133.

16 L. H. Slaugh and R. D. Mullineaux, *U.S. Patent 3*, 1966, **239**, 570.

17 L. Maier, '*Organic Phosphorus Compounds*', ed. G. M. Kosolapoff and L. Maier, Wiley-Interscience, 1972, **1**, 32.

18 D. G. Gilheany and C. M. Mitchell, '*The Chemistry of Organophosphorus Compounds*', ed. F. R. Hartley, Wiley, 1990, **1**, 151.

19 W. Voskuil and F. Arens, *Recl. Trav. Chim. Pays-Bas*, 1963, **82**, 302.

20 M. Karlsson, M. Johansson and C. Andersson, *J. Chem. Soc., Dalton Trans.*, 1999, 4187.

21 G. P. Schiemenz and E. Papageorgiou, *Phosphorus Sulfur*, 1982, **13**, 41.

22 S. B. Sembiring, S. B. Colbran and D. C. Craig, *J. Chem. Soc., Dalton Trans.*, 1999, 1543.

23 G. P. Schiemenz and H. Kaack, *Justus Liebigs Ann. Chem.*, 1973, 1480.

24 W. E. McEwen, K. F. Kumli, A. Bladé-Font, M. Zanger, and C. A. Vander der Werf, *J. Am. Chem. Soc.*, 1964, **86**, 2378.

25 A. Mingoia, *Gazz. Chim. Ital.*, 1930, **60**, 144.

26 C. Screttas and A. F. Isbell, *J. Org. Chem.*, 1962, **27**, 2573.

27 H. Hoffmann and P. Schellenbeck, *Chem. Ber.* 1967, **100**, 692.

28 A. Antiñolo, F. Carrillo-Hermosilla, E. Díez-Barra, J. Fernández-Baeza, M. Fernández-López, A. Lara-Sánchez, A. Moreno, A. Otero, A. M. Rodriguez and J. Tejeda, *J. Chem. Soc., Dalton Trans.*, 1998, 3737.

29 X. Bei, T. Uno, J. Norris, H. W. Turner, W. H. Weinberg and A. S. Guram, *Organometallics*, 1999, **18**, 1840.

30 J. Fawcett, S. Friedrichs, J. H. Holloway, E. G. Hope, V. McKee, M. Nieuwenhuyzen, D. R. Russell and G. C. Saunders, *J. Chem. Soc., Dalton Trans.*, 1998, 1477.

31 J. F. Nobis, L. F. Moormeier and R. E. Robinson, *Advan. Chem. Ser.*, 1959, **23**, 63.

32 M. A. Jalil, S. Fujinami, H. Senda and H. Nishikawa, *J. Chem. Soc., Dalton Trans.*, 1999, 1655.

33 P. Braunstein, M. D. Fryzuk, F. Naud and S. J. Rettig, *J. Chem. Soc., Dalton Trans.*, 1999, 589.

34 S. S. Moore and G. M. Whitesides, *J. Org. Chem.*, 1982, **47**, 1489.

35 F. Langer and P. Knochel, *Tetrahedron Lett.*, 1995, **36**, 4591.

36 K. Weyer, *Doctoral Thesis*, Technische Hochschule Aachen, 1956.

37 H. Hartmann and H. Fratzscher, *Naturwissenschaften*, 1964, **51**, 213.

38 W. Siebert, W. E. Davidsohn and M. C. Henry, *J. Organomet. Chem.*, 1969, **17**, 65.

39 M. Zablocka, Y. Miquel, A. Igau, J.-P. Majoral and A. Skowronska, *J. Chem. Soc., Chem. Commun.*, 1998, 1177.

40 C. Hay, D. Le Vilain, V. Deborde, L. Toupet and R. Réau, *J. Chem. Soc., Chem. Commun.*, 1999, 345.

41 P. Rosa, L. Ricard, F. Mathey and P. Le Floch, *J. Chem. Soc., Chem. Commun.*, 1999, 537.

42 S. R. Gilbertson and G. W. Starkey, *J. Org. Chem.*, 1996, **61**, 2922.

43 E. Costa, P. G. Pringle and K. Worboys, *J. Chem. Soc., Chem. Commun.*, 1998, 49.

44 B.-L. Chen, K.-F. Mok and S.-C. Ng, *J. Chem. Soc., Dalton Trans.*, 1998, 2861.

45 E. Lindner, H. Rauleder, C. Scheytt, H. A. Mayer, W. Hiller, R. Fawzi and P. Wegner, *Z. Naturforsch. Teil B*, 1984, **39**, 632.

46 T. Kauffmann, J. Ennen, H. Lhotak, A. Rensing, F. Steinseifer and A. Woltermann, *Angew. Chem., Int. Ed. Engl.*, 1980, **19**, 328; K. Berghus, A. Hamsen, A. Rensing, A. Woltermann and T. Kauffmann, *Angew. Chem., Int. Ed. Engl.*, 1981, **20**, 117.

47 R. Fields, R. N. Hazseldine and J. Kirman, *J. Chem. Soc., C*, 1970, 197.

48 A. A. Oswald, L. L. Murrel and L. J. Boucher, *Am. Chem. Soc., Div Pet. Chem. Prepr.*, 1974, **19**, 155, 162; *Chem. Abstr.*, 1975, **83**, 198225; *Chem Abstr.*, 1976, **84**, 105685.

49 G. P. Schiemenz and H.-U. Siebeneick, *Chem. Ber.*, 1969, **102**, 1883.

50 I. G. M. Campbell and J. K. Way, *J. Chem. Soc.*, 1961, 2133.

51 T. B. Rauchfuss, J. L. Clements, S. F. Agnew and D. M. Roundhill, *Inorg. Chem.*, 1977, **16**, 775.

52 E. Lindner, S. Meyer, P. Wegner, B. Karle, A. Sickinger and B. Steger, *J. Organomet. Chem.*, 1987, **335**, 59.

53 J. I. Dulebohn, S. C. Haefner, K. A. Berglund and K. R. Dunbar, *Chem. Mater.*, 1992, **4**, 506.

54 A. Benefiel, D. M. Roundhill, W. C. Fultz and A. L. Rheingold, *Inorg. Chem.*, 1984, **23**, 3316.

55 A. Bader and E. Lindner, *Coord. Chem. Rev.*, 1991, **108**, 27.

56 C. S. Slone, D. A. Weinberger and C. A. Mirkin, *Prog. Inorg. Chem.*, 1999, **48**, 233.

57 P. Braunstein, Y. Chauvin, J. Nähring, A. DeCian and J. Fischer, *J. Chem. Soc., Dalton Trans.*, 1995, 863.

58 P. Braunstein, D. Matt, F. Mathey and D. Thavard, *J. Chem. Res. (S)*, 1978, 232.

59 B. Demerseman, C. Renouard, R. Le Lagadec, M. Gonzalez, P. Crochet and P. H. Dixneuf, *J. Organomet. Chem.*, 1994, **471**, 229.

60 N. W. Alcock, A. W. G. Platt and P. G. Pringle, *J. Chem. Soc., Dalton Trans.*, 1987, 2273.

61 N. W. Alcock, A. W. G. Platt and P. G. Pringle, *J. Chem. Soc., Dalton Trans.*, 1989, 139.

62 J. Andrieu, P. Braunstein, A. Tiripicchio and F. Ugozzoli, *Inorg. Chem.*, 1996, **35**, 5975.

63 S. J. Higgins, R. Taylor and B. L. Shaw, *J. Organomet. Chem.*, 1987, **325**, 285.

64 S. Mecking and W. Keim, *Organometallics*, 1996, **15**, 2650.

65 E. Lindner, Q. Wang, H. A. Mayer, A. Bader, H. Kühbauch and P. Weger, *Organometallics*, 1993, **12**, 3291.

66 L. Horner and G. Simons, *Z. Naturforsch. Teil B*, 1984, **39**, 497.

67 E. Lindner, R. Speidel, R. Fawzi and W. Hiller, *Chem. Ber.*, 1990, **123**, 2255.

68 E. Lindner, A. Sickinger and P. Wegner, *J. Organomet. Chem.*, 1988, **349**, 75.

69 E. Lindner and B. Andres, *Chem. Ber.*, 1988, **121**, 829.

70 E. Lindner, M. Kemmler, T. Schneller and H. A. Mayer, *Inorg. Chem.*, 1995, **34**, 5489.

71 E. Lindner, R. Schreiber, T. Schneller, P. Weger, H. Mayer, W. Göpel and C. Ziegler, *Inorg. Chem.*, 1996, **35**, 514.

72 E. Valls, J. Suades, B. Donadieu and R. Mathieu, *J. Chem. Soc., Chem. Commun.*, 1996, 771.

73 S. Sabata, J. Vcelák and J. Hetflejs, *Collect. Czech. Chem. Commun.*, 1995, **60**, 127.

74 P. Braunstein, T. M. G. Carneiro, D. Matt, F. Balegroune and D. Grandjean, *J. Organomet. Chem.*, 1989, **367**, 117.

75 J. E. Hoots, T. B. Rauchfuss and D. A. Wrobleski, *Inorg. Synth.*, 1982, **21**, 175.

76 P. Braunstein, Y. Chauvin, J. Nähring, A. DeCian, J. Fischer, A. Tiripicchio and F. Ugozzoli, *Organometallics*, 1996, **15**, 5551.

77 E. Lindner, K. Gierling, B. Keppeler and H. A. Mayer, *Organometallics*, 1997, **16**, 3531.

78 S. J. Chadwell, S. J. Coles, P. G. Edwards and M. B. Hursthouse, *J. Chem. Soc., Dalton Trans.*, 1996, 1105.

79 L. A. Hamilton and P. S. Landis, in *'Organic Phosphorus Compounds'*, ed. G. M. Kosolapoff and L. Maier, Wiley-Interscience, 1972, **4**, 504.

80 T. Hosokawa, Y. Wakabayashi, K. Hosokawa, T. Tsuji and S.-I. Murahashi, *Chem. Commun.*, 1996, 859.

81 K. G. Gaw, A. M. Z. Slawin and M. B. Smith, *Organometallics*, 1999, **18**, 3255.

82 D. J. Birdsall, J. Green, T. Q. Ly, J. Novosad, M. Necas, A. M. Z. Slawin, J. D. Woollins and Z. Zak, *Eur. J. Inorg. Chem.*, 1999, 1445.

83 S. Naïli, J.-F. Carpentier, F. Agbossou, A. Mortreux, G. Nowogrocki and J.-P. Wignacourt, *Organometallics*, 1995, **14**, 401.

84 I. Suisse, H. Bricout and A. Mortreux, *Tetrahedron Lett.*, 1994, **35**, 413.

85 S. M. Aucott, A. M. Z. Slawin and J. D. Woollins, *Phosphorus, Sulfur,* 1997, **124-5**, 473.

86 W. Schirmer, U. Flörke and H.-J. Haupt, *Z. Anorg. Allg. Chem.*, 1987, **545**, 83.

87 S. M. Aucott, A. M. Z. Slawin and J. D. Woollins, *J.Organomet. Chem.,* 1999, **582**, 83.

88 J.-M. Brunel and G. Buono, *Tetrahedron Lett.*, 1999, **40**, 3561.

89 P. A. Bella, O. Crespo, E. J. Fernández, A. K. Fischer, P. G. Jones, A. Laguna, J. M. López-de-Luzuriaga and M. Monge, *J. Chem. Soc., Dalton Trans.*, 1999, 4009.

90 M. S. Balakrishna, R. M. Abhyankar and J. T. Mague, *J. Chem. Soc., Dalton Trans.*, 1999, 1407.

91 F.-Y. Zhang, C.-C. Pai and A. S. C. Chan, *J. Am. Chem. Soc.*, 1998, **120**, 5808.

92 T. Q. Ly, A. M. Z. Slawin and J. D. Woollins, *J. Chem. Soc., Dalton Trans.*, 1997, 1611.

93 K. Osakada, T. Ikariya, M. Saburi and S. Yoshikawa, *Chem. Lett.*, 1981, 1691.

94 T. Q. Ly and J. D. Woollins, *Coord. Chem. Rev.*, 1998, 451.

95 P. Bhattacharyya and J. D. Woollins, *Polyhedron*, 1995, 3367.

96 N. C. Payne and D. W. Stephan, *J. Organomet. Chem.*, 1981, **221**, 203.

97 P. Bhattacharyya, A. M. Z. Slawin, M. B. Smith and J. D. Woollins, *Inorg. Chem.*, 1996, **35**, 3675.

98 A. M. Z. Slawin, M. B. Smith and J. D. Woollins, *J. Chem. Soc., Dalton Trans.*, 1996, 1283.

99 A. M. Z. Slawin, M. B. Smith and J. D. Woollins, *J. Chem. Soc., Dalton Trans.*, 1996, 4575.

100 T. Q. Ly, A. M. Z. Slawin and J. D. Woollins, *J. Chem. Soc., Dalton Trans.*, 1997, 1611.

101 F. Agbossou, J.-F. Carpentier, F. Hapiot, I. Suisse and A. Mortreux, *Coord. Chem. Rev.*, 1998, 1615.

102 Y. Pottier, A. Mortreux and F. Petit, *J. Organomet. Chem.*, 1989, **370**, 333.

103 A. Karim, A. Montreux and F. Petit, *Tetrahedron Lett.*, 1986, **27**, 345.

104 N. Kokel, A. Mortreux and F. Petit, *J. Mol. Catal.*, 1989, **57**, L5.

105 C. Hatat, A. Karim, N. Kokel, A. Mortreux and F. Petit, *Tetrahedron Lett.*, 1988, **29**, 3675.

106 C. Hatat, A. Karim, N. Kokel, A. Mortreux and F. Petit, *New J. Chem.*, 1990, **14**, 141.

107 P. Cros, G. Buono, G. Peiffer, P. Denis, A. Mortreux and F. Petit, *New J. Chem.*, 1987, **11**, 573.

108 K. G. Moloy and J. L. Petersen, *J. Am. Chem. Soc.*, 1995, **117**, 7696.

109 S. Serron, S. P. Nolan, K. G. Moloy, *Organometallics*, 1996, **15**, 4301.

110 A. Huang, J. E. Marcone, K. L. Mason, W. J. Marshall and K. G. Moloy, *Organometallics*, 1997, **16**, 3377.

111 A. M. Trzeciak, T. Glowiak, R. Grzybek and J. J. Ziolkowski, *J. Chem. Soc. Dalton Trans.*, 1997, 1831.

112 A. M. Trzeciak, T. Glowiak and J. J. Ziolkowski, *J. Organomet. Chem.*, 1998, **552**, 159.

113 P.S. Pregosin and R. W. Kunz, '*^{31}P and ^{13}C NMR of Transition Metal Phosphine Complexes*', Springer-Verlag, Berlin Heidelberg, 1979.

114 P. E. Garrou, *Chem. Rev.*, 1981, 229.

115 R. H. Crabtree, '*The Organometallic Chemistry of the Transition Metals*', Wiley-Interscience, Singapore, 1988, 219.

116 E. A. V. Ebsworth, D. W. H. Rankin and S. Cradock, '*Structural Methods in Inorganic Chemistry*', Blackwell, Oxford, 1991.

Chapter 2

Ether-Functionalised Phosphinoamines

2.0 Introduction

Phosphines are one of the most important groups of ligands in coordination and organometallic chemistry, in part due to the ready customisation of their electronic and steric properties. The ability to easily modify the properties of phosphine ligands has been crucial in the development of their transition metal complexes as homogeneous catalysts for a vast range of processes.

In contrast to the considerable chemistry of phosphines and phosphites, the use of phosphinoamines (also called aminophosphines) containing P-N bonds remains relatively undeveloped. One potential reason for the lack of interest in the chemistry of phosphinoamines is the assumed ease of P-N bond cleavage.[1] However, the mild reaction conditions required for the synthesis of phosphinoamines means that they may be a convenient source of bifunctional phosphines, containing an additional functionality. Phosphinoamines that contain P-N bonds have been know for many years,[2,3] but incorporation of additional functionalities within these ligands has been given little attention.[4,5,6]

The incorporation into phosphines of functional groups that contain additional donor atoms such as an ether oxygen is of potential interest in the synthesis of complexes suitable for catalysis. The combination of a phosphorus atom, which forms strong bonds to a late transition metal, and a more labile ether oxygen atom, provides the donor combination required for reversible monodentate-bidentate coordination.[7] The weakly coordinated end of the ligand may undergo facile dissociation generating a vacant coordination site, a property known as hemilability (Figure 1).

Figure 1.

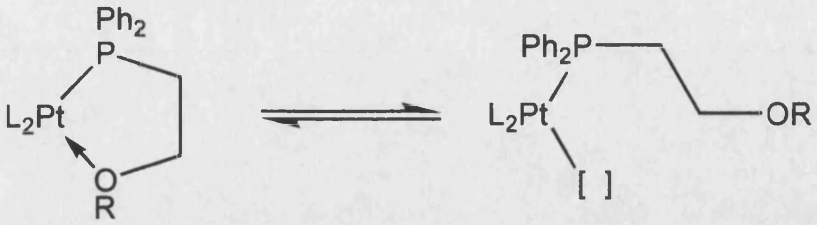

2.1 Results and Discussion

2.1.1 Synthesis of Ether-Functionalised Phosphinoamines

It is possible to synthesise phosphinoamines of the general formula Ph_2PNHR using mild reaction conditions[5,6,8] thus allowing incorporation of additional functionalities into the R group. The synthetic route is based on the deprotonation of the functionalised amine using NEt_3 followed by the reaction with Ph_2PCl. The solvent used is THF due to the insolubility of $NEt_3H^+Cl^-$, which precipitates on formation, thus driving the equilibrium over to the formation of the phosphinoamine. This route was used in the synthesis of a range of phosphinoamine ligands containing ether functionalities (Scheme 1).

Scheme 1

$$H_2NR + Et_3N \rightleftharpoons Et_3NH^+RHN^- \xrightarrow[THF]{Ph_2PCl} Ph_2PNHR + Et_3NH^+Cl^-$$

R = $CH_2CH_2OCH_3$ (L^1),
$CH_2CH_2CH_2OCH_3$ (L^2),
$CH_2CH(OCH_3)_2$ (L^3),
$C_6H_4OCH_3$-2 (L^4).

The ligands L^1-L^4 were synthesised in high yield as colourless or pale yellow oils, and characterised using multinuclear NMR and infrared spectroscopy and microanalysis. The $^{31}P\{^1H\}$ NMR spectra for L^1-L^4 showed single phosphorus resonances in the range δ(P) 41-43 ppm for L^1-L^3 and δ(P) 27.2 ppm for L^4 (Table 1). The $^{31}P\{^1H\}$ NMR chemical shift for L^4 is similar to other Ph_2PNHAr ligands such as the recently reported $Ph_2PNH(C_6H_4)C(O)Me$-2 [δ(P) 25.6ppm][5] and $C_6H_4(NHPPh_2)_2$-1,2 [δ(P) 32.5 ppm].[6] The difference between δ(P) for L^1-L^3 and δ(P) for L^4 can be attributed to the different electronic and steric properties of the alkyl and aryl substituents on the nitrogen atom.[9]

Table 1 Selected $^{31}P\{^1H\}$, ^1H NMR and infrared data for compounds L^1-L^6.

	Compound	δ(P)/ppm	δ(NH)/ppm	ν(NH)/cm^{-1}
L^1	$Ph_2PNHCH_2CH_2OCH_3$	42.0	2.46m	3370m
L^2	$Ph_2PNHCH_2CH_2CH_2OCH_3$	41.9	2.20m	3370m
L^3	$Ph_2PNHCH_2CH(OCH_3)_2$	42.9	2.23m	3368m
L^4	$Ph_2PNH(C_6H_4)OCH_3$-2	27.2	5.32d	3381m
L^5	$(Ph_2P)_2NCH_2CH_2OCH_3$	65.1	-	-
L^6	$Ph_2P(S)NH(C_6H_4)OCH_3$-2	52.7	5.66d	3366m

The ^1H NMR spectra for L^1-L^4 were as expected: L^1 and L^2 gave signals for the methylene, methyl and NH groups, L^3 showed signals for the methylene, methine, methyl and NH groups and L^4 showed distinctive signals for the methyl and NH groups (Table 1 & Experimental Section). The $^{13}C\{^1H\}$ NMR spectra for L^1-L^3 showed the expected signals due to the diphenylphosphino unit, and well-defined signals for the alkyl chain carbon atoms and the terminal methyl group. The

methylene carbons showed coupling [$^2J(C,P) \approx 10$ Hz and $^3J(C,P) \approx 6$ Hz] to the phosphorus nuclei.

The bis(diphenylphosphino)amine $(Ph_2P)_2NCH_2CH_2OMe$ ($\mathbf{L^5}$) was synthesised by both a one step and a two step process (Scheme 2).

Scheme 2

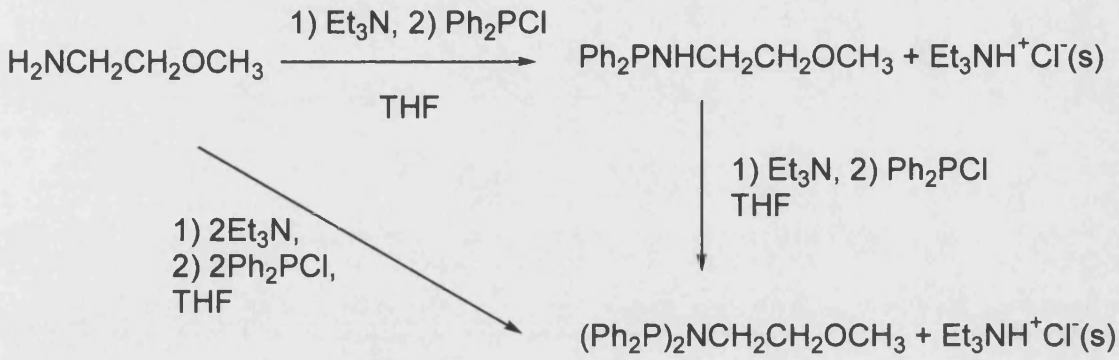

The $^{31}P\{^1H\}$ NMR spectra confirmed that the products of both these synthetic routes were identical, showing a singlet at $\delta(P)$ 65.1 ppm. Both the ^1H NMR and IR spectra confirmed the absence of the NH group.

During the syntheses of $\mathbf{L^1}$-$\mathbf{L^5}$ the $^{31}P\{^1H\}$ NMR spectra sometimes showed the presence of a by-product observed as a pair of doublets [$\delta(P_A)$ 36.8 ppm, $\delta(P_B)$ -22.1 ppm, $^1J(P,P)$ 228 Hz]. This was identified as tetraphenyldiphosphine monoxide, $Ph_2PP(O)Ph_2$, formed from the reaction between trace amounts of water and Ph_2PCl in the presence of NEt_3.[2] Consequently care has to be taken to exclude water from the reaction mixture during synthesis.

The ligands $\mathbf{L^1}$-$\mathbf{L^5}$ are moisture sensitive, decomposing in wet solvents or on exposure to air to give a number of phosphorus containing products including $Ph_2PP(O)PPh_2$ and $Ph_2P(O)OH$ [$\delta(P) \approx 25$ ppm].[10] The P-N bond can also be cleaved

by reaction with an alcohol ROH to give the diphenylphosphinite Ph_2POR.[11,12] To compare the sensitivity of the P-N(aryl) and P-N(alkyl) bonds to alcoholysis, the phosphines $\mathbf{L^1}$ and $\mathbf{L^4}$ were reacted with excess methanol in dichloromethane solution. $^{31}P\{^1H\}$ NMR studies showed that complete conversion of $\mathbf{L^4}$ to Ph_2POMe occurred within 30 minutes, whereas the analogous reaction with $\mathbf{L^1}$ took over 24 hours to reach completion. The ease in which the P-N bond in $\mathbf{L^4}$ is cleaved by methanol is in marked contrast to the stability of the P-N bond in the previously reported phosphinoamine $C_6H_4(NHPPh_2)_2$-1,2, which is air stable indefinitely.[6]

Oxidation of the phosphorus atoms by oxygen, sulfur or selenium (E), has been shown in the related systems to yield products such as $Ph_2P(E)NHPPh_2$, $Ph_2P(E)NHP(E)PPh_2$ and $C_6H_4\{NHP(E)Ph_2\}_2$, which are able to coordinate to metal centres through the lone pairs of E.[13] Oxidation of the ether-functionalised phosphinoamine $\mathbf{L^4}$ was achieved by reaction with sulfur in a THF solution at room temperature to give the phosphorus(V) compound $Ph_2P(S)NH(C_6H_4)OMe$-2 ($\mathbf{L^6}$) (Scheme 3), with no cleavage of the P-N bond. This compound was characterised on the basis of multinuclear NMR and infrared spectroscopy. In the $^{31}P\{^1H\}$ NMR spectrum a singlet was observed at δ(P) 52.7 ppm, and in the ^1H NMR spectrum δ(NH) was observed as a doublet at δ(H) 5.66 ppm, [$^2J(H,P)$ = 8 Hz]. The $^{31}P\{^1H\}$ NMR spectrum shows a downfield shift compared to $\mathbf{L^4}$ as expected on oxidising P^{III} to P^V.

Scheme 3

$$Ph_2NH(C_6H_4)OCH_3\text{-}2 \xrightarrow[THF]{S_8} Ph_2P(S)NH(C_6H_4)OCH_3\text{-}2$$

2.1.2 Complexes of the Ether-Functionalised Phosphinoamines

2.1.2.1 Synthesis of $[MCl_2L_2]$ (M = Pd and Pt)

The reaction of two equivalents of phosphinoamines $\mathbf{L^1}$-$\mathbf{L^4}$ with $[MCl_2(cod)]$ (M = Pd or Pt) in dichloromethane gave virtually quantitative yields of the complexes $[MCl_2L_2]$ (L = $\mathbf{L^1}$-$\mathbf{L^4}$). These compounds were characterised on the basis of microanalysis, infrared and multinuclear NMR spectroscopy (see Experimental Section).

2.1.2.1.1 Characterisation of $[PdCl_2L_2]$ (L = L^1-L^4)

The $^{31}P\{^1H\}$ NMR spectra of the complexes $[PdCl_2L_2]$ for $\mathbf{L^1}$, $\mathbf{L^2}$ and $\mathbf{L^3}$ showed two phosphorus resonances, which were assigned to the *cis* and *trans* isomers. The formation of an equilibrium mixture of these isomers was observed by following

Table 2 Selected $^{31}P\{^1H\}$, ^1H NMR and infrared data for complexes **1-4**.

	Complex	δ(P)/ppm	δ(NH)/ppm	δ(OCH_3)/ppm	ν(NH)/cm^{-1}
1	*trans*-$[PdCl_2(\mathbf{L^1})_2]$	46.4s	4.28m	3.22s	3351w
	cis-$[PdCl_2(\mathbf{L^1})_2]$	59.0s	4.40m	3.28s	-
2	*trans*-$[PdCl_2(\mathbf{L^2})_2]$	46.4s	4.11m	3.19s	3332w
	cis-$[PdCl_2(\mathbf{L^2})_2]$	58.8s	4.47m	3.23s	-
3	*trans*-$[PdCl_2(\mathbf{L^3})_2]$	46.9s	4.29m	3.25s	3331w
	cis-$[PdCl_2(\mathbf{L^3})_2]$	59.2s	4.42m	3.23s	-
4	*trans*-$[PdCl_2(\mathbf{L^4})_2]$	-	-	-	3300w

the slow isomerisation of the crystallographically characterised isomers *trans*-[$PdCl_2(\mathbf{L^1})_2$] (**1**) and *trans*-[$PdCl_2(\mathbf{L^3})_2$] (**3**) (see below) over a period of 24 hours. The $^{31}P\{^1H\}$ NMR spectra in both cases showed a 1:1 mixture of the *cis* and *trans* isomers at equilibrium in $CDCl_3$. The chemical shifts for the *trans* isomers are in the range δ(P) 46-47 ppm, while the chemical shifts of the *cis* isomers are in the range δ(P) 58-59 ppm (Table 2).[14] The difference in the chemical shifts (Δδ) between the *cis* and *trans* isomers are similar to other [$PdCl_2(PPh_2NHR)_2$] complexes, such as the recently reported [$PdCl_2(PPh_2NHP(O)Ph_2)_2$] [$\delta(P)_{trans}$ 46.7 ppm, $\delta(P)_{cis}$ 58.3 ppm],[15] which like **1** and **3** exists in the *trans* form in the solid state and as a *cis-trans* mixture in solution, though in this case with a ratio of 1:3.7 of the *cis* and *trans* isomers at equilibrium in $CDCl_3$.

The ^1H NMR spectra were as expected, with distinctive signals for the methylene, methine (where relevant), methyl and NH protons for the two isomers. Signals for the *cis* and *trans* isomers can be readily assigned, as spectra recorded after several minutes show only the *trans* isomer. [$PdCl_2L_2$] crystallises exclusively as the *trans* isomer (Section 2.1.2.1.3) and in all cases one ν(NH) vibration was observed in the solid state infrared spectrum. The complex [$PdCl_2(\mathbf{L^4})_2$] (**4**) was insoluble in common solvents so only characterised on the basis of microanalysis and infrared spectroscopy (see Experimental Section). The infrared spectrum of complex **4** showed a similar pattern to those observed for **1**, **2** and **3** with the presence of only one band for ν(NH) suggesting that **4** also exists as the *trans* isomer in the solid state. The FAB mass spectrum of complex **1** showed the presence of a very weak peak at *m/z* 697 for $[M]^+$, with the next highest observed peak at *m/z* 661 for $[M - Cl]^+$. The spectrum of complex **3** showed a peak at *m/z* 756 corresponding to $[M + H]^+$.

2.1.2.1.2 Characterisation of *cis*-$[PtCl_2L_2]$ (L = L^1, L^3 and L^4) and *cis*-$[PtBr_2(L^1)_2]$

The $^{31}P\{^1H\}$ NMR spectra for *cis*-$[PtCl_2L_2]$ [L = L^1 (**5**) L^3 (**6**) and L^4 (**7**)] and *cis*-$[PtBr_2(L^1)_2]$ (**8**) show a single phosphorus resonance with platinum satellites (Table 3 and Figure 2). The chemical shifts of these complexes are similar to other $[PtCl_2(PPh_2NHR)_2]$ complexes, such as *cis*-$[PtCl_2(PPh_2NHP(O)Ph_2\text{-}P)_2]$ δ(P) 35.7 ppm, [^{1}J(P,Pt) 3955 Hz].[15] The ^{1}J(P,Pt) values for complexes **5-7** (Table 3), are typical of phosphines *trans* to a ligand with a relatively weak *trans* influence such as a chloride,[14] indicating the phosphines are mutually *cis*. This is typical of reactions of $[PtCl_2(cod)]$.[15,16] The $^{31}P\{^1H\}$ NMR spectra for complexes **5**, **6** and **7** did not show

Table 3. Selected $^{31}P\{^1H\}$, ^1H NMR and infrared data for complexes **5-8**.

	Complex	δ(P) /ppm	^{1}J(P,Pt) /Hz	δ(NH) /ppm	δ(CH_3) /ppm	ν(NH) /cm^{-1}
5	*cis*-$[PtCl_2(L^1)_2]$	35.5	3940	4.08m	3.14s	3380, 3293w
6	*cis*-$[PtCl_2(L^3)_2]$	35.8	3940	4.09m	3.14s	3350, 3247m
7	*cis*-$[PtCl_2(L^4)_2]$	30.1	3934	6.82m	3.65s	3371, 3199m
8	*cis*-$[PtBr_2(L^1)_2]$	36.7	3904	3.97m	3.16s	3399, 3293m

the presence of any *cis-trans* isomerisation occurring within solution. The ^1H NMR spectra of **5**, **6** and **7** were as expected. The infrared spectra of all three complexes showed two weak bands for ν(NH), which is in contrast to complexes **1-4**, which show only one band. The complexes **5** and **7** showed the expected parent ion peaks at *m/z* 785 and 880 respectively in the positive-ion FAB mass spectra.

The reaction of two equivalents of the phosphine L^1 with $[PtBr_2(cod)]$ in dichloromethane gave the complex *cis*-$[PtBr_2(L^1)_2]$ (**8**). The ^{1}J(P,Pt) of 3904 Hz is

typical for a phosphine *trans* to a bromide, again indicating the phosphines are mutually *cis*. The ^{1}H NMR was virtually identical to that for **5**, with a small shift to high field for the amine hydrogen [$\Delta\delta$(NH) = 0.08 ppm].

Figure 2

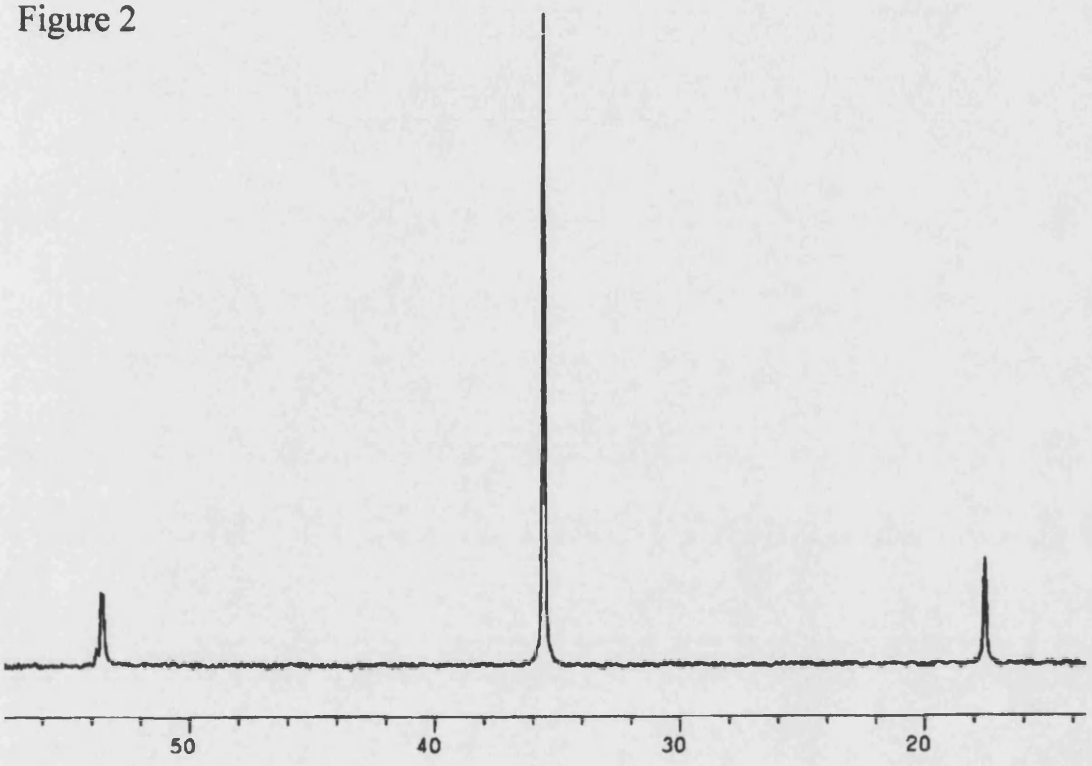

2.1.2.1.3 X-ray Crystal Structures of *trans*-[$PdCl_2(L^1)_2$] (1) and *trans*-[$PdCl_2(L^3)_2$] (3)

Compounds **1** and **3** were recrystallised from dichloromethane-diethyl ether as yellow needle shaped single crystals suitable for X-ray crystallographic studies. The crystal structures confirmed the proposed formulations; selected bond lengths and angles are given in Table 4 and 5.

Table 4. Selected bond lengths [Å] and angles [°] for complex **1**.

Pd(1)-Cl(1)	2.2963(10)	O(1)-C(15)	1.420(5)
Pd(1)-P(1)	2.3158(10)	O(1)-C(14)	1.410(5)
P(1)-N(1)	1.643(3)	C(13)-C(14)	1.513(6)
N(1)-C(13)	1.464(5)		
Cl(1)-Pd(1)-P(1)'	88.49(4)	C(15)-O(1)-C(14)	112.5(3)
Cl(1)-Pd(1)-P(1)	91.51(4)	N(1)-C(13)-C(14)	109.6(3)
N(1)-P(1)-Pd(1)	111.59(13)	O(1)-C(14)-C(13)	107.5(3)
C(13)-N(1)-P(1)	127.6(3)		

Primed atoms generated by the symmetry transformation *-x*, *-y*, *-z*+1.

Table 5. Selected bond lengths [Å] and angles [°] for complex **3**.

Pd(1)-Cl(1)	2.2957(12)	O(1)-C(14)	1.419(6)
Pd(1)-P(1)	2.3304(12)	O(2)-C(14)	1.398(5)
P(1)-N(1)	1.644(4)	O(2)-C(15)	1.445(6)
N(1)-C(13)	1.456(5)	C(13)-C(14)	1.499(6)
O(1)-C(16)	1.405(7)		
Cl(1)-Pd(1)-P(1)	88.23(4)	C(14)-O(2)-C(15)	113.2(4)
Cl(1)-Pd(1)-P(1)'	91.77(4)	N(1)-C(13)-C(14)	110.7(4)
N(1)-P(1)-Pd(1)	111.31(14)	O(2)-C(14)-O(1)	111.9(4)
C(13)-N(1)-P(1)	127.9(3)	O(2)-C(14)-C(13)	107.2(4)
C(16)-O(1)-C(14)	114.8(4)	O(1)-C(14)-C(13)	112.5(4)

Primed atoms generated by the symmetry transformation *-x*, *-y*, *-z*.

The asymmetric units of complexes **1** and **3** contain only half of the molecule, with the remaining portion in both cases being generated by inversion through a centre of symmetry on which the palladium atom sits with half-site occupancy.

The palladium(II) centres in complexes **1** and **3** are approximately square planar with *cis* angles of 88.49(4) and 91.51(4)° for **1**, and 88.23(4) and 91.77(4)° for **3**, with the two monodentate phosphine ligands arranged mutually *trans* to each other.

The sum of the angles around the nitrogen atom in complexes **1** and **3** are 354° and 360° respectively, indicating the nitrogen atoms have significant sp^2 character.

The Pd-P and Pd-Cl bond lengths in **1** and **3** are unremarkable.[17] The P-N bond distance in complexes **1** [1.643(3) Å] and **3** [1.644(4) Å] are shorter than the generally accepted range for P-N single bonds (*e.g.* 1.689-1.727 Å in *N*-piperidinophosphines[18]). This shortening of the P-N bond length has been previously ascribed to the overlap of the nitrogen lone pair with the P-C σ* orbitals.[12,19]

The structure of **1** (Figure 3) shows the presence of an intramolecular hydrogen bond between the NH proton of N(1) and the chloride ligand Cl(1) [N(1)···Cl(1)' 3.170(3), H(1)···Cl(1)' 2.54(4) Å; N(1)-H(1)···Cl(1)'126(3)°]. N-H···Cl hydrogen bonds have been observed in a number of other complexes containing both phosphinoamines and chloride ligands *cis* to each other.[15,20,21] In these previous examples, N···Cl distances range from 3.00 to 3.12 Å, and H···Cl distances from 2.1 to 2.5 Å. The presence of a much weaker interaction between the NH proton of N(1) and the ether oxygen O(1) [N(1)···O(1) 2.777(4), H(1)···O(1) 2.42(3) Å; N(1)-H(1)···O(1) 104(2)°], is suggested by the orientation of the ether group (see Figure 3). Similar weak components of bifurcated hydrogen bonds have been observed in the crystal structures of nucleosides and nucleotides.[22] The hydrogen bonding can therefore be

more accurately described as an unsymmetrical bifurcated hydrogen bond. The interaction with the ether oxygen atom is weak as a result of the unfavourable angular geometry of the strained 5-membered hydrogen-bond ring.

Figure 3

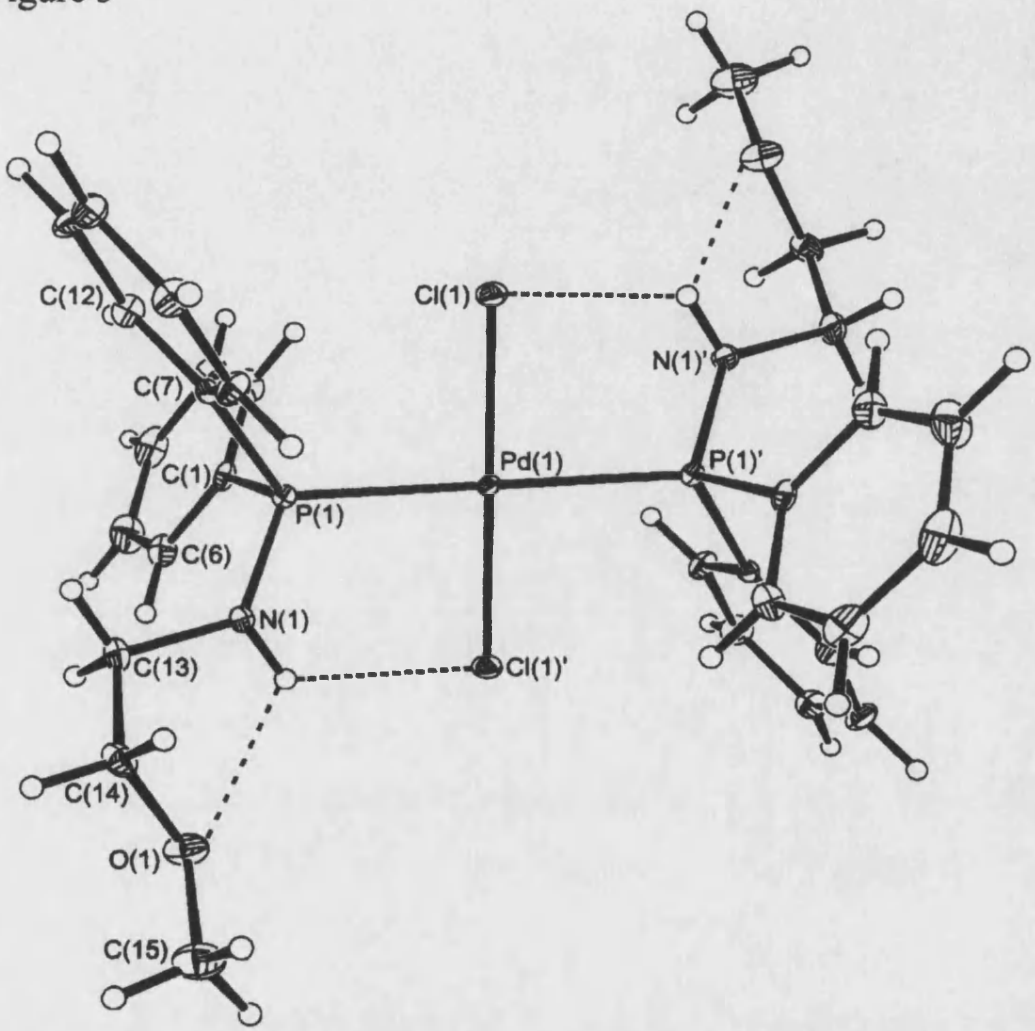

The structure of **3** (Figure 4) shows a similar unsymmetrical bifurcated hydrogen bond as in **1**, with one of the ether groups of $\mathbf{L}^3$ orientated towards the NH proton of N(1), though the NH···O hydrogen bond is longer than in **1** [N(1)···Cl(1)'

3.140(3), H(1)···Cl(1)' 2.49(3) Å; N(1)-H(1)···Cl(1)'131° and N(1)···O(1) 2.860(4), H(1)···O(1) 2.56 Å; N(1)-H(1)···O(1) 100°].

Figure 4

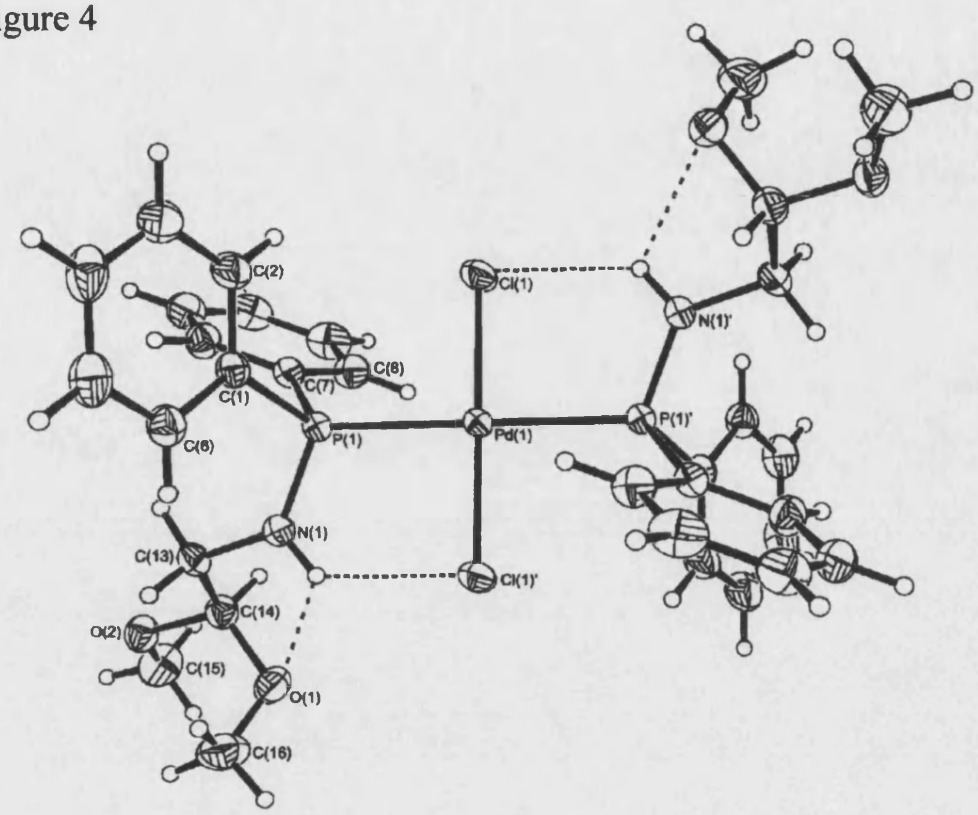

2.1.2.1.4 Reactions of $[MCl_2L_2]$ (M = Pd and Pt)

2.1.2.1.4.1 Abstraction of Chloride from *cis*-$[PtCl_2L_2]$ (L = L^1 and L^4) and *trans*-$[PdCl_2(L^1)_2]$

To examine the potential bidentate coordination of the ether-functionalised phosphinoamines, the complexes *cis*-$[PtCl_2L_2]$ (L = $\mathbf{L^1}$ and $\mathbf{L^4}$) and *trans*-$[PdCl_2(\mathbf{L^1})_2]$ were reacted with $AgBF_4$ (Scheme 4). Two equivalents (or a slight excess) of $AgBF_4$ was added to *cis*-$[PtCl_2L_2]$ (L = $\mathbf{L^1}$ and $\mathbf{L^4}$) and *trans*-$[PdCl_2(\mathbf{L^1})_2]$ in dichloromethane, with the rapid formation of silver chloride. The products were

characterised as *cis*-[Pt(L-*P,O*)$_2$](BF$_4$)$_2$ [L = **L^1** (**9**) and **L^4** (**10**)] and *trans*-[Pd(**L^1**-*P,O*)$_2$](BF$_4$)$_2$ (**11**), on the basis of microanalysis, multinuclear NMR and infrared spectroscopy.

Scheme 4

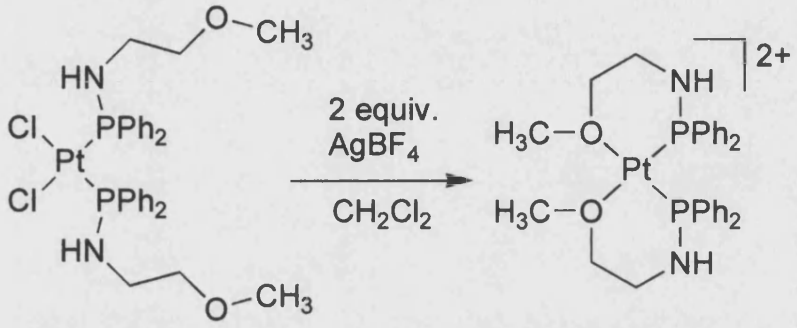

Table 6. Selected $^{31}P\{^1H\}$, ^1H NMR and infrared data for complexes **9-14**.

	Complex	δ(P) /ppm	^1J(P,Pt) /Hz	δ(NH) /ppm	δ(CH$_3$) /ppm	ν(NH) /cm^{-1}
9	*cis*-[Pt(**L^1**-*P,O*)$_2$](BF$_4$)$_2$	39.6	4346	3.87m	3.77s	3326w
10	*cis*-[Pt(**L^4**-*P,O*)$_2$](BF$_4$)$_2$	27.7	4162	6.48d	3.79s	3296w
11	*trans*-[Pd(**L^1**-*P,O*)$_2$](BF$_4$)$_2$	80.1	-	4.07m	3.65s	3316w
12	[Pd(μ-Cl)(**L^1**)$_2$]$_2$(BF$_4$)$_2$	61.4	-	4.39br	3.26s	3274w
13	*cis*-[Pt(**L^1**)$_2$(CNXyl)$_2$](BF$_4$)$_2$	38.6	2069	4.83m	3.17s	3306w
14	*cis*-[Pt(**L^1**)$_2$(NCCH$_3$)$_2$](BF$_4$)$_2$	25.9	3924	4.33m	3.27s	3305w

The $^{31}P\{^1H\}$ NMR spectra for [Pt(L-*P,O*)$_2$](BF$_4$)$_2$ (L = **L^1** and **L^4**) show single phosphorus resonances with platinum satellites (see Table 6). The increase in ^1J(P,Pt) for complexes **9** and **10** relative to complexes **5** and **7** (ΔJ = +406 for **L^1**, +228 Hz for **L^4**) is indicative of the phosphine lying *trans* to a weaker *trans* influence ligand such

as an ether oxygen atom.[23] Further evidence to support the coordination of the ether oxygen atoms is observed in the ^{1}H NMR spectra, where the chemical shifts show deshielding of the methoxy protons ($\Delta\delta$ = 0.63 ppm for **9** with respect to **5**, 0.14 ppm for **10** with respect to **7**). Similar deshielding is also observed in the chemical shift of the methylene protons of **9**, which are now attached to a 6-membered chelate ring. In the complex $[Pt\{PPh_2(C_6H_4)NMe_2\text{-}2\}_2](ClO_4)_2$ a similar downfield shift in the ^{1}H NMR spectrum for the methyl protons is observed on coordination of the NMe_2 group.[24] In contrast to the deshielding of the methyl and methylene protons, the NH protons show significant shielding on formation of the chelate rings ($\Delta\delta$ = -0.21 ppm for **9** with respect to **5**, -0.34 ppm for **10** with respect to **7**). This is likely to be due to the loss of hydrogen bonding to the NH protons.

Extraction of the chloride ligands from the complexes *cis*-$[PtCl_2(\mathbf{L^1})_2]$ **5** [δ(P) 35.5 ppm] and *cis*-$[PtCl_2(\mathbf{L^4})_2]$ **7** [δ(P) 30.1 ppm] can lead to either a small increase [δ(P) 39.6 ppm **9**, $\Delta\delta$ = +4.31 ppm] or a small decrease [δ(P) 27.7 ppm **10**, $\Delta\delta$ = -2.4 ppm] in the observed chemical shift. It would appear that two opposing factors are affecting the phosphorus chemical shifts: formation of a six membered chelate ring containing the phosphorus atom leads to δ(P) being shifted to higher field,[14] whereas replacement of the chloride by a weaker *trans* influencing ligand results in δ(P) being shifted to lower field.[14]

The $^{31}P\{^1H\}$ NMR spectrum for *trans*-$[Pd(\mathbf{L^1}\text{-}P,O)_2](BF_4)_2$ (**11**) showed a single phosphorus resonance at δ(P) 80.1 ppm. This is significantly deshielded relative to **2** [δ(P) 46.4 ppm]. As in the platinum containing complexes **9** and **10**, the ^{1}H NMR spectrum of **11** shows the deshielding of the methoxy protons ($\Delta\delta$ = 0.43 ppm for **11** with respect to **1**) and the methylene protons, as well as the shielding of the NH proton ($\Delta\delta$ = -0.21 ppm for **11** with respect to **1**). These features are again

consistent with the coordination of the ether oxygen atom forming a 6-membered chelate ring. Due to the moisture sensitivity of **11**, microanalysis was not successfully obtained.

The reaction of **1** with only one equivalent of $AgBF_4$ (Scheme 5) did not lead to the formation of a *P,O*-coordinated phosphinoamine, but instead gave exclusively the chloro-bridged dimer $[Pd(\mu\text{-}Cl)(\mathbf{L^1})_2]_2(BF_4)_2$ (**12**) which was characterised on the basis of microanalysis, FAB-MS, multinuclear NMR and infrared spectroscopy. The ^1H NMR spectrum showed the methoxy ($\Delta\delta$ = +0.04 ppm for **12** with respect to **1**), methylene and NH protons were all very slightly deshielded with respect to **1**, in marked contrast to the observations for complexes **9-11**.

Lindner and co-workers[25,26] have previously shown that the reaction of *trans*-$[PdCl_2L_2]$ (L = range of ether-phosphines) with one equivalent of $AgClO_4$ resulted in the formation of the cationic complexes $[PdClL_2]^+$, containing one bidentate *P,O*-coordinated phosphine and one unidentate *P*-coordinated phosphine. Only for ether-phosphines in which the oxygen atom is less basic were dimers observed. In this case, the formation of the chloro-bridged dimer **12** is likely to be the result of the unfavourable formation of a 6-membered chelate ring.

Scheme 5

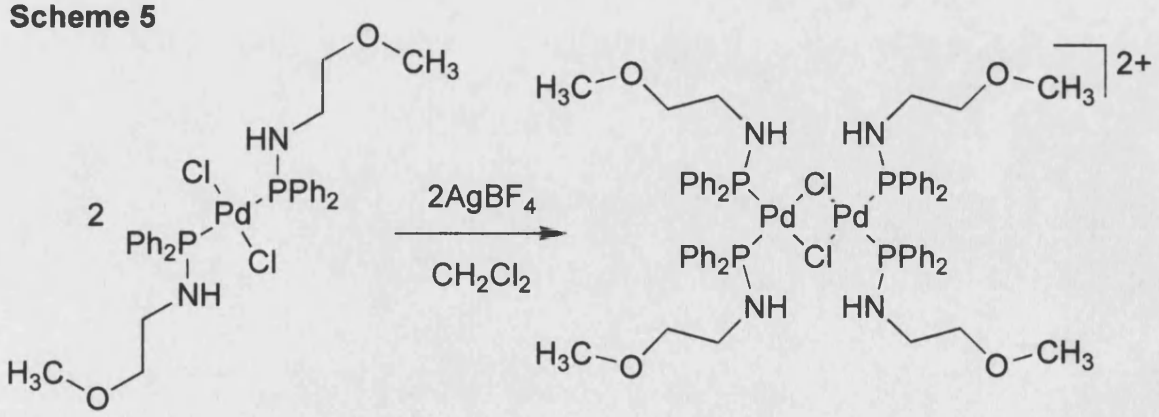

2.1.2.1.4.2 Lability of Coordinated Ether Oxygen

The lability of the coordinated ether oxygen in complexes **9** and **10** should allow this atom to be readily displaced.

The reaction of two equivalents of xylyl isocyanide with **9** in dichloromethane gave the complex *cis*-$[Pt(\mathbf{L^1})_2(CNXyl)_2](BF_4)_2$ (**13**). This compound was characterised on the basis of microanalysis, multinuclear NMR and infrared spectroscopy. The $^{31}P\{^1H\}$ NMR spectrum showed a single phosphorus resonance with platinum satellites [δ(P) 38.6 ppm, $^1J(P,Pt)$ 2069 Hz]. The considerably reduced coupling constant in **13** relative to **5** and **9** is consistent with the higher *trans*-influence of the isocyanide ligand relative to Cl^- and O-donors respectively.[27] The infrared spectrum of **13** showed a band for the NH group [ν(NH) 3306 cm^{-1}], and a characteristic band for the terminally coordinated isocyanide group [ν(CN) 2214 cm^{-1}].

The reaction of an excess of acetonitrile with **9** in dichloromethane gave the complex *cis*-$[Pt(\mathbf{L^1})_2(NCCH_3)_2](BF_4)_2$ (**14**), which was characterised on the basis of multinuclear NMR and infrared spectroscopy. The $^{31}P\{^1H\}$ NMR spectrum showed a single phosphorus resonance with platinum satellites [δ(P) 25.9 ppm, $^1J(P,Pt)$ 3924 Hz]. The ^1H NMR spectrum was as expected with distinctive signals for the methylene, methyl and NH groups of the ligand $\mathbf{L^1}$ as well as a signal for the methyl group of acetonitrile [$\delta(CH_3)$ 2.00 ppm]. The infrared spectrum of **14** showed a broad band for the NH group [ν(NH) 3305 cm^{-1}]. This compound was found to be very moisture sensitive and as such proved difficult to characterise fully. Reaction of **9** with CO led to decomposition to platinum metal. This is not surprising as compounds of the type $[Pt(CO)_2(PR_3)_2]^{2+}$ are unknown.[23]

2.1.2.1.4.3 Methanolysis of the P-N Bonds of Coordinated Phosphinoamines

Cleavage of the P-N bond was observed to readily occur on reaction of the free ligand $\mathbf{L^1}$ with an excess of methanol (Section 2.1.1). In order to compare the stability of the P-N bond in the free ligand with that of the coordinated ligand, excess methanol was added to a dichloromethane solution of the complex $[PdCl_2(\mathbf{L^1})_2]$. After one hour the $^{31}P\{^1H\}$ NMR spectra showed no change, demonstrating that coordination stabilises the P-N bond to cleavage by methanol. This is in marked contrast to diphosphazanes ($Ph_2PNRPPh_2$) for which the free phosphines are stable in methanol at room temperature for several days, but on coordination the P-N bonds readily undergoes cleavage.[11] Similarly, $Ph_2PNHP(O)Ph_2$ is activated to methanolysis on coordination to platinum.[21]

2.1.2.1.4.4 Synthesis of *cis*-$[PtX(NO_2)(\mathbf{L^1})_2]$ [X = Cl and Br] and *cis*-$[Pt(NO_2)_2(\mathbf{L^1})_2]$

The substitution of one or both of the halides from *cis*-$[PtX_2(\mathbf{L^1})_2]$ (X = Cl and Br) by a nitrite group was carried out to assess the ease of Pt-X bond substitution and determine the effects of substitution on the intramolecular hydrogen bonding.

An excess of aqueous sodium nitrite was reacted with complexes **5** and **8** in acetone. The reactions were followed by $^{31}P\{^1H\}$ NMR spectroscopy, and this showed the formation of the complexes *cis*-$[PtX(NO_2)(\mathbf{L^1})_2]$ [X = Cl (**15**) and Br (**16**)] (Table 7) reached a maximum yield after approximately 4 hours. On continuation of the reaction for a further 24 hours, $^{31}P\{^1H\}$ NMR spectroscopy showed that the complex *cis*-$[Pt(NO_2)_2(\mathbf{L^1})_2]$ (**17**) was the major product in both cases, but it did not prove possible to isolate this compound from the reaction mixture.

Table 7. Selected $^{31}P\{^{1}H\}$, ^{1}H NMR and infrared data for complexes **15-17**.

	δ(P) /ppm	$^{1}J(P,Pt)$ /Hz	$^{2}J(P,P)$ /Hz	δ(NH) /ppm	$\delta(CH_3)$ /ppm	ν(NH) /cm^{-1}
cis-$[PtCl(NO_2)(\mathbf{L^1})_2]$	33.8	4115	24	4.4,	3.20,	3396,
(**15**)	25.5	3186		3.5	3.17	3264w
cis-$[PtBr(NO_2)(\mathbf{L^1})_2]$	33.8	4101	23	4.2,	3.21,	3397,
(**16**)	25.5	3166		3.3	3.19	3311w
cis-$[Pt(NO_2)_2(\mathbf{L^1})_2]$	26.8	3370	-	3.54m	3.22s	-
(**17**)						

Complexes **15** and **16** were characterised on the basis of microanalysis, multinuclear NMR and infrared spectroscopy. The $^{31}P\{^{1}H\}$ NMR spectra of **15** and **16** (Figure 5) both showed two well-separated doublets each with platinum satellites.

Figure 5

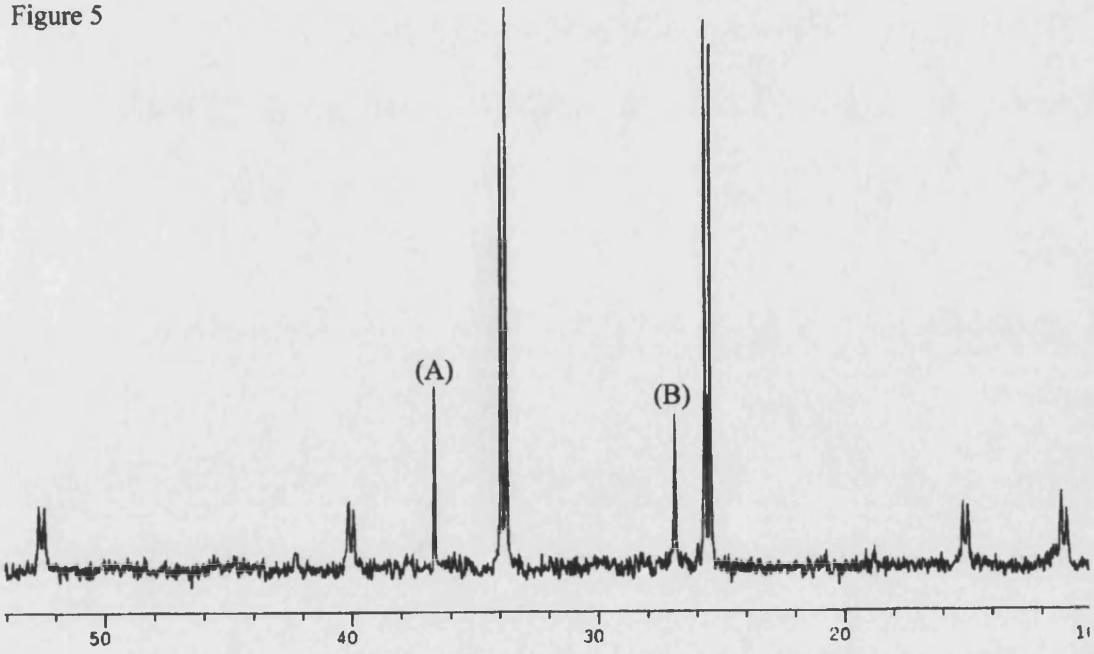

(**A**) = *cis*-$[PtBr_2(\mathbf{L^1})_2]$ and (**B**) = *cis*-$[Pt(NO_2)_2(\mathbf{L^1})_2]$

This coupling pattern is the result of the two phosphorus atoms becoming inequivalent due to the substitution of one halide by a nitrite. For the two phosphorus atoms to be inequivalent, the phosphines must still be *cis* to each other. This is further supported by the coupling constants $^1J(P,Pt)$ for complexes **15** and **16.** The doublets can be assigned on the basis of $^1J(P,Pt)$, the value of which is greater for the phosphorus atom *trans* to the halide.

Two sets of resonances were as expected observed in the ^1H NMR of complexes **15** and **16** for δ(NH), $\delta(CH_3)$ and $\delta(CH_2)$ (see Experimental Section). Comparison of the ^1H NMR spectra of **15** and **16** with those for *cis*-$[PtCl_2(\mathbf{L^1})_2]$ (**5**) and *cis*-$[PtBr_2(\mathbf{L^1})_2]$ (**8**) show that one of the amine hydrogen atoms has become significantly shielded (Δδ = -0.58 ppm for **15** with respect to **5**, Δδ -0.67 ppm for **16** with respect to **8**). This shielding of one of the NH protons is likely to be a consequence of the loss of the intramolecular N-H···X hydrogen bonding for this proton. The infrared spectra of complexes **15** and **16** showed two weak bands for the ν(NH). The FAB mass spectrum of complex **16** did not show the parent ion; the highest observed peak was at *m/z* 793 for $[M - NO_2]^+$.

The $^{31}P\{^1H\}$ NMR spectra of *cis*-$[Pt(NO_2)_2(\mathbf{L^1})_2]$ (**17**) shows a single phosphorus resonance with platinum satellites. The different electronic effects of the halide and nitrite on $^1J(P,Pt)$ is reflected in the coupling constant for **17** which is 570 Hz less than that for **5**. The ^1H NMR spectra of **17** (Table 7) shows that both the NH protons have been shielded when compared to the NH protons in **5** and **8**, again consistent with a loss of N-H···X hydrogen bonding.

2.1.2.1.4.4.1 X-ray Crystal Structure of *cis*-[PtBr(NO_2)(L^1)$_2$] (16)

Compound **16** was recrystallised from dichloromethane-hexane as colourless block shaped single crystals suitable for X-ray crystallographic studies. The crystal structure (Figure 6) confirmed the proposed formulation. Selected bond lengths and angles are given in Table 8.

Table 8. Selected bond lengths [Å] and angles [°] for complex **16**.

Pt(1)-P(1)	2.256(2)	P(2)-N(2)	1.661(5)
Pt(1)-P(2)	2.2684(14)	N(1)-C(13)	1.471(8)
Pt(1)-Br(1)	2.4889(8)	N(2)-C(28)	1.475(8)
Pt(1)-N(3)	2.150(6)	N(3)-O(1)	1.2235(14)
P(1)-N(1)	1.653(5)	N(3)-O(2)	1.2246(10)
N(3)-Pt(1)-Br(1)	83.19(12)	N(1)-P(1)-Pt(1)	110.9(2)
N(3)-Pt(1)-P(1)	91.91(12)	C(13)-N(1)-P(1)	127.8(4)
N(3)-Pt(1)-P(2)	173.86(13)	N(2)-P(2)-Pt(1)	110.1(2)
P(1)-Pt(1)-P(2)	93.78(5)	C(28)-N(2)-P(2)	126.6(4)
P(1)-Pt(1)-Br(1)	174.96(4)	O(1)-N(3)-Pt(1)	113.3(5)
P(2)-Pt(1)-Br(1)	91.07(4)		

The platinum(II) centre in **16** is distorted square-planar with *cis* angles between 83.19(12) and 93.78(5)°. The two monodentate $Ph_2PNHCH_2CH_2OMe$ ligands are arranged mutually *cis*.

The Pt-P and Pt-Br bond distances in complex **16** are similar to the expected values.[17] The P-N bond distances in complex **16** [P(1)-N(1) 1.653(5) Å and P(2)-N(2) 1.661(5) Å] are slightly longer than those observed in **1** [1.643(3) Å] and **3** [1.644(4)

Å], but are still shorter than that expected for a P-N single bond (1.68 to 1.73 Å).[18] The sum of the angles around the N(1) and N(2) atoms is 355 and 352° respectively, showing as with **1** and **3**, significant sp^2 character.

Figure 6

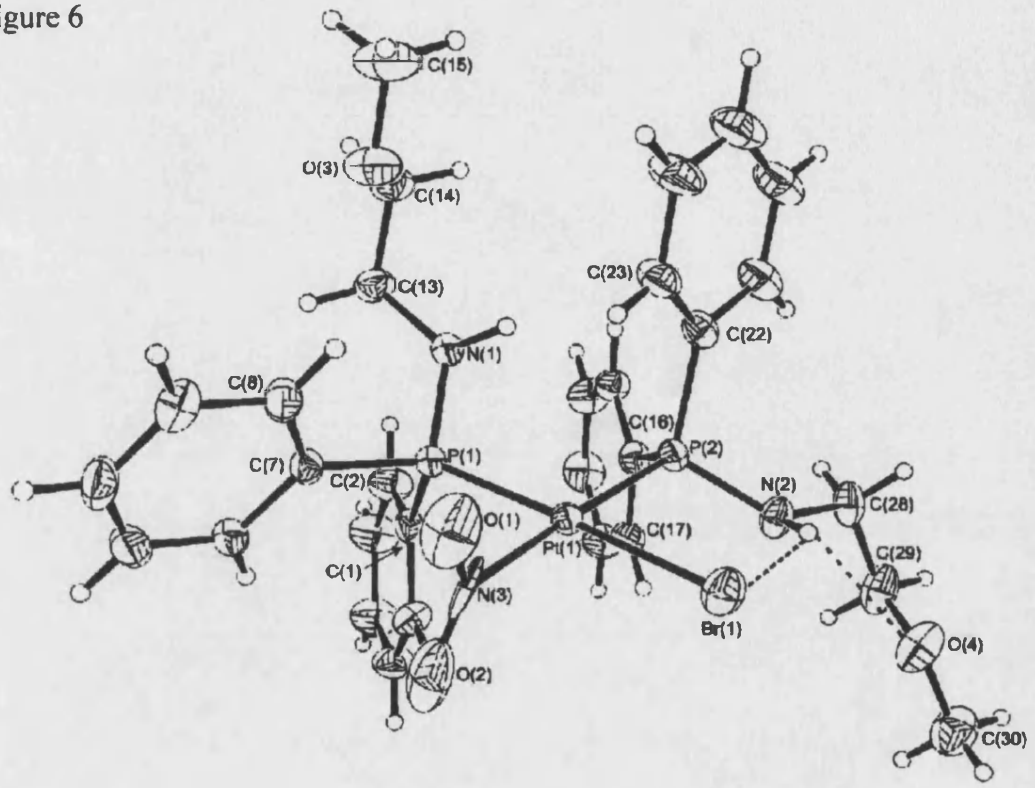

An intramolecular hydrogen bond was observed between the N(2)-H(2A) proton and the bromine atom [N(2)···Br(1) 3.175(4), H(2A)···Br(1) 2.48(6) Å; N(2)-H(2A)···Br(1) 128(4)°]. As with **1** and **3**, the orientation of the ether chain suggests the presence of a weak intramolecular hydrogen bond between the oxygen atom O(4) and the N(2)-H(2A) proton [N···O 2.791(7) Å, H···O 2.67(7) Å, N-H···O 87(4)°]. The crystal structure showed that there was no interaction between the amine proton H(1A), and either the ether oxygen atom O(3) or the oxygen atoms of the nitrite group. This relates well to the ^{1}H NMR spectra of **16** in which the chemical

shifts of the two N-H protons are no longer equivalent, suggesting that the solution structure is the same as that in the solid state.

2.1.2.2 Synthesis of [Pd(dmba)Cl(L)] (L = L^1-L^4) and [Pt(dmba)Cl(L)] (L = L^1, L^3 and L^4)

Complexes **9**, **10** and **11** were found to readily decompose in solution, which made their characterisation and study difficult. In order to try and increase the stability of compounds containing *P,O*-coordinated ligands L^1-L^4, a group of compounds [M(dmba)Cl(L)] (M = Pd and Pt; Hdmba = *N,N*-dimethylbenzylamine) were synthesised containing only one phosphine ligand per molecule. In these cyclometallated compounds the chelating dmba ligand blocks two coordination sites of the metal complex, so simplifying the possible reactions that the complexes can undergo (Figure 7).

Figure 7

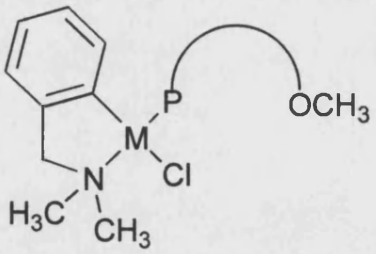

M = Pd or Pt

The reaction of two equivalents of phosphine L with the cyclometallated complex $[M(dmba)(\mu\text{-}Cl)]_2$ (M = Pd or Pt) in dichloromethane resulted in cleavage of the chloride bridges to give the complex [M(dmba)Cl(L)] in virtually quantitative

yield. These compounds were characterised on the basis of microanalysis, infrared and multinuclear NMR spectroscopy (see Experimental Section).

2.1.2.2.1 Characterisation of [Pd(dmba)Cl(L)] (L = L^1-L^4)

The $^{31}P\{^1H\}$ NMR spectra of the complexes [Pd(dmba)Cl(L)] [L = $\mathbf{L^1}$ (**18**), $\mathbf{L^2}$ (**19**), $\mathbf{L^3}$ (**20**) and $\mathbf{L^4}$ (**21**)] showed single phosphorus resonances, with chemical shifts in the range δ(P) 67-69 ppm for **18-20** and δ(P) 59.7 ppm for **21** (Table 9). In contrast to **1-3**, no isomerisation was observed in solution. The ^1H NMR spectra of **18-21** were

Table 9. Selected $^{31}P\{^1H\}$, ^1H NMR and infrared data for complexes **18-21**.

	Complex	δ(P) /ppm	δ(NH) /ppm	$\delta(OCH_3)$ /ppm	ν(NH) /cm^{-1}
18	[Pd(dmba)Cl($\mathbf{L^1}$)]	68.4	4.41m	3.23s,br	3285m
19	[Pd(dmba)Cl($\mathbf{L^2}$)]	67.6	4.40br	3.19s	3303w,br
20	[Pd(dmba)Cl($\mathbf{L^3}$)]	68.4	4.48m	3.25s	3284m
21	[Pd(dmba)Cl($\mathbf{L^4}$)]	59.7	6.3d	3.81s	3197w

as expected, though due to the overlap of the methylene and methyl signals of the phosphine and dmba, unambiguous determination of the chemical shifts was not always possible. The *trans* N-Pd-P arrangement of the ligands in complexes **18-21** can be deduced from the observed $^4J(H,P)$ coupling constants to the methyl and methylene groups within dmba,[28] [$^4J(CH_3,P) \approx 3$ Hz, $^4J(CH_2,P) \approx 2$ Hz] in the ^1H NMR spectra of **20** and **21**, and from the broadness of $\delta(NCH_3)$ and $\delta(NCH_2)$ in complexes **18** and **19**. This arrangement of the phosphine *trans* to the nitrogen has

been previously observed in [Pd(dmba)Cl($PPh_2CH_2C(O)OC_2H_5$)][28] and the presence of only one of the possible isomers, was ascribed to the lability of the phosphine ligand *trans* to σ-bonded carbon. The infrared spectra of all four complexes showed one band for ν(NH). The positive-ion FAB mass spectrum of complex **18** showed the parent ion peak at *m/z* 535.

2.1.2.2.2 Characterisation of [Pt(dmba)Cl(L)] (L = L^1, L^3 and L^4)

The $^{31}P\{^1H\}$ NMR spectra for [Pt(dmba)Cl(L)] [L = L^1 (**22**) L^3 (**23**) and L^4 (**24**)] show single phosphorus resonances with $^1J(P,Pt)$ in the range 4460-4470 Hz (Table 10). The large value of $^1J(P,Pt)$ suggests the phosphine is *trans* to the nitrogen atom of dmba,[14] and this is consistent with the geometry adopted in the solid state (Section 2.1.2.2.3). From the ^1H NMR spectra of **22**, **23** and **24**, the observed coupling

Table 10. Selected $^{31}P\{^1H\}$, ^1H NMR and infrared data for complexes **22-24**.

	Complex	δ(P) /ppm	$^1J(P,Pt)$ /Hz	δ(NH) /ppm	δ(OCH_3) /ppm	ν(NH) /cm^{-1}
22	[Pt(dmba)Cl(**L^1**)]	42.1	4460	4.23dt	3.25s	3308w,br
23	[Pt(dmba)Cl(**L^3**)]	42.3	4470	4.24dt	3.28s	3294w,br
24	[Pt(dmba)Cl(**L^4**)]	34.8	4464	6.37d	3.80s	3214w,br

between the phosphorus and the methyl and methylene protons of dmba is also consistent with this arrangement [$^4J(CH_3,P) \approx 3$ Hz, $^4J(CH_2,P) \approx 3$ Hz]. $^{31}P\{^1H\}$ NMR spectra of crude samples of **22** showed the presence of an additional compound [δ 53.9, $^1J(P,Pt)$ 2170 Hz] (Figure 8A). The value of $^1J(P,Pt)$ is consistent with this peak

being due to the isomer with the phosphine *trans* to carbon. On leaving the reaction mixture overnight, this compound is converted to **22** (Figure 8B). It has previously been shown that the reaction of cyclometallated platinum chloro-bridged dimers with pyridines can give either *N,N-cis* or *N,N-trans* products, depending on the reaction conditions and the substituents on the pyridine ligand.[29]

Figure 8

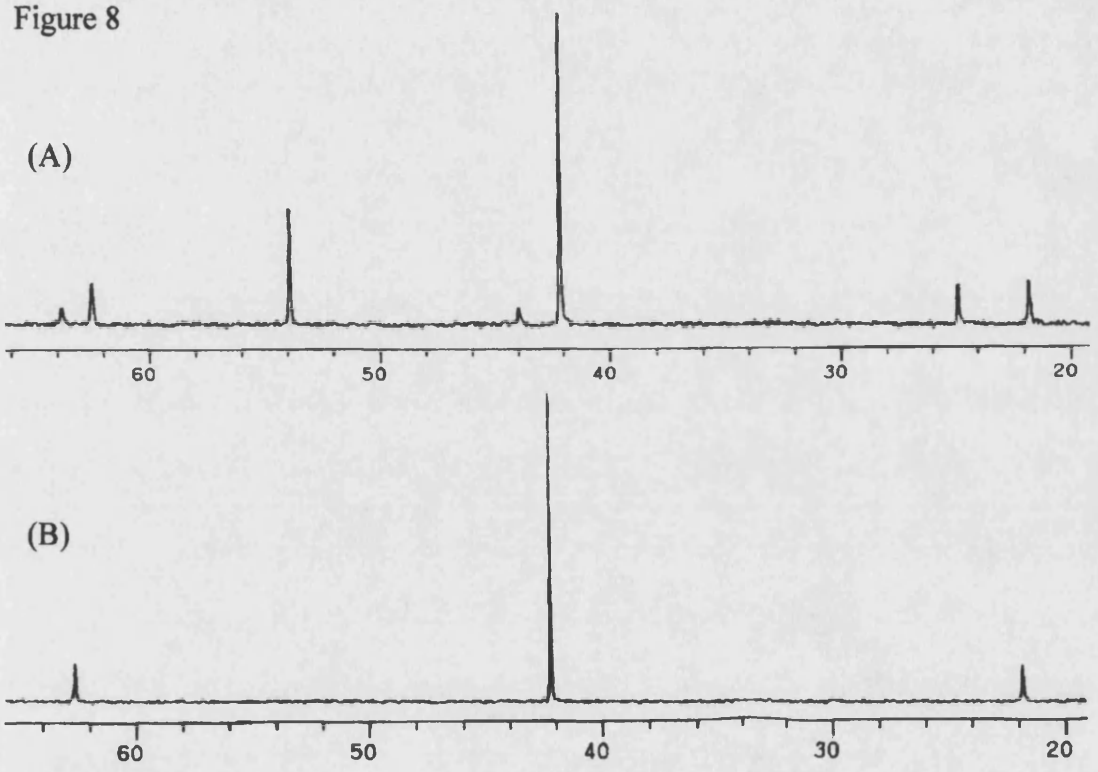

2.1.2.2.3 X-ray Crystal Structures of [Pd(dmba)Cl(L^1)] (18) and [Pd(dmba)Cl(L^2)] (19)

Complexes **18** and **19** were recrystallised from dichloromethane-pentane and dichloromethane-diethyl ether, respectively, as needle shaped single crystals suitable for X-ray crystallographic studies. The crystal structures (Figures 9 & 10) confirmed

the proposed formulation; selected bond lengths and angles are given in Table 11 and Table 12.

Table 11. Selected bond lengths [Å] and angles [°] for complex **18**.

Pd(1)-C(13)	1.955(6)	Pd(1)-Cl(1)	2.365(2)
Pd(1)-N(2)	2.141(5)	P(1)-N(1)	1.616(6)
Pd(1)-P(1)	2.247(2)	N(1)-C(19)	1.470(8)
C(13)-Pd(1)-N(2)	80.1(2)	N(2)-Pd(1)-Cl(1)	92.5(2)
C(13)-Pd(1)-P(1)	96.7(2)	P(1)-Pd(1)-Cl(1)	92.51(6)
N(2)-Pd(1)-P(1)	169.53(14)	N(1)-P(1)-Pd(1)	111.2(2)
C(13)-Pd(1)-Cl(1)	166.0(2)	C(19)-N(1)-P(1)	124.9(4)

Table 12. Selected bond lengths [Å] and angles [°] for complex **19**.

Pd(1)-C(17)	2.034(4)	Pd(1)-Cl(1)	2.3886(11)
Pd(1)-N(2)	2.156(3)	P(1)-N(1)	1.649(3)
Pd(1)-P(1)	2.2471(8)	N(1)-C(13)	1.455(4)
C(17)-Pd(1)-N(2)	82.72(13)	N(2)-Pd(1)-Cl(1)	90.16(9)
C(17)-Pd(1)-P(1)	96.80(10)	P(1)-Pd(1)-Cl(1)	90.07(3)
N(2)-Pd(1)-P(1)	177.49(8)	N(1)-P(1)-Pd(1)	109.37(10)
C(17)-Pd(1)-Cl(1)	170.91(10)	C(13)-N(1)-P(1)	128.1(2)

The palladium(II) centre in complex **18** shows significant deviation from square-planar geometry, with *cis* angles between 80.1(2) and 96.7(2)°. The complex has a slight tetrahedral distortion, with Cl(1) and C(13) lying above (by 0.16 and 0.22

Å respectively), and P(1) and N(2) lying below (by 0.17 and 0.21 Å respectively) the Pd(1)Cl(1)N(2)C(13)P(1) mean plane. The crystal structure of **19** shows a smaller deviation from square-planar geometry about the palladium(II) centre, with *cis* angles between 82.69(13) and 96.82(10)°. The Pd(1), Cl(1), N(2), C(17) and P(1) atoms in **19** show a much smaller deviation from planarity, with the Cl(1) and the C(17) lying below (by 0.04 and 0.05 Å respectively), and Pd(1), P(1) and N(2) lying above (by 0.06, 0.01 and 0.02 Å respectively) the Pd(1)Cl(1)N(2)C(17)P(1) mean plane. The monodentate phosphines $\mathbf{L^1}$ and $\mathbf{L^2}$ in complexes **18** and **19** are both located *trans* to the nitrogen atom of dmba, consistent with the NMR data.

Figure 9

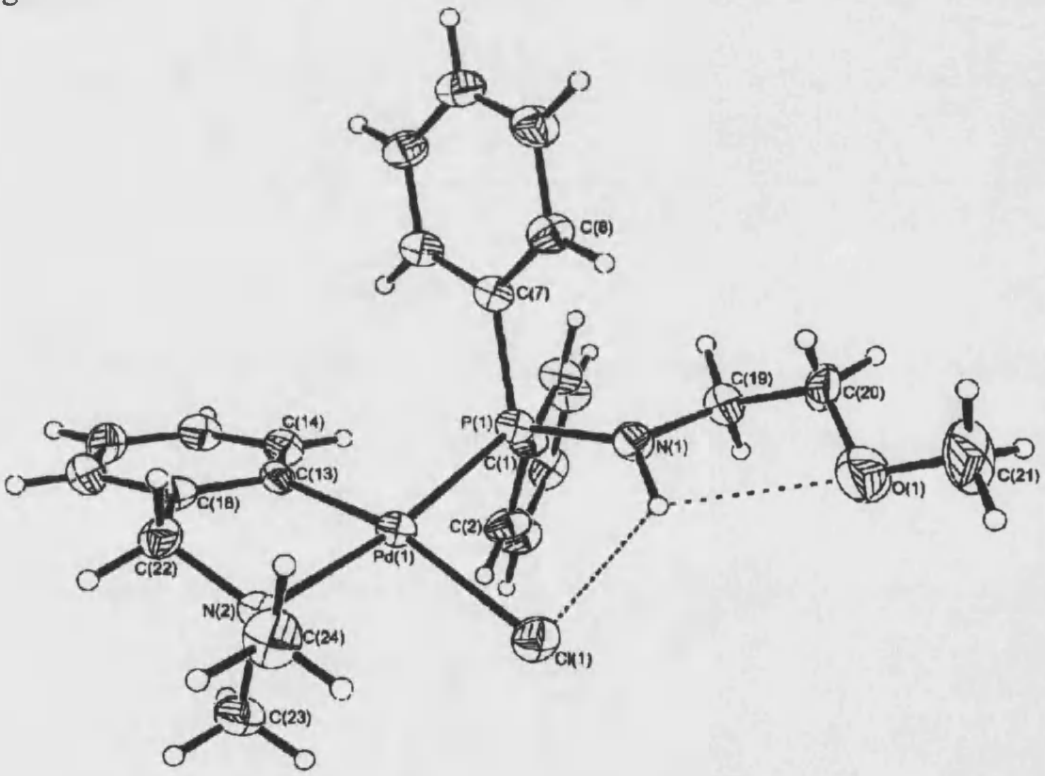

The sum of the angles around the N(1) atom of the phosphine ligand $\mathbf{L^1}$ in complex **18** is 352° and the $\mathbf{L^2}$ ligand in **19** is 358°, showing as in complexes **1** and **3** significant sp^2 character.[18]

The Pd-P and Pd-Cl distances in complex **18** and **19** are similar to those previously reported for Pd-P and Pd-Cl bonds.[17] The P-N bond distances in both **18** [1.616(6) Å] and **19** [1.649(3) Å], are shorter than would normally be expected for a P-N single bond,[18] and in the case of **18** the P-N bond length is significantly shorter than those in **19**, **1** [1.643(3) Å] and **3** [1.644(4) Å].

Figure 10

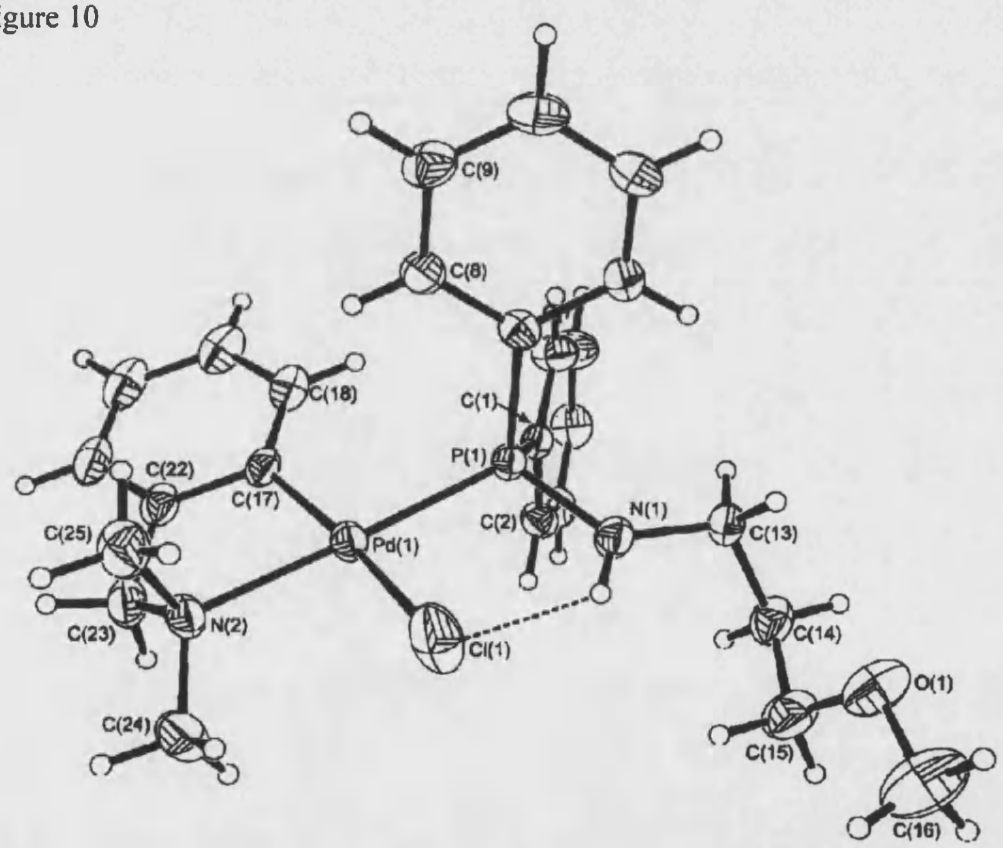

The bite angles of the dmba chelate in complexes **18** [80.1(2)°] and **19** [82.69(13)°] are as expected when compared to other related complexes containing

this ligand.[30] The reduction in the bite angle in complex **18** compared to **19** is probably the result of the larger distortion in **18** from a square planar geometry about the palladium(II) centre.

As in complexes **1** and **3**, the structure of **18** (Figure 9) shows the presence of an unsymmetrical intramolecular bifurcated hydrogen bond between the N(1)-H(1) proton and both the chlorine Cl(1) and ether oxygen O(1) atoms, with the major component to the chloride [N···Cl 3.087(6) H···Cl 2.42(5) Å, N-H···Cl 125(4)°] and the minor component to the oxygen atom [N···O 2.904(8), H···O 2.53(5) Å, N-H···O 103(3)°]. The structure of **19** (Figure 10) only shows the presence of a N-H···Cl interaction [N···Cl 3.087(3), H···Cl 2.43(3) Å, N-H···Cl 137(2)°], due to the ether oxygen O(1) atom being directed away from the N(1)-H(1) proton, so the N-H···O interaction is absent [N···O 3.626(4), H···O 3.39(3) Å, N-H···O 100(2)°]. This is somewhat surprising, since an intramolecular 6-membered hydrogen-bonded ring might have been expected to be more favourable than a 5-membered hydrogen-bonded ring, due to the improved geometry for hydrogen-bonding inherent in a 6-membered ring.

2.1.2.2.4 Reactions of [M(dmba)Cl(L)] (M = Pd and Pt)

2.1.2.2.4.1 Abstraction of Chloride from [Pt(dmba)Cl(L)] (L = L^1 and L^4) and [Pd(dmba)Cl(L^1)]

To examine the potential bidentate coordination of the ether-functionalised phosphinoamines, the complexes [M(dmba)Cl(L)] (M = Pd, Pt) were reacted with Ag^+. One equivalent (or a slight excess) of $AgBF_4$ or $AgPF_6$ was reacted with the complexes [Pt(dmba)Cl(L)] (L = L^1 and L^4) and [Pd(dmba)Cl(L^1)] in

dichloromethane, with the rapid formation of silver chloride (Scheme 6). The resulting complexes were characterised as [Pt(dmba)(L-*P,O*)](BF_4) [L = $\mathbf{L^1}$ (**25**) and $\mathbf{L^4}$ (**26**)] and [Pd(dmba)($\mathbf{L^1}$-*P,O*)]X [X = BF_4 (**27**) and PF_6 (**28**)], on the basis of multinuclear NMR, infrared spectroscopy and microanalysis.

Scheme 6

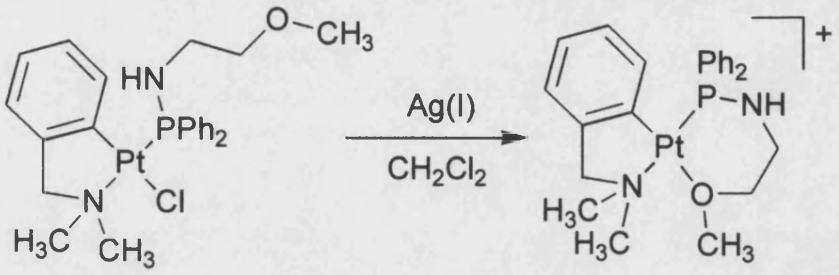

Table 13. Selected $^{31}P\{^1H\}$, ^1H NMR and infrared data for complexes **25-28**.

	Complex	δ(P) /ppm	^1J(P,Pt) /Hz	δ(NH) /ppm	δ(OCH_3) /ppm	ν(NH) /cm^{-1}
25	[Pt(dmba)($\mathbf{L^1}$-*P,O*)](BF_4)	48.8	4396	3.15m,br	3.52	3308w
26	[Pt(dmba)($\mathbf{L^4}$-*P,O*)](BF_4)	60.9	4393	6.0br	4.17	3390
27	[Pd(dmba)($\mathbf{L^1}$-*P,O*)](BF_4)	75.2	-	3.40br	3.33	-
28	[Pd(dmba)($\mathbf{L^1}$-*P,O*)](PF_6)	69.5	-	3.56m	3.50	-

The $^{31}P\{^1H\}$ NMR spectra for [Pt(dmba)(L-*P,O*)](BF_4) (L = $\mathbf{L^1}$ and $\mathbf{L^4}$) show single phosphorus resonances with platinum satellites (Table 13). The small decrease in the coupling constants between the phosphorus and platinum atoms in complexes **25** and **26** relative to complexes [Pt(dmba)Cl($\mathbf{L^1}$)] (**22**) and [Pt(dmba)Cl($\mathbf{L^4}$)] (**24**) [ΔJ = -64 for **25** with respect to **22**, and -71 for **26** with respect to **24**] can be ascribed to the combination of several different effects on the value of ^1J(P,Pt), such as changing

the ligand *cis* to the phosphine, the presence of a positive charge on the metal centre and the formation of a chelate ring.[31]

The ^{1}H NMR spectra of complexes **25** and **26** show that the methoxy protons are slightly deshielded [$\Delta\delta$ = 0.27 for **25** with respect to **22**, and 0.37 for **26** with respect to **24**], as are the methylene protons in **25**. This downfield shift is consistent with ether oxygen coordination and was also observed in both complexes *cis*-[Pt(**L**^{1}-*P,O*)$_2$](BF$_4$)$_2$ (**9**) and *cis*-[Pt(**L**^{4}-*P,O*)$_2$](BF$_4$)$_2$ (**10**) (Section 2.1.2.1.4.1). The NH protons show significant shielding on formation of the chelate rings ($\Delta\delta$ = -1.08 ppm for **25** with respect to **22**, -0.4 ppm for **26** with respect to **24**). As in **9** and **10**, this is likely to be due to the loss of hydrogen bonding between the NH protons and chloride ligands.

The ^{31}P{^{1}H} NMR spectrum for [Pd(dmba)(**L**^{1}-*P,O*)](BF$_4$) **27** showed a single phosphorus resonance [δ(P) 75.2 ppm], while complex [Pd(dmba)(**L**^{1}-*P,O*)](PF$_6$) **28** showed a single phosphorus resonance plus a septet due to the PF_6^- counter ion [δ(P) 69.5 ppm, -143.6 ppm, sep, ^{1}J(P,F) 711 Hz]. As in complex **25**, the ^{1}H NMR spectrum of **27** and **28** show deshielding of the methoxy [$\Delta\delta$ = 0.12 for **27** with respect to **18**, and 0.26 for **28** with respect to **18**] and methylene protons, indicating the coordination of the ether oxygen. In addition to significant shielding of the NH proton [$\Delta\delta$ = -1.01 for **27** with respect to **18**, and -0.85 for **28** with respect to **18**], consistent with the loss of the hydrogen bonding.

Unfortunately the solutions of complexes **26-28** in dichloromethane were found to decompose, and as a result only **25** could be isolated and purified.

2.1.2.2.4.2 Lability of the Coordinated Ether Oxygen

The coordinated ether oxygen atoms in **25** and **26** are expected to be relatively labile.[23] To access the ease of rupturing the Pt-O bond, a range of ligands, including carbon monoxide (CO), acetonitrile ($NCCH_3$) and xylyl isocyanide (CNXyl) were reacted in solution with the complexes [Pt(dmba)(L-*P,O*)](BF_4) (L = $\mathbf{L^1}$, $\mathbf{L^3}$ and $\mathbf{L^4}$).

Carbon monoxide was bubbled through dichloromethane solutions of the complexes [Pt(dmba)(L-*P,O*)](BF_4) (L = $\mathbf{L^1}$, $\mathbf{L^3}$ and $\mathbf{L^4}$), for approximately 10 minutes with no obvious colour change to give the complexes [Pt(dmba)(L)(CO)](BF_4) [L = $\mathbf{L^1}$ (**29**), $\mathbf{L^3}$ (**30**) and $\mathbf{L^4}$ (**31**)] (Scheme 7). These compounds were characterised on the basis of microanalysis, infrared and multinuclear NMR spectroscopy (see Experimental Section).

Scheme 7

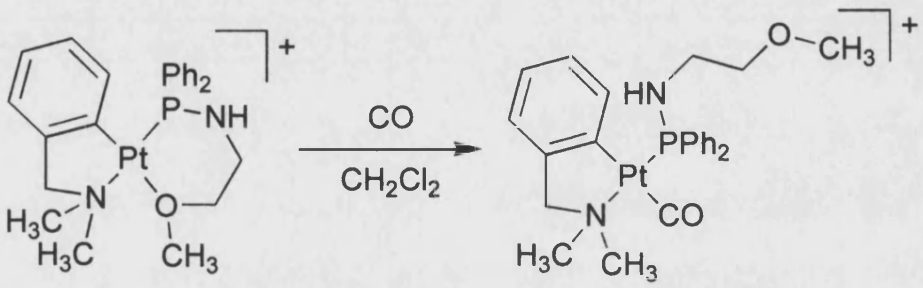

The $^{31}P\{^1H\}$ NMR spectra of complexes **29-31** showed single phosphorus resonances with platinum satellites (Table 14). Observation of the coupling between the phosphorus and the methyl and methylene protons of the dmba ligand with platinum satellites in the ^1H NMR spectra [$^4J(CH_3,P) \approx 3$ Hz, $^4J(CH_2,P) \approx 3$ Hz], is consistent with **29-31** retaining the *trans* N-Pt-P arrangement of the ligands as in complexes **22-24**.

Complexes **29** and **31** show a significant decrease in $^{1}J(P,Pt)$ on replacing the coordinated ether oxygen atom with a carbonyl ligand. [ΔJ = -730 for **29** with respect to **25** and -697 for **31** with respect to **26**]. There are a number of factors that may contribute to this decrease in the value of $^{1}J(P,Pt)$ such as a change in the ligand *cis* to the phosphine and the loss of the 6-membered chelate ring. The high values for the $\nu(CO)$ band, observed in the infrared spectra of **29**, **30** and **31** (2114, 2106 and 2105 cm^{-1} respectively) indicate that there is relatively little back-bonding from the platinum to the carbonyl.[32] These high values for $\nu(CO)$ are similar to those observed in complexes of the type *trans*-$[PtX(CO)(PR_3)_2]^+$.[33]

Both complexes **30** and **31** were observed to decompose on standing in solution to give a black insoluble material, so characterisation by microanalysis was not possible. In contrast complex **29** was found to be relatively stable thus allowing purification.

Table 14. Selected $^{31}P\{^{1}H\}$, ^{1}H NMR and infrared data for complexes **29-31**.

	Complex	δ(P) /ppm	$^{1}J(P,Pt)$ /Hz	δ(NH) /ppm	$\delta(OCH_3)$ /ppm	ν(CO) /cm^{-1}
29	$[Pt(dmba)(\mathbf{L^1})(CO)](BF_4)$	38.8	3666	3.57m	3.26br	2114s[a]
30	$[Pt(dmba)(\mathbf{L^3})(CO)](BF_4)$	39.1	3622	4.12m	3.36s	2106s[b]
31	$[Pt(dmba)(\mathbf{L^4})(CO)](BF_4)$	35.4	3696	5.90m	3.76s	2105s[b]

(IR a = KBr disk; b = CH_2Cl_2 solution)

The reaction of **25** and **26** with an excess of acetonitrile in dichloromethane gave the complexes $[Pt(dmba)(L)(NCCH_3)](BF_4)$ [L = $\mathbf{L^1}$ (**32**) and $\mathbf{L^4}$ (**33**)]. These compounds were characterised on the basis of multinuclear NMR and infrared

spectroscopy. The $^{31}P\{^{1}H\}$ NMR spectrum showed a single phosphorus resonance with platinum satellites (Table 15). The $^{1}J(P,Pt)$ values for complexes **32** and **33** show a significantly reduction [ΔJ = -208 for **32** with respect to **22**, and -208 for **33** with respect to **24**] in the $^{1}J(P,Pt)$ compared to **22** and **24**, though this reduction is considerably less than seen for **29** and **30**. The observation of $^{4}J(H,P)$ in the ^{1}H NMR spectrum suggests the phosphine remains *trans* to the nitrogen atom of the dmba ligand, as previously observed in complexes **22-24**. These compounds slowly decomposed in solution, and as a result proved difficult to characterise fully.

Table 15. Selected $^{31}P\{^{1}H\}$, ^{1}H NMR and infrared data for complexes **32-33**.

	δ(P) /ppm	$^{1}J(P,Pt)$ /Hz	$\delta(CH_3)$ /ppm	$\delta(NCCH_3)$ /ppm	ν(NH) /cm^{-1}
$[Pt(dmba)(\mathbf{L^1})(NCCH_3)]BF_4$ (**32**)	44.4	4252	3.28s	2.02s	3350
$[Pt(dmba)(\mathbf{L^4})(NCCH_3)]BF_4$ (**33**)	38.5	4256	3.77s	1.83s	3370w

The reaction of one equivalent of xylyl isocyanide with **26** in dichloromethane gave the complex $[Pt(dmba)(\mathbf{L^4})(CNXyl)](BF_4)$ (**34**). This compound was characterised on the basis of multinuclear NMR and infrared spectroscopy (see Experimental Section). The $^{31}P\{^{1}H\}$ NMR spectrum showed a single phosphorus resonance with platinum satellites δ(P) 36.7 ppm [$^{1}J(P,Pt)$ 3897 Hz]. The observed $^{4}J(H,P)$ [$^{4}J(CH_3,P) \approx 3$ Hz, $^{4}J(CH_2,P) \approx 3$ Hz] is consistent with the complex retaining the *trans* N-Pt-P arrangement of the ligands as in complexes **22-24**. The infrared spectrum of **34** showed a characteristic band for the coordinated isocyanide group

[ν(CN) 2179 cm^{-1}]. The high value of the ν(CN) band indicates there is little backbonding from the platinum to the isocyanide group, as observed in **29-31**.

2.1.2.2.4.3 Formation of [Pt(dmba)(μ-PPh_2O)]$_2$

Attempts to recrystallise complex [Pt(dmba)(L^1-*P,O*)](BF_4) (**25**) to obtain crystals suitable for X-ray analysis were unsuccessful resulting in decomposition to give a number of compounds, as observed in the $^{31}P\{^1H\}$ NMR spectra. One of these compounds crystallised from dichloromethane-pentane and was isolated as colourless block shaped crystals suitable for X-ray crystallography. From analysis of these crystals the complex was revealed to be [Pt(dmba)(μ-PPh_2O)]$_2$ (**35**). The formation of **35** is believed to be due to cleavage of the P-N bond of the *P,O*-coordinated phosphinoamine in **25**, by a trace amount of water.

2.1.2.2.4.3.1 X-ray Crystal Structure of [Pt(dmba)(μ-PPh_2O)]$_2$ (35)

The crystal structure (Figure 11) revealed that complex **35** was a dinuclear species with bridging phosphito (μ-PPh_2O) units. Selected bond lengths and angles are given in Table 16.

The crystal structure analysis showed that complex **35** crystallised with one molecule of dichloromethane per unit cell. Each of the platinum centres in **35** is coordinated to bidentate cyclometallated dmba ligand, a phosphorus atom and an oxygen atom, thus giving a 6-membered ring. The platinum centres both show significant deviation from a square-planar arrangement with *cis* angles between 82.1(7) and 98.9(6)° for Pt(1) and between 82.6(8) and 98.7(7)° for Pt(2). The

phosphorus atoms of the bridging phosphito (PPh_2O^-) units are arranged *trans* to the nitrogen atoms [N(1) and N(2)] of the dmba ligands.

Figure 11

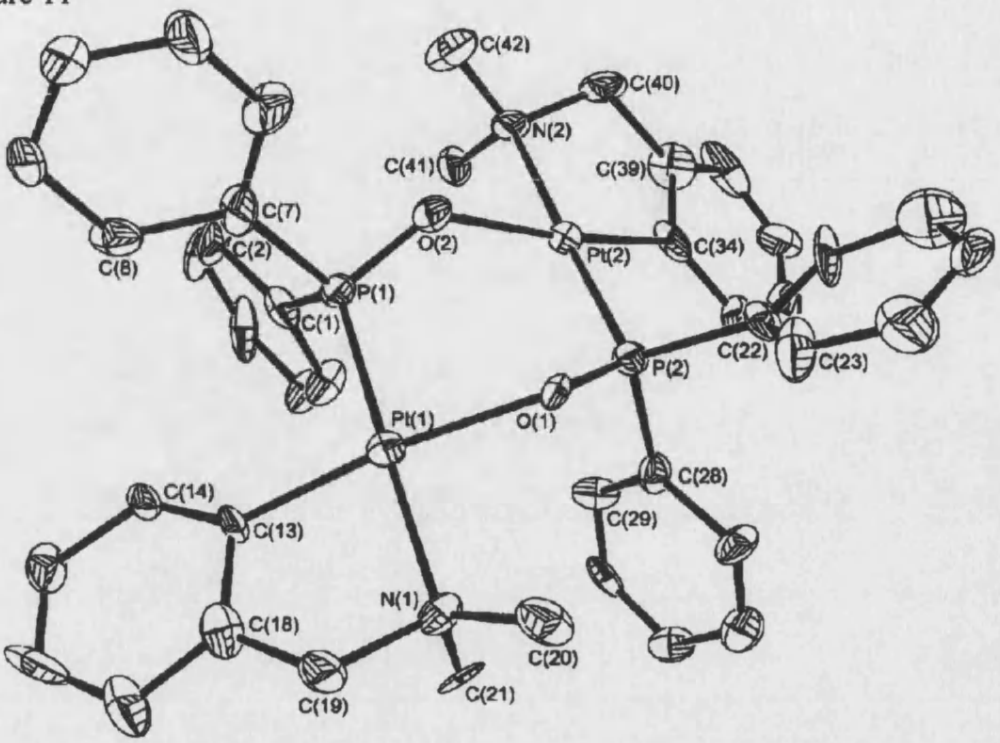

The conformation of the six membered ring is best described as two distorted square planar platinum units linked at an O···O hinge, with the angle between the Pt(1)-P(1)-O(1)-O(2) and Pt(2)-P(2)-O(1)-O(2) least squares planes being 48°. This is in marked contrast to the conformation observed in $[Pd\{PPh_2CH{=}C(O)Ph\}(\mu\text{-}PPh_2O)]_2$[34] which is best described as a boat with the palladium atoms in the prows. The Pt-P [2.205(5) Å for Pt(1)-P(1), and 2.217(5) Å Pt(2)-P(2)], P-O [1.531(13) Å for P(1)-O(2) and 1.556(12) Å for P(2)-O(1)] and Pt-O [2.116(11) Å for Pt(1)-O(1), and 2.098(11) Å for Pt(2)-O(2)] bond distances within the 6-membered ring are similar to those in the complexes

$[Pt_3(\mu_3\text{-}OH)(\mu\text{-}PPh_2O)_3(PR_3)_3]^{2+}$ [35] and $[Pt_2Cl(PEt_3)_3(\mu\text{-}PPh_2O)_2]^{+}$ [36] which also contains the μ-PPh_2O ligand.

Table 16. Selected bond lengths [Å] and angles [°] for complex **35**.

Pt(1)-C(13)	2.00(2)	Pt(2)-O(2)	2.098(11)
Pt(1)-O(1)	2.116(11)	Pt(2)-N(2)	2.15(2)
Pt(1)-N(1)	2.160(15)	Pt(2)-P(2)	2.217(5)
Pt(1)-P(1)	2.205(5)	P(1)-O(2)	1.531(13)
Pt(2)-C(34)	2.01(2)	P(2)-O(1)	1.556(12)
C(13)-Pt(1)-O(1)	170.4(7)	O(2)-Pt(2)-N(2)	88.8(8)
C(13)-Pt(1)-N(1)	82.1(7)	C(34)-Pt(2)-P(2)	98.7(7)
O(1)-Pt(1)-N(1)	88.9(5)	O(2)-Pt(2)-P(2)	89.9(4)
C(13)-Pt(1)-P(1)	98.9(6)	N(2)-Pt(2)-P(2)	176.2(4)
O(1)-Pt(1)-P(1)	90.1(3)	O(2)-P(1)-Pt(1)	115.4(5)
N(1)-Pt(1)-P(1)	179.0(4)	O(1)-P(2)-Pt(2)	115.5(5)
C(34)-Pt(2)-O(2)	171.3(8)	P(2)-O(1)-Pt(1)	126.1(7)
C(34)-Pt(2)-N(2)	82.6(8)	P(1)-O(2)-Pt(2)	128.6(7)

2.1.2.3 Complexes of Molybdenum

Since it had not proved possible to obtain crystals of a platinum or palladium complex containing $\mathbf{L^4}$, complexes of molybdenum were prepared to compare the solid state ligand structure of $\mathbf{L^4}$ with those for $\mathbf{L^1}$-$\mathbf{L^3}$.

2.1.2.3.1 Synthesis of $[Mo(CO)_4L_2]$ (L = L^1, L^3 and L^4)

The reaction of two equivalents of phosphinoamines $\mathbf{L^1}$, $\mathbf{L^3}$ and $\mathbf{L^4}$ with $[Mo(CO)_4(pip)_2]$ (pip = piperidine) in dichloromethane gave good yields of the complexes $[Mo(CO)_4L_2]$ [L = $\mathbf{L^1}$ (**36**), $\mathbf{L^3}$ (**37**) and $\mathbf{L^4}$ (**38**)]. These compounds were purified by recrystallisation and characterised on the basis of microanalysis, FAB-MS, infrared and multinuclear NMR spectroscopy (see Experimental Section).

2.1.2.3.2 Characterisation of $[Mo(CO)_4L_2]$ (L = L^1, L^3 and L^4)

The $^{31}P\{^1H\}$ NMR spectra of the complexes **36-38** showed single phosphorus resonances, with chemical shifts in the range δ(P) 70-79 ppm for **36-38** (Table 17).

Table 17. Selected $^{31}P\{^1H\}$, ^1H NMR and infrared data for complexes **36-38**.

	Complex	δ(P) /ppm	δ(NH) /ppm	δ(OCH_3) /ppm	ν(NH) /cm^{-1}	ν(CO) /cm^{-1}
36	$[Mo(CO)_4(\mathbf{L^1})_2]$	77.2s	2.95m	3.28s	3400, 3380w	2016vs, 1900vs(vbr)[a]
37	$[Mo(CO)_4(\mathbf{L^3})_2]$	78.4s	2.78m	3.20d	-	-
38	$[Mo(CO)_4(\mathbf{L^4})_2]$	70.9s	5.88m	3.74s	3399m	2022vs, 1906vs, 1870vs,br[b]
39	$[Mo(CO)_3(\mathbf{L^3})_3]$	78.7s	3.81m	3.23s	3297m,br	1939vs, 1842vs,br[a]

(a = KBr, b = nujol)

The infrared spectra of complexes **36-38** showed one weak/broad band for the ν(NH). The number of carbonyl bands in the infrared spectra was difficult to determine due to the broadness of the ν(CO) bands. The positive-ion FAB mass spectra of complexes **36** and **38** showed the expected parent ions at *m/z* 726 and 822 respectively.

The coordination of $\mathbf{L^1}$, $\mathbf{L^3}$ and $\mathbf{L^4}$ in **36-38** stabilised the ligands to methanolysis and hydrolysis as previously observed for the palladium and platinum complexes **1-8**. The addition of excess wet methanol to a dichloromethane solution of **36-38** led to no change in the $^{31}P\{^1H\}$ NMR spectrum over a period of 2 days. This is in marked contrast to the free ligands, which react readily with methanol.

2.1.2.3.3 X-ray Crystal Structure of *cis*-$[Mo(CO)_4(L^4)_2]$ (38)

Complex **38** was recrystallised from dichloromethane-methanol as colourless block shaped single crystals suitable for X-ray crystallographic studies. Selected bond lengths and angles are given in Table 18.

The crystal structure of complex **38** (Figure 12) shows that the ligands around the molybdenum(0) centre adopt a distorted octahedral arrangement, with the phosphine ligands mutually *cis*. *Cis* angles in the complex range from 86.0(2) to 100.24(9)° with the widest angle, as expected, that which separates the two phosphinoamines. The molecule is disposed about a crystallographic 2-fold axis passing through the molybdenum atom and bisecting the angle between P(1) and P(1)'.

Table 18. Selected bond lengths [Å] and angles [°] for complex **38**.

Mo(1)-C(2)	1.978(8)	N(1)-C(15)	1.404(9)
Mo(1)-C(1)	2.016(8)	O(1)-C(1)	1.153(8)
Mo(1)-P(1)	2.540(2)	O(2)-C(2)	1.139(8)
P(1)-N(1)	1.680(6)		
P(1)'-Mo(1)-P(1)	100.24(9)	C(2)-Mo(1)-C(1)'	90.9(3)
C(1)-Mo(1)-P(1)	93.6(2)	C(2)-Mo(1)-C(1)	87.7(3)
C(1)-Mo(1)-P(1)'	87.6(2)	O(1)-C(1)-Mo(1)	176.7(7)
C(2)-Mo(1)-P(1)	86.0(2)	O(2)-C(2)-Mo(1)	175.9(7)
C(2)-Mo(1)-P(1)'	172.4(2)	N(1)-P(1)-Mo(1)	106.9(2)
C(1)'-Mo-C(1)	178.1(4)	C(15)-N(1)-P(1)	132.1(6)
C(2)-Mo(1)-C(2)'	88.0(4)		

Primed atoms generated by the symmetry transformation *-x, y, -z+1/2*

The Mo(1)-P(1) distance [2.540(2) Å for **38**] is significantly longer than the generally accepted Mo-P bond distance to a phosphinoamine.[17] The Mo-C bonds are similar to the generally accepted range for Mo-C bonds,[17] with the Mo-C bond distances for the carbonyl ligands *trans* to another carbonyl [Mo(1)-C(1) 2.016(8) Å] longer than those for the carbonyl ligands *trans* to the phosphinoamine ligand (**L**^{4}) [Mo(1)-C(2) 1.978(8) Å]. This is consistent with previous observations on the related complex $[Mo(CO)_4(PPh_2NH_2)_2]$, and can be attributed to the carbonyl ligands being better π-acceptors than the phosphinoamine ligands.[37]

The P-N bond distance in complex **38** [1.680(6) Å] is significantly longer than those observed in complexes *trans*-$[PdCl_2(\mathbf{L}^1)_2]$ (**1**) [1.643(3) Å], *trans*-$[PdCl_2(\mathbf{L}^3)_2]$ (**3**) [1.644(4) Å], [Pd(dmba)Cl(**L**^{1})] (**18**) [1.616(6) Å] and [Pd(dmba)Cl(**L**^{2})] (**19**)

[1.649(3) Å], suggesting a weaker P-N bond than in the P-N(alkyl) complexes (Section 2.1.2.1). The sum of angles around the nitrogen atoms in **38** is 359° consistent with the nitrogen having significant sp^2 character (Section 2.1.2.1).

Figure 12

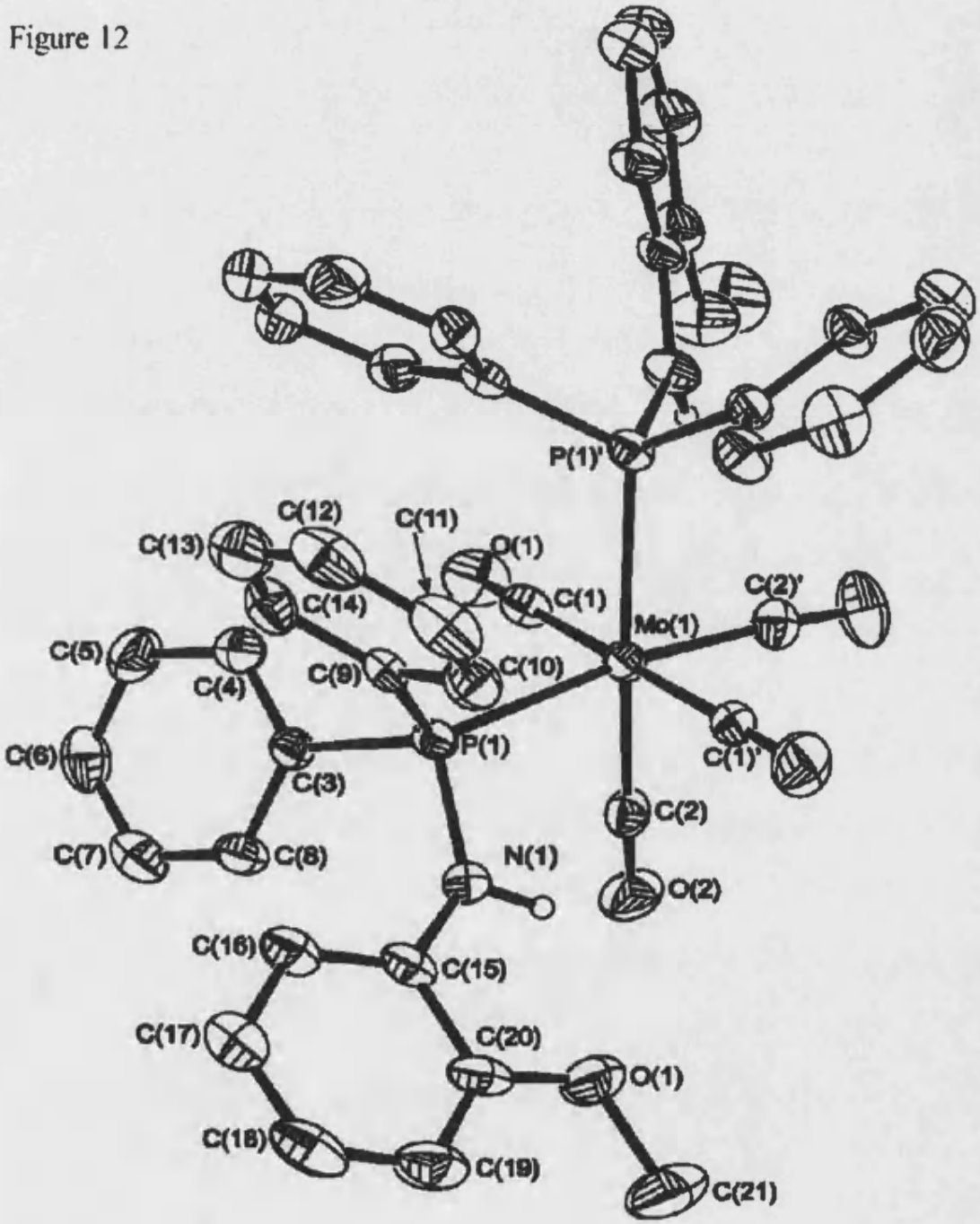

The structure of **38** shows the presence of intramolecular hydrogen bonding between the N(1)-H(1) proton and the ether group oxygen atom [N···O 2.587(8) Å, H···O 2.11(4) Å, N-H···O 112(3)°]. This N-H···O interaction is considerably shorter than those seen in **1, 3, 17** and **18**; this may be the consequence of both the geometry imposed by the aromatic system, as well as the absence of any N-H···Cl hydrogen bonding.

2.1.2.3.4 Synthesis of $[Mo(CO)_3(L^3)_3]$

The reaction of two equivalents of the phosphine L^3 with $[Mo(C_7H_8)(CO)_3]$ in toluene gave only the complex $[Mo(CO)_3(L^3)_3]$ (**39**) as observed from the $^{31}P\{^1H\}$ NMR spectrum. This compound was characterised on the basis of microanalysis, infrared and multinuclear NMR spectroscopy (see Experimental Section).

The $^{31}P\{^1H\}$ NMR spectra of the complex $[Mo(CO)_3(L^3)_3]$ **39** show a single phosphorus resonance, with a chemical shift of δ(P) 78.7 ppm. The ^1H NMR spectrum of **39** was as expected. The *fac* P-Mo-P arrangement of the ligands in complex **39** is suggested by the absence of any coupling between the phosphorus nuclei. The presence of only two ν(CO) bands in the infrared spectrum is also consistent with this arrangement, as it retains C_{3v} symmetry.

2.1.2.4 Complexes of Rhodium

2.1.2.4.1 Synthesis of $[RhCl(CO)L_2]$ (L = L^1, L^3 and L^4)

The reaction of four equivalents of phosphine L (L = L^1, L^3 and L^4) with $[Rh(\mu\text{-}Cl)(CO)_2]_2$ in dichloromethane resulted in the rapid evolution of CO gas, with

the formation in good yield of the complex *trans*-[RhCl(CO)L_2] [L = $\mathbf{L^1}$ (**40**), $\mathbf{L^3}$ (**41**) and $\mathbf{L^4}$ (**42**)] (Scheme 8). These compounds were characterised on the basis of microanalysis, infrared and multinuclear NMR spectroscopy (see Experimental Section).

Scheme 8

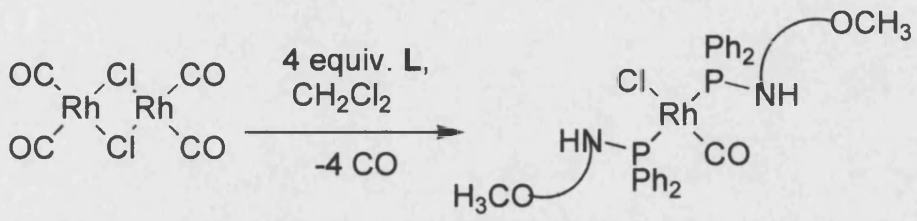

2.1.2.4.2 Characterisation of [RhCl(CO)L_2] (L = $\mathbf{L^1}$, $\mathbf{L^3}$ and $\mathbf{L^4}$)

The $^{31}P\{^1H\}$ NMR spectra of **40-42** each show a doublet with $^1J(P,Rh)$ between 124 and 131 Hz (Table 19 and Figure 13) indicating *trans* geometry. The

Table 19. Selected $^{31}P\{^1H\}$, ^1H NMR and infrared data for complexes **40-42**.

	Complex	δ(P) /ppm	$^1J(P,Rh)$ /Hz	δ(NH) /ppm	δ(CH_3) /ppm	ν(CO) /cm^{-1}
40	*trans*-[RhCl(CO)($\mathbf{L^1}$)$_2$]	60.0	124	4.22m	3.30	1988vs[a], 1977vs[b]
41	*trans*-[RhCl(CO)($\mathbf{L^3}$)$_2$]	60.3	127	4.24m	3.30	1958vs[a], 1977vs[b]
42	*trans*-[RhCl(CO)($\mathbf{L^4}$)$_2$]	53.2	131	-	3.89	1965vs[a], 1980vs[b]

(IR a = KBr, b = CH_2Cl_2)

coupling constants of **40-42** lie close to the previously reported[14] range [^{1}J(P,Rh) 117-129 Hz] for *trans*-[RhCl(CO)P_2] (P_2 = a variety of monodentate and bidentate phosphine ligands). The infrared spectrum of **40-42** showed one strong band for ν(CO).

Figure 13

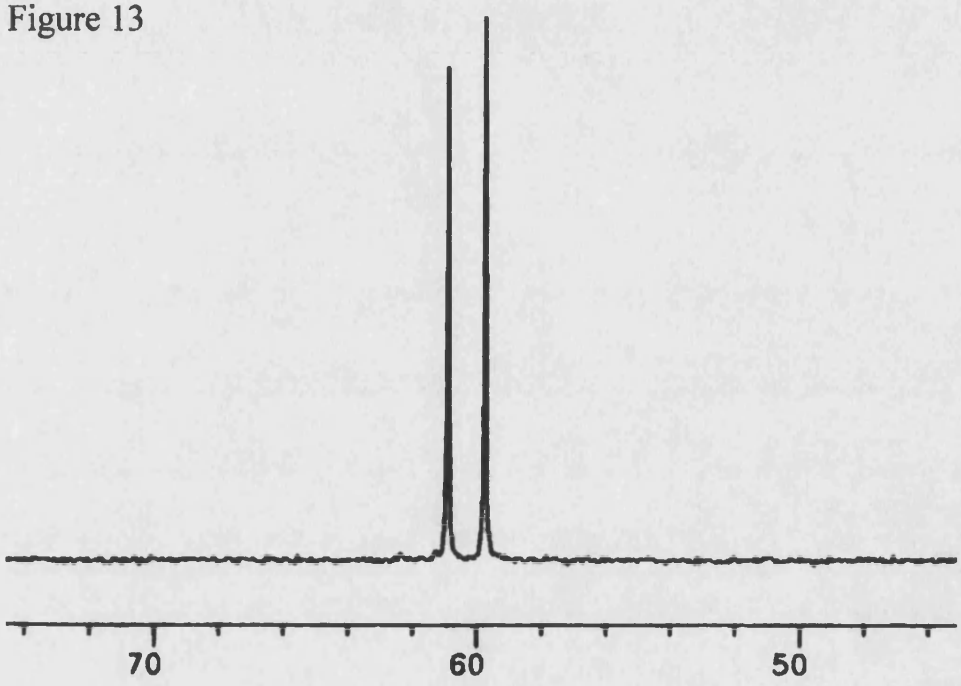

Infrared spectroscopy of **40-42** was used to examine the electronic properties of the phosphine ligands. Back-bonding to the CO from an electron rich metal results in a lowering of the C-O bond order and thereby reduces the ν(CO) stretching frequency whereas the reverse is true of electron deficient complexes.[32,38] The electronic properties of the attached phosphine ligands affect the electron density on the metal centre, which in turn affects the ν(CO) stretching frequency. Therefore, ν(CO) can be used as a probe of the electronic properties of phosphines. A comparison of the carbonyl frequencies of **40-42** against a selection of the equivalent

rhodium(I) complexes *trans*-[RhCl(CO)(**L**)$_2$] (**L** = alkyl and aryl phosphines and phosphites, *N*-pyrrolidinyl and *N*-pyrrolyl phosphines) is shown in Table 20.

Table 20 Carbonyl stretching frequency ν(CO) for *trans*-[RhCl(CO)(**L**)$_2$].

Ligand (**L**)	ν(CO)/cm^{-1}	ref
PBu^n_3	1953	39
PEt_3	1954.5	39
PMe_3	1966	39
$PMePh_2$	1974	39
$PPh_2NHCH_2CH_2OMe$ (**L**^{1})	1977	this work
$PPh_2NHCH_2CH(OMe)_2$ (**L**^{3})	1977	this work
PPh_3	1978	39
$PPh_2NHC_6H_4OMe$-2 (**L**^{4})	1980	this work
$PPh_2(OMe)$	1986.5	39
PPh_2(*N*-pyrrolyl)	1993	38
$P(OMe)_3$	1998	39
P(*N*-pyrrolyl)$_3$	2024	38

Using the reported correlation[39] between ν(CO) for *trans*-[RhCl(CO)(PR$_3$)$_2$] and [Ni(CO)$_3$(PR$_3$)] (A$_1$ band), the ν(CO) for [Ni(CO)$_3$(L)] (L = **L**^{1}, **L**^{3} and **L**^{4}) (A$_1$ band) can be estimated and used to calculate the electronic parameter[9] χ for the ether-functionalised phosphinoamine ligands using Equation 1 (Table 21). These calculations are only approximate as small errors in the recorded value of ν(CO) can have a significant effect on the calculated value of χ_i.

For $PX_1X_2X_3$ $\nu = 2056.1 + \sum_{i=1}^{3} \chi_i$ (Equation 1)

ν = ν(CO) of the A_1 carbonyl mode of $[Ni(CO)_3(PX_1X_2X_3)]$ in CH_2Cl_2

χ_i = substituent contribution

Table 21 Estimated ν(CO) for $Ni(CO)_3L$ (A_1 band) and electronic parameter χ_i.

Ligand	ν(CO)/cm^{-1}	χ_i
L^1	2069	4.3
L^2	2069	4.3
L^4	2070	5.3

Comparison of these electronic parameters with those for *N*-pyrrolyl (χ_i = 12), methoxy (χ_i = 7.7) and phenyl (χ_i = 4.3) groups, show that the electronic contribution (χ_i) for **L**^{1} and **L**^{3} is approximately the same as for the phenyl group, while the electronic contribution for **L**^{4} is between that of a methoxy and a phenyl group. This suggests that for **L**^{1} and **L**^{3} the substitution of a phenyl group from PPh_3 by a primary alkyl-amine has little effect on the electronic properties of the phosphine despite the increased electronegativity of the amine nitrogen atom compared to carbon. This has previously been attributed to the presence of π-backbonding from the nitrogen to the phosphorus, which effectively reduces the electronegativity of the nitrogen.[38] Evidence for this was observed in the X-ray crystal structures of the complexes containing the ether-functionalised phosphinoamines **L**^{1} and **L**^{3}, which showed significant shortening of the P-N bond distances. The difference in the electronic parameter for **L**^{4} with respect to **L**^{1} and **L**^{3} suggests that **L**^{4} is a poorer σ-donor, possibly due to reduced π-bonding between the nitrogen and the phosphorus as

observed in the complex *cis*-[Mo(CO)$_4$($\mathbf{L^4}$)$_2$] in which the P-N bond is significantly longer than observed for complexes containing $\mathbf{L^1}$ and $\mathbf{L^3}$.

2.2 Conclusions

Phosphinoamines containing ether functionalities can be easily synthesised in good yield and purity. These ligands coordinate to Pt(II), Pd(II), Mo(0) and Rh(I) and abstraction of halide has been shown to lead to bidentate coordination involving the ether oxygen atom. However, the oxygen atom can be readily displaced from the metal centre by acetonitrile, carbon monoxide and xylyl isocyanide.

The crystal structures of complexes **1, 3, 16, 18, 19** and **38** show that the P-N bond is significantly shorter than expected for a P-N single bond. This is further supported by the planarity of the amine nitrogen, which indicates that the nitrogen atom is significantly sp^2 hybridised.

The single crystal X-ray analyses of complexes **1, 3, 16** and **28** showed the presence of unsymmetrical bifurcated hydrogen bonds with the major component between the NH proton and halide atom, and the minor component between the NH proton and the oxygen atom of the ether chain. In **19** increasing the ether chain length led to the loss of the interaction between the NH proton and the ether oxygen atom, while retaining the hydrogen bond between the NH proton and the chloride.

The uncoordinated phosphinoamines were shown to be susceptible to hydrolysis and methanolysis but were stabilised to these on coordination to palladium(II), platinum(II) or molybdenum(0).

2.3 References

1 L. A. Hamilton and P. S. Landis, in *'Organic Phosphorus Compounds'*, ed. G. M. Kosolapoff and L. Maier, Wiley-Interscience, 1972, **4**, 504.

2 J. McKechnie, D. S. Payne and W. Sim, *J. Chem. Soc.*, 1965, 3500.

3 R. F. Hudson, R. J. G. Searle and F. H. Devitt, *J. Chem. Soc. (C)*, 1966, 1001; W. A. Hart and H. H. Sisler, *Inorg. Chem.*, 1964, 617.

4 S. M. Aucott, A. M. Z. Slawin and D. J. Woollins, *Phosphorus, Sulfur,* 1997, 473; J.-M. Brunel and G. Buono, *Tetrahedron Lett.*, 1999, 3561.

5 K. G. Gaw, A. M. Z. Slawin and M. B. Smith, *Organometallics*, 1999, **18**, 3255.

6 T. Q. Ly, A. M. Z. Slawin and J. D. Woollins, *J. Chem. Soc., Dalton Trans.*, 1997, 1611.

7 A. Bader and E. Lindner, *Coord. Chem. Rev.*, 1991, 27; C. S. Slone, D. A. Weinberger, C. A. Mirkin, *Prog. Inorg. Chem.*, 1999, **48**, 233.

8 F. Agbossou, J.-F. Carpentier, F. Hapiot, I. Suisse and A. Montreux, *Coord. Chem. Rev.*, 1998, 1615.

9 C. A. Tolman, *Chem. Rev.*, 1977, **77**, 313.

10 V. Mark, C. H. Dungan, M. M. Crutchfield and J. R. Van Wazer, *Topics in Phosphorus Chemistry*, 1967, **5**, 227.

11 R. P. K. Babu, S. S. Krishnamurthy and M. Nethaji, *Polyhedron*, 1996, **15**, 2689.

12 A. Badía, L. R. Falvello, R. Navarro and E. P. Urriolabeitia, *J. Organomet. Chem.* 1997, 121.

13 T. Q. Ly and J. D. Woollins, *Coord. Chem. Rev.*, 1998, 451.

14 P.S. Pregosin and R. W. Kunz, *^{31}P and ^{13}C NMR of Transition Metal Phosphine Complexes'*, ed. P. Diehl, E. Fluck and R. Kosfeld, Springer-Verlag, Berlin Heidelberg, 1979, 53.

15 P. Bhattacharyya, A. M. Z. Slawin, M. B. Smith and J. D. Woollins, *Inorg. Chem.*, 1996, **35**, 3675.

16 V.V. S. Reddy, J. E. Whitten, K. A. Redmill, A. Varshney and G. M. Gray, *J. Organomet. Chem.*, 1989, **372**, 207; N. W. Alcock, A. W. G. Platt and P. Pringle, *J. Chem. Soc. Dalton Trans.*, 1987, 2273.

17 A. G. Orpen, L. Brammer, F. H. Allen, O. Kennard, D. G. Watson and R. Taylor, *J. Chem. Soc. Dalton Trans.*,1989, S1.

18 R. A. Burrow, D. H. Farrar and C. H. Honeyman, *Acta Cryst.*, 1994, **C50**, 681.

19 R. Murugavel, S. S. Krishnamurthy, J. Chandrasekhar and M. Nethaji, *Inorg. Chem.*, 1993, **32**, 5447.

20 A. M. Z. Slawin, M. B. Smith and J. D. Woollins, *J. Chem. Soc., Dalton Trans.*, 1996, 1283.

21 A. M. Z. Slawin, M. B. Smith and J. D. Woollins, *J. Chem. Soc., Dalton Trans.*, 1996, 4567.

22 G. A. Jeffrey, *'An Introduction to Hydrogen Bonding'*, O.U.P., New York, 1997, and references therein.

23 G. K. Anderson and R. Kumar, *Inorg. Chem.*, 1984, **23**, 4064.

24 T. B. Rauchfuss, F. T. Patino and D. M. Roundhill, *Inorg. Chem.*, 1975, **14**, 652; H. P. Fritz, I. R. Gordon, K. E. Schwarzhans and L. M. Venanzi, *J. Chem. Soc.*, 1965, 5210.

25 E. Lindner, R. Speidel, R. Fawzi and W. Hiller, *Chem. Ber.*, 1990, **123**, 2255.

26 E. Lindner, J. Dettinger, H. A. Mayer, H. Kühbauch, R. Fawzi and M. Steimann, *Chem. Ber.*, 1993, **126**, 1317.

27 T. G. Appleton, H. C. Clark and L. E. Manzer, *Coord. Chem. Rev.*, 1973, **10**, 335.

28 P. Braunstein, D. Matt, Y. Dusausoy, J. Fischer, A. Mitschler and L. Ricard, *J. Am. Chem. Soc.*, 1981, **103**, 5115.

29 A. D. Ryabov, L. G. Kuz'mina, V. A. Polyakov, G. M. Kazankov, E. S. Ryabova, M. Pfeffer and R. van Eldik, *J. Chem. Soc. Dalton Trans.*, 1995, 999.

30 P. Braunstein, D. Matt, D. Nobel, S.-E. Bouaoud and D. Grandjean, *J. Organomet. Chem.*, 1986, **301**, 401.

31 P. E. Garrou, *Chem. Rev.*, 1981, 229.

32 R. H. Crabtree *'The Organometallic Chemistry of the Transition Metals'*, Wiley, New York, 1988.

33 W. J. Cherwinski and H. C. Clark, *Inorg. Chem.*, 1971, **10**, 2263.

34 D. Matt, F. Ingold, F. Balegroune and D. Grandjean, *J. Organomet. Chem.*, 1990, **399**, 349.

35 N. W. Alcock, P. Bergamini, T. M. Gomes-Carniero, R. D. Jackson, J. Nicholls, A. G. Orpen, P. G. Pringle, S. Sostero and O. Traverso, *J. Chem. Soc. Chem Comm.*, 1990, 980.

36 D. E. Berry, K. A. Beveridge, J. Browning, G. W. Bushnell, and K. R. Dixon, *Can. J. Chem.*, 1986, **64**, 1903.

37 G. M. Gray and Y. Zhang, *J. Cryst. Spect. Res.*, 1993, 711.

38 K. G. Moloy and J. L. Petersen, *J. Am. Chem. Soc.*, 1995, **117**, 7696.

39 S. Vastag, B. Heil and L. Markó, *J. Mol. Cat.*, 1979, **5**, 189.

Chapter 3

Amine-Functionalised Phosphinoamines

3.0 Introduction

The chemistry of hemilabile amine-functionalised phosphines[1] is not as extensive as that of the analogous ether-functionalised ligands. This is in part due to the greater number of substitutionally inert *P,N*-chelates, which form due to the greater bonding ability of amino groups as compared with ether groups, for late transition metal centres.

The hemilabile coordination of amine-functionalised phosphine ligands such as $Ph_2PC_6H_4NMe_2$-2 has been shown to have potential catalytic implications. For example, the iridium(I)[2] and palladium(II)[3] complexes of amine-functionalised phosphines have been used to catalyse the chemoselective hydrogenation of α,β-unsaturated ketones, and the amination reactions of aryl halides respectively. In both these processes, the reversible coordination of the amine nitrogen is believed to be an important step in the catalytic mechanism.

The hemilabile properties of amine-functionalised phosphine ligands on coordination have been shown in the dynamic behaviour of *trans*-[RhCl{P(*i*-Pr)$_2$CH$_2$CH$_2$CH$_2$NMe$_2$-*P,N*}{P(*i*-Pr)$_2$CH$_2$CH$_2$CH$_2$NMe$_2$-*P*}],[4] in which the complex undergoes an exchange of bound and unbound amino groups at room temperature in a non-coordinating solvent (CD_2Cl_2).

3.1 Results and Discussion

3.1.1 Ligand Synthesis

The synthetic route for the preparation of $Ph_2PNMeCH_2CH_2NMe_2$ ($\mathbf{L^7}$) was based on that used to synthesise ether-functionalised phosphinoamines $\mathbf{L^1}$-$\mathbf{L^4}$ (Section 2.1.1). Deprotonation of the amine $Me_2NCH_2CH_2NHMe$ using NEt_3 followed by reaction with an equimolar quantity of Ph_2PCl in THF (Scheme 1) produced $\mathbf{L^7}$ in good yield. As was the case of the ether-functionalised phosphinoamines, care has to be taken to exclude water, in order to prevent the formation of $Ph_2PP(O)Ph_2$, which is catalysed by NEt_3.[5]

Scheme 1

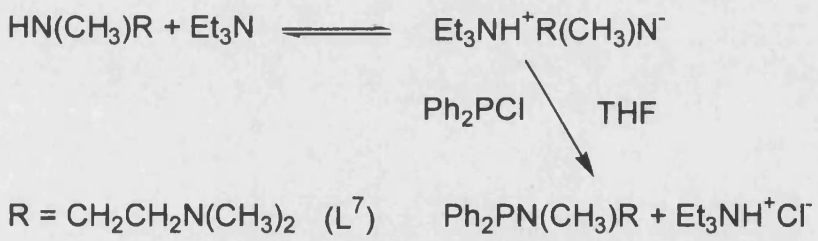

In contrast to this, the synthesis of $Ph_2PNHCH_2CH_2NMe_2$ ($\mathbf{L^8}$) required a different approach as the reaction of equimolar quantities of Ph_2PCl with the appropriate amine in the presence of NEt_3 led to a mixture of products as shown by the $^{31}P\{^1H\}$ NMR spectra. Comparison of the $^{31}P\{^1H\}$ NMR spectra of these products to that of $(Ph_2P)_2NCH_2CH_2OMe$ ($\mathbf{L^5}$) [δ(P) 65.1 ppm] suggested that $(Ph_2P)_2NCH_2CH_2NMe_2$ ($\mathbf{L^9}$) [δ(P) 64.2 ppm] was being formed in addition to $\mathbf{L^8}$, indicating that deprotonation of $\mathbf{L^8}$ occurs far more readily than seen previously for

Table 1 Selected $^{31}P\{^1H\}$, ^1H NMR and infrared data for compounds L^7-L^9.

	Compound	δ(P)/ppm	δ(NH) /ppm	δ(NCH_3) /ppm	ν(NH) /cm^{-1}
L^7	$Ph_2PN(CH_3)CH_2CH_2N(CH_3)_2$	65.4	-	2.52d, 2.17s	-
L^8	$Ph_2PNHCH_2CH_2N(CH_3)_2$	41.6	2.49m	2.08s	3370m
L^9	$(Ph_2P)_2NCH_2CH_2N(CH_3)_2$	64.2	-	-	-

L^1-L^4 (Section 2.1.1) under the same reaction conditions. The identity of L^9 was confirmed by the reaction of excess NEt_3 with $Me_2NCH_2CH_2NH_2$ and 2 equivalents of Ph_2PCl, which gave L^9 as the major product as observed from the $^{31}P\{^1H\}$ NMR spectra.

The alternative route to L^8 used *n*-butyllithium to deprotonate the amine at -78°C in THF, followed by reaction with Ph_2PCl. The reaction mixture was warmed to room temperature and the solvent removed under reduced pressure to give a waxy solid, from which extraction using cold diethyl ether gave L^8 as an oil in good yield (Scheme 2).

Scheme 2

$$H_2NR + BuLi \longrightarrow Li^+RHN^- \xrightarrow[THF]{Ph_2PCl} Ph_2PNHR + LiCl$$

$$R = CH_2CH_2N(CH_3)_2 \quad (L^8)$$

The ligands L^7 and L^8 were characterised using multinuclear NMR and infrared spectroscopy and microanalysis. The $^{31}P\{^1H\}$ NMR spectra for $L^7$and L^8

showed single phosphorus resonances at δ(P) 65.4 and 41.6 ppm respectively (Table 1). The $^{31}P\{^{1}H\}$ NMR chemical shift for $\mathbf{L^8}$ is similar to those of the ether-phosphinoamines $\mathbf{L^1}$-$\mathbf{L^3}$ which showed single phosphorus resonances in the range δ(P) 41-43 ppm (Section 2.1.1).

The ^{1}H NMR spectra for $\mathbf{L^7}$ and $\mathbf{L^8}$ were as expected: $\mathbf{L^7}$ gave signals for the methylene, methyl groups, and $\mathbf{L^8}$ showed signals for the methylene, methyl and NH groups (Table 1 & Experimental Section). The $^{13}C\{^{1}H\}$ NMR spectra for $\mathbf{L^7}$ and $\mathbf{L^8}$ showed the expected signals due to the diphenylphosphino unit, plus well-defined signals for the alkyl chain carbon atoms and methyl groups. The methylene carbons showed coupling [^{2}J(C,P) 11-21 Hz and ^{3}J(C,P) 6-7 Hz] to the phosphorus nucleus.

3.1.2 Complexes of the Amine-Functionalised Phosphinoamines

3.1.2.1 Synthesis of $[PtCl_2L_2]$ (L = $\mathbf{L^7}$ and $\mathbf{L^8}$)

The reaction of two equivalents of $\mathbf{L^7}$ and $\mathbf{L^8}$ with $[PtCl_2(cod)]$ in dichloromethane gave the complexes *cis*-$[PtCl_2(\mathbf{L^7})_2]$ (**43**) and *cis*-$[PtCl_2(\mathbf{L^8})_2]$ (**44**), though due to the difficulty in separating the products from the reaction mixtures the complexes were only isolated in yields of 50% and 70% respectively. Complexes **43** and **44** were characterised on the basis of microanalysis, multinuclear NMR and infrared spectroscopy.

Table 2. Selected $^{31}P\{^{1}H\}$, ^{1}H NMR and infrared data for complexes **43-45**.

	Complex	δ(P) /ppm	$^{1}J(P,Pt)$ /Hz	δ(NH) /ppm	$\delta(NCH_3)$ /ppm	ν(NH) /cm^{-1}
43	*cis*-$[PtCl_2(\mathbf{L}^7)_2]$[a]	50.1	3904	-	2.51d, 2.39s	-
44	*cis*-$[PtCl_2(\mathbf{L}^8)_2]$[b]	36.8	3906	4.69br	2.12br	3370
45	*cis*-$[PtCl_2(\mathbf{L}^7\text{-}P,N)]$[c]	32.8	4175	-	3.12br, 2.38d	-

(a = CD_2Cl_2, b = d^6-acetone, c = $CDCl_3$)

On cooling **43** from 25°C to -78°C in d^2-dichloromethane, the $^{31}P\{^{1}H\}$ NMR spectra showed that the original broad singlet with platinum satellites was split to give a pair of broad signals each with platinum satellites (Table 3 and Figure 1). Although the signals were too broad to resolve the $^{2}J(P,P)$ coupling, the relative intensities suggest the signals result from inequivalent phosphorus atoms in the same species. The difference in the two $^{1}J(P,Pt)$ values can be ascribed to a phosphine *trans* to a chloride [$^{1}J(P_a,Pt)$ = 4209 Hz], and *trans* to an amine[6] [$^{1}J(P_b,Pt)$ = 3202 Hz] respectively. This suggests that the phosphines are mutually *cis* which is consistent with the formation of the complex *cis*-$[PtCl(\mathbf{L}^7\text{-}P,N)(\mathbf{L}^7\text{-}P)]Cl$. It has previously been demonstrated that the amino group in *cis*-$[PtCl_2\{PPh_2(CH_2)_nNMe_2\}_2]$ (n = 2 and 3)[7] can displace a chloride when a 5-membered chelate ring (n = 2) results, but not when a 6-membered chelate ring (n = 3) would be formed.

Figure 1

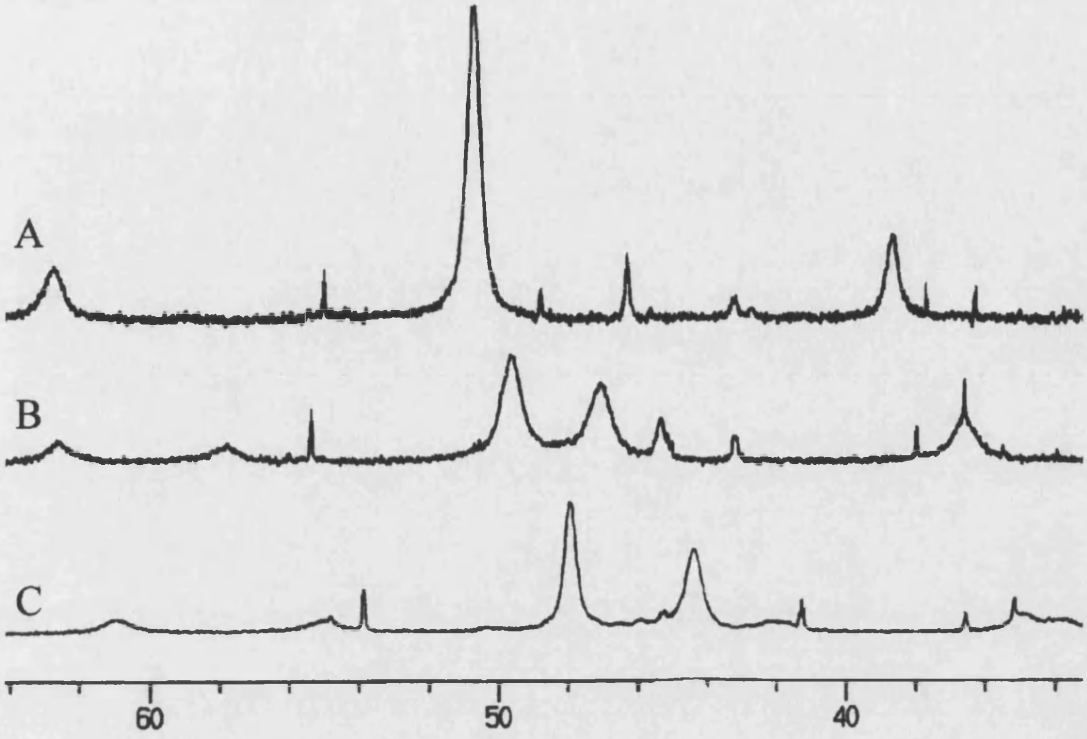

(A = +25, B = -25 and C = -50°C)

Table 3. Selected low temperature $^{31}P\{^{1}H\}$ NMR data for complex **43**.

Temp./°C	$\delta(P_a)$ /ppm	$^{1}J(P_a,Pt)$ /Hz	$\delta(P)$ /ppm	$^{1}J(P,Pt)$/ Hz	$\delta(P_b)$ /ppm	$^{1}J(P_b,Pt)$ /Hz	$^{2}J(P_a,P_b)$ /Hz
25			50.1	3899			-
-50	49.5	4206			46.9	3202	-

The $^{31}P\{^{1}H\}$ NMR spectra for *cis*-$[PtCl_2(\mathbf{L}^8)_2]$ (**44**) shows a single broad phosphorus resonance with platinum satellites at room temperature (Table 2), with the width of the signals dependent on the solvent. In acetone the signals were well resolved but in dichloromethane and chloroform the linewidth was much greater. The

chemical shift of **44** is similar to the complexes of the ether-functionalised phosphinoamines described in section 2.1.2.1.2.

Table 4. Selected low temperature $^{31}P\{^{1}H\}$ NMR data for complex **44**.

Temp./°C	$\delta(P_a)$ /ppm	$^{1}J(P_a,Pt)$ /Hz	$\delta(P)$ /ppm	$^{1}J(P,Pt)$/ Hz	$\delta(P_b)$ /ppm	$^{1}J(P_b,Pt)$ /Hz	$^{2}J(P_a,P_b)$ /Hz
25			35.1	3936			
0	38.4		35.0	3930	32.7		
-20	38.4	3951	34.9	3930	30.4	3593	
-40	38.4	3953	34.7	3914	29.9	3601	18
-60	38.1	3961	34.0	3936	29.0	3581	12

As with **43,** cooling **44** in d^2-dichloromethane resulted in the appearance of a pair of signals each with platinum satellites (Table 4 and Figure 2). The low temperature $^{31}P\{^{1}H\}$ NMR spectra showed that the original broad singlet with platinum satellites was retained but on cooling to -60°C the intensity of the signal was considerably diminished whilst the intensity of the new pair of signals increased. At these low temperatures, the new signals both split into doublets suggesting coupling between the two inequivalent phosphorus atoms. Due to the large linewidths the value of $^{2}J(P,P)$ could only be approximately calculated [$^{2}J(P,P)$ = 18 Hz], this small value for $^{2}J(P,P)$ is indicative of the phosphinoamines being mutually *cis*.[8] The difference in the two $^{1}J(P,Pt)$ values suggest that one of the phosphine is *trans* to a chloride [$^{1}J(P_a,Pt)$ = 3953 Hz], whilst the other is *trans* to an amine [$^{1}J(P_b,Pt)$ = 3601 Hz] as

Figure 2

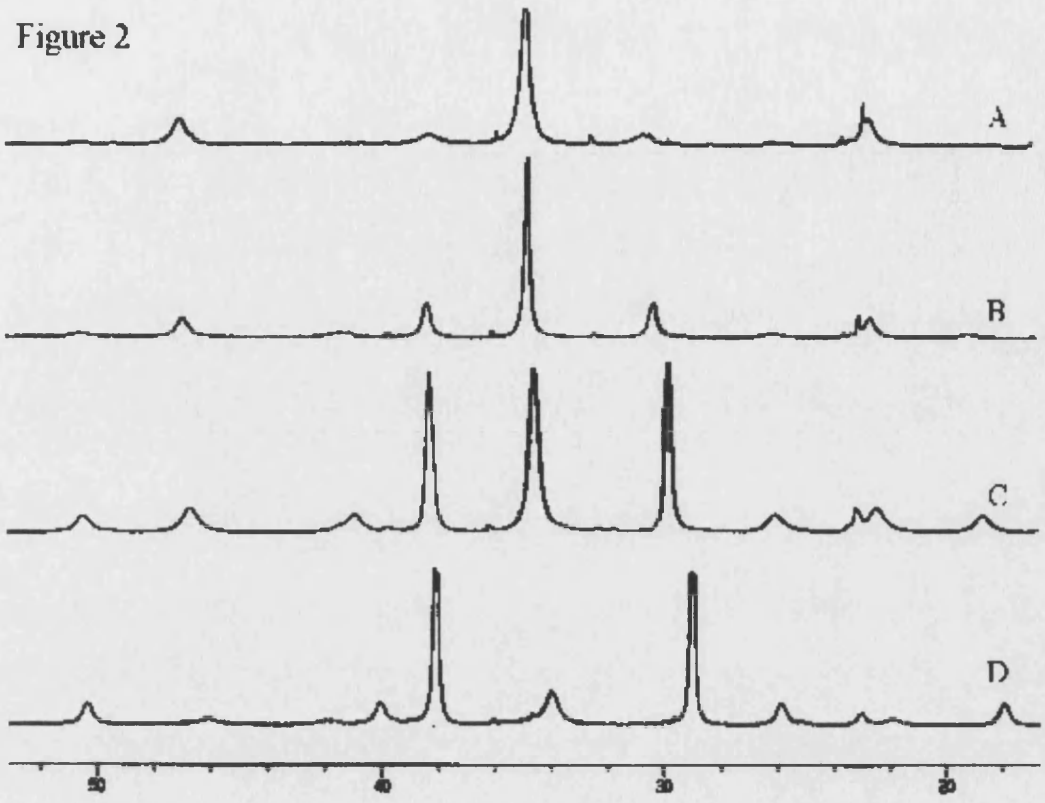

(A = 0, B = -20, C = -40 and D = -60 °C)

observed previously in **43.** This data is consistent with the formation of the cationic complex *cis*-[PtCl(**L**^{8}-*P,N*)(**L**^{8}-*P*)]Cl at low temperatures (Scheme 3). The rate of exchange at low temperature between the two complexes in Scheme 3 is sufficiently slow within the NMR timescale to allow the two separate species to be observed.

Scheme 3

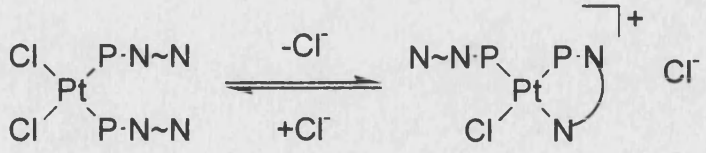

The ^{1}H NMR spectrum of **43** showed the expected signals with distinctive peaks for the methylene and methyl protons. In contrast the ^{1}H NMR spectrum of **44**

showed considerable broadening of the proton resonances so making assignment of the spectra difficult, this is consistent with the ligands undergoing a fluxional process.

The low temperature $^{31}P\{^{1}H\}$ NMR studies of **43** and **44** both show the formation of a 6-membered *P,N*-chelate consistent with the formation of the cationic complex *cis*-[Pt(**L**-*P,N*)(**L**-*P*)]Cl. This stabilisation of a chelating bidentate phosphine has previously been observed at low temperatures for phosphino alcohol platinum(II) complexes (e.g. $[PtCl_2\{PPh_2CH_2C(CH_3)_2OH\}_2]$).[8] At room temperatures these complexes exhibit fluxionality but on cooling the chelate structure forms, in which one of the alcohol oxygen atoms is coordinated to the metal.

The $^{31}P\{^{1}H\}$ NMR spectra of the crude sample of **43** showed two distinct phosphorus resonances with platinum satellites, one gave a broad signal indicating fluxionality, while the other signal was well resolved. These two sets of peaks were attributed to the complexes *cis*-$[PtCl_2(\mathbf{L}^7)_2]$ (**43**) and *cis*-$[PtCl_2(\mathbf{L}^7\text{-}P,N)]$ (**45**) (see below).

The reaction of $[PtCl_2(cod)]$ with one equivalent of $\mathbf{L}^7$ in dichloromethane gave *cis*-$[PtCl_2(\mathbf{L}^7\text{-}P,N)]$ (**45**) quantitatively. This was characterised on the basis of microanalysis, multinuclear NMR and infrared spectroscopy. The $^{31}P\{^{1}H\}$ NMR spectra (Table 2) showed a singlet with platinum satellites [δ(P) 32.8 ppm, ^{1}J(P,Pt) 4175 Hz], which match those of the well resolved component observed in the crude sample of **43** [δ(P) 32.8 ppm, ^{1}J(P,Pt) 4179 Hz]. The ^{1}H NMR shows evidence of the coordination of the tertiary amine nitrogen atom, with the chemical shift of the methyl protons deshielded relative to **43** (Δδ = 0.73 ppm for **45** with respect to **43**).

3.1.2.1.1 Abstraction of Chloride from *cis*-[$PtCl_2(L^8)_2$]

The low temperature studies on complexes **43** and **44** showed that the amine nitrogen of amine-functionalised phosphinoamines was sufficiently nucleophilic to displace a chloride so forming a 6-membered *P,N*-chelate ring. This was in marked contrast to complexes containing ether-functionalised phosphinoamines (Section 2.1.2.1.4.1) which required chloride abstraction using Ag^+ to provide a vacant site to which the ether oxygen could coordinate.

In order to examine the bidenate coordination of the amine-functionalised phosphinoamine ($\mathbf{L^8}$), the complex *cis*-[$PtCl_2(\mathbf{L^8})_2$] (**44**) was reacted with excess $TlPF_6$ or $NaBF_4$.

Table 5. Selected $^{31}P\{^1H\}$, ^1H NMR and infrared data for complexes **46-47**.

	Complex	δ(P) /ppm	^1J(P,Pt) /Hz	δ(NH) /ppm	δ(NCH_3) /ppm	ν(NH) /cm^{-1}
46	*cis*-[PtCl($\mathbf{L^8}$-*P,N*)($\mathbf{L^8}$-*P*)]PF_6	40.3	4038	3.32m	2.06s	3367,
		33.2	3587		2.99d	3212
47	*cis*-[PtCl($\mathbf{L^8}$-*P,N*)($\mathbf{L^8}$-*P*)]BF_4	40.2	4008	3.31br	1.97s	3436,
		32.8	3595		2.96br	3280

Reaction of **44** with excess $TlPF_6$ in dichloromethane gave in good yield the complex *cis*-[PtCl($\mathbf{L^8}$-*P,N*)($\mathbf{L^8}$-*P*)]PF_6 (**46**). The $^{31}P\{^1H\}$ NMR spectra (Figure 3) showed two doublets each with platinum satellites (Table 5), plus a septet due to the PF_6^- counter ion [δ(P) 69.5 ppm, -143.6 ppm, sep, ^1J(P,F) 711 Hz]. ^1J(P,Pt) values are similar to those observed in the low temperature spectra of **43** and **44**, suggesting that

one of the phosphines is *trans* to a chloride [$^1J(P_a,Pt)$ 4038 Hz], whilst the other is *trans* to an amine [$^1J(P_b,Pt)$ 3587 Hz].

Figure 3

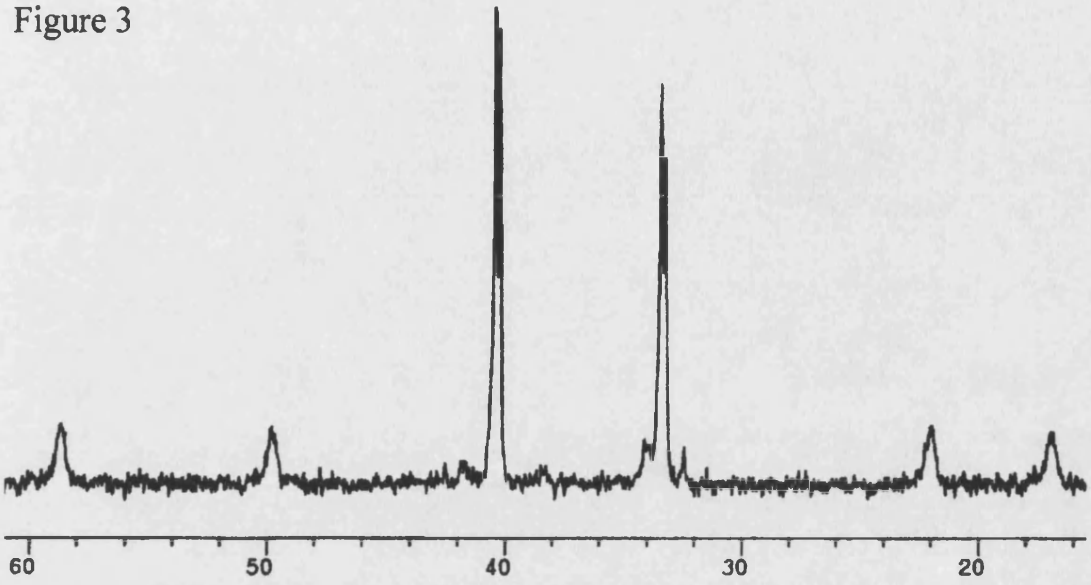

The ^1H NMR spectra of **46** show two resonances for $\delta(NCH_3)$, separated by approximately 0.9 ppm. Comparison of these values with those of **44** ($\Delta\delta$ = 0.87 ppm and -0.06 ppm for **46** with respect to **44**) shows significant deshielding of one of the amine methyl groups. The complex $[Pt\{PPh_2(C_6H_4)N(CH_3)_2\text{-}2\}_2](ClO_4)_2$ showed a similar downfield shift in the ^1H NMR spectrum for the methyl protons of the amine group on coordination of the amine nitrogen.[9] This indicates that the nitrogen atom of one of the amine groups is coordinated to the metal, while the other amine group remains uncoordinated. The infrared spectra showed two weak bands for $\nu(NH)$ and a strong band for $\nu(PF_6)$.

Even in the presence of excess $TlPF_6$, the second chloride was not abstracted. A similar observation was previously made with the complex *cis*-$[PtCl\{PPh_2(CH_2)_3N(CH_3)_2\}_2]BF_4$,[7] this lack of reactivity was attributed to the difficulty in forming two 6-membered chelate rings using this type of ligand. A search

of the Cambridge Structural Database[10] confirmed there are no examples of the dication $[Pt(\mathbf{L}\text{-}P,N)_2]^{2+}$ that have been crystallographically characterised.

A 10 fold excess of $NaBF_4$ was reacted with a methanol/water solution of **44**, to give *cis*-$[PtCl(\mathbf{L}^8\text{-}P,N)(\mathbf{L}^8\text{-}P)]BF_4$ (**47**) which was characterised by NMR and infrared spectroscopy. As with **46** the $^{31}P\{^1H\}$ NMR spectra showed the formation of a pair of doublets with platinum satellites (Table 5). The δ(P) and $^1J(P,Pt)$ are similar to **46** indicating the amine-functionalised phosphinoamines ($\mathbf{L}^8$) are arranged mutually *cis*, with one of the ligands forming a 6-membered *P,N*-chelate ring. The ^1H NMR spectrum matches that of **46** with two resonances for $\delta(NCH_3)$, separated by approximately 1 ppm. The $\delta(NCH_3)$ as in **46,** indicates that the nitrogen atom of one of the amine groups is coordinated to the metal, while the other amine group remains uncoordinated ($\Delta\delta$ = 0.84 ppm and -0.15 ppm for **47** with respect to **44**). The infrared spectrum for **47** showed two weak bands for ν(NH) and a strong broad band for $\nu(BF_4)$.

The sharpness of the $^{31}P\{^1H\}$ NMR spectra of **46** and **47** is in contrast to the broad signals observed for **44,** suggesting that removal of the chloride stops the fluxionality. This supports the theory that the fluxional processes involve the reversible coordination of chloride.

As with the ether-functionalised phosphinoamine complexes (Section 2.1.2.1.4.3) coordination stabilised the amine-functionalised phosphinoamine $\mathbf{L}^8$ to methanolysis and hydrolysis as observed during the synthesis of **47** in which the $^{31}P\{^1H\}$ NMR of the crude product showed the absence of any decomposition products after 1 hour.

3.1.2.2 Synthesis of [M(dmba)Cl(L^7)] (M = Pd and Pt)

Complexes of the type [M(dmba)Cl(L)] containing an amine-functionalised phosphinoamine ($\mathbf{L^7}$) were synthesised to allow comparison of their properties and reactions with respect to those of the related ether-functionalised phosphinoamine complexes **18-24** (Section 2.1.2.2). The reaction of two equivalents of $\mathbf{L^7}$ with $[M(dmba)(\mu\text{-}Cl)]_2$ (M = Pd, Pt) gave the complexes [Pd(dmba)Cl($\mathbf{L^7}$)] (**48**) or [Pt(dmba)Cl($\mathbf{L^7}$)] (**49**). The $^{31}P\{^1H\}$ NMR spectra of both the reaction mixtures showed that **48** and **49** were only formed in moderate yields with other products also formed.

Table 6. Selected $^{31}P\{^1H\}$, ^1H NMR and infrared data for complexes **48-51**.

	Complex	δ(P) /ppm	^1J(P,Pt) /Hz	δ($PNCH_3$) /ppm	δ(NCH_3) /ppm
48	[Pd(dmba)Cl($\mathbf{L^7}$)]	93.2br	-	2.66d, ^3J(H,P) 10 Hz	2.15s
49	[Pt(dmba)Cl($\mathbf{L^7}$)]	66.4	4618	2.75d, ^3J(H,P) 11 Hz	2.14s
	minor component	80.3	2126		
50	[Pt(dmba)($\mathbf{L^7}$-*P,N*)]PF_6	51.2	4880	2.44d, ^3J(H,P) 9 Hz	2.92s
51	[Pt(dmba)($\mathbf{L^7}$-*P,N*)]BF_4	51.2	4876	2.44d, ^3J(H,P) 9 Hz	2.90s

The $^{31}P\{^1H\}$ NMR spectra of **48** showed a single broad phosphorus resonance suggesting fluxionality, in marked contrast to the ether-functionalised phosphinoamine analogues, which gave sharp signals. Unfortunately solutions of complex **48** in dichloromethane were found to decompose, and as a result it could not be isolated and purified.

The $^{31}P\{^{1}H\}$ NMR spectra of **49** showed a single phosphorus resonance with $^{1}J(P,Pt)$ of 4618 Hz (Table 6). The large value of $^{1}J(P,Pt)$ suggests the phosphine is *trans* to the nitrogen atom of dmba.[11] The observed $^{4}J(H,P)$ coupling between the phosphorus and the methyl and methylene protons of dmba in the ^{1}H NMR spectrum is also consistent with this arrangement [$^{4}J(CH_3,P) \approx 3$ Hz, $^{4}J(CH_2,P) \approx 3$ Hz].

$^{31}P\{^{1}H\}$ NMR spectra of crude samples of **49** showed the presence of an additional compound [δ(P) 80.3 ppm, $^{1}J(P,Pt)$ 2126 Hz] (Figure 4). The value of $^{1}J(P,Pt)$ suggests this to be due to the isomer with the phosphinoamine *trans* to the carbon of dmba.

Figure 4

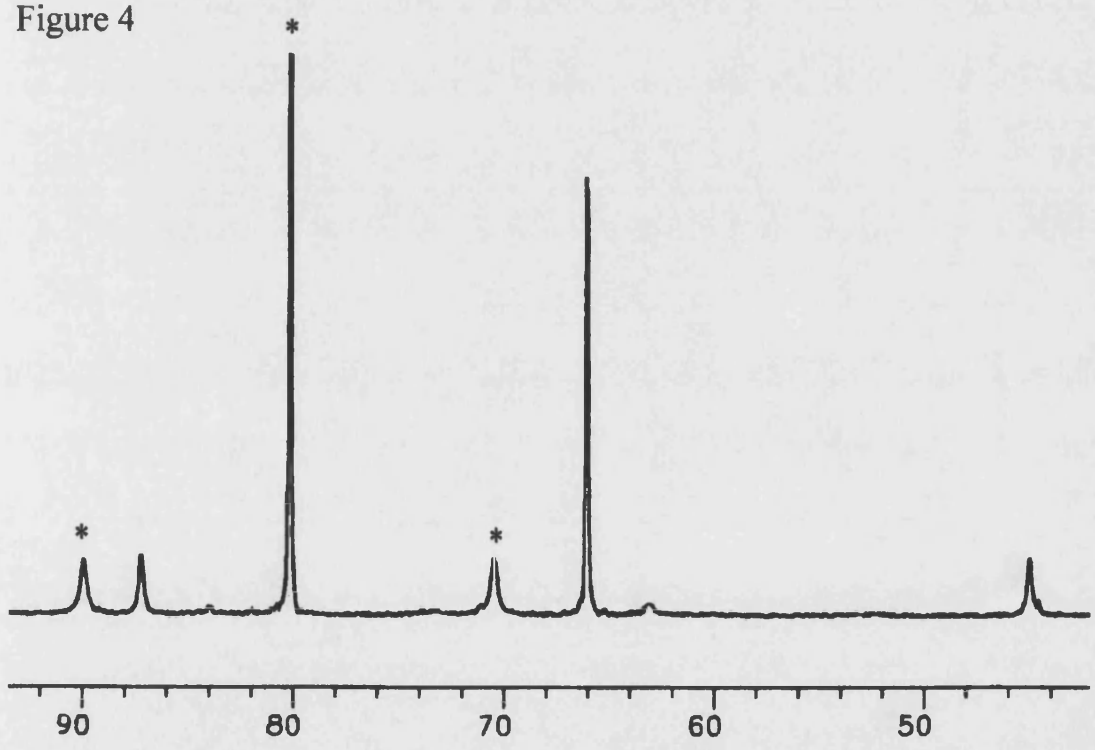

(Peaks marked with * due to isomer with the phosphinoamine *trans* to the carbon of dmba)

3.1.2.2.1 Abstraction of Chloride from [Pt(dmba)Cl(L^7)]

The potential bidentate coordination of the amine-functionalised phosphinoamine was examined by reacting the complex [Pt(dmba)Cl(L^7)] with $AgBF_4$ and $TlPF_6$. A slight excess of $AgBF_4$ or $TlPF_6$ was reacted with the complex [Pt(dmba)Cl(L^7)] in dichloromethane with the resulting complexes characterised as [Pt(dmba)(L^7-*P,N*)]X [X = BF_4 (**50**) and PF_6 (**51**)] on the basis of multinuclear NMR and infrared spectroscopy (Table 6).

The $^{31}P\{^1H\}$ NMR spectra of [Pt(dmba)(L^7-*P,N*)]X show single phosphorus resonances with $^1J(P,Pt)$ of approximately 4880 Hz, as well as a septet due to the PF_6^- counter ion in complex **51**.

The ^1H NMR spectra of **50** and **51** show that the methyl protons of the amine group are deshielded [$\Delta\delta$ = 0.78 for **50** with respect to **49**, and 0.76 for **51** with respect to **49**]. This downfield shift is consistent with the amine nitrogen coordinating to the metal as observed earlier for complexes of the type *cis*-[PtCl(L^8-*P,N*)(L^8-*P*)]PF_6 (Section 3.1.2.1.1) and is similar to that observed for [Pt(dmba)(L-*P,O*)]BF_4 [L = L^1 (**25**) and L^4 (**26**)] (Section 2.1.2.2.4.1).

3.1.2.3 Formation of *cis*-[Pt(L^7-*P,N*)(μ-L^7)$CoCl_3$]

The presence of four uncoordinated nitrogen atoms in the complex [$PtCl_2(PPh_2N\{CH_3\}CH_2CH_2N\{CH_3\}_2)_2$] (**43**) provides the potential for the further coordination of a first row transition metal (Figure 5). The structures of the complexes containing ether-functionalised phosphinoamines (Chapter 2) showed the nitrogen atom bonded to the phosphorus was significantly sp^2-hybridised, as a consequence of this, for coordination to this atom to occur a change in hybridisation would be required.

Figure 5

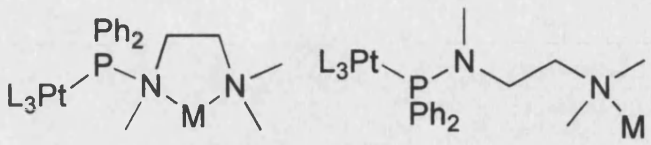

In order to examine the potential coordination of the nitrogen donor groups, the complex *cis*-[$PtCl_2(\mathbf{L}^7)_2$] (**43**) was reacted with one equivalent of $CoCl_2 \cdot 6H_2O$ or $ZnCl_2 \cdot 6H_2O$ in acetone. The solvent was removed from the reaction mixture to give a blue or colourless solid respectively, from which extraction using dichloromethane followed by recrystallisation gave a product which contained a 1:1 ratio of **43** and MCl_2 (M = Co or Zn) as determined by elemental analysis. Unfortunately multinuclear NMR spectroscopy was of limited help in characterising these compounds due to the cobalt complex being paramagnetic and the zinc compound giving very broad signals.

The cobalt complex crystallised from dichloromethane-diethyl ether and was isolated as blue block shaped crystals suitable for X-ray crystallography. From analysis of these crystals the complex was revealed to be the bimetallic species *cis*-[$Pt(\mathbf{L}^7\text{-}P,N)(\mu\text{-}\mathbf{L}^7)CoCl_3$] (**52**). The highest observed peak in the FAB mass spectrum of complex **52** was at *m/z* 803 for $[M - CoCl_3]^+$.

The blue colour of **52** in the solid state and in dichloromethane is indicative of tetrahedral cobalt. On addition of excess methanol to a solution of **52** in dichloromethane a rapid colour change to pink was observed. This can be attributed to the coordination of the two methanol molecules to the cobalt centre to give an octahedral geometry. This coordination of methanol was found to be reversible, with the blue complex reforming after removal of the solvent under reduced pressure.

3.1.2.3.1 X-ray Crystal Structure of *cis*-[Pt(L^7-*P,N*)(μ-L^7)$CoCl_3$] (52)

The crystal structure revealed that complex **52** was a bimetallic species with the cobalt coordinated to the terminal nitrogen of one of the amine-functionalised phosphinoamines while the nitrogen of the second terminal amine group coordinated to the platinum to give a 6-membered *P,N*-chelate ring (Figure 6). Selected bond lengths and angles are given in Table 7.

Table 7. Selected bond lengths [Å] and angles [°] for **52**.

Pt(1)-N(2)	2.167(5)	Co(1)-Cl(3)	2.214(2)
Pt(1)-P(1)	2.247(2)	Co(1)-Cl(4)	2.246(2)
Pt(1)-P(2)	2.271(2)	Co(1)-Cl(5)	2.249(2)
Pt(1)-Cl(1)	2.365(2)	P(1)-N(1)	1.673(5)
Co(1)-N(4)	2.118(6)	P(2)-N(3)	1.657(5)
N(2)-Pt(1)-P(1)	90.85(13)	N(4)-Co(1)-Cl(3)	104.8(2)
N(2)-Pt(1)-P(2)	170.38(13)	N(4)-Co(1)-Cl(4)	108.7(2)
P(1)-Pt(1)-P(2)	97.44(6)	Cl(3)-Co(1)-Cl(4)	115.71(10)
N(2)-Pt(1)-Cl(1)	88.23(13)	N(4)-Co(1)-Cl(5)	106.9(2)
P(1)-Pt(1)-Cl(1)	169.30(6)	Cl(3)-Co(1)-Cl(5)	113.91(9)
P(2)-Pt(1)-Cl(1)	84.53(6)	Cl(4)-Co(1)-Cl(5)	106.44(8)

The platinum centre in **52** is distorted square-planar with *cis* angles between 84.53(6) and 97.44(6)°. The two phosphorus atoms are arranged mutually *cis*.

The Pt-P, Pt-N and Pt-Cl bond distances in complex **52** are unremarkable.[12] One feature of the Pt-P bonds is the significantly longer Pt(1)-P(2) bond *trans* to the tertiary amine nitrogen relative to the Pt(1)-P(1) bond *trans* to chloride [Pt(1)-P(1)

2.247(2) Å and Pt(1)-P(2) 2.271(2) Å]. This maybe indicative of the greater *trans* influence of the tertiary amine compared to a chloride, though steric crowding may also be a factor.

Figure 6

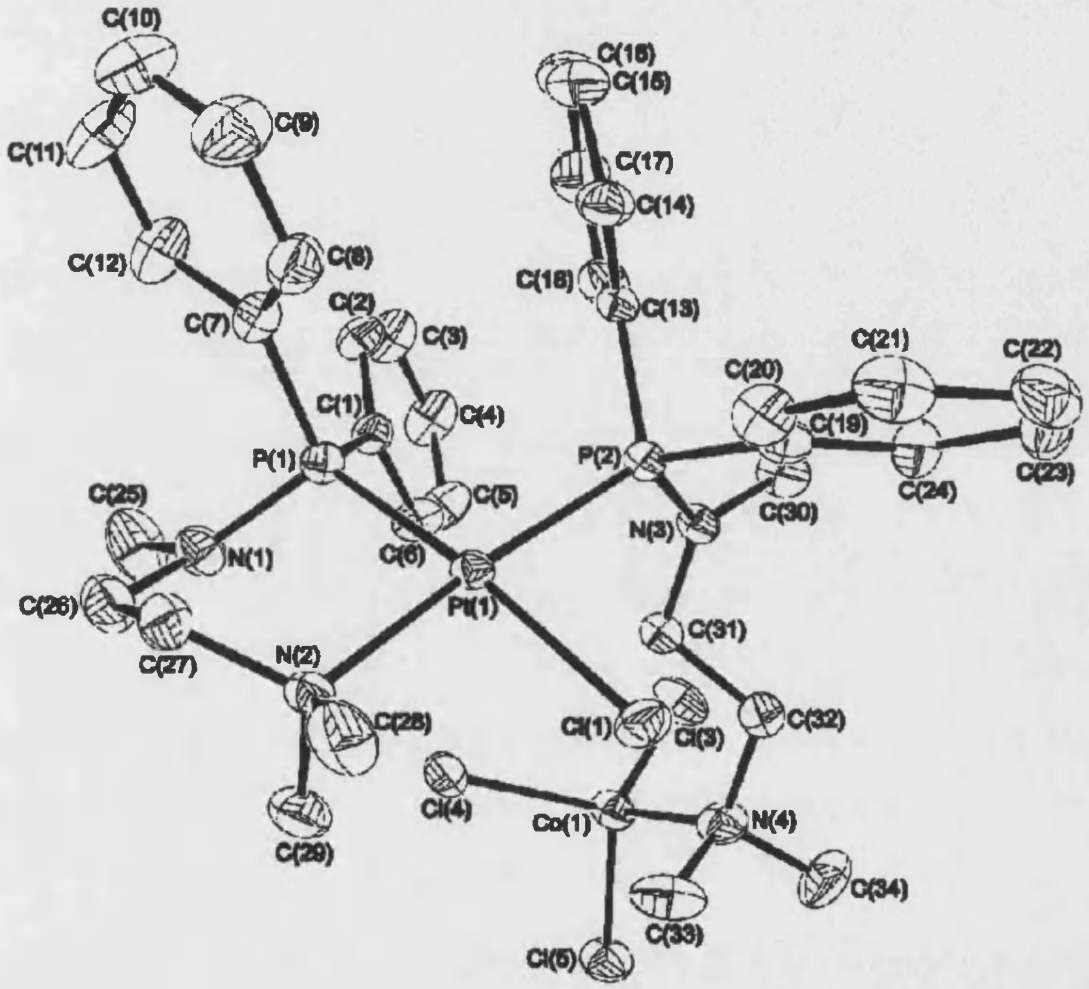

The P-N bond distances in complex **52** [P(1)-N(1) 1.673(5) Å and P(2)-N(3) 1.657(5) Å] are similar to those observed in the complexes containing ether-functionalised phosphinoamines [range of P-N bond distances = 1.616-1.680 Å (Chapter 2)], and are shorter than the generally accepted range for P-N single bonds (*e.g.* 1.689-1.727 Å in *N*-piperidinophosphines[13]). The sum of the angles around the

N(1) and N(3) atoms is 354° and 360° respectively, showing as with the ether-functionalised phosphinoamine complexes, significant sp^2 character of the nitrogen.

The cobalt(II) centre in **52** is distorted tetrahedral with *cis* angles between 104.8(2) and 115.71(10)°, with three chloride ligands and a tertiary amine ligand. The Co-N and Co-Cl bond distances in complex **52** are similar to the expected values for a Co-N bond to a tertiary amine and a Co-Cl bond.[12]

Comparison of the Co-Cl bond distances in **52** with reported structures of tetrahedral coordinated cobalt(II) having a 3Cl + 1N coordination donor set, shows that two of the Co-Cl bond distances [Co(1)-Cl(4) 2.246(2) Å and Co(1)-Cl(5) 2.249(2) Å] are within the observed range of 2.22-2.26 Å[14] whilst the Co(1)-Cl(3) [2.214(2) Å] is significantly shorter. The Co-N bond [Co(1)-N(4) 2.118(6) Å] is significantly longer than the observed range of 2.02-2.05 Å[14] for Co-N distances.

The combination of a positive charge on the platinum(II) and a negative charge on the cobalt(II) results in the complex being zwitterionic. The presence of the positive and negative charges on the metal centres may explain the ordering observed within the crystal lattice in which molecules of **52** stack along the *b* axis with intermolecular Pt···Co distances of 6.3 Å, similar to those observed within the molecule (6.0 Å). Closer intermolecular contact of the metal centres is prevented by the presence of the phenyl groups.

3.1.2.4 Synthesis of $[Pt(O_2C_6H_3{}^tBu)(L^7)_2]$

In order to prevent the ligand L^7 from forming 6-membered *P,N*-chelates, complexes in which both chlorides were replaced by a bidentate ligand were prepared. *t*-Butyl catechol was used as a bidentate dicationic *O,O*-donor ligand precursor,

replacing the chlorides with a 5-membered chelate ring. This would remove any possible fluxional process involving the labile chloride ligands.

Two equivalents of $\mathbf{L}^7$ were reacted with [Pt($O_2C_6H_3{}^tBu$-4)(cod)] in dichloromethane, to give [Pt($O_2C_6H_3{}^tBu$)($\mathbf{L}^7$)$_2$] (**53**) in good yield. This complex was characterised on the basis of microanalysis, infrared and multinuclear NMR spectroscopy (see Experimental Section).

The $^{31}P\{^1H\}$ NMR spectra of **53** showed two sets of doublets each with platinum satellites as expected for complexes containing two inequivalent phosphorus atoms (Table 8). The external signal of both doublets was attenuated while the internal signals were enhanced (Figure 7) this roof effect is typical of a simple AB system, in which the coupling constant is of similar magnitude to the difference in the chemical shift between the two nuclei. The inequivalence is due to the unsymmetrical nature of *t*-butyl catechol (Figure 8).

Table 8. Selected $^{31}P\{^1H\}$, ^1H NMR and infrared data for complex **53**.

	Complex	δ(P) /ppm	^1J(P,Pt) /Hz	δ($PNCH_3$) /ppm	δ(NCH_3) /ppm
53	*cis*-[Pt($OC_6H_3{}^tBu$)($\mathbf{L}^7$)$_2$]	55.4 54.5	3796 3800	2.83m	2.12s, 2.15s

The ^1H NMR spectrum of **53** was as expected with distinctive signals for the methylene and methyl groups. The inequivalence caused by the *t*-butyl catechol results in two resonances for the methylene and methyl protons respectively, though overlap of the methylene signals obscures this small separation.

Figure 7

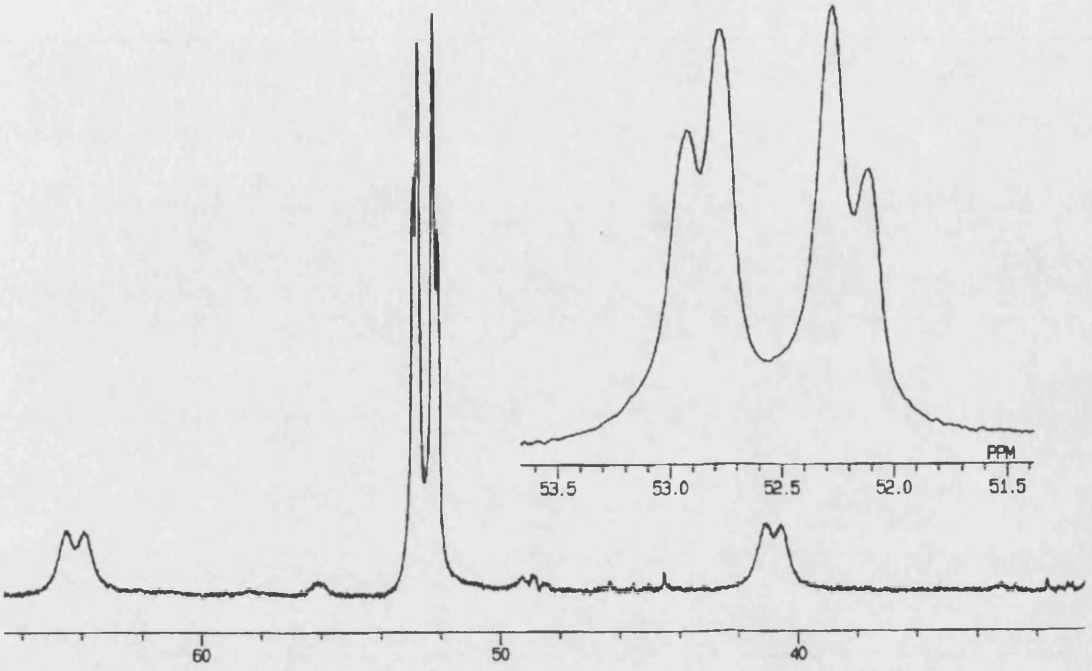

Figure 8

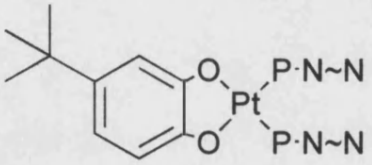

In order to examine the potential coordination of the nitrogen donor groups, **53** was reacted with one equivalent of $CoCl_2 \cdot 6H_2O$ in methanol. Analysis of the isolated product by elemental analysis and infrared spectroscopy showed that unexpectedly complex **52** had been formed. This suggested that the reaction of **53** with $CoCl_2 \cdot 6H_2O$ resulted in the cleavage of Pt-O bonds, with a chloride being transferred from the cobalt to the platinum.

3.1.2.5 Synthesis of [RhCl(CO)(L^8-*P,N*)] and [RhCl(CO)(L^8)$_2$]

The reaction of two and four equivalents of L^8 with [Rh(μ-Cl)(CO)$_2$]$_2$ in dichloromethane resulted in the rapid evolution of CO gas, with the formation in good yield of the complex [RhCl(CO)(L^8-*P,N*)] (**54**) and *trans*-[RhCl(CO)(L^8)$_2$] (**55**) respectively. These compounds were characterised on the basis of infrared and multinuclear NMR spectroscopy (see Experimental Section).

The $^{31}P\{^1H\}$ NMR spectra of **54** and **55** show a doublet with $^1J(P,Rh)$ of 181 and 128 Hz respectively. The $^1J(P,Rh)$ of **54** and **55** are typical of a phosphorus *trans* to a chloride, and a phosphorus *trans* to a phosphorus respectively.[11] The coupling constant associated with **55** is similar to those previously observed for the equivalent ether-functionalised phosphinoamine complexes (Section 2.1.2.4) The ^1H NMR spectra of **54** and **55** were as expected with distinctive signals for the NH, methylene and methyl groups. Evidence to support the formation of a 6-membered *P,N*-chelate ring in **54** is observed in the ^1H NMR spectra, where the chemical shifts show deshielding of the amine methyl protons ($\Delta\delta$ = 0.36 ppm for **54** with respect to **55**)

Table 9. Selected $^{31}P\{^1H\}$, ^1H NMR and infrared data for complexes **54-55**.

	Complex	δ(P) /ppm	$^1J(P,Rh)$ /Hz	δ(NH) /ppm	δ(NCH_3) /ppm	ν(CO) /cm^{-1}
54	*trans*-[RhCl(CO)(L^8-*P,N*)]	75.7	181	2.96m	2.55s	1988[a], 1995[b]
55	*trans*-[RhCl(CO)(L^8)$_2$]	59.9	128	4.26m	2.19s	1976[b]

(a = KBr, b = CH_2Cl_2)

and methylene protons. Similar deshielding of the methyl and methylene protons was observed in the platinum(II) complexes **50** and **51**.

The infrared spectra of **54** and **55** show one band for ν(CO) consistent with only one carbonyl group in **54,** and the *trans* geometry of **55**.

From the estimated value for ν(CO) of 2068.5 cm^{-1} for the $[Ni(CO)_3(\mathbf{L^8})]$ (A_1 band) obtained using the reported correlation between ν(CO) for *trans*-$[RhCl(CO)(PR_3)_2]$ and $[Ni(CO)_3(PR_3)]$ (A_1 band),[15] the electronic substituents contribution χ_i for the $-NHCH_2CH_2NMe_2$ group can be estimated as $\chi_i = 3.8$ using Equation 1 (Section 2.1.2.4.2).[16] Comparison of this with the values of χ_i estimated for the ether-functionalised phosphinoamines complexes *trans*-$[RhCl(CO)L_2]$ (L = $\mathbf{L^1}$ and $\mathbf{L^3}$) (Section 2.1.2.4.2) shows that the electronic substituents contribution of the amine-functionalised amine group in $\mathbf{L^8}$ is slightly smaller than χ_i for the phenyl and ether-functionalised amine groups.

3.2 Conclusions

As with the ether-functionalised phosphinoamines, $Ph_2PNMeCH_2CH_2NMe_2$ ($\mathbf{L^7}$) could easily be synthesised in good yield and purity. In contrast, the synthesis of $Ph_2PNHCH_2CH_2NMe_2$ ($\mathbf{L^8}$) was complicated by the ease in which this product could be deprotonated, which resulted in a mixture of the ligand $\mathbf{L^8}$ and $(Ph_2P)_2NCH_2CH_2NMe_2$ ($\mathbf{L^9}$). An alternative synthetic strategy was developed for $\mathbf{L^8}$ using the low temperature deprotonation of the amine with BuLi followed by reaction with Ph_2PCl to give the desired product without contamination by $\mathbf{L^9}$

The phosphinoamines $\mathbf{L^7}$ and $\mathbf{L^8}$ have been shown to readily coordinate to Pt(II), though in a number of these complexes the broad signals observed in the $^{31}P\{^1H\}$ and ^1H NMR spectra indicated the complexes were fluxional.

The relative ease in which 6-membered *P,N*-chelate rings formed is in contrast to the difficulty in forming 6-membered *P,O*-chelate rings in complexes containing the ether-functionalised phosphinoamines. The ability of the amino functionalised phosphinoamines to coordinate via both the phosphorus and the nitrogen groups was observed in both the synthesis of *cis*-[$PtCl_2(\mathbf{L^7}$-*P,N*)] (**45**) and the mixed metal species [$Pt(\mathbf{L^7}$-*P,N*)(μ-$\mathbf{L^7}$)$CoCl_3$] (**52**). These observations are all consistent with the greater bonding ability to late transition metal centres of the amino groups compared with the equivalent ether groups.

3.3 References

1 C. S. Slone, D. A. Weinberger and C. A. Mirkin, *Prog. Inorg. Chem.*, 1999, **48**, 233.

2 E. Farnetti, G. Nardin and M. Graziani, *J. Organomet. Chem.*, 1991, **417**, 163.

3 X. Bei, T. Uno, J. Norris, H. W. Turner, W. H. Weinberg and A. S. Guram, *Organometallics*, 1999, **18**, 1840.

4 H. Werner, A. Hampp and B. Windmüller, *J. Organomet. Chem.*, 1992, **435**, 169.

5 J. McKechnie, D. S. Payne and W. Sim, *J. Chem. Soc.*, 1965, 3500.

6 G. K. Anderson, H. C. Clark and J. A. Davies, *Inorg. Chem.*, 1983, **22**, 434.

7 G. K. Anderson and R. Kumar, *Inorg. Chem.*, 1984, **23**, 4064

8 N. W. Alcock, A. W. G. Platt and P. Pringle, *J. Chem. Soc. Dalton Trans.*, 1987, 2273; N. W. Alcock, A. W. G. Platt and P. G. Pringle, *J. Chem. Soc. Dalton Trans.*, 1989, 139.

9 T. B. Rauchfuss, F. T. Patino and D. M. Roundhill, *Inorg. Chem.*, 1975, **14**, 652; H. P. Fritz, I. R. Gordon, K. E. Schwarzhans and L. M. Venanzi, *J. Chem. Soc.*, 1965, 5210; L. Crociani, G. Bandoli, A. Dolmella, M. Basato and B. Corain, *Eur. J. Inorg. Chem.*, 1998, 1811.

10 D. A. Fletcher, R. F. McMeeking and D. Parkin, *J. Chem. Inf. Comput. Sci.*, 1996, **36**, 746-749; F. H. Allen and O. Kennard, *Chem. Des. Automat. News*, 1993, **8**, 1 & 31-37.

11 P.S. Pregosin and R. W. Kunz, *^{31}P and ^{13}C NMR of Transition Metal Phosphine Complexes'*, ed. P. Diehl, E. Fluck and R. Kosfeld, Springer-Verlag, Berlin Heidelberg, 1979.

12 A. G. Orpen, L. Brammer, F. H. Allen, O. Kennard, D. G. Watson and R. Taylor, *J. Chem. Soc. Dalton Trans.*,1989, S1.

13 R. A. Burrow, D. H. Farrar and C. H. Honeyman, *Acta Cryst.*, 1994, **C50**, 681.

14 J. A. Cooley, P. Kamaras and M. Rapta, *Acta Cryst.*, 1995, **C51**, 1811; A. Marzotto, D. A. Clemente and G. Valle, *Acta. Cryst.*, 1999, **C55**, 43.

15 S. Vastag, B. Heil and L. Markó, *J. Mol. Cat.*, 1979, **5**, 189.

16 C. A. Tolman, *Chem. Rev.*, 1977, **77**, 313.

Chapter 4

Keto-Functionalised *N*-Pyrrolyl Phosphines

4.0 Introduction

The chemistry of *N*-pyrrolyl substituted phosphines has currently received interest due to their exceptional π acceptor properties, which can exceed those of phosphites such as $P(OPh)_3$.[1,2] Aromatic delocalization of the nitrogen lone pair into the 5-membered ring contributes to the *N*-pyrrolyl groups strong electron withdrawing properties, which result in the phosphines acting as relatively poor σ donors and as good π acceptors.

Complexes containing *N*-pyrrolyl substituted phosphines have been shown to be of catalytic relevance. For example, the rhodium(I) complexes of *N*-pyrrolyl substituted phosphines have been used to catalyse the hydroformylation of hex-1-ene[3] and the hydrogenation of olefins and arenes.[4]

Work by Braunstein et al[5] has shown that the carbonyl group of ketone- and ester-functionalised phosphines generally coordinates more strongly to late transition metal centres than the corresponding ether group of ether-functionalised phosphines. This results in *P,O*-coordinated ketone- and ester-functionalised phosphine complexes exhibiting increased stability and static nature compared to equivalent ether-functionalised phosphine complexes. For example, $[Rh\{PPh_2CH_2C(O)Ph\text{-}P,O\}_2]PF_6$ is stable at room temperature whereas the analogous ether-functionalised complex $[Rh(PPh_2CH_2CH_2OCH_3\text{-}P,O)_2]BPh_4$[6] is unstable above -30°C. This increased bond strength of the carbonyl oxygen-metal bond in ketone- and ester-functionalised phosphine complexes has also been observed to result in a number of ketone- and ester-functionalised phosphine complexes being static at room temperature, in contrast to the equivalent ether-functionalised phosphine complexes many of which exhibit fluxionality under similar conditions. For example, the

P,O-chelate ring in [RhCl{$PPh_2CH_2C(O)Ph$-*P,O*}{$PPh_2CH_2C(O)Ph$-*P*}][5] is non-fluxional at room temperature in contrast to [$RhClH_2(PCy_2CH_2CH_2OMe$-*P,O*)-($PCy_2CH_2CH_2OMe$-*P*)].[7]

N-pyrrolyl phosphines can easily be synthesised using mild reaction conditions[1] allowing the facile incorporation of additional functional groups such as the ketone group in 2-acetylpyrrole. This provides the potential mixed donor combination required for coordination through either, or both the phosphorus and oxygen atoms to a transition metal centre.

4.1 Results and Discussion

4.1.1 Ligand Synthesis

$Ph_2PNC_4H_3(COCH_3$-2) (**L**[10]) was synthesised in a similar manner to the ether-functionalised phosphinoamines (Section 2.1.1), using NEt_3 to deprotonate 2-acetylpyrrole, followed by reaction with an equimolar quantity of Ph_2PCl in THF (Scheme 1). This reaction produced **L**[10] in good yields but, in contrast to the rapid formation of the ether-functionalised phosphinoamines, the synthesis of **L**[10] took over two days to reach completion. As previously observed for the synthesis of the functionalised phosphinoamines, care has to be taken to exclude water, in order to prevent the formation of $Ph_2PP(O)Ph_2$.

Scheme 1

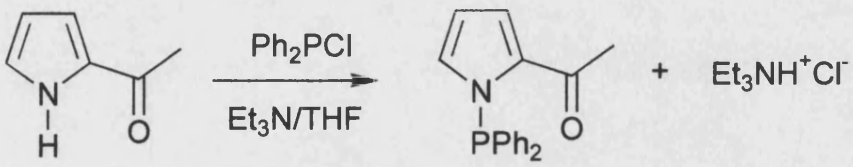

Replacement of NEt_3 by the stronger base 1,8-diazabicyclo[5.4.0]undec-7-ene (Dbu), decreased the reaction time to a few hours (see Experimental Section).

$\mathbf{L^{10}}$ was synthesised in good yield as colourless crystals, and characterised using microanalysis, multinuclear NMR and infrared spectroscopy. The $^{31}P\{^1H\}$ NMR spectra for $\mathbf{L^{10}}$ showed a single phosphorus resonance at δ(P) 55.8 ppm (Table 1). The $^{31}P\{^1H\}$ NMR chemical shift for $\mathbf{L^{10}}$ shows the phosphorus nucleus to be deshielded relative to the ether-functionalised phosphinoamines $\mathbf{L^1}$-$\mathbf{L^4}$ which showed single phosphorus resonances in the range δ(P) 27-43 ppm (Section 2.1.1). This is consistent with the pyrrolyl ring acting as a more electron withdrawing group[1] than the *N*-alkyl and *N*-aryl groups of $\mathbf{L^1}$-$\mathbf{L^4}$.

Table 1 Selected $^{31}P\{^1H\}$, ^1H NMR and infrared data for compounds $\mathbf{L^{10}}$-$\mathbf{L^{11}}$.

	Compound	δ(P)/ppm	$\delta(CH_3)$/ppm	$\nu(C{=}O)/cm^{-1}$
$\mathbf{L^{10}}$	$Ph_2PNC_4H_3(COCH_3\text{-}2)$	55.8	2.43s	1643vs
$\mathbf{L^{11}}$	$Ph_2P(S)NC_4H_3(COCH_3\text{-}2)$	67.3	2.29s	1664s

The ^1H NMR spectrum for $\mathbf{L^{10}}$ was as expected with distinctive signals for the methyl and pyrrolyl protons (Table 1 & Experimental Section). The $^{13}C\{^1H\}$ NMR spectra for $\mathbf{L^{10}}$ showed well-defined signals for the diphenylphosphino unit, carbonyl, methyl and pyrrolyl carbons.

Oxidation of the phosphorus atom in $\mathbf{L^{10}}$ by sulfur occurred readily as observed for the ether-functionalised phosphinoamine $\mathbf{L^4}$ (Section 2.1.1). The reaction of sulfur with $\mathbf{L^{10}}$ in a THF solution at room temperature gave the phosphorus(V) compound $Ph_2P(S)NC_4H_3(COCH_3\text{-}2)$ ($\mathbf{L^{11}}$) [Scheme 2], which was characterised on the basis of multinuclear NMR and infrared spectroscopy.

Scheme 2

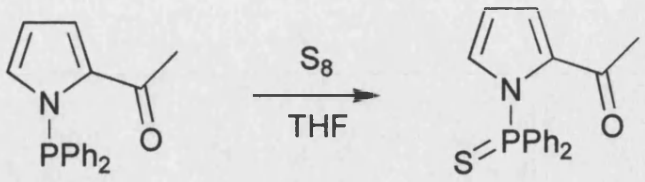

The $^{31}P\{^{1}H\}$ NMR spectrum of $\mathbf{L^{11}}$ showed a single phosphorus resonance at δ(P) 67.3 ppm. The deshielding of the phosphorus (Δδ = 11.5 ppm for $\mathbf{L^{11}}$ with respect to $\mathbf{L^{10}}$) was also observed for $\mathbf{L^{6}}$ (Δδ = 25.5 ppm for $\mathbf{L^{6}}$ with respect to $\mathbf{L^{4}}$), and is as expected on oxidising P^{III} to P^{V}.

As with the ether-functionalised phosphinoamines $\mathbf{L^{1}}$-$\mathbf{L^{4}}$ the P-N bond of $\mathbf{L^{10}}$ was found to be susceptible to alcoholysis, with the reaction of $\mathbf{L^{10}}$ with methanol forming Ph_2POMe. However the reaction of $\mathbf{L^{10}}$ with methanol took 2 days to reach completion compared with 24 hours for $\mathbf{L^{1}}$ and 30 minutes for $\mathbf{L^{4}}$ under similar reaction conditions. Comparison of the stability of $\mathbf{L^{10}}$ and the *N*-pyrrolyl phosphine $P(NC_4H_4)_3$, which is stable to alcoholysis, shows that the phosphorus atom of $\mathbf{L^{10}}$ is a better nucleophile than that in $P(NC_4H_4)_3$.[1]

4.1.2 Complexes of 2-Acetyl *N*-Pyrrolyl Phosphine

4.1.2.1 Synthesis of $[MCl_2(L^{10})_2]$ (M = Pd and Pt)

The reaction of two equivalents of $\mathbf{L^{10}}$ with $[MCl_2(cod)]$ (M = Pd and Pt) in dichloromethane gave the complexes $[PdCl_2(\mathbf{L^{10}})_2]$ (**56**) and *cis*-$[PtCl_2(\mathbf{L^{10}})_2]$ (**57**) in good yields. Complex **56** and **57** were characterised on the basis of microanalysis and infrared spectroscopy, though due to the poor solubilities of both complexes in common solvents, attempts to obtain $^{31}P\{^{1}H\}$ and ^{1}H NMR spectra were unsuccessful.

The infrared spectra of **56** and **57** both showed one band for ν(C=O) at 1644 cm^{-1}, similar to that of the free ligand $\mathbf{L^{10}}$ [ν(C=O) 1643 cm^{-1}] suggesting that the carbonyl oxygens are uncoordinated.

The combination of both an oxygen and sulfur donor groups in $\mathbf{L^{11}}$ provides the potential for coordination to a metal centre either through the oxygen or the sulfur group. No reaction between $\mathbf{L^{11}}$ and [$PtCl_2$(cod)] was observed indicating that the donor groups of $\mathbf{L^{11}}$ were insufficiently basic to displace the cod moiety from platinum(II).

4.1.2.2 Synthesis of [M(dmba)Cl($\mathbf{L^{10}}$)] (M = Pd and Pt)

Due to the poor solubility of **56** and **57**, complexes of the type [M(dmba)Cl(L)] containing $\mathbf{L^{10}}$ were synthesised to allow comparison of their properties with the equivalent ether- and amine-functionalised phosphinoamine complexes (Sections 2.1.2.2 and 3.1.2.2). The reaction of two equivalents of $\mathbf{L^{10}}$ with [M(dmba)(μ-Cl)]$_2$ (M = Pd, Pt) gave the complexes [Pd(dmba)Cl($\mathbf{L^{10}}$)] (**58**) and [Pt(dmba)Cl($\mathbf{L^{10}}$)] (**59**) in virtually quantitative yields.

The $^{31}P\{^1H\}$ NMR spectrum of **58** showed a single phosphorus resonance and the ^1H NMR spectrum was as expected with distinctive signals for the pyrrolyl and methyl protons. As with the amine- and ether-functionalised phosphinoamine complexes the *trans* N-Pd-P arrangement of the ligands in complex **58** can be deduced from the observed ^4J(H,P) coupling constants to the methyl protons within dmba, [$^4J(CH_3,P) \approx 3$ Hz], though due to the broadness of the methylene signal of dmba no ^4J(H,P) coupling could be observed. The infrared spectrum showed one

strong band for ν(C=O) at 1649 cm^{-1}, consistent with an uncoordinated carbonyl group.

Table 2. Selected $^{31}P\{^{1}H\}$, ^{1}H NMR and infrared data for complexes **58-63**.

	Complex	δ(P) /ppm	$^{1}J(P,Pt)$ /Hz	$\delta(CH_3)$ /ppm	ν(C=O) /cm^{-1}
58	[Pd(dmba)Cl(**L**^{10})]	88.6	-	2.04s	1649s
59	[Pt(dmba)Cl(**L**^{10})]	63.6	5097	2.06s	1657s
60	[Pd(dmba)(**L**^{10}-*P,O*)]BF_4	87.1	-	2.72s	1594, 1580s
61	[Pd(dmba)(**L**^{10}-*P,O*)]PF_6	87.4, -143.6sep	-	2.70s	1596s
62	[Pt(dmba)(**L**^{10}-*P,O*)]BF_4	62.6	4423	2.73s	1583s
63	[Pt(dmba)(**L**^{10}-*P,O*)]PF_6	62.8, -143.6sep	4437	2.68s	1579s

The $^{31}P\{^{1}H\}$ NMR spectrum for [Pt(dmba)Cl(**L**^{10})] (**59**) shows a singlet with $^{1}J(P,Pt)$ of 5097 Hz. The large value of $^{1}J(P,Pt)$ suggests the phosphine is *trans* to the nitrogen atom of dmba, and this is further supported by the presence of a $^{4}J(H,P)$ coupling in the ^{1}H NMR spectra [$^{4}J(CH_3,P) \approx 3$ Hz, $^{4}J(CH_2,P) \approx 3$ Hz]. The infrared spectrum of **59** shows ν(C=O) at 1657 cm^{-1} for the uncoordinated carbonyl group.

4.1.2.2.1 Abstraction of Chloride from [M(dmba)Cl(L^{10})] (M = Pd and Pt)

In order to examine and compare the potential bidentate coordination mode of **L**^{10} with that of the ether- and amine-functionalised phosphinoamines, complexes **58**

and **59** were reacted with $AgBF_4$ and $TlPF_6$. The abstraction of chloride from [M(dmba)Cl($\mathbf{L^{10}}$)] (M = Pd, Pt) in dichloromethane using $AgBF_4$ or $TlPF_6$ readily occurred with the formation of [Pd(dmba)($\mathbf{L^{10}}$-*P,O*)]X [X = BF_4 (**60**), X = PF_6 (**61**)] and [Pt(dmba)($\mathbf{L^{10}}$-*P,O*)]X [X = BF_4 (**62**), X = PF_6 (**63**)], which were characterised using microanalysis, multinuclear NMR and infrared spectroscopy.

The $^{31}P\{^1H\}$ NMR spectrum of **60** showed a single phosphorus resonance, while **61** showed a single phosphorus resonance plus a septet due to the PF_6^- counter ion (Table 2). Comparison of the chemical shifts of **60** and **61** with **58** show little change on coordination of the ketone group [$\Delta\delta$ between -1.2 and -1.5 ppm for **60** and **61** with respect to **58**], a similar observation was made for the ether-functionalised complexes [Pd(dmba)($\mathbf{L^1}$)]X [X = BF_4 (**27**) and PF_6 (**28**)] (Section 2.1.2.2.4.1). This small change in the chemical shifts on forming a 6-membered chelate ring has previously been observed[8] in the complex *cis*-[Pt{$PPh_2(CH_2)_3NMe_2$-*P,N*}-{$PPh_2(CH_2)_3NMe_2$-*P*}]BF_4.[9]

The $^{31}P\{^1H\}$ NMR spectrum of **62** showed a singlet with platinum satellites, whilst **63** showed an additional septet due to the PF_6^- counter ion. As with **60** and **61** the coordination of the ketone group had little effect on the phosphorus chemical shifts relative to **59** [$\Delta\delta$ between -0.8 and -1 ppm for **62** and **63** with respect to **59**]. The ^1J(P,Pt) for **62** and **63** show a significant decrease compared to **59** [ΔJ between -660 and -674 for **62** and **63** with respect to **59**], which is due to the combination of a range of different effects on the value of ^1J(P,Pt), such as changing the chloride ligand *cis* to the phosphine with the ketone oxygen atom, the presence of a positive charge on the metal centre and the formation of a chelate ring. The size of ΔJ is larger than observed for the ether-functionalised phosphinoamine complexes [Pt(dmba)($\mathbf{L^1}$-*P,O*)]BF_4 (**25**) and [Pt(dmba)($\mathbf{L^4}$-*P,O*)]BF_4 (**26**) (Section 2.1.2.2.4.1),

this difference in the values for ^{1}J(P,Pt) is possibly due to changing the ether oxygen atom with a ketone oxygen atom and changes to the flexibility of the chelate ring. The ^{1}H NMR spectra showed the presence of a ^{4}J(H,P) coupling between the methyl protons of dmba and the phosphorus atom [^{4}J(C*H*$_3$,P) ≈ 3 Hz], the presence of ^{4}J(H,P) coupling to the methylene protons is not observed due to the broadness of this resonance.

The ^{1}H NMR spectra of **60-63** showed significant deshielding of the methyl protons of the coordinated ketone group compared to **58** [Δδ between 0.66 and 0.68 ppm for **60** and **61** with respect to **58**] and **59** [Δδ between 0.62 and 0.67 ppm for **62** and **63** with respect to **59**]. This deshielding of the methyl and methylene protons on coordination of either the ether oxygen and amine nitrogen has been previously observed for the *P,O*- and *P,N*-chelate complexes containing ether- and amine-functionalised phosphinoamines (Sections 2.1.2.2.4.1 and 3.1.2.2.1).

The infrared spectra of **60-63** show a marked decrease in the ν(C=O) stretching frequency from 1643 cm^{-1} for free **L^{10}** to 1579-1596 cm^{-1}, consistent with formation of the 6-membered *P,O*-chelate ring through coordination of the ketone group.[10]

4.1.2.2.1.1 X-ray Crystal Structure of [Pt(dmba)(L^{10}-*P,O*)]PF$_6$ (63)

Complex **63** was recrystallised from dichloromethane/pentane as block shaped crystals suitable for X-ray crystallographic studies. The crystal structure confirmed the *trans* arrangement of the phosphorus and nitrogen as well as coordination of the ketone group to give a 6-membered *P,O*-chelate ring (Figure 1); selected bond lengths and angles are given in Table 3.

Table 3. Selected bond lengths [Å] and angles [°] for **63**.

Pt(1)-C(13)	2.016(6)	Pt(1)-P(1)	2.193(2)
Pt(1)-O(1)	2.089(4)	P(1)-N(1)	1.731(5)
Pt(1)-N(2)	2.135(5)	O(1)-C(26)	1.259(8)
C(13)-Pt(1)-O(1)	169.0(2)	O(1)-Pt(1)-P(1)	93.49(13)
C(13)-Pt(1)-N(2)	82.2(2)	N(2)-Pt(1)-P(1)	178.96(14)
O(1)-Pt(1)-N(2)	86.9(2)	N(1)-P(1)-Pt(1)	110.1(2)
C(13)-Pt(1)-P(1)	97.3(2)	C(26)-O(1)-Pt(1)	133.6(4)

Figure 1

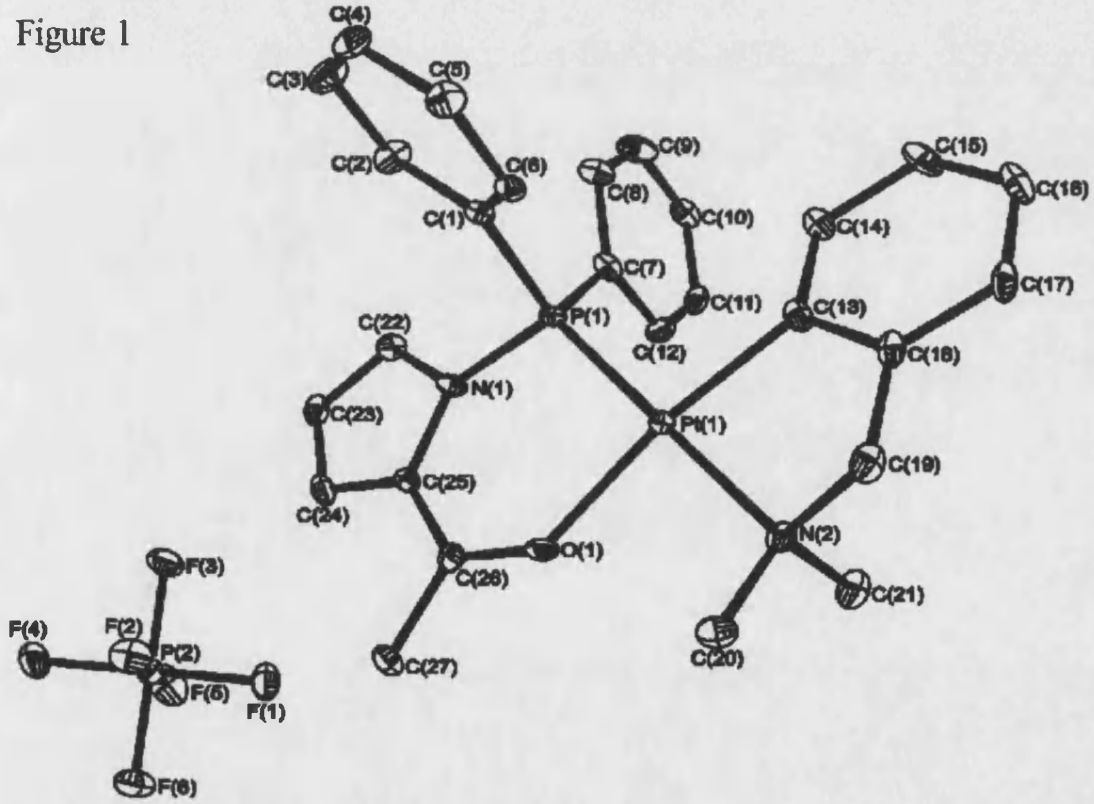

The platinum(II) centre in **63** is distorted square-planar, with *cis* angles between 82.2(2) and 97.3(2)°. The phosphorus atom of the bidentate *N*-pyrrolyl

phosphine ligand $\mathbf{L^{10}}$ is *trans* to the amine nitrogen atom, consistent with the NMR data, while the ketone oxygen atom is *trans* to the carbon atom of dmba ligand.

The sum of the angles around the nitrogen atom N(1) is 359° which is similar to that found in the free ligand $\mathbf{L^{10}}$ [N(1) 360°],[11] and is consistent with the nitrogen being sp^2 hybridised. The P-N bond distance of 1.731(5) Å is significantly longer than seen for complexes containing ether-functionalised phosphinoamine [1.616-1.680 Å] (Chapter 2), and is consistent with the generally accepted range for a P-N single bond.[12] This is marked contrast to the ether-functionalised phosphinoamines, which showed significant double bond character. Comparison with the P-N bond length in the free ligand $\mathbf{L^{10}}$ [1.7637(14) Å][11] shows that coordination to give the 6-membered *P,O*-chelate ring results in shortening of the P-N bond, suggesting more double bond character than in the free ligand due to increased π-donation from the nitrogen to phosphorus.[1]

The Pt-P bond distance of 2.193(2) Å is significantly shorter than those found in the ether-functionalised phosphinoamine complex *cis*-$[PtBr(NO_2)(\mathbf{L^1})_2]$ (**16**) [2.256(2) and 2.2684(14) Å] (Section 2.1.2.1.4.4.1) as well as the generally accepted Pt-P bond to triphenylphosphine (2.25-2.33 Å).[13] This shortening of Pt-P bond is similar to that observed for the Rh-P bonds in *trans*-$[RhCl(CO)\{P(pyrrolyl)_3\}_2]$,[1] in which the short Rh-P bond lengths were attributed to increased π-backbonding from rhodium to the phosphorus.

In **63** the coordinated ketone is bonded through a lone pair on the oxygen. The Pt-O bond distance of 2.089(4) Å is shorter than those found in the acetone complexes $[Pt(CH_2PPh_2CH_2PPh_2\text{-}C,P)(PPh_3)(OCMe_2)](PF_6)_2$[14] [2.133(16) Å] and *trans*-$[Pt(PPhMe_2)_2Me(OCMe_2)]PF_6$[15] [2.168(5) Å], whilst the C=O bond length of 1.259(8) in **63** is comparable, 1.25(4) and 1.226(9) Å respectively. On coordination,

the C=O bond length increases compared with the free ligand [1.216(2) Å] suggesting less double bond character, though it is still shorter than expected for a C-O single bond.[13,16]

Comparison of the Pt-C and Pt-N bond distances and bite angle that the dmba chelate makes with the platinum(II) centre in **63** [Pt(1)-C(13) 2.016(6), Pt(1)-N(2) 2.135(5) Å and 82.2(2)°] with that observed in [Pt(dmba)(μ-PPh_2O-*P,O*)]$_2$ (**35**) (Section 2.1.2.2.4.3.1) show that the dmba ligand is relatively unaffected on changing the phosphine *trans* to the nitrogen.

4.1.2.2.2 Lability of the Coordinated Ketone Oxygen

The ketone oxygen atom is expected to form stronger bonds to the metal centre than the ether oxygen atoms of complexes **25** and **26**, which consequently may decrease its lability.[5] A range of ligands, including carbon monoxide (CO), acetonitrile ($NCCH_3$), diphenylacetylene (PhCCPh) and xylyl isocyanide (CNXyl) were added to a solution of [Pt(dmba)(**L**^{10}-*P,O*)]PF_6 in dichloromethane. The reaction mixtures were analysed by infrared spectroscopy, using the ν(C=O) stretching frequencies to check if the ketone group remained coordinated.

These experiments demonstrated that only xylyl isocyanide was able to displace the keto group. The infrared spectra showed a strong band for ν(C=O) at 1653 cm^{-1}, consistent with the uncoordinated ketone, as well as a band for ν(CN) at 2180 cm^{-1}, which is similar to the stretching frequency observed for the coordinated isocyanide group in [Pt(dmba)(**L**^{4})(CNXyl)]BF_4 [ν(CN) 2179 cm^{-1}] (Section 2.1.2.2.4.2).

4.1.2.3 Rhodium(I) Complexes

4.1.2.3.1 Synthesis of [RhCl(CO)(L^{10}-*P,O*)]

The reaction of two equivalents of $\mathbf{L^{10}}$ with $[Rh(\mu\text{-}Cl)(CO)_2]_2$ in dichloromethane gave the *P,O*-chelate [RhCl(CO)($\mathbf{L^{10}}$-*P,O*)] (**64**), which was characterised on the basis of microanalysis, infrared and multinuclear NMR spectroscopy (see Experimental Section).

The $^{31}P\{^1H\}$ NMR spectrum of **64** showed a doublet with $^1J(P,Rh)$ of 178 Hz. The $^1J(P,Rh)$ of **64** is similar to that observed for the 6-membered *P,N*-chelate rhodium(I) complex [RhCl(CO)($\mathbf{L^8}$-*P,N*)] (**54**) [$^1J(P,Rh)$ = 181 Hz] (Section 3.1.2.5) and typical for a phosphorus *trans* to a chloride in a rhodium(I) system.[17]

Table 4. Selected $^{31}P\{^1H\}$, ^1H NMR and infrared data for complexes **64-66**.

	Complex	δ(P) /ppm	$^1J(P,Rh)$ /Hz	δ(CH_3) /ppm	ν(CO) /cm^{-1}	ν(C=O) /cm^{-1}
64	*trans*-[RhCl(CO)($\mathbf{L^{10}}$-*P,O*)]	93.6	178	2.60s	1989vs	1576s
65	*trans*-[RhCl(CO)($\mathbf{L^{10}}$)$_2$]	84.4	158	2.40s	1963vs	1650s
66	$[RhCl(CO)(PPh_2OPPh_2)]_2$	-	-	-	1964vs 1793m	-

The ^1H NMR spectrum of **64** was as expected, with the methyl protons deshielded relative to **64** [Δδ = 0.40 ppm for **64** with respect to **65**] suggesting the coordination of the ketone oxygen atom to form a 6-membered *P,O*-chelate ring. The infrared spectrum of **64** showed a single band for ν(C=O) at 1576 cm^{-1}, also consistent with the coordination of the ketone group.

In order to examine the lability of the Rh-O bond, **64** was reacted with a range of ligands, including carbon monoxide (CO), diphenylacetylene (PhCCPh) and xylyl isocyanide (CNXyl). The reactions in dichloromethane were analysed using NMR and infrared spectroscopy, using the ν(C=O) stretching frequencies to check the coordination of the ketone group.

The addition of diphenylacetylene to a solution of **64** in dichloromethane, showed no change in both the $^{31}P\{^{1}H\}$ NMR and infrared spectrum, consistent with the ketone group remaining coordinated. Bubbling CO through a dichloromethane solution of **64**, resulted in the broadening of the phosphorus signals as observed from the $^{31}P\{^{1}H\}$ NMR spectrum (Figure 2). The infrared spectrum showed two broad carbonyl bands [ν(CO)] at 2078 and 2002 cm^{-1}, and three bands for the ketone group [ν(C=O)] at 1645, 1621 and 1587 cm^{-1}. The ν(C=O) band at 1645 cm^{-1} is consistent with the presence of an uncoordinated ketone group suggesting formation of $[RhCl(CO)_2(\mathbf{L^{10}})]$ whereas the band at 1587 cm^{-1} is consistent with the presence of a coordinated ketone and formation of $[Rh(CO)_2(\mathbf{L^{10}}\text{-}P,O)]Cl$. However, degassing the reaction mixture led to the reformation of **64**, demonstrating that the interaction of the CO ligand with the rhodium(I) metal centre is reversible.

The infrared and NMR spectra of the product from the reaction of **64** with xylyl isocyanide showed a mixture of products to have resulted. From the infrared spectrum, the presence of both the coordinated [ν(C=O) 1584 cm^{-1}] and uncoordinated [ν(C=O) 1653 cm^{-1}] ketone group as well as two bands attributed to ν(CN) [2099 cm^{-1}] and ν(CO) [1994 cm^{-1}] suggested that the isocyanide has not only displaced the keto group but also substituted another ligand.

Figure 2

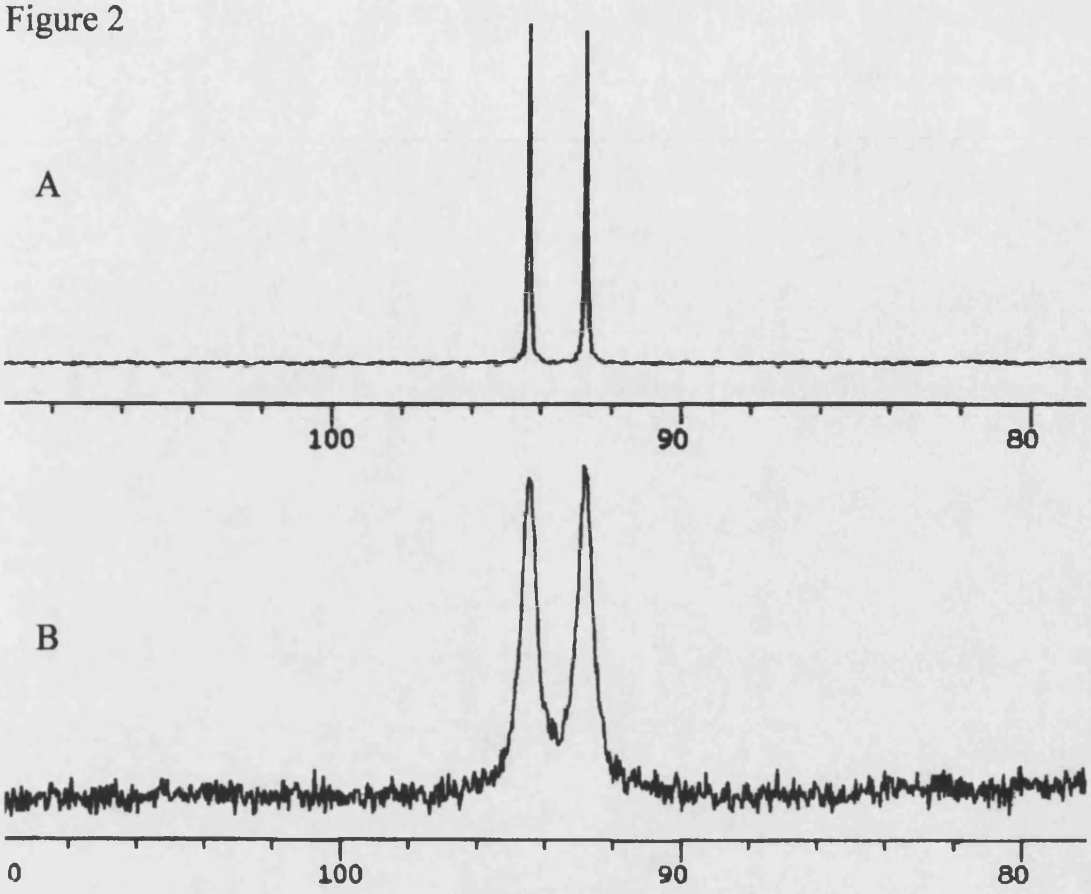

(**A** = No CO added, **B** = CO saturated solution)

4.1.2.3.2 Synthesis of *trans*-[RhCl(CO)(L^{10})$_2$]

The reaction of four equivalents of L^{10} with [Rh(μ-Cl)(CO)$_2$]$_2$ in toluene resulted in the rapid evolution of CO gas with the formation of a yellow solution. After 5 minutes the yellow product *trans*-[RhCl(CO)(L^{10})$_2$] **65** began to precipitate from solution. **65** was characterised on the basis of microanalysis, infrared and multinuclear NMR spectroscopy (see Experimental Section).

The $^{31}P\{^1H\}$ NMR spectrum of **65** showed a broad doublet (δ 84.4 ppm) with $^1J(P,Rh)$ of 158 Hz. The coupling constant of **65** is similar to that of the previously reported complex *trans*-[RhCl(CO){PPh$_2$(pyrrolyl)}$_2$][1] [$^1J(P,Rh)$ 140 Hz] suggesting the phosphorus atoms are *trans* to each other. This is also indicated by the presence of

only one phosphorus environment. The infrared spectrum in dichloromethane showed a band for ν(C=O) at 1650cm^{-1}, similar to that of the free ligand indicating the ketone group is uncoordinated, and one band for ν(CO) at 1981 cm^{-1}.

Using the reported correlation[18] between ν(CO) for *trans*-[RhCl(CO)(PR$_3$)$_2$] and [Ni(CO)$_3$(PR$_3$)] (A$_1$ band), the ν(CO) for [Ni(CO)$_3$(**L**^{10})] (A$_1$ band) is estimated to be approximately 2070 cm^{-1} from which using equation 1[19] the value of the electronic parameter χ for **L**^{10} is 14.4. From which the substituent contribution χ_i for the 2-acetyl *N*-pyrrolyl group can be determined as the value of the χ_i for a phenyl group is known, this gives an estimate of χ_i for the 2-acetyl *N*-pyrrolyl as 5.8. Comparison of the electronic parameter with that for the unsubstituted *N*-pyrrolyl (χ_i = 12)[1], functionalised amine (Sections 2.1.2.4.2 and 3.1.2.5) and phenyl groups (χ_i = 4.3), shows that its electronic contribution (χ_i) is considerably less than that of an unsubstituted *N*-pyrrolyl group, though larger than that for phenyl and functionalised amine groups.

4.1.2.3.3 Formation of [RhCl(CO)(μ-PPh$_2$OPPh$_2$)]$_2$

Dissolution of **65** in dichloromethane gave a yellow solution, which on standing at room temperature for a few hours turned red and gave red crystals, from which a suitable sample for single crystal X-ray analysis was obtained. Analysis of these revealed the complex to be the dinuclear species [RhCl(CO)(μ-PPh$_2$OPPh$_2$)]$_2$ (**66**). Unfortunately, due to the poor solubility of the red crystalline material in most common solvents, analysis by NMR was unsuccessful. The infrared spectrum of **66** showed two ν(CO) bands at 1964 and 1793 cm^{-1}, consistent with a terminal and bridging carbonyl group respectively. The absence of a band for ν(C=O) shows that

the ketone group has been lost. Cooling the yellow solution of **65** in dichloromethane to below 10°C was found to stabilise **65** to decomposition, but on warming to room temperature the sample decomposes to give a red solution and precipitate. The formation of **66** is believed to be due to catalytic cleavage of the P-N bond of $Ph_2PNC_4H_3(COCH_3\text{-}2)$ ($\mathbf{L^{10}}$) by a trace amount of water.

4.1.2.3.3.1 X-ray Crystal Structure of $[RhCl(CO)(\mu\text{-}PPh_2OPPh_2)]_2$ (66)

The crystal structure revealed that the complex **66** was a dinuclear species with bridging PPh_2OPPh_2 ligands (Figure 3). Selected bond lengths and angles are given in Table 5.

The asymmetric unit in **66** consists of one half of a rhodium dimer and one dichloromethane molecule with half-site occupancy. The remaining portion of the dimer is generated via the 1-*x*, -*y*, -*z* transformation. The coordination geometry around each rhodium centre is distorted trigonal bipyramidal, with two phosphorus atoms from different bridging bis(diphenylphosphine) monoxide ligands arranged *trans* to each other in the axial positions. Coordination around each rhodium centre is completed by one terminal and two bridging ligands, which occupy the equatorial positions. The equatorial ligands are carbonyls and chlorides which are disordered equally between the terminal and bridging positions, with each of these ligands in the crystal structure modelled as 50% chloride and 50% carbonyl.

Table 5. Selected bond lengths [Å] and angles [°] for **66**.

Rh(1)-C(26)	1.83(2)	Rh(1)-Cl(2)	2.464(5)
Rh(1)-C(27)	1.84(2)	P(1)-O(3)	1.636(3)
Rh(1)-P(1)	2.2917(13)	P(2)-O(3)	1.651(3)
Rh(1)-P(2)'	2.2986(13)	O(1)-C(26)	1.12(2)
Rh(1)-Cl(1)	2.361(5)	O(2)-C(27)	1.17(2)
C(26)-Rh(1)-C(27)	151.3(6)	P(1)-Rh(1)-Rh(1)'	91.50(4)
C(26)-Rh(1)-P(1)	90.8(4)	P(2)'-Rh(1)-Rh(1)'	89.94(4)
C(27)-Rh(1)-P(1)	87.5(4)	Cl(1)-Rh(1)-Rh(1)'	145.98(7)
C(26)-Rh(1)-P(2)'	89.3(4)	Cl(2)-Rh(1)-Rh(1)'	65.10(8)
C(27)-Rh(1)-P(2)'	91.2(4)	O(3)-P(1)-Rh(1)	113.17(13)
P(1)-Rh(1)-P(2)'	177.46(5)	O(3)-P(2)-Rh(1)'	113.73(12)
C(27)-Rh(1)-Cl(1)	148.5(4)	C(26)-Cl(1)-O(1)	160(2)
P(1)-Rh(1)-Cl(1)	89.43(7)	O(1)-Cl(1)-Rh(1)	169.6(11)
P(2)'-Rh(1)-Cl(1)	90.55(7)	O(2)-Cl(2)-C(27)	143(2)
C(26)-Rh(1)-Cl(2)	151.7(4)	O(2)-Cl(2)-Rh(1)	146.2(12)
P(1)-Rh(1)-Cl(2)	85.45(7)	C(27)-Cl(2)-Rh(1)	6.0(13)
P(2)'-Rh(1)-Cl(2)	93.27(7)	P(1)-O(3)-P(2)	125.9(2)
Cl(1)-Rh(1)-Cl(2)	148.74(11)	Cl(1)-C(26)-Rh(1)	166(2)
C(26)-Rh(1)-Rh(1)'	143.2(4)	O(1)-C(26)-Rh(1)	176.3(13)
C(27)-Rh(1)-Rh(1)'	65.5(4)	O(2)-C(27)-Rh(1)	165.7(12)

Primed atoms generated by the symmetry transformations $-x+1, -y, -z$.

Double primed atoms generated by the symmetry transformation $-x+2, -y, -z$.

Figure 3

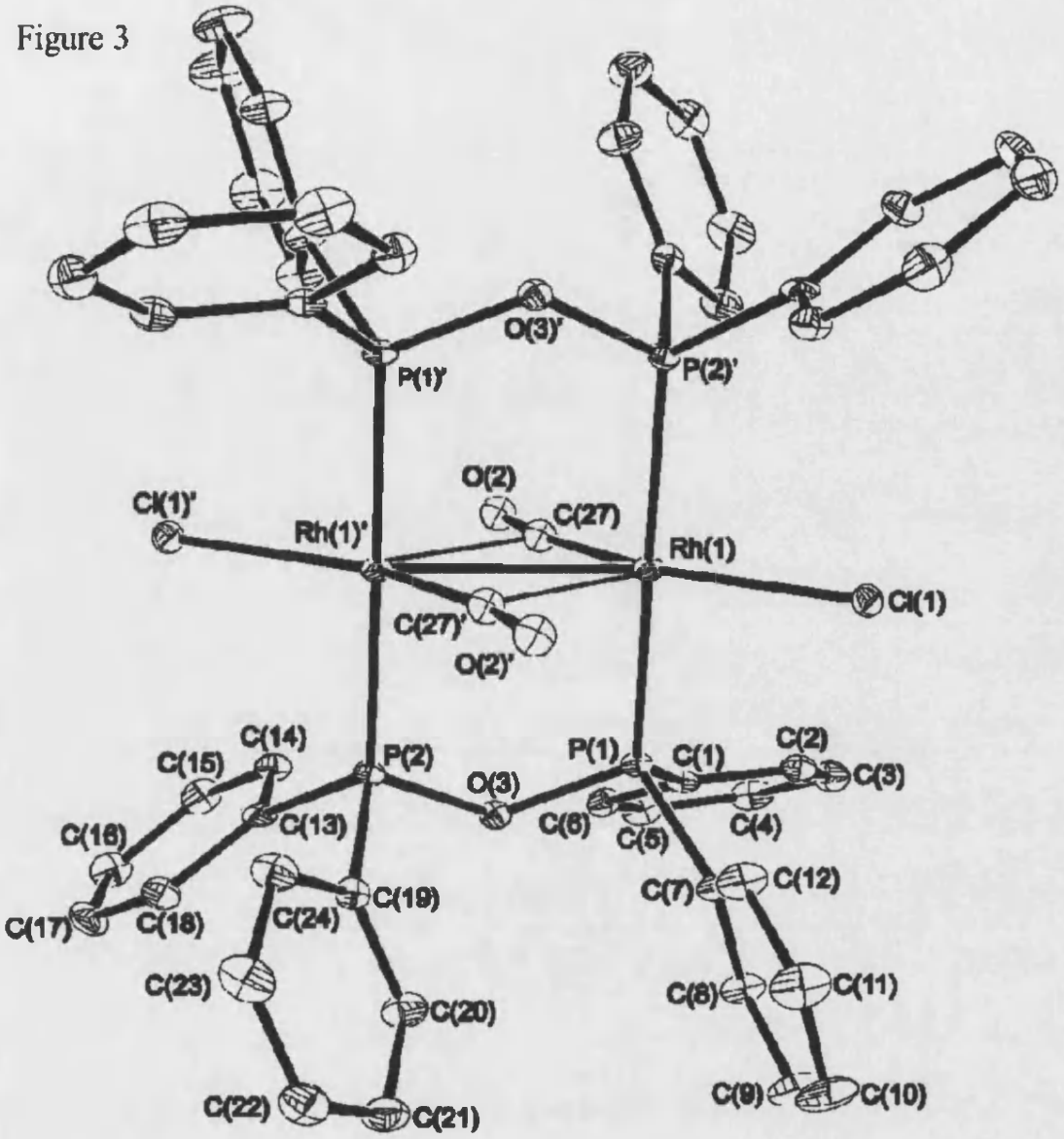

A search of the Cambridge Structural Database[20] showed that **66** is the first crystallographically characterised example of a rhodium dimer with bridging PPh_2OPPh_2 ligands. In contrast, a considerable number of rhodium dimers in which the related bridging ligand bis(diphenylphosphino)methane (dppm) is present have been crystallographically characterised. Analysis of the Rh-Rh distances from the complexes containing the $Rh_2(\mu\text{-dppm})_2$ skeleton, showed that the Rh-Rh distance in **66** (2.8683(9) Å) lies within the ranges observed for compounds which both contain a formal Rh-Rh single bond [2.52-3.01 Å (mean 2.77 Å)] and also for those in which a

formal Rh-Rh bond is absent [2.83-3.47 Å (mean 3.16 Å)]. However, a number of other structural factors suggest the presence of a Rh-Rh bond. For example, the P···P separation between the phosphorus atoms of the same ligand (2.93 Å) is longer than the Rh-Rh distance indicating compression along the Rh-Rh internuclear axis. In addition, the Cl···Cl (4.54 Å) and C···C (3.60 Å) distances across the central 'square' are significantly longer than the Rh-Rh distance.

Although the structural parameters suggest a Rh-Rh bond to be present, the disorder within the crystal structure makes it difficult to confirm this on the basis of electron counting rules. Indeed, neither $[Rh_2(\mu\text{-}Cl)_2(\mu\text{-}PPh_2OPPh_2)_2(CO)_2]$ nor $[Rh_2Cl_2(\mu\text{-}PPh_2OPPh_2)_2(\mu\text{-}CO)_2]$ would be expected to have Rh-Rh bonds.

The Rh-CO and Rh-Cl terminal bond distances in complex **66** are similar to the expected values for terminal Rh-CO, and Rh-Cl bonds respectively.[13] The bridging ligands are very asymmetric, with the Rh-C(27) distances 1.84(2) and 2.69 Å and the Rh-Cl(2) distances 2.464(5) and 2.889 Å. This asymmetry is also reflected in the bond angles, with the bridging carbonyl ligands [Rh(1)-C(27)-O(2) 165.7(12)°] showing only a small deviation from the linear conformation observed for the terminal carbonyl [O(1)-C(26)-Rh(1) 176.3(13)°]. In addition, the bond angle Cl(1)-Rh(1)-Rh(1)' of 145.98(7)° shows a significant deviation from the expected linear [180°] arrangement expected for a symmetrical structure. Comparison of the C-O bond distances of the terminal and bridging carbonyls 1.12(2) and 1.17(2) Å respectively shows that the C-O bond length is significantly increased for the bridging carbonyl consistent with a reduction in the C-O bond order. The presence of both bridging and a terminal carbonyls in the crystal structure of **66** is consistent with the observed ν(CO) bands for terminal [ν(CO) 1964 cm^{-1}] and bridging [ν(CO) 1793 cm^{-1}] carbonyls in the infrared spectrum.

The dppm complex $[Rh_2Cl_2(\mu\text{-dppm})_2(CO)_2]$[21] is similar in terms of its chemical formula to **66**, but comparison of the structural features for the two compounds shows a number of important differences. In $[Rh_2Cl_2(\mu\text{-dppm})_2(CO)_2]$ the Rh···Rh separation of 3.2386(5) Å is consistent with there being no Rh-Rh bond, and in addition none of the carbonyl or chloride ligands are bridging. The Rh-Rh distance in **66** is similar to that observed in the cationic complexes $[Rh_2(\mu\text{-Cl})(CO)_2(\mu\text{-CO})(dppm)_2]X$ (X = BPh_4 and $[RhCl_2(CO)_2]$) [2.8415(7)[22] and 2.838(1) Å[23] respectively], though these complexes differ significantly from **66** in that the bridging chloride and carbonyl ligands are more symmetrical.

4.1.2.3.4 Synthesis of $[Rh(L^{10}\text{-}P,O)_2]X$ (X = Cl and PF_6)

The reaction of four equivalents of L^{10} with $[Rh(\mu\text{-Cl})(cod)]_2$ in dichloromethane gave the complex $[Rh(L^{10}\text{-}P,O)_2]Cl$ (**67**) which was characterised on the basis of multinuclear NMR and infrared spectroscopy.

The $^{31}P\{^1H\}$ NMR spectrum of **67** showed a doublet with $^1J(P,Rh)$ of 204 Hz. The large value of $^1J(P,Rh)$ suggests that the phosphines are mutually *cis*.[17] The ^1H NMR spectrum was as expected, with the methyl protons deshielded compared to the free ligand (L^{10}) ($\Delta\delta$ = 0.2 ppm for **67** with respect to L^{10}), consistent with the deshielding of the methyl protons as observed in $[RhCl(CO)(L^{10}\text{-}P,O)]$ **64** on forming a *P,O*-chelate ring. The infrared spectrum showed one strong band for ν(C=O) at 1574 cm^{-1} consistent with both ketone groups being coordinated to the rhodium(I) metal centre.

Table 6. Selected $^{31}P\{^{1}H\}$, ^{1}H NMR and infrared data for complexes **67-68**.

	Complex	δ(P)/ppm	^{1}J(P,Rh) /Hz	δ(CH_3) /ppm	ν(C=O) /cm^{-1}
67	[Rh(**L**^{10}-*P,O*)$_2$]Cl	108.0	204	2.63s	1574s
68	[Rh(**L**^{10}-*P,O*)$_2$]PF_6	108.3, -143.5 sep	205	2.71s	1570s

Unfortunately **67** was found to decompose in solution to give a number of rhodium-phosphorus containing products as shown by $^{31}P\{^{1}H\}$ NMR, and as a result it could not be isolated and purified. In order to stabilise **67** the chloride was replaced by a non-coordinating anion PF_6^-.

A slight excess of NH_4PF_6 was reacted *in situ* with [Rh(**L**^{10}-*P,O*)$_2$]Cl in dichloromethane, with the rapid precipitation of NH_4Cl, and formation of [Rh(**L**^{10}-*P,O*)$_2$]PF_6 (**68**). Complex **68** was considerably more stable than **67** and as a result could be characterised on the basis of microanalysis, infrared and multinuclear NMR spectroscopy. The $^{31}P\{^{1}H\}$ NMR spectrum showed a doublet [^{1}J(P,Rh) 205 Hz] plus a septet due to the PF_6^- counter ion. The chemical shift and coupling constant of **68** are virtually identical to those of **67** suggesting that the cations in the two compounds are identical. The infrared spectrum showed one band for ν(C=O) at 1570 cm^{-1} which compares well with that observed for the coordinated ketone group in **67**.

In order to examine if CO could displace the keto group from **67,** CO was bubbled through a solution of **67** in dichloromethane and results monitored by $^{31}P\{^{1}H\}$ NMR spectroscopy. On saturating the solution with CO, decomposition occurred with the colour changing rapidly to give a red solution and precipitate. The

$^{31}P\{^{1}H\}$ NMR spectrum of this red solution showed a mixture of phosphorus-rhodium containing products.

4.2 Conclusion

The synthetic route used for the synthesis of the amine- and ether-functionalised phosphinoamines was successfully adapted to allow the synthesis of $\mathbf{L^{10}}$ in good yield and purity. In contrast to the rapid formation of the amine- and ether-functionalised phosphinoamines, deprotonation of the NH group of 2-acetylpyrrole proved very slow with NEt_3, though could be speeded up using a stronger base.

As with the amine- and ether-functionalised phosphinoamines $\mathbf{L^{10}}$ readily coordinated to platinum(II), palladium(II) and rhodium(I). The relative ease in which the oxygen of the ketone coordinated to give a static and stable platinum(II) and palladium(II) complexes containing 6-membered *P,O*-chelate rings, is in contrast to the amine- and ether-functionalised phosphinoamine chelate rings which exhibited fluxionality and poor stability respectively.

The single crystal X-ray analysis of **63** showed that the P-N bond is significantly longer than observed for the amine- and ether-functionalised phosphinoamines, with the bond length being consistent with a P-N single bond.

The stability of the rhodium(I) complex $[RhCl(CO)(\mathbf{L^{10}})_2]$ in dichloromethane, was found to be dependent on the temperature of the solution, with reaction with trace amounts of water occurring above 10°C to give the dimer $[Rh_2Cl_2(CO)_2(PPh_2OPPh_2)_2]$ (**66**). In contrast, the analogous ether-functionalised phosphinoamine complexes were stable under similar conditions.

The single crystal X-ray structure of **66** showed that the rhodium atoms are bridged by two Ph_2POPPh_2 ligands arranged *trans* to each other in the axial positions, whilst in the equatorial plane the chlorides and carbonyl ligands are disordered between the bridging and terminal positions.

4.3 References

1 K. G. Moloy and J. L. Petersen, *J. Am. Chem. Soc.*, 1995, **117**, 7696.

2 S. Serron, S. P. Nolan, K. G. Moloy, *Organometallics*, 1996, **15**, 4301.

3 A. M. Trzeciak, T. Glowiak, R. Grzybek and J. J. Ziólkowski, *J. Chem. Soc. Dalton Trans.*, 1997, 1831.

4 A. M. Trzeciak, T. Glowiak and J. J. Ziólkowski, *J. Organomet. Chem.*, 1998, **552**, 159.

5 P. Braunstein, Y. Chauvin, J. Nähring, A. DeCian, J. Fischer, A. Tiripicchio and F. Ugozzoli, *Organometallics*, 1996, **15**, 5551.

6 A. Badar and E. Lindner, *Coord. Chem. Rev.*, 1991, **108**, 27.

7 E. Lindner, K. Gierling, B. Keppeler and H. A. Mayer, *Organometallics*, 1997, **16**, 3531.

8 P. E. Garrou, *Chem. Rev.*, 1981, 229.

9 G. K. Anderson and R. Kumar, *Inorg. Chem.*, 1984, **23**, 4064.

10 S.-E. Bouaoud, P. Braunstein, D. Grandjean, D. Matt and D. Nobel, *Inorg. Chem.*, 1986, **25**, 3765.

11 A. D. Burrows, M. F. Mahon and C. D. Andrews, *Unpublished results.*

12 R. A. Burrow, D. H. Farrar and C. H. Honeyman, *Acta Cryst.*, 1994, **C50**, 681.

13 A. G. Orpen, L. Brammer, F. H. Allen, O. Kennard, D. G. Watson and R. Taylor, *J. Chem. Soc., Dalton Trans.*,1989, S1.

14 T. Ghaffar, A. Kieszkiewicz, S. C. Nyburg and A. W. Parkins, *J. Organomet. Chem.*, 1996, **517**, 227.

15 A. G. Thayer and N. C. Payne, *Acta. Cryst.*, 1986, **C42**, 1302.

16 N. W. Alcock, A. W. G. Platt and P. Pringle, *J. Chem. Soc., Dalton Trans.*, 1987, 2273.

17 P. S. Pregosin and R. W. Kunz, *^{31}P and ^{13}C NMR of Transition Metal Phosphine Complexes'*, ed. P. Diehl, E. Fluck and R. Kosfeld, Springer-Verlag, Berlin Heidelberg, 1979.

18 S. Vastag, B. Heil and L. Marko, *J. Mol. Cat.*, 1979, **5**, 189.

19 C. A. Tolman, *Chem. Rev.*, 1977, **77**, 313.

20 D. A. Fletcher, R. F. McMeeking and D. Parkin, *J. Chem. Inf. Comput. Sci.*, 1996, **36**, 746-749; F. H. Allen and O. Kennard, *Chem. Des. Automat. News*, 1993, **8**, 1 & 31-37.

21 M. Cowie and S. K. Dwight, *Inorg. Chem.*, 1980, **19**, 2500.

22 M. Cowie, *Inorg. Chem.*, 1979, **18**, 286.

23 M. M. Olmstead, C. H. Lindsay, L. S. Benner and A. L. Balch, *J. Organomet. Chem.*, 1979, **179**, 289.

Chapter 5

Late Transition Metal Complexes of Silasesquioxanes

5.0 Introduction

Incompletely condensed silasesquioxanes have received considerable attention due to their potential use as models for silica and the immobilised catalysts based on such supports.[1] These heterogeneous catalysts are used in a vast number of chemical processes, in particular in the petrochemical industry where their uses vary from oxidation of hydrocarbons to polymerisation.[2] The extreme difficulty of investigating the mechanistic pathways involved with immobilised compounds led to the development of compounds which would model the surface morphologies of the silica supports and their interactions with the immobilised compounds. From this initial interest has developed a wide range of syntheses for complexes of main group and transition metals in which the silasesquioxanes are coordinated as ligands.[3,4]

Silasesquioxanes provide a variety of coordination environments, which can be varied by substitution of the basic trisilanol unit by chlorotrimethylsilane to reduce the number of free silanol groups (Figure 1).

Figure 1

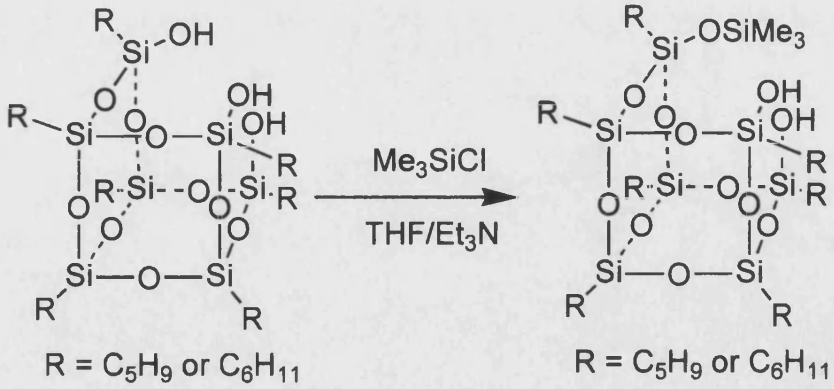

A number of strategies for the synthesis of silasesquioxane complexes have been developed by Feher et. al. (Figure 2)[3,4] The first involves the reaction between

the silanols and less acidic alkyl, alkoxide or amide ligands, the second uses amine assisted metathesis of a metal-halide complex and finally metathetic replacement of metal-halide bonds by a silasesquioxide anion equivalent.

Figure 2

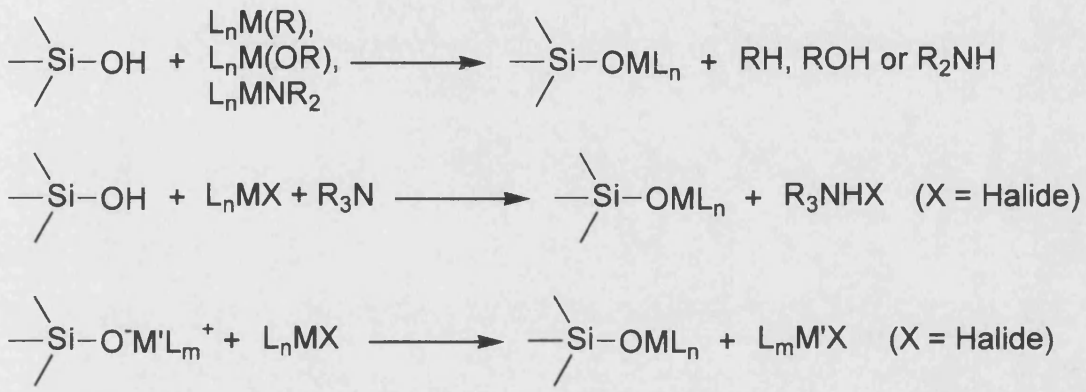

The direct reaction of silanols with reactive alkoxide, amide or alkyl ligands works well, but is limited to the availability of suitable metal complexes. Other factors also limit the effectiveness of these routes, for example the direct reaction of silanols with metal alkyl complexes is only effective for electropositive metals (e.g. Zr, Ti, Al, Ga), but for the late transition metals where the metal-carbon bond is less reactive this route is of little synthetic use.

The amine assisted metathesis of SiO-H for metal-halide bonds is of greater synthetic use compared with the direct reaction of silanols with amides, alkoxides or alkyls ligands, and has been successfully applied to the synthesis of a number of compounds, for example see Figure 3. This reaction is again of limited use as a reactive metal halide complex is required. In addition a common side reaction of this route is the base assisted cyclodeprotonation of the silasesquioxane. This has been found to be particularly a problem where high valent metal complexes are used.[4]

Figure 3

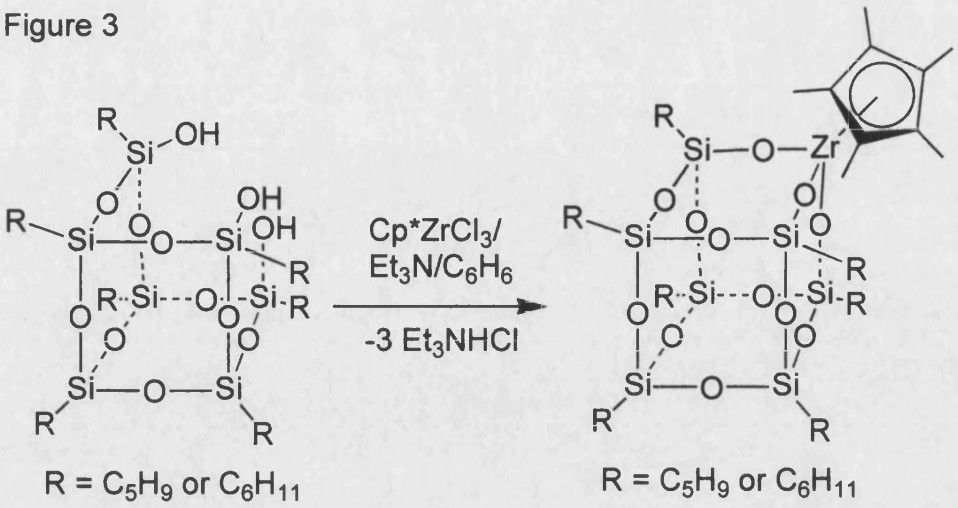

Of particular synthetic interest is the use of anionic equivalents of silasesquioxanes such as the thallium(I) or tetraalkylstibonium siloxides. These soft anion sources do not promote skeletal degradation of the silasesquioxane and provide a useful source of silasesquioxide anions which react with complexes of the late transition metal series such as $[Pt(cod)I_2]$[4] (Figure 4) though full experimental details have not been published to date.

Figure 4

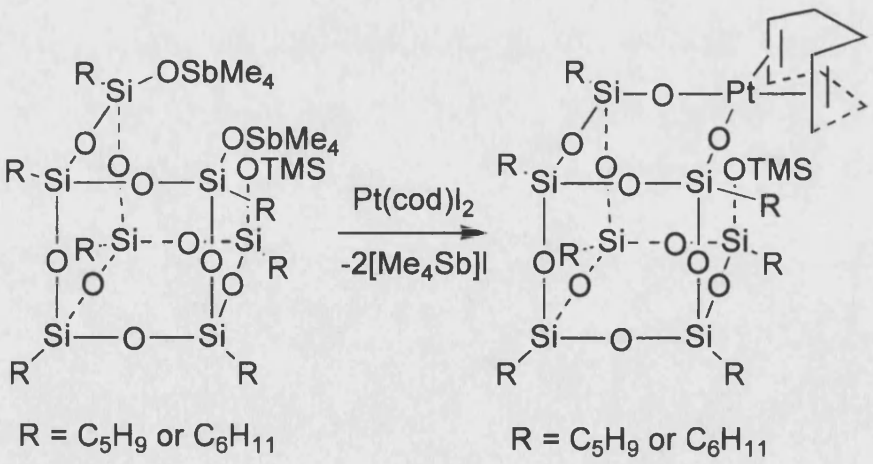

5.1 Results and Discussion

5.1.1 Introduction

Anionic equivalents of silasesquioxanes using thallium(I) or tetraalkylstibonium, have found limited use in the synthesis of complexes containing late transition metals, and other high oxidation state metals.[4,5] The aims of this work were to develop alternative synthetic strategies based on the acidity of the free silanol groups, as well as the activation of the late transition metal complex to silanol coordination via the extraction of chloride ligands. This removes the need to use transmetallating agents such as thallium salts, and the problems that these entail.

5.1.2 Synthesis of the Palladium(II) and Platinum(II) Complexes of Silasesquioxanes

Two synthetic routes were developed to form the platinum(II) and palladium(II) silasesquioxane complexes, both of which gave the desired complexes in good yields. The first method utilises the reactivity of the acidic silasequioxane silanol groups with the carbonate functionality in [$Pt(CO_3)$(dppe)] [dppe = bis(diphenylphosphino)ethane] (Scheme 1). The reaction of one equivalent of [$Pt(CO_3)$(dppe)] with (c-$C_5H_9)_7Si_7O_9(OH)_2OSiMe_3$ (**S**^{1})^6, (c-$C_6H_{11})_7Si_7O_9(OH)_2OSiMe_3$ (**S**^{2})^6 and (c-$C_5H_9)_7Si_7O_9(OH)_3$ (**S**^{3})^6 in dichloromethane, yielded the complexes [(c-$C_5H_9)_7Si_7O_9(OSiMe_3)O_2Pt$(dppe)] (**69**), [($c$-$C_6H_{11})_7Si_7O_9(OSiMe_3)O_2Pt$(dppe)] (**70**) and [($c$-$C_5H_9)_7Si_7O_9(OH)O_2Pt$(dppe)] (**71**) respectively. In all cases the reactions are clean, with **69**, **70** and **71** the only observed products, but these reactions are slow with full conversion only occurring after several days.

Scheme 1

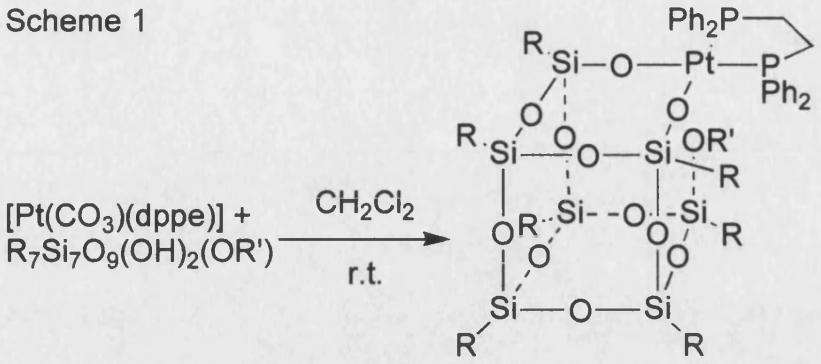

R = *c*-C_5H_9 or *c*-C_6H_{11}
R' = $SiMe_3$ or H

Complexes **69-71** were characterised on the basis of microanalysis, multinuclear NMR and infrared spectroscopy. The $^{31}P\{^1H\}$ NMR spectra of **69-71** showed a singlet with platinum satellites (Table 1), with chemical shifts in the range δ(P) 26.9-27.7 ppm and $^1J(P,Pt)$ coupling constants between 3729-3776 Hz. All three complexes showed an upfield shift and larger $^1J(P,Pt)$ coupling constants relative to [$Pt(CO_3)$(dppe)]. The chemical shifts and coupling constants of **69-71** are similar to those reported previously for [$Pt(OSiMe_3)_2$(dppe)][7] [δ(P) 27.1 ppm, $^1J(P,Pt)$ 3595 Hz] and [$Pt(OMe)_2$(dppe)][8] [δ(P) 28.5 ppm, $^1J(P,Pt)$ 3342 Hz], though the coupling constants are slightly larger, reflecting the lower *trans* influence of the silasesquioxane. The ^1H NMR spectra of **69-71** were as expected with broad signals for the phenyl groups of dppe and the alkyl groups of the silasesquioxane ligands. The FAB mass spectrum of complex **69** showed the presence of a peak at *m/z* 1539 corresponding to $[M + H]^+$ and a peak at *m/z* 1469 corresponding to $[M - SiMe_3]^+$. The spectrum of complex **70** showed a peak at *m/z* 1046 corresponding to $[M - Pt(dppe)]^+$.

The reaction of [$Pt(CO_3)$(dppe)] with $\mathbf{S^1}$ is in marked contrast to those of [$Pt(CO_3)(PPh_3)_2$] and [$Pt(CO_3)$(dppp)] for which no reaction with $\mathbf{S^1}$ was observed after several days. A similar trend for the reactivities of the

bis(phosphine)platinum(II) carbonates has been reported previously for their reactions with vicinal diols.[9]

The second preparative route utilised the reaction of the silasesquioxane silanol groups of $\mathbf{S^1}$ [6] and $\mathbf{S^2}$ [6] with $[MCl_2(dppe)]$ [M = Pd(II) or Pt(II)] in refluxing dichloromethane in the presence of the base silver(I) oxide (Scheme 2). The reaction is slow as for the carbonate route, though it also allowed the synthesis of the palladium(II) silasesquioxane complex (**72**).

Scheme 2

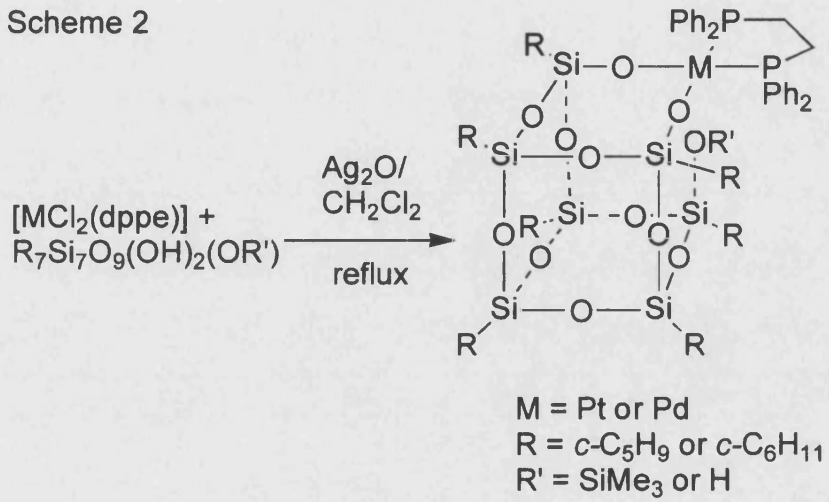

Table 1. Selected $^{31}P\{^1H\}$ NMR data for complexes **69-72**.

	Complex	δ(P)/ppm	^1J(P,Pt)/Hz
69	$[(c\text{-}C_5H_9)_7Si_7O_9(OSiMe_3)O_2Pt(dppe)]$	27.3	3773
70	$[(c\text{-}C_6H_{11})_7Si_7O_9(OSiMe_3)O_2Pt(dppe)]$	27.7	3776
71	$[(c\text{-}C_5H_9)_7Si_7O_9(OH)O_2Pt(dppe)]$	26.9	3729
72	$[(c\text{-}C_5H_9)_7Si_7O_9(OSiMe_3)O_2Pd(dppe)]$	33.7	-

Comparison of the $^{31}P\{^1H\}$ and ^1H NMR spectra of the products from the reaction of $\mathbf{S^1}$ and $\mathbf{S^2}$ with $[PtX(dppe)]$ (where X = Cl_2 or CO_3), showed that the two

synthetic routes are equivalent. The only difference was found in purification of the final products, with the carbonate reaction tending to give a cleaner synthesis, while the final product from the silver(I) oxide route were often contaminated by a brown discolouration.

During the synthesis of **69** via the silver(I) oxide route the $^{31}P\{^{1}H\}$ NMR spectra showed that on prolonged reaction with silver(I) oxide the simple singlet with platinum satellites due to **69**, was replaced by a complex pattern of singlets with platinum satellites centred at approximately δ 27 ppm with coupling constants [$^{1}J(P,Pt)$] between 3700 to 3780 Hz. Unfortunately it did not prove possible to identify these compounds.

The reaction of $[PdCl_2(dppe)]$ with $\mathbf{S^1}$ was carried out via the silver(I) oxide route to check that the reaction was general for both palladium(II) and platinum(II). The reaction took approximately one week to reach completion, with the $^{31}P\{^{1}H\}$ NMR spectra showing a singlet at δ 33.7 ppm. The ^{1}H NMR of the purified product showed the typical broad signals expected for the alkyl groups of the silasesquioxane as well as the presence of the phenyl and alkyl groups of the dppe ligand (Experimental Section).

The complexes **70-72** were found to be difficult to purify due to the formation of a waxy residue on recrystallisation. As a result of this difficulty in purifying samples, microanalysis of **71** and **72** were not successfully obtained.

The interest in using the trisilanol silasesquioxane (c-$C_5H_9)_7Si_7O_9(OH)_3$ ($\mathbf{S^3}$), is that on coordination to a transition metal fragment such as Pt(dppe) one of the silanol groups remains uncoordinated. This leaves a potential reactive site to which various functional groups or a second metal atom may be introduced.

5.1.2.1 X-ray Crystal Structure of *cis*-[(*c*-C_5H_9)$_7$$Si_7O_9$($OSiMe_3$)$O_2$Pt(dppe)] (69)

Single crystals of complex **69** were grown from slow diffusion of acetonitrile into a toluene solution. The crystal structure (Figure 4) confirmed the identity of **69**. Selected bond lengths and angles are given in Table 2.

Table 2. Selected bond lengths [Å] and angles [°] for **69**.

Pt(1)-O(1)	2.031(6)	Pt(2)-O(2)	2.036(4)
Pt(1)-P(1)	2.195(2)	Pt(1)-P(2)	2.204(2)
Si(1)-O(1)	1.573(6)	Si(2)-O(2)	1.566(6)
O(1)-Pt(1)-O(2)	90.3(2)	O(2)-Pt(1)-P(1)	90.2(2)
P(1)-Pt(1)-P(2)	86.90(8)	P(2)-Pt(1)-O(1)	92.5(2)
Pt(1)-O(1)-Si(1)	146.2(4)	Pt(1)-O(2)-Si(2)	148.3(4)
Si(3)-O(12)-Si(8)	152.8(5)		

The platinum(II) centre in **69** is distorted square planar with *cis* angles between 86.9 to 92.5°. The Pt-O and Pt-P bond distances in complex **69** are similar to the expected values for a Pt-O and Pt-P bonds.[10] Comparison of these bond distances with the isoelectronic complex [Pt(OCH_3)$_2$(dppe)][8] [Pt-P = 2.222(3), 2.228(3) Å, Pt-O = 2.037(7), 2.041(7) Å] shows the Pt-O distances to be similar whereas the Pt-P bonds in **69** are slightly shorter than those in [Pt(OCH_3)$_2$(dppe)] which is consistent with the lower *trans* influence of the silasesquioxane. The Si-O bond distances in the platinum siloxy functions [Si(1)-O(1) = 1.573(6) Å; Si(2)-O(2) = 1.566(6) Å] are significantly shorter than those present in the silasesquioxane skeleton [1.597-1.647 Å; typical 1.63 Å], while the equivalent Si-O bond distances from the crystal structure of the

silasesquioxane silanol $(c\text{-}C_5H_9)_7Si_7O_9(OH)_2(OSiMe_3)$[11] (**S**[1]), are 1.619(7) and 1.616(7) Å respectively. This bond shortening may be ascribed to the absence of electron donation from the oxygen lone pairs to the electron rich platinum centre which will lead to a stronger Si-O bond by enhanced electron donation to silicon; this effect is absent or the reverse in high oxidation state early transition metal silasesquioxanes.[12]

Figure 4

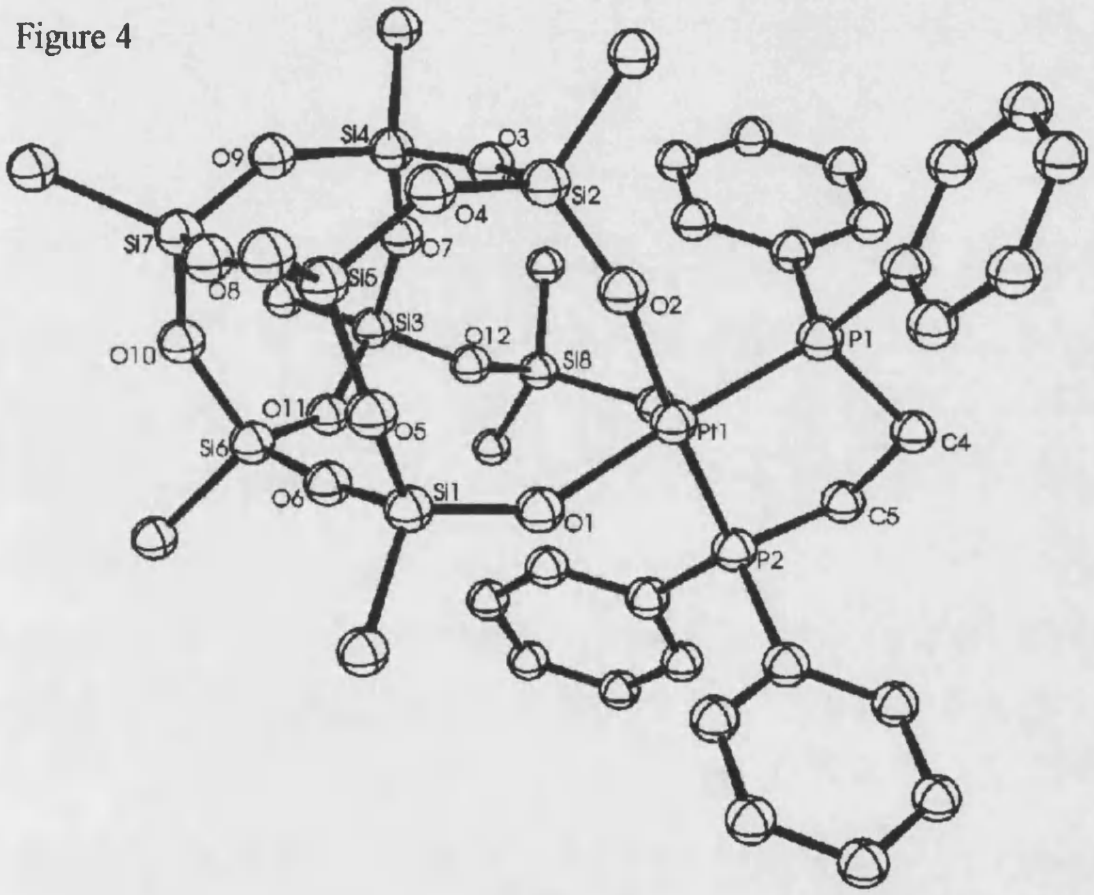

Comparison of the Si/O skeleton of **69** with that of the silasesquioxane disilanol **S**[1] shows that they are both very similar. For example, the intramolecular distance between the ligating oxygen atoms O(1) and O(2) in **69** is 2.88(1) Å compared with 2.67(1) Å in **S**[1], while the intramolecular distance Si(1)-Si(3) in **69**,

which can be considered as a measure of the binding cavity, of 5.22(1) Å is virtually identical in S^1 of 5.21(1) Å. These results suggest that the silasesquioxane diol is ideally preorganised for coordination to platinum(II) centre following deprotonation.

5.2 Conclusion

Both the carbonate and the silver(I) oxide routes have been shown to lead to transition metal complexes of the silasesquioxanes **69-72**, though both reactions are slow. Initial results appear to indicate that the silver(I) oxide route is more general in that it works for both palladium(II) and platinum(II).

The single crystal X-ray analysis of complex **69** showed that the platinum is bound to the two deprotonated silanol groups of the silasesquioxane S^1 in a *cis* arrangement with the dppe ligand taking up a slightly distorted configuration.

5.3 References

1 F. J. Feher, D. A. Newman and J. F. Walzer, *J. Am. Chem. Soc.*, 1989, **111**, 1741.

2 F. T. Edelmann, *Angew. Chem., Int. Ed. Engl.*, 1992, **31**, 586.

3 F. J. Feher, T. A. Budzichowski, K. Rahimian and J. W. Ziller, *J. Am. Chem. Soc.*, 1992, **114**, 3859.

4 F. J. Feher and T. A. Budzichowski, *Polyhedron*, 1995, **14**, 3239.

5 H. C. L. Abbenhuis, unpublished work.

6 Silasesquioxane starting materials kindly supplied by H. C. L. Abbenhuis, Schuit Institute of Catalysis, Eindhoven Univeristy of Technology, The Netherlands.

7 M. A. Andrews and G. L. Gould, *Organometallics*, 1991, **10**, 387.

8 H. E. Bryndza, J. C. Calabrese, M. Marsi, D. C. Roe, W. Tam and J. E. Bercaw, *J. Am. Chem. Soc.*, 1986, **108**, 4805.

9 M. A. Andrews, E. J. Voss, G. L. Gould, W. T. Klooster and T. F. Koetzle, *J. Am. Chem. Soc.*, 1994, **116**, 5730.

10 A. G. Orpen, L. Brammer, F. H. Allen, O. Kennard, D. G. Watson and R. Taylor, *J. Chem. Soc. Dalton Trans.*,1989, S1.

11 H. C. L. Abbenhuis, A. D. Burrows, H. Kooijman, M. Lutz, M. T. Palmer, R. A. van Santen and A. L. Spek, *J. Chem. Soc., Chem. Commun.*, 1998, 2627.

12 F. J. Feher, *J. Am. Chem. Soc.*, 1986, **108**, 3850; F. J. Feher and R. L. Blanski, *J. Chem. Soc., Chem. Commun.*, 1990, 1614; M. Crocker, R. H. M. Herold and A. G. Orpen, *J. Chem. Soc., Chem. Commun.*, 1997, 2411.

Chapter 6

Self Assembly and Silver Isonicotinate Structure

6.0 Introduction

The synthetic technique of self-assembly in which simple chemical systems self-organise to form supramolecular structures provides a very powerful tool in the synthesis of a vast range of compounds with interesting structures.

Out of the vast range of polygons that can be potentially synthesised using self-assembly, molecular squares such as $[Pt(dppp)(4,4'\text{-bipyridyl})]_4(OSO_2CF_3)_8$[1] are one of the simplest and have attracted considerable interest.[2,3] Their design and assembly incorporates non-chelating bidentate linear linkage units in conjunction with 90° angular binding units. Square planar group 10 metals containing two mutually *cis* reactive sites, and two ancillary ligands (L), for example *cis*-$[Pd(OSO_2CF_3)_2(PEt_3)_2]$, have been exploited to provide the required 90° angles which when combined with linear linkage units such as 4,4'-bipyridyl allow self assembly to occur to give the tetranuclear, macrocyclic molecular squares (Figure 1). The dimensions of the cavity produced can be varied by use of different linking ligands, for example the incorporation of 2,9-diazadibenzo[*cd*,*lm*]perylene as the linear linkage units increases the size of the cavity. This control is of particular interest in relation to the possible host guest chemistry. The versatility of this synthetic method has been utilised in the preparation of a vast range of functionalised molecular squares, with the incorporation of mixed metallic,[4] crown ethers,[2] porphyrin[5] and chiral[6] groups.

Figure 1

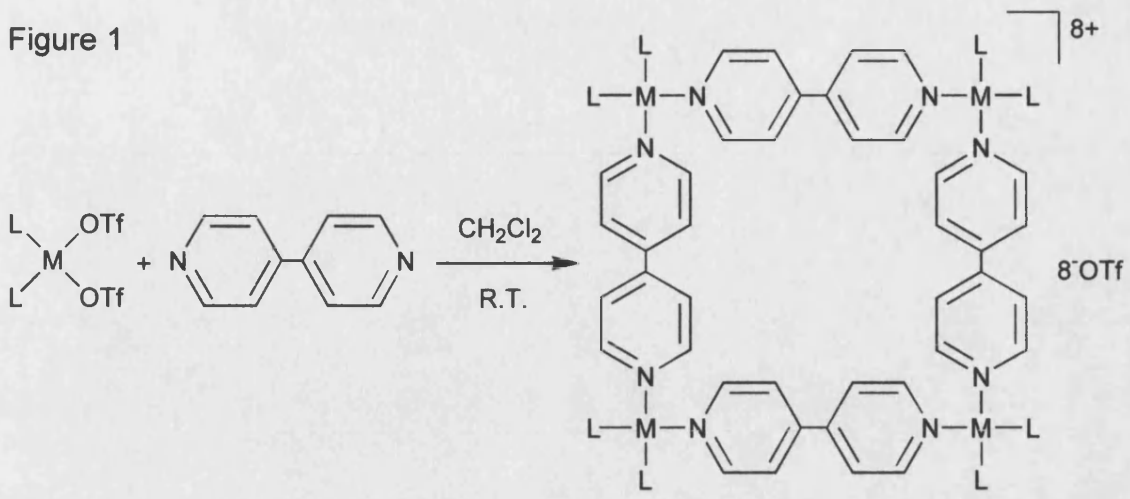

Control over molecular assembly using a combination of coordinative bonds and hydrogen bonding groups to facilitate the crystal engineering of structures based on metal complexes is currently of considerable interest.[7,8] When such hydrogen bonding groups are incorporated into transition metal complexes the metal acts as a rigid framework around which the complex can be built.[8,9] Use of suitable matching hydrogen bonding pairs contained within the ligands as in $[Pt(H_2L)(PPh_3)_2]$[10] (H_4L = 5-aminoorotic acid), or by addition of molecules containing the complementary hydrogen bonding groups for example the hydrogen bonding between bis(thiosemicarbazide)nickel(2+) and dicarboxylate anions (Figure 2),[11] provides for the possible linkage of such molecules into supramolecular structures.

Figure 2

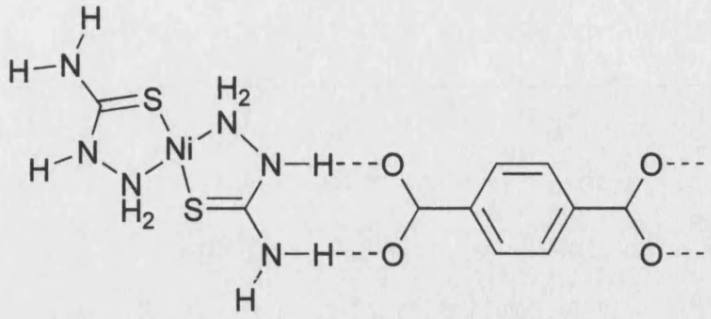

The carboxylic acid group (-COOH) has been shown to self-assemble to form either discrete dimeric or linear structures (Figure 3). The formation of discrete

Figure 3

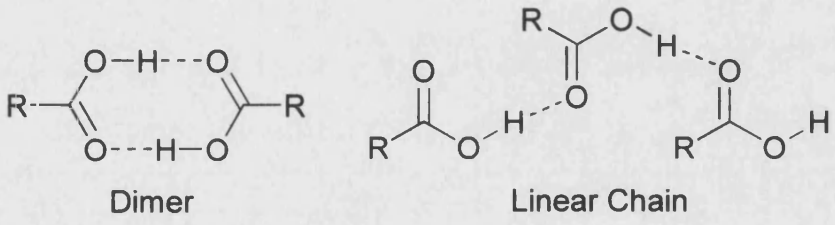

dimeric pairs in compounds that contain two or more carboxylic acid groups can have a significant effect on the formation of a range of 1D, 2D and 3D polymeric structures depending on spatial orientation of the carboxylic acid groups. For example the hydrogen-bonding network observed in the crystal structure of trimesic acid (Figure 4).[12]

Figure 4

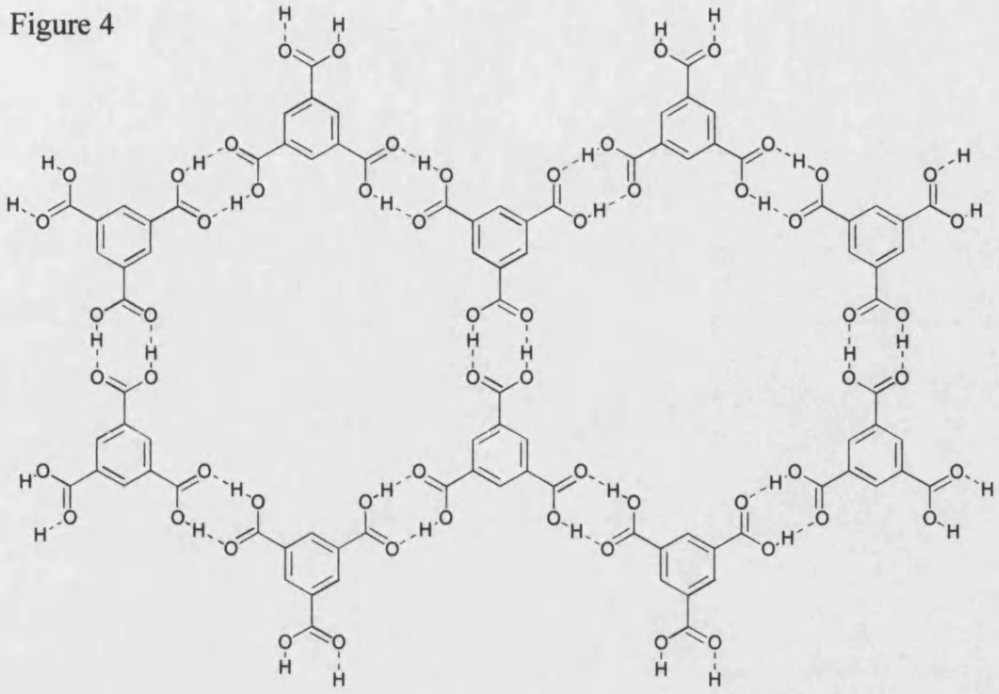

The main impetus for the work in this chapter was to determine if molecular squares could be made by the self assembly of transition metal complexes containing complementary hydrogen bonding groups, instead of the linkage being made up of ligands such as 4,4'-bipyridine. For the geometry of the transition metal complexes to be suitable for the formation of supramolecular squares, as opposed to chains, the ligands containing the hydrogen bonding functionality have to be arranged mutually *cis*, with the angle between the two ligands as close to 90° as possible. It was hoped that the linkage of two carboxylic acid groups from isonicotinic acid to give the dimer would effectively act as a hydrogen-bonded analogue of 4,4'-bipyridine (Figure 5).

Figure 5

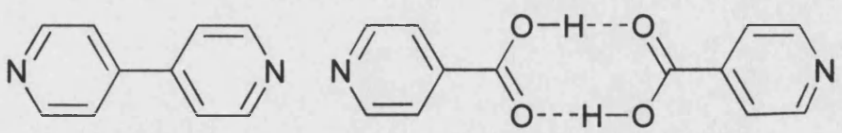

4,4'-Bipyridine Isonicotinic acid dimer

6.1 Results and Discussion

6.1.1 Synthesis of *cis*-[M(dppe)(isonicH)$_2$](BF$_4$)$_2$ (M = Pd and Pt)

Previous attempts to use the self-complementary hydrogen bonding groups of isonicotinic acid (isonicH) in the complexes [Pt(dppe)(isonicH)$_2$](OSO$_2$CF$_3$)$_2$,[13] to self assemble via the formation of carboxylic acid dimer pairs giving platinum molecular squares were unsuccessful due to hydrogen bonding of the carboxylic acid group to the triflate counter ion so preventing dimerisation (Figure 6). To avoid this a counter ion was needed which would not be involved in hydrogen bonding to the isonicotinic acid, for example tetrafluoroborate (BF_4^-).

Figure 6

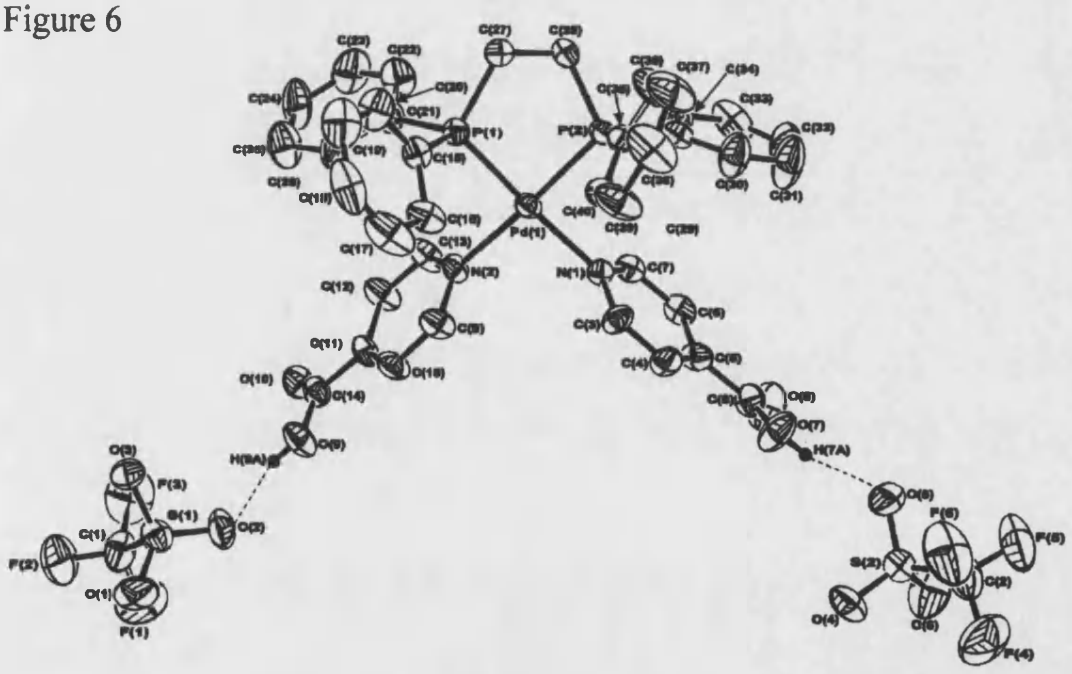

The reaction of two equivalents of isonicotinic acid with the reactive intermediate [M(dppe)(S)$_2$](BF$_4$)$_2$ (S = THF, acetone) which was formed *in situ* from [MCl$_2$(dppe)] and AgBF$_4$ gave the complexes *cis*-[Pd(dppe)(isonicH)$_2$](BF$_4$)$_2$ (**73**) and

cis-[Pt(dppe)(isonicH)$_2$](BF$_4$)$_2$ (**74**) which were characterised on the basis of multinuclear NMR and infrared spectroscopy.

The $^{31}P\{^1H\}$ NMR spectrum of **73** showed a single phosphorus resonance, while complex **74** showed a singlet with platinum satellites (Table 1). The chemical shifts and coupling constant are both similar to those observed for the complexes [M(dppe)(isonicH)$_2$](OSO$_2$CF$_3$)$_2$ (M = Pd and Pt) [δ= 67.7 ppm; δ 39.0 ppm, ^1J(P,Pt) 3236 Hz respectively], suggesting that **73** and **74** have similar structures. The ^1H NMR spectra of **73** and **74** were as expected with the signal integration's consistent with a ratio of 1:2 for dppe and isonicotinic acid. The infrared spectra of **73** and **74** show one strong band ν(CO$_2$H) at 1734 and 1733 cm^{-1}, which is consistent with the protonated carboxylic acid, as well as a strong band for ν(BF$_4$) at 1060 cm^{-1}.

Unfortunately complexes **73** and **74** could not be purified sufficiently to get accurate microanalyses, so were only characterised by multinuclear NMR and infrared spectroscopy. As no suitable crystals for X-ray crystallographic studies could be obtained of either **73** or **74,** examination of their potential self-assembly was not possible.

Table 1. Selected $^{31}P\{^1H\}$ NMR and infrared data for complexes **73-74.**

	Complex	δ(P)/ppm	^1J(P,Pt)/Hz	ν(CO$_2$H)/cm^{-1}
73	*cis*-[Pd(dppe)(isonicH)$_2$](BF$_4$)$_2$	68.3	-	1734
74	*cis*-[Pt(dppe)(isonicH)$_2$](BF$_4$)$_2$	39.2	3233	1733

6.1.2 Formation of $[Ag_3(isonic)_2]BF_4$

Reactions in which $AgBF_4$ was reacted directly with $[PdCl_2(dppe)]$ and isonicotinic acid in acetone gave unexpected results. The $^{31}P\{^1H\}$ NMR spectra of the reaction mixture showed a singlet at δ 68.1, consistent with the formation of $[Pd(dppe)(isonicH)_2]^{2+}$. However on crystallisation, the solution gave two distinct crystal types; the major product formed pale yellow crystals, which lost solvent very rapidly and therefore were not suitable for X-ray analysis, whereas the minor component formed small colourless air stable crystals. Spectroscopic data suggested that these crystals contained neither palladium nor dppe, and were instead a silver isonicotinate complex $[Ag_3(isonic)_2]BF_4$ (**75**). Further evidence for this conclusion was obtained by the formation of similar crystals from the reaction of silver(I) tetrafluoroborate with two equivalents of isonicotinic acid in the absence of $[PdCl_2(dppe)]$. The product of this reaction was isolated as colourless block shaped crystals, and characterised on the basis of microanalysis, X-ray crystallography, multinuclear NMR, and infrared spectroscopy as $[Ag_3(isonic)_2]BF_4$ (**75**). The ^1H NMR spectra of **75** showed two doublets which were attributed to the protons of the isonicotinate ligands at δ 9.24 [$^3J(H,H)$ = 7 Hz] and 8.65 [$^3J(H,H)$ = 7 Hz]. The $^{13}C\{^1H\}$ NMR spectrum for **75** showed the expected signals due to the isonicotinate ligand. The infrared spectrum showed bands for both $\nu(CO_2)$ at 1580 and 1547 cm^{-1}, and $\nu(BF_4)$ at 1156, 1092, 1026 and 1009 cm^{-1} (Experimental Section).

6.1.2.1 X-ray Crystal Structure of $[Ag_3(isonic)_2]BF_4$ (75)

Compound **75** was recrystallised from acetone-hexane as colourless block shaped crystals suitable for X-ray crystallographic studies. The crystal structure

revealed that complex **75** had an unusual polymeric structure consisting of Ag_3 triangles linked together pair wise by two isonicotinate ligands. Selected bond lengths and angles are given in Table 2.

Table 2. Selected bond lengths [Å] and angles [°] for **75**.

Ag(1)-Ag(2)	3.011(2)	Ag(1)-Ag(3)	2.969(5)
Ag(2)-Ag(3)	3.236(5)	Ag(2)-N(1)	2.172(7)
Ag(3)-N(2)	2.160(6)	Ag(1)-O(1)^{ii}	2.146(6)
Ag(1)-O(3)^{I}	2.134(5)	Ag(2)-O(4)^{I}	2.134(6)
Ag(3)-O(2)^{ii}	2.129(5)	Ag(1)-Ag(1)^{iii}	3.062(5)
Ag(1)···F(2)	2.808(6)	Ag(1)···F(3)	2.889(7)
Ag(2)···F(2)^{v}	2.870(6)	Ag(2)···F(4)^{v}	3.130(7)
Ag(3)···F(4)^{v}	2.948(6)	Ag(2)···F(2)^{vi}	2.898(8)
Ag(3)···F(3)^{vii}	2.857(7)	Ag(3)···F(4)^{vii}	2.922(7)
Ag(3)-Ag(1)-Ag(2)	65.51(10)	Ag(1)-Ag(2)-Ag(3)	56.61(9)
Ag(1)-Ag(3)-Ag(2)	57.88(10)	Ag(3)-Ag(1)-Ag(1)^{iii}	136.23(8)
Ag(2)-Ag(1)-Ag(1)^{iii}	74.07(9)	O(1)^{ii}-Ag(1)-O(3)^{I}	173.9(2)
O(4)^{i}-Ag(2)-N(1)	179.5(3)	O(2)^{ii}-Ag(3)-N(2)	175.2(3)

Primed atoms generated by the following symmetry transformations: i $-x + 1, -y + 1, -z + 1$, ii $-x, -y, -z$, iii $-x, -y, -z + 1$, v $-1 + x, y, z$, vi $1 - x, -y, -z$ and vii $-x, 1 - y, -z$, respectively.

The asymmetric unit (Figure 7) consists of three silver atoms at the apices of a triangle, two isonicotinate anions and one tetrafluoroborate anion. The nitrogen atoms of the isonicotinate ligands N(1) and N(2), are coordinated to the silver atom Ag(2)

and Ag(3) respectively, with the Ag-N bond distances [Ag(2)-N(1) 2.172(7), Ag(3)-N(2) 2.160(6) Å] similar to the Ag-N bond distances reported for the complex $[Ag(NC_5H_4CO_2)(NC_5H_4CO_2H)].4H_2O$ (2.166 Å).[14] The silver-silver distances range from 2.969(5) to 3.236(5) Å (Table 2).

Figure 7

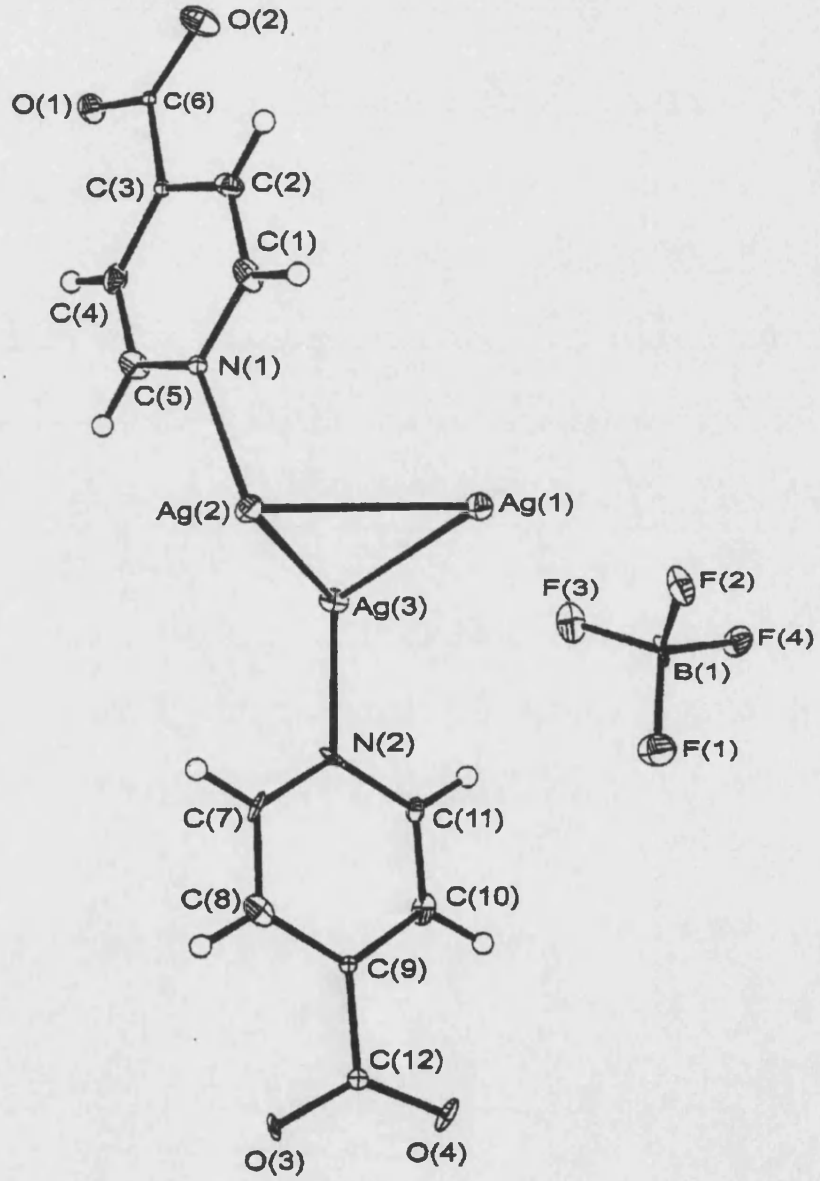

The extended structure of **75** shows that all four oxygen atoms of the carboxylate groups within the two isonicotinate anions are coordinated to silver

atoms, with O(1) and O(2) bonded to Ag(1) and Ag(3) in the asymmetric unit generated via the symmetry operator *-x*, *-y*, 1 - *z*, and O(3) and O(4) are bonded to Ag(1) and Ag(2) in asymmetric unit generated via the symmetry operator 1 - *x*, 1 - *y*, -1 - *z*. The combined effect of these bonds is to render a series of one-dimensional columnar polymers within the crystal lattice (Figure 8). Considering these polymers in isolation, all the silver atoms are four-coordinate, assuming the silver-silver bonds to be present. The three silver-silver contacts within each triangle are composed of two which are bridged by a carboxylate group [Ag(1)-Ag(2) 3.011(2), Ag(1)-Ag(3) 2.969(5) Å] while the silver-silver contact between Ag(2) and Ag(3) is unbridged, and it is this edge that is the longest [3.236(5) Å].

A centre of inversion proximate to Ag(1) (at 0.5, 0, 0) has the effect of interlinking these polymers into sheets with a short Ag(1)···Ag(1) contact, hence raising the coordination of Ag(1) to five. This silver-silver contact is unbridged and significantly shorter [3.062(5) Å] than observed for the unbridged edge of the Ag_3 triangle [Ag(2)···Ag(3)].

The presence of these two unbridged silver-silver interactions, which are both shorter than twice the van der Waals' radius of silver, suggests that significant Ag···Ag interactions are present. Indeed similar Ag···Ag interactions have been observed in the structure of $[Ag(imidazole)_2]_6(ClO_4)_6$[15] in which $Ag(imidazole)_2$ units are linked together into a triangle solely by silver-silver interactions with Ag···Ag contacts considerably longer [3.493 Å] than either of the two unbridged contacts observed in **75**. These contacts have been previously ascribed to d^{10}-d^{10} interactions, though such interactions have mainly been observed for gold(I)[16] with a few examples reported for both copper(I) and silver(I).[17]

Figure 8

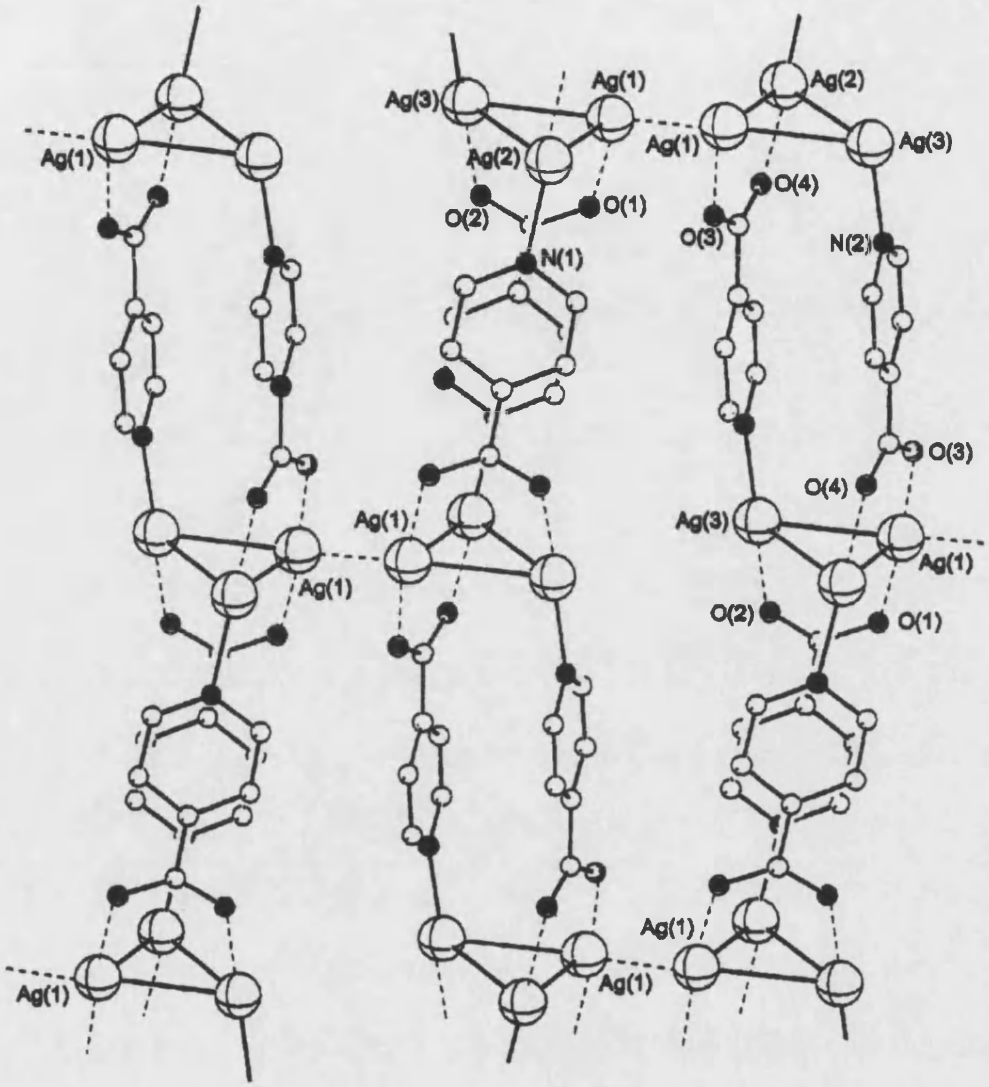

The angles between the plane of the silver atoms and the planes of the isonicotinate ligands show some distortion from the perpendicular, being 88.3(2) [for the isonicotinate containing N(1)] and 77.2(2)° [for the isonicotinate containing N(2)]. Examination of the torsion angles involving the carboxylates revealed that this functionality in the isonicotinate containing N(2) is considerably more twisted from the pyridyl plane [13(1)°] than that in the isonicotinate containing N(1) [2(1)°].

Within the plane containing the silver triangles there are, in addition to the Ag···Ag interactions, significant interactions between the silver atoms and the tetrafluoroborate anions (Figure 9). These anions are orientated such that one fluorine atom F(1) is pointing in the direction of the polymeric chains, whereas each of the other three fluorine atoms interact with the three silver atoms. The Ag···F distances range from 2.808(6) to 3.130(7) Å, all within the combined van der Waals' radii for both atoms (3.19 Å). Previous examples in which silver(I) and BF_4^- interact have been observed before for example, $[Ag(2,6\text{-dimethylpyridine})_2]BF_4$[18] in which Ag···F interactions [3.011(8) Å] serve to link the cations into chains. In this compound as in **75**, interaction with BF_4^- leads to a reduction in the anion symmetry in the solid state and several $\nu(BF_4^-)$ stretches are observed in the infrared spectrum.

Figure 9

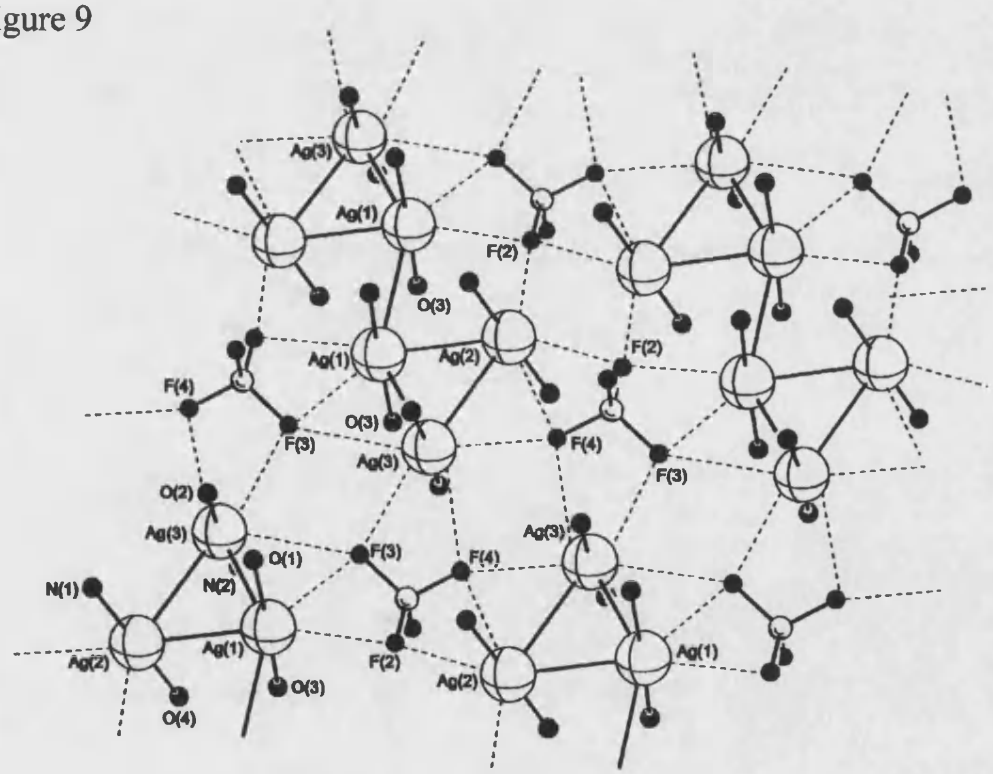

6.2 Conclusion

The incorporation of isonicotinic acid into the palladium and platinum coordination spheres, has led to complexes with the *cis*-$[M(dppe)(isonicH)_2]^{2+}$ geometry required for self assembly into supramolecular squares. However, unfortunately no suitable crystals have been obtained for these compounds to verify whether such a self-assembly process does occur.

The minor component formed by the reaction of $[PdCl_2(dppe)]$, isonicH and $AgBF_4$ was shown to be the compound $[Ag_3(isonic)_2]BF_4$ (**75**). Compound **75** was also synthesised directly from the reaction of isonicH and $AgBF_4$. The crystal structure of **75** contained both unbridged and bridged short Ag···Ag contacts within the Ag_3 triangles and polymeric structure.

6.3 References

1 P. J. Stang, D. H. Cao, S. Saito and A. M. Arif, *J. Am. Chem. Soc.*, 1995, **117**, 6273.

2 P. J. Stang and D. H. Cao, *J. Am. Chem. Soc.*, 1994, **116**, 4981; P. J. Stang, D. H. Cao, K. Chen, G. M. Gray, D. C. Muddiman and R. D. Smith, *J. Am. Chem. Soc.*, 1997, **119**, 5163.

3 M. Fujita, O. Sasaki, T. Mitsuhashi, T. Fujita, J. Yazaki, K. Yamaguchi and K. Ogura, *J. Chem. Soc., Chem. Commum.*, 1996, 1535.

4 P. J. Stang, B. Olenyuk, J. Fan and A. M. Arif, *Organometallics*, 1996, **15**, 904.

5 P. J. Stang, J. Fan, B. Olenyuk, *J. Chem. Soc., Chem. Commun.*, 1997, 1453.

6 P. J. Stang and B. Olenyuk, *Angew. Chem., Int. Ed. Engl.*, 1996, **35**, 732.

7 J.-M. Lehn, *Angew. Chem., Int. Ed. Engl.*, 1990, **29**, 1304; D. Philp and J. F. Stoddart, *Angew. Chem., Int. Ed. Engl.*, 1996, 35, 1154; C. B. Aakeröy and K. R. Seddon, *Chem. Soc. Rev.*, 1993, 397.

8 S. Subramanian and M. J. Zaworotko, *Coord. Chem. Rev.*, 1994, **137**, 357

9 A. D. Burrows, C.-W Chan, M. M. Chowdhry, J. E. McGrady and D. M. P. Mingos, *Chem. Soc. Rev.*, 1995, 329.

10 A. D. Burrows, D. M. P. Mingos, A. J. P. White and D. J. Williams, *J. Chem. Soc., Dalton Trans.*, 1996, 3805.

11 A. D. Burrows, D. M. P. Mingos, A. J. P. White and D. J. Williams, *J. Chem. Soc., Chem. Commun.*, 1996, 97.

12 D. J. Duchamp and R. E. Marsh, *Acta. Cryst.*, 1969, **B25**, 5.

13 A. D. Burrows and M. F. Mahon, unpublished results.

14 F. Jaber, F. Charbonnier, R. Faure and M. Petit-Ramel, *Z. Kristallogr.*, 1994, **209**, 536.

15 G. W. Eastland, M. A. Mazid, D. R. Russell and M. C. R. Symons, *J. Chem. Soc., Dalton Trans.*, 1980, 1682.

16 H. Schmidbaur, *Chem. Soc. Rev.*, 1995, **24**, 391.

17 M. Jenson, *Angew. Chem., Int. Ed. Engl.*, 1987, **26**, 1098; P. Pyykkö, *Chem. Rev.*, 1997, **97**, 597.

18 E. Horn, M. R. Snow and E. R. T. Tiekink, *Aust. J. Chem.*, 1987, **40**, 761.

Chapter 7

Experimental Section

7.0 General Experimental

Reactions were routinely carried out using Schlenk-line techniques under pure dry dinitrogen using dry dioxygen-free solvents unless noted otherwise. Microanalyses (C, H and N) were carried out by Mr. Alan Carver (University of Bath Microanalytical Service). Infrared spectra were recorded on a Nicolet 510P spectrometer as KBr pellets, nujol mulls or dichloromethane solutions in KBr cells. ^{1}H, $^{13}C\{^{1}H\}$ and $^{31}P\{^{1}H\}$ NMR spectra were recorded on a JEOL JNM-EX270 spectrometer operating at 270 MHz referenced to TMS and 109.4 MHz referenced to H_3PO_4, respectively. $^{31}P\{^{1}H\}$ NMR spectra were also recorded on a Varian Mercury 400 MHz NMR spectrometer. FAB mass spectra were recorded on a VG AutoSpec-Q spectrometer using 3-nitrobenzyl alcohol as the matrix. $[PtX_2(cod)]$ (X = Cl, Br),[1] $[PdCl_2(cod)]$,[2] $[Pt(CO_3)(dppe)]$,[3] $[M(dmba)(\mu\text{-}Cl)]_2$ (M = Pd, Pt)[4], $[Mo(CO)_4(NHC_5H_{10})_2]$,[5] $[Mo(C_7H_8)(CO)_3]$,[6] $[Rh(\mu\text{-}Cl)(CO)_2]_2$[7] and $[Rh(\mu\text{-}Cl)(cod)]_2$[8] were prepared by standard literature methods. $(c\text{-}C_5H_9)_7Si_7O_9(OH)_2OSiMe_3$ ($\mathbf{S^1}$), $(c\text{-}C_6H_{11})_7Si_7O_9(OH)_2OSiMe_3$ ($\mathbf{S^2}$) and $(c\text{-}C_5H_9)_7Si_7O_9(OH)_3$ ($\mathbf{S^3}$) were kindly supplied by H. C. L. Abbenhuis[9] and used without further purification. Dichloromethane was distilled under a nitrogen atmosphere from CaH_2, diethyl ether, THF, toluene, pentane and hexane were pre-dried over sodium wire, distilled from sodium-potassium alloy or sodium-benzophenone under a nitrogen atmosphere. $\mathbf{L^1}$-$\mathbf{L^4}$, $\mathbf{L^7}$, $\mathbf{L^8}$ and $\mathbf{L^{10}}$ were isolated in 80-90% yield, the palladium, platinum, molybdenum and rhodium complexes in 50-90% yields unless noted otherwise.

7.1 Safety

The awareness of safety issues within laboratories is of immense importance to minimise the risks to yourself to those around you. You should work carefully and be aware of the hazards of the chemicals, solvents and equipment that you are using. Whilst working in a laboratory you should always wear safety glasses, protective clothing (lab coat, gloves) and use fume cupboards when handling toxic chemicals.

Particular care must be taken to remove any possible sources of ignition whilst using solvents such as diethyl ether, pentane, hexane, toluene and THF as they are highly flammable. Sodium-potassium alloy, sodium and CaH_2 react violently with both water and alcohols and as such it is essential to use clean dry glassware and equipment when working with solvent stills containing these drying agents.

7.2 Syntheses

Synthesis of $Ph_2PNHCH_2CH_2OCH_3$ (L^1)

Triethylamine (NEt_3) (0.566 g, 5.5 mmol) and chlorodiphenylphosphine (PPh_2Cl) (1.23 g, 5.5 mmol) were added sequentially with stirring to a solution of 2-methoxyethylamine (0.41 g, 5.5 mmol) in tetrahydrofuran (THF) (20 cm^3). The reaction mixture was stirred for 30 minutes and the solution filtered to remove NEt_3HCl. The resulting solution was evaporated under reduced pressure to give a pale yellow, viscous oil. (Found: C, 69.3; H, 6.96; N, 5.15. $C_{15}H_{18}NOP$ requires C, 69.5; H, 7.00; N, 5.40 %). $^{31}P\{^1H\}$ NMR ($CDCl_3$) δ 42.0; ^1H NMR ($CDCl_3$) δ 7.47 - 7.40 (m, 4H, Ar), 7.33 - 7.24 (m, 6H, Ar), 3.32 (t, 2H, $^3J(H,H)$ 5 Hz, CH_2O), 3.23 (s, 3H, CH_3), 3.07 (dt, 2H, CH_2N), 2.46 (m, 1H, NH); $^{13}C\{^1H\}$ NMR ($CDCl_3$) δ 141.2 (d, $^1J(C,P)$ 12 Hz, C_{ipso}), 130.8 (d, $^2J(C,P)$ 20 Hz, C_{ortho}), 128.0 (s, C_{para}), 127.7 (d, $^3J(C,P)$

6 Hz, C_{meta}), 73.5 (d, $^3J(C,P)$ 6 Hz, CH_2O), 58.1 (s, CH_3), 45.3 (d, $^2J(C,P)$ 14 Hz, CH_2N). IR (NaCl plates, cm^{-1}): 3370 [m (br), ν(NH)].

$Ph_2PNHCH_2CH_2CH_2OCH_3$ (L^2): as for **L^1** using NEt_3 (1.11 g, 11 mmol), PPh_2Cl (2.41 g, 11 mmol) and 3-methoxypropylamine (0.98 g, 11 mmol). Product extracted with diethyl ether at -78°C followed by hexane. (Found: C, 70.8; H, 7.20; N, 4.67. $C_{16}H_{20}NOP$ requires C, 70.3; H, 7.38; N, 5.12%). $^{31}P\{^1H\}$ NMR ($CDCl_3$) δ 41.9; ^1H NMR ($CDCl_3$) δ 7.52 - 7.46 (m, 4H, Ar), 7.40 - 7.33 (m, 6H, Ar), 3.44 (t, 2H, $^3J(H,H)$ 6 Hz, CH_2O), 3.32 (s, 3H, CH_3), 3.07 (m, 2H, CH_2N), 2.20 (m, 1H, NH), 1.76 (qui, 2H, CH_2C_2); $^{13}C\{^1H\}$ NMR ($CDCl_3$) δ141.3 (s, C_{ipso}), 130.9 (d, $^2J(C,P)$ 18 Hz, C_{ortho}), 127.8 (s, C_{para}), 127.7 (s, C_{meta}), 70.2 (s, CH_2O), 58.0 (s, CH_3), 43.1 (d, $^2J(C,P)$ 11 Hz, CH_2N), 32.1 (s, CH_2C_2). IR (NaCl plates, cm^{-1}): 3370 [m (br), ν(NH)].

$Ph_2PNHCH_2CH(OCH_3)_2$ (L^3): as for **L^1** using NEt_3 (1.13 g, 11 mmol), PPh_2Cl (2.46 g, 11 mmol) and 2,2-dimethoxyethylamine (1.17 g, 11 mmol). Product extracted with diethyl ether at -78°C. (Found: C, 66.4; H, 6.86; N, 4.70. $C_{16}H_{20}NO_2P$ requires C, 66.4; H, 6.97; N, 4.84%). $^{31}P\{^1H\}$ NMR ($CDCl_3$) δ 42.9; ^1H NMR ($CDCl_3$) δ 7.39 - 7.23 (m, Ar), 4.13 (t, 1H, $^3J(H,H)$ 6 Hz, CH), 3.22 (s, 6H, CH_3), 3.00 (m, 2H, CH_2), 2.23 (m, 1H, NH); $^{13}C\{^1H\}$ NMR (CD_2Cl_2) δ 141.4 (d, $^1J(C,P)$ 12 Hz, C_{ipso}), 130.7 (d, $^2J(C,P)$ 20 Hz, C_{ortho}), 127.8 (s, C_{para}), 127.6 (d, $^3J(C,P)$ 6 Hz, C_{meta}), 104.3 (d, $^3J(C,P)$ 6 Hz, CH), 53.0 (s, CH_3), 47.2 (d, $^2J(C,P)$ 14 Hz, CH_2). IR (NaCl plates, cm^{-1}): 3368 [m (br), ν(NH)].

$Ph_2PNH(C_6H_4)OCH_3$-2 (L^4): as for L^1 using NEt_3 (1.13 g, 11 mmol), PPh_2Cl (2.46 g, 11 mmol) and *o*-anisidine (1.38 g, 11 mmol). Product extracted with diethyl ether at -78°C. (Found: C, 73.3; H, 6.11; N, 4.95. $C_{19}H_{18}NOP$ requires C, 74.2; H, 5.90; N, 4.56%). $^{31}P\{^1H\}$ NMR ($CDCl_3$) δ 27.2; ^1H NMR ($CDCl_3$) δ 7.70 - 7.64 (m, 4H, Ar), 7.55 - 7.44 (m, 6H, Ar), 7.06 - 6.97 (m, 2H, Ar), 6.95 - 6.90 (m, 2H, Ar), 5.32 (d, 1H, ^2J(H,P) 7 Hz, NH), 3.93 (s, 3H, CH_3); $^{13}C\{^1H\}$ NMR ($CDCl_3$) δ147.3 (d, ^3J(C,P) 4 Hz, C2), 139.8 (d, ^2J(C,P) 12 Hz, C_{ipso}), 135.7 (d, ^2J(C,P) 18 Hz, C1), 130.6 (d, ^2J(C,P) 21 Hz, C_{ortho}), 128.5 (s, C_{para}), 128.0 (d, ^3J(C,P) 7 Hz, C_{meta}), 120.7 (s, C5), 118.3 (s, C4), 113.6 (d, ^3J(C,P) 21 Hz, C6), 109.6 (s, C3), 54.9 (s, CH_3). IR (NaCl plates, cm^{-1}): 3381 [m, ν(NH)].

Synthesis of $(Ph_2P)_2NCH_2CH_2OCH_3$ (L^5)

Two methods for the synthesis of L^5 were used:

(**Method 1**) NEt_3 (0.566 g, 5.5 mmol) and PPh_2Cl (1.23 g, 5.5 mmol) were added sequentially with stirring to a solution of L^1 (1.43 g, 5.5 mmol) in THF (20 cm^3). The reaction mixture was stirred for two hours and the solution filtered to remove NEt_3HCl. The resulting solution was evaporated under reduced pressure to give a viscous oil.

(**Method 2**) NEt_3 (1.13 g, 11 mmol) and PPh_2Cl (2.46 g, 11 mmol) were added sequentially with stirring to a solution of 2-methoxyethylamine (0.41 g, 5.5 mmol) in THF (20 cm^3). The reaction mixture was stirred for 2 hours and the solution filtered to remove NEt_3HCl. The resulting solution was evaporated under reduced pressure to give a viscous oil.

(Found: C, 70.4; H, 5.86; N, 2.92. $C_{27}H_{27}ONP_2$ requires C, 73.1; H, 6.14; N, 3.16%). $^{31}P\{^1H\}$ NMR ($CDCl_3$) δ 65.1; ^1H NMR ($CDCl_3$) δ 7.54 (m (br), Ar), 7.45 - 7.40 (m (br), Ar), 3.62 (m, CH_2N), 3.10 (s, CH_3), 3.04 (t, $^3J(H,H)$ 7 Hz,CH_2O).

Synthesis of $Ph_2P(S)NH(C_6H_4)OCH_3$-2 (L^6)

Sulfur (0.032 g, 1.00 mmol) was added with stirring to a solution of $Ph_2PNH(C_6H_5)OCH_3$-2 (0.307 g, 1.00 mmol) in THF (10 cm^3). The reaction mixture was stirred for 2 days and the resulting solution was evaporated under reduced pressure and the solid washed with cold diethyl ether (2 × 10 cm^3), and the white insoluble material dried under reduced pressure. (Found: C, 66.3; H, 5.30; N, 4.06. $C_{19}H_{18}NOPS$ requires C, 67.2; H, 5.35; N, 4.13 %). $^{31}P\{^1H\}$ NMR ($CDCl_3$) δ 52.7; ^1H NMR ($CDCl_3$) δ 8.08 - 7.99 (m, 4H, Ar), 7.60 - 7.43 (m, 6H, Ar), 7.02 (d, 1H, Ar), 6.87 - 6.82 (m, 2H, Ar), 6.74 - 6.68 (m, 1H, Ar), 5.66 (d, 1H, $^2J(H,P)$ 8 Hz, NH), 3.84 (s, 3H, CH_3). IR (KBr, cm^{-1}): 3366 [m, ν(NH)].

$Ph_2PN(CH_3)CH_2CH_2N(CH_3)_2$ (L^7): as for L^1 using NEt_3 (1.13 g, 11 mmol), PPh_2Cl (2.46 g, 11 mmol) and $HN(CH_3)CH_2CH_2N(CH_3)_2$ (1.14 g, 11 mmol). Product extracted with diethyl ether at -78°C. The resulting solution was evaporated under reduced pressure to give a colourless oil. (Found: C, 71.1; H, 7.96; N, 9.31. $C_{17}H_{23}N_2P$ requires C, 71.3; H, 8.10; N, 9.78 %). $^{31}P\{^1H\}$ NMR ($CDCl_3$) δ 65.4; ^1H NMR ($CDCl_3$) δ 7.41 - 7.34 (m, 4H, Ar), 7.33 - 7.28 (m, 6H, Ar), 3.22 - 3.12 (m, 2H, CH_2NP), 2.52 (d, 3H, $^3J(H,P)$ 6 Hz, CH_3NP), 2.35 (t, 2H, $^3J(H,H)$ 7 Hz, CH_2N), 2.17 (s, 6H, CH_3N); $^{13}C\{^1H\}$ NMR ($CDCl_3$) δ 139.0 (d, $^1J(C,P)$ 16 Hz, C_{ipso}), 131.5 (d,

^{2}J(C,P) 20 Hz, C_{ortho}), 127.8 (s, C_{para}), 127.6 (d, ^{3}J(C,P) 7 Hz, C_{meta}), 58.1 (d, ^{2}J(C,P) 6 Hz, CH_2N), 54.2 (d, ^{2}J(C,P) 29 Hz, CH_2NP), 45.3 (s, CH_3N), 36.9 (s, CH_3NP).

Synthesis of $Ph_2PNHCH_2CH_2N(CH_3)_2$ (L^8)

n-Butyllithium (BuLi) in hexane (6.96 cm^3, 1.6 M, 11 mmol) and Ph_2PCl (2.46 g, 11 mmol) were added sequentially with stirring to a solution of $H_2NCH_2CH_2N(CH_3)_2$ (0.980 g, 11 mmol) in THF (40 cm^3) at -78°C. The reaction mixture was stirred for 2 hours and then slowly warmed to room temperature. The solvent was removed under reduced pressure and the product extracted with ice cold diethyl ether. The resulting solution was evaporated under reduced pressure to give a pale yellow oil. (Found: C, 71.1; H, 7.68; N, 9.60. $C_{16}H_{21}N_2P$ requires C, 70.6; H, 7.77; N, 10.3 %). $^{31}P\{^1H\}$ NMR ($CDCl_3$) δ 41.6; ^{1}H NMR ($CDCl_3$) δ 7.41 - 7.37 (m, 4H, Ar), 7.30 - 7.15 (m, 6H, Ar), 2.89 (dt, 2H, ^{3}J(H,P) 14 Hz, ^{3}J(H,H) 6 Hz, CH_2NP), 2.49 (m, 1H, NH), 2.24 (t, 2H, ^{3}J(H,H) 6 Hz, CH_2N), 2.08 (s, 6H, CH_3); $^{13}C\{^1H\}$ NMR ($CDCl_3$) δ 140.9 (d, ^{1}J(C,P) 13 Hz, C_{ipso}), 130.7 (d, ^{2}J(C,P) 20 Hz, C_{ortho}), 127.5 (d, ^{3}J(C,P) 7 Hz, C_{meta}), 127.3 (s, C_{para}), 60.3 (d, ^{3}J(C,P) 7 Hz, CH_2N), 44.6 (s, CH_3), 42.3 (d, ^{2}J(C,P) 11 Hz, CH_2NP). IR (NaCl, cm^{-1}): 3370 [m (br), ν(NH)].

$(Ph_2P)_2NCH_2CH_2N(CH_3)_2$ (L^9): as for **L^1** using NEt_3 (1.13 g, 11 mmol), PPh_2Cl (2.46 g, 11 mmol) and $H_2NCH_2CH_2N(CH_3)_2$ (0.49 g, 5.5 mmol). The resulting solution was evaporated under reduced pressure to give a viscous oil. $^{31}P\{^1H\}$ NMR ($CDCl_3$) mixture of **L^9** and **L^8** δ 64.2 and 41.6.

Synthesis of $Ph_2PNC_4H_3(COCH_3\text{-}2)$ (L^{10})

Two methods for the synthesis of L^{10} were used:

(**Method 1**): as for L^1 using NEt_3 (1.31 g, 13 mmol) and PPh_2Cl (2.41 g, 11 mmol) were added sequentially with stirring to a solution of 2-acetylpyrrole (1.19 g, 11 mmol) in THF (40 cm^3). The reaction mixture was stirred for two days and the solution filtered to remove NEt_3HCl. The resulting solution was evaporated under reduced pressure to give a white solid. Recrystallisation from dichloromethane-hexane followed by THF-hexane gave block shaped crystals.

(**Method 2**) Dbu (1.83 g, 12 mmol) and PPh_2Cl (2.41 g, 11 mmol) were added sequentially with stirring to a solution of 2-acetylpyrrole (1.19 g, 11 mmol) in THF (40 cm^3). The reaction mixture was stirred for 2 hours and the solution filtered to remove [DbuH]Cl. The resulting solution was evaporated under reduced pressure to give a white solid. Product washed with hexane then recrystallised from THF-hexane to give block shaped crystals.

(Found: C, 73.4; H, 5.62; N, 4.75. $C_{18}H_{16}NOP$ requires C, 73.7; H, 5.50; N, 4.78 %). $^{31}P\{^1H\}$ NMR ($CDCl_3$) δ 55.8; ^1H NMR ($CDCl_3$) δ 7.40 - 7.38 (m, 6H, Ar), 7.32 - 7.27 (m, 4H, Ar), 7.16 (m, 1H, CH), 6.44 (m, 1H, CH), 6.24 (m, 1H, CH), 2.43 (s, 3H, CH_3); $^{13}C\{^1H\}$ NMR ($CDCl_3$) δ 187.4 (s, CO), 136.9 (d, ^1J(C,P) 20 Hz, C_{ipso}), 132.0 (d, J(C,P) 23 Hz, C_{ortho}), 129.4 (s, C_{para}), 128.2 (d, J(C,P) 8 Hz, C_{meta}), 121.1 (s, CH), 110.9 (s, CH), 25.7 (s, CH_3). IR (KBr, cm^{-1}): 1643 [vs, ν(C=O)].

$Ph_2P(S)NC_4H_3(COCH_3\text{-}2)$ (L^{11}): as for L^6 using sulfur (0.011 g, 0.34 mmol) and $Ph_2PNC_4H_3(COCH_3\text{-}2)$ (0.10 g, 0.34 mmol). Product extracted using diethyl ether. $^{31}P\{^1H\}$ NMR ($CDCl_3$) δ 67.3; ^1H NMR ($CDCl_3$) δ 7.78 - 7.69 (m, 4H, Ar), 7.58 -

7.40 (m, 6H, Ar), 7.20 (m, 1H, CH), 6.96 (m, 1H, CH), 6.28 (m, 1H, CH), 2.29 (s, 3H, CH_3). IR (KBr, cm^{-1}): 1664 [s, ν(C=O)].

Synthesis of $[PdCl_2(L^1)_2]$ (1)

$[PdCl_2(cod)]$ (0.100 g, 0.35 mmol) was added with stirring to a solution of $\mathbf{L^1}$ (0.182 g, 0.70 mmol) in dichloromethane (40 cm^3). After 30 min., the solution was concentrated under reduced pressure, and diethyl ether added to give yellow crystals of **1**. (Found: C, 50.9; H, 5.20; N, 3.87. $C_{30}H_{36}Cl_2N_2O_2P_2Pd \cdot \frac{1}{4}CH_2Cl_2$ requires C, 50.7; H, 5.13; N, 3.91%). $^{31}P\{^1H\}$ NMR ($CDCl_3$) *trans* isomer δ 46.4; *cis* isomer δ 59.0; ^1H NMR ($CDCl_3$) *trans* isomer δ 7.85 - 7.75 (m, Ar), 7.47 - 7.36 (m, Ar), 4.28 (m (br), 1H, NH), 3.23 (t, 2H, $^3J(H,H)$ 6 Hz, CH_2O), 3.22 (s, 3H, CH_3), 2.80 (m, 2H, CH_2N); *cis* isomer δ 7.8 - 7.3 (m, Ar), 4.40 (m (br), 1H, NH), 3.28 (s, 3H, CH_3), 3.16 (t, 2H, $^3J(H,H)$ 6 Hz, CH_2O), 2.56 (m, 2H, CH_2N); FAB-MS, *m/z* 697 $[M+H]^+$, 661 $[M-Cl]^+$. IR (KBr, cm^{-1}) *trans* isomer: 3351 [w, ν(NH)].

$[PdCl_2(L^2)_2]$ (2): as for **1** using $[PdCl_2(cod)]$ (0.103 g, 0.36 mmol) and $\mathbf{L^2}$ (0.198 g, 0.73 mmol). (Found: C, 53.0; H, 5.58; N, 3.82. $C_{32}H_{40}Cl_2N_2O_2P_2Pd$ requires C, 53.1; H, 5.57; N, 3.87%). $^{31}P\{^1H\}$ NMR ($CDCl_3$) *trans* isomer δ 46.4; *cis* isomer δ 58.8; ^1H NMR ($CDCl_3$) *cis-trans* mixture δ 7.86 - 7.80 (m, Ar), 7.60 - 7.36 (m, Ar), 7.31 - 7.25 (m, Ar), 4.47 (br, NH), 4.11 (br, NH), 3.32 (t, $^3J(H,H)$ 6 Hz, CH_2O), 3.25 (m, CH_2O), 3.23 (s, CH_3), 3.19 (s, CH_3), 2.73 (m, CH_2N), 2.48 (m, CH_2N), 1.58 (qui, CH_2C_2), 1.50 (qui, CH_2C_2). IR (KBr, cm^{-1}) *trans* isomer: 3332 [w, ν(NH)].

$[PdCl_2(L^3)_2]$ (3): as for **1** using $[PdCl_2(cod)]$ (0.100 g, 0.35 mmol) and L^3 (0.203 g, 0.70 mmol). (Found: C, 50.6; H, 5.31; N, 3.68. $C_{32}H_{40}Cl_2N_2O_4P_2Pd$ requires C, 50.8; H, 5.33; N, 3.71%). $^{31}P\{^1H\}$ NMR ($CDCl_3$) *trans* isomer δ 46.9; *cis* isomer δ 59.2; ^1H NMR ($CDCl_3$) *trans* isomer δ 7.90 – 7.82 (m, 4H, Ar), 7.53 – 7.44 (m, 6H, Ar), 4.29 (m (br), 1H, NH), 4.05 (t, 1H, $^3J(H,H)$ 6 Hz, CH), 3.25 (s, 6H, CH_3), 2.75 (m, 2H, CH_2N); *cis* isomer δ 7.94 – 7.86 (m, Ar), 7.58 – 7.35 (m, Ar), 4.42 (m, 1H, NH), 4.02 (t, 1H, $^3J(H,H)$ 6 Hz, CH), 3.23 (s, 6H, CH_3), 2.52 (m, 2H, CH_2N); FAB-MS, *m/z* 756 $[M+H]^+$, 721 $[M-Cl]^+$. IR (KBr, cm^{-1}) *trans* isomer: 3331 [w, ν(NH)].

$[PdCl_2(L^4)_2]$ (4): as for **1** using $[PdCl_2(cod)]$ (0.100 g, 0.35 mmol) and L^4 (0.216 g, 0.70 mmol). (Found: C, 57.3; H, 4.66; N, 3.46. $C_{38}H_{36}Cl_2N_2O_2P_2Pd$ requires C, 57.6; H, 4.58; N, 3.54%). IR (KBr, cm^{-1}): 3300 [w, ν(NH)].

$[PtCl_2(L^1)_2]$ (5): as for **1** using $[PtCl_2(cod)]$ (0.100 g, 0.27 mmol) and L^1 (0.138 g, 0.53 mmol). Colourless crystals. (Found: C, 44.2; H, 4.57; N, 3.37. $C_{30}H_{36}Cl_2N_2O_2P_2Pt\cdot\frac{1}{2}CH_2Cl_2$ requires C, 44.3; H, 4.51; N, 3.39%); $^{31}P\{^1H\}$ NMR ($CDCl_3$) δ 35.5 [$^1J(P,Pt)$ 3940 Hz]; ^1H NMR ($CDCl_3$) δ 7.57 (m, 4H, Ar), 7.43 (m, 2H, Ar), 7.30 (m, 4H, Ar), 4.08 (m (br), 1H, NH), 3.14 (s, 3H, CH_3), 3.09 (t, 2H, $^3J(H,H)$ 5 Hz, CH_2O), 2.52 (m, 2H, CH_2N); FAB-MS, *m/z* 785 $[M+H]^+$, 749 $[M-Cl]^+$. IR (KBr, cm^{-1}): 3380, 3293 [w, ν(NH)].

$[PtCl_2(L^3)_2]$ (6): as for **1** using $[PtCl_2(cod)]$ (0.136 g, 0.36 mmol) and L^3 (0.210 g, 0.73 mmol). Colourless crystals. (Found: C, 44.1; H, 4.72; N, 3.07. $C_{32}H_{40}Cl_2N_2O_4P_2Pt\cdot\frac{1}{2}CH_2Cl_2$ requires C, 44.0; H, 4.66; N, 3.16%); $^{31}P\{^1H\}$ NMR

($CDCl_3$) δ 35.8 [^1J(P,Pt) 3940 Hz]; ^1H NMR ($CDCl_3$) δ 7.56 (m, 4H, Ar), 7.45 (m, 2H, Ar), 7.32 (m, 4H, Ar), 4.09 (m (br), 1H, NH), 3.93 (t, 1H, ^3J(H,H) 5 Hz, CH), 3.14 (s, 6H, CH_3), 2.45 (m, 2H, CH_2). IR (KBr, cm^{-1}): 3350, 3247 [m, ν(NH)].

[$PtCl_2(L^4)_2$] (7): as for **1** using [$PtCl_2$(cod)] (0.100 g, 0.27 mmol) and $\mathbf{L^4}$ (0.164 g, 0.53 mmol). (Found: C, 50.1; H, 4.09; N, 2.72. $C_{38}H_{36}Cl_2N_2O_2P_2Pt \cdot \frac{1}{2}CH_2Cl_2$ requires C, 50.1; H, 4.04; N, 3.03%); $^{31}P\{^1H\}$ NMR (CD_2Cl_2) δ 30.1 [^1J(P,Pt) 3934 Hz]; ^1H NMR (CD_2Cl_2) δ 7.62 (m, 4H, Ar), 7.46 (m, 2H, Ar), 7.30 (m, 4H, Ar), 6.82 (m, 1H, NH), 6.74 (m, Ar), 6.72 (m, Ar), 6.33 (m, Ar), 6.07 (d, 1H, Ar), 3.65 (s, 3H, CH_3); FAB-MS *m/z* 880 $[M]^+$, 844 $[M–Cl]^+$, 808 $[M\text{-}2Cl]^+$. IR (KBr, cm^{-1}): 3371, 3199 [m, ν(NH)].

[$PtBr_2(L^1)_2$] (8): as for **1** using [$PtBr_2$(cod)] (0.100 g, 0.21 mmol) and $\mathbf{L^1}$ (0.112 g, 0.43 mmol). Colourless crystals. (Found: C, 40.3; H, 4.01; N, 2.75. $C_{30}H_{36}Br_2N_2O_2P_2Pt \cdot \frac{1}{2}CH_2Cl_2$ requires C, 40.0; H, 4.07; N, 3.06%); $^{31}P\{^1H\}$ NMR ($CDCl_3$) δ 36.7 [^1J(P,Pt) 3904 Hz]; ^1H NMR ($CDCl_3$) δ 7.62 (m, 4H, Ar), 7.45 (m, 2H, Ar), 7.35 (m, 4H, Ar), 3.97 (m (br), 1H, NH), 3.16 (s, 3H, CH_3), 3.12 (t, 2H, ^3J(H,H) 6 Hz, CH_2O), 2.55 (m, 2H, CH_2N). IR (KBr, cm^{-1}): 3399, 3293 [m, ν(NH)].

Reaction of [$PtCl_2(L^1)_2$] with $AgBF_4$: Synthesis of [$Pt(L^1)_2$](BF_4)$_2$ (9)

$AgBF_4$ (0.060 g, 0.31 mmol) was added to a solution of [$PtCl_2(L^1)_2$] (0.100 g, 0.13 mmol) in dichloromethane (20 cm^3) and the mixture stirred in darkness for 30 minutes. The resulting solution was filtered, the residue washed with dichloromethane, and the filtrate and washings combined. This solvent was then

evaporated under reduced pressure to give **9** as a white solid. Recrystallisation from dichloromethane-hexane gave colourless microcrystals. (Found: C, 38.1; H, 4.15; N, 2.56. $C_{30}H_{36}B_2F_8N_2O_2P_2Pt{\cdot}CH_2Cl_2$ requires C, 38.3; H, 3.94; N, 2.88%); $^{31}P\{^1H\}$ NMR ($CDCl_3$) δ 39.6 [^1J(P,Pt) 4346 Hz]; ^1H NMR ($CDCl_3$) δ 7.61 (m, Ar), 7.52 (m, Ar), 7.35 (m, Ar), 4.20 (s (br), 2H, CH_2O), 3.87 (m (br), 1H, NH), 3.77 (s, 3H, CH_3), 3.22 (m (br), 2H, CH_2N). IR (KBr, cm^{-1}): 3326 [w, ν(NH)], 1070 [vs (br), ν(BF_4)].

[Pt(L^4)$_2$](BF_4)$_2$ (10): as for **9** using $AgBF_4$ (0.117 g, 0.60 mmol) and **7** (0.213 g, 0.30 mmol). Recrystallisation from dichloromethane-hexane gave yellow microcrystals. (Found: C, 46.4; H, 3.79; N, 2.48. $C_{38}H_{36}B_2F_8N_2O_2P_2Pt$ requires C, 46.4; H, 3.69; N, 2.85%); $^{31}P\{^1H\}$ NMR (CD_2Cl_2) δ 27.7 [^1J(P,Pt) 4162 Hz]; ^1H NMR (CD_2Cl_2) δ 7.44 (m, Ar), 7.22 (m, Ar), 6.82 (m, 2H, Ar), 6.48 (d, ^2J(H,P) 8 Hz, NH), 6.40 (m, 2H, Ar), 3.79 (s, 3H, CH_3). IR (KBr, cm^{-1}): 3296 [w, ν(NH)], 1060 [vs (br), ν(BF_4)]. (Yield 32%).

[Pd(L^1)$_2$](BF_4)$_2$ (11): as for **9** using $AgBF_4$ (0.093 g, 0.48 mmol) and **1** (0.150 g, 0.22 mmol). The solvent was then evaporated under reduced pressure to give **11** as an orange solid. $^{31}P\{^1H\}$ NMR ($CDCl_3$) δ 80.1; ^1H NMR ($CDCl_3$) δ 7.59 (m, Ar), 7.39 (m, Ar), 4.07 (m (br), 1H, NH), 3.93 (s (br), 2H, CH_2O), 3.65 (s, 3H, CH_3), 3.20 (m (br), 2H, CH_2N). IR (KBr, cm^{-1}): 3316 [w, ν(NH)], 1080 [vs (br), ν(BF_4)].

[Pd(μ-Cl)(L^1)$_2$]$_2$(BF_4)$_2$ (12): as for **9** using $AgBF_4$ (0.030 g, 0.15 mmol) and **1** (0.107 g, 0.15 mmol). (Found: C, 47.1; H, 4.83; N, 3.66. $C_{60}H_{72}B_2Cl_2F_8N_4O_4P_4Pd_2{\cdot}½CH_2Cl_2$ requires C, 47.3; H, 4.79; N, 3.65%); $^{31}P\{^1H\}$ NMR ($CDCl_3$) δ 61.4; ^1H NMR

($CDCl_3$) δ 7.35 (m, Ar), 4.39 (br, 1H, NH), 3.32 (t, 2H, ^{3}J(H,H) 6 Hz, CH_2O), 3.26 (s, 3H, CH_3), 2.72 (t (br), 2H, CH_2N); FAB-MS *m/z* 1407 $[M–BF_4]^+$, 1321 $[M–2BF_4]^+$, 660 $[PdCl(L^1)_2]^+$. IR (KBr, cm^{-1}): 3274 [w, ν(NH)], 1080 [vs (br), ν(BF_4)].

Reaction of 9 with XylNC: Synthesis of $[Pt(L^1)_2(CNXyl)_2](BF_4)_2$ (13)

CNXyl (0.044 g, 0.34 mmol) was added to a solution of **9**, formed *in situ* from $AgBF_4$ (0.069 g, 0.35 mmol) and **5** (0.133 g, 0.17 mmol). Recrystallisation from dichloromethane-diethyl ether followed by acetone-diethyl ether to give colourless crystals. (Found: C, 50.1; H, 4.82; N, 4.77. $C_{48}H_{54}B_2F_8N_4O_2P_2Pt$ requires C, 50.1; H, 4.73; N, 4.87%); $^{31}P\{^1H\}$ NMR (CD_2Cl_2) δ 38.6 [^{1}J(P,Pt) 2069 Hz]; ^{1}H NMR (CD_2Cl_2) δ 7.7 (m, Ar), 7.42 (m, Ar), 7.26 (t, Ar), 7.03 (d, Ar), 4.83 (m, 1H, NH), 3.47 (t, 2H, ^{3}J(H,H) 5 Hz, CH_2O), 3.17 (s, 3H, CH_3O), 3.07 (m, 2H, CH_2N), 1.93 (s, 6H, CH_3C). IR (KBr, cm^{-1}): 3306 [m, ν(NH)], 2214 [s, ν(CN)], 1070 [vs (br), ν(BF_4)].

Reaction of 9 with Acetonitrile: Synthesis of $[Pt(L^1)_2(NCCH_3)_2](BF_4)_2$ (14)

Excess acetonitrile (2 cm^3) was added to a solution of **9**, formed *in situ* from $AgBF_4$ (0.130 g, 0.67 mmol) and **5** (0.217 g, 0.28 mmol). The resulting solution was evaporated under reduced pressure to give **14** as a pale yellow solid. $^{31}P\{^1H\}$ NMR (CD_2Cl_2) δ 25.9 [^{1}J(P,Pt) 3924 Hz]; ^{1}H NMR (CD_2Cl_2) δ 7.55 (m, Ar), 7.46 (m, Ar), 4.33 (m (br), NH), 3.39 (t (br), CH_2O), 3.28 (s, CH_3O), 2.95 (m (br), CH_2N), 2.00 (s (br), CH_3CN). IR (KBr, cm^{-1}): 3305 [w (br), ν(NH)], 1070 [vs (br), ν(BF_4)].

Synthesis of $[PtCl(NO_2)(L^1)_2]$ (15)

A solution of $NaNO_2$ (0.070 g, 1.0 mmol) in water (4 cm^3) was added with stirring to a solution of **5** (0.150 g, 0.19 mmol) in acetone (20 cm^3). The mixture was stirred for 5 hours, after which the solvent was removed under reduced pressure, the product extracted with dichloromethane (3 × 20 cm^3) and recrystallised from dichloromethane-diethyl ether, followed by dichloromethane-hexane to give colourless crystals. (Found: C, 42.2; H, 4.24; N, 4.82. $C_{30}H_{36}ClN_3O_4P_2Pt{\cdot}CH_2Cl_2$ requires C, 42.3; H, 4.35; N, 4.77%); $^{31}P\{^1H\}$ NMR ($CDCl_3$) δ_a 33.8 [$^1J(P_a,Pt)$ 4115 Hz], δ_b 25.5 [$^1J(P_b,Pt)$ 3186 Hz], $^2J(P,P)$ 24 Hz; ^1H NMR ($CDCl_3$) δ 7.68 – 7.28 (m (br), Ar), 4.40 (m (br), NH), 3.50 (m (br), NH), 3.20-3.17 (m, CH_2O/CH_3O), 2.72 (m, CH_2N), 2.58 (m, CH_2N). IR (KBr, cm^{-1}): 3396, 3264 [w (br), ν(NH)], 1333 [s, $\nu(NO_2)$].

$[PtBr(NO_2)(L^1)_2]$ (16): as for **15** using $NaNO_2$ (0.300 g, 4.35 mmol) and **8** (0.377 g, 0.43 mmol). Recrystallisation from dichloromethane-hexane gave colourless crystals. (Found: C, 42.8; H, 4.34; N, 4.92. $C_{30}H_{36}BrN_3O_4P_2Pt$ requires C, 42.9; H, 4.32; N, 5.01%); $^{31}P\{^1H\}$ NMR ($CDCl_3$) δ_a 33.8 [$^1J(P_a,Pt)$ 4101 Hz], δ_b 25.5 [$^1J(P_b,Pt)$ 3166 Hz], $^2J(P,P)$ 23 Hz; ^1H NMR ($CDCl_3$) δ 7.60 (m, Ar), 7.43 (m, Ar), 7.32 (m, Ar), 4.20 (m, NH), 3.30 (m, NH), 3.21 (s, CH_3), 3.19 (s, CH_3), 3.16 (m, CH_2O), 2.73 (m, CH_2N), 2.56 (m, CH_2N); FAB-MS *m/z* 793 $[M–NO_2]^+$, 712 $[M–NO_2–Br]^+$. IR (KBr, cm^{-1}): 3397, 3311 [w, ν(NH)], 1403, 1332 [s (br), $\nu(NO_2)$]. (Yield 45%).

$[Pt(NO_2)_2(L^1)_2]$ (17): as for **15** using $NaNO_2$ (0.300 g, 4.35 mmol) and **8** (0.377 g, 0.43 mmol). The mixture was stirred overnight, after which the solvent was removed

under reduced pressure, the crude product extracted with dichloromethane (4 × 10 cm^3). The solvent was then evaporated under reduced pressure to give **17** as a pale yellow solid. $^{31}P\{^1H\}$ NMR ($CDCl_3$) δ 26.8 [^1J(P,Pt) 3370 Hz]; ^1H NMR ($CDCl_3$) δ 7.59 (m, Ar), 7.45 (m, Ar), 7.34 (m, Ar), 3.54 (m (br), NH), 3.22 (s, CH_3), 3.18 (t, ^3J(H,H) 6 Hz, CH_2O), 2.71 (m, CH_2N).

Synthesis of [Pd(dmba)Cl(L^1)] (18)

[Pd(dmba)(μ-Cl)]$_2$ (0.400 g, 0.75 mmol) was added to a solution of L^1 (0.375 g, 1.45 mmol) in dichloromethane (30 cm^3). The solution was stirred for 1 hour, after which the solution was concentrated under reduced pressure, filtered and pentane added, to give yellow crystals of **18**. (Found: C, 53.5; H, 5.66; N, 5.19. $C_{24}H_{30}ClN_2OPPd$ requires C, 53.8; H, 5.65; N, 5.23%); $^{31}P\{^1H\}$ NMR ($CDCl_3$) δ 68.4; ^1H NMR ($CDCl_3$) δ 7.85 (m, Ar), 7.35 (m, Ar), 6.93 (d, Ar), 6.82 (t, Ar), 6.53 (m, Ar), 4.41 (m (br), NH), 3.91 (m (br), CH_2N (dmba)), 3.23 (m (br), CH_2O/CH_3O), 2.76 (m, CH_2N, CH_3N); FAB-MS *m/z* 535 $[M+H]^+$, 499 $[M-Cl]^+$. IR (KBr, cm^{-1}): 3285 [m, ν(NH)].

[Pd(dmba)Cl(L^2)] (19): as for **18** using [Pd(dmba)(μ-Cl)]$_2$ (0.100 g, 0.18 mmol) and L^2 (0.099 g, 0.36 mmol). Recrystallisation from dichloromethane-diethyl ether gave yellow crystals. (Found: C, 54.2; H, 5.85; N, 5.01. $C_{25}H_{32}ClN_2OPPd$ requires C, 54.7; H, 5.87; N, 5.10%); $^{31}P\{^1H\}$ NMR ($CDCl_3$) δ 67.6; ^1H NMR ($CDCl_3$) δ 7.80 (m, Ar), 7.40 (m, Ar), 6.89 (d, 1H, Ar), 6.78 (m, 1H, Ar), 6.50 (m, 2H, Ar), 4.40 (m, 1H, NH), 3.89 (s, 2H, CH_2N (dmba)), 3.30 (t, 2H, ^3J(H,H) 6 Hz, CH_2O), 3.19 (s, 3H, CH_3O), 2.74 (m (br), CH_2N/CH_3N), 1.57 (m, 2H, CH_2C_2). IR (KBr, cm^{-1}): 3303 [w (br), ν(NH)].

[Pd(dmba)Cl(L^3)] (20): as for **18** using [Pd(dmba)(μ-Cl)]$_2$ (0.200 g, 0.36 mmol) and L^3 (0.210 g, 0.73 mmol). Recrystallisation from dichloromethane-pentane gave yellow crystals. (Found: C, 52.4; H, 5.61; N, 4.80. $C_{25}H_{31}ClN_2O_2PPd$ requires C, 53.2; H, 5.54; N, 4.96%); $^{31}P\{^1H\}$ NMR ($CDCl_3$) δ 68.4; ^1H NMR ($CDCl_3$) δ 7.85 (m, 4H, Ar), 7.42 (m, 6H, Ar), 6.95 (d, 1H, Ar), 6.82 (m, 1H, Ar), 6.55 (m, 2H, Ar), 4.48 (m, 1H, NH), 4.14 (t, 1H, ^3J(H,H) 6 Hz, CH), 3.93 (s, 2H, CH_2N (dmba)), 3.25 (s, 6H, CH_3O), 2.78 (d, 6H, ^4J(H,P) 3 Hz, CH_3N), 2.74 (m, 2H, CH_2). IR (KBr, cm^{-1}): 3284 [m, ν(NH)].

[Pd(dmba)Cl(L^4)] (21): as for **18** using [Pd(dmba)(μ-Cl)]$_2$ (0.275 g, 0.90 mmol) and L^4 (0.247 g, 0.45 mmol). Recrystallisation from dichloromethane-pentane gave yellow microcrystals. (Found: C, 49.9; H, 4.53; N, 3.91. $C_{28}H_{30}ClN_2OPPd\cdot{}^3/_2CH_2Cl_2$ requires C, 49.9; H, 4.68; N, 3.94%); $^{31}P\{^1H\}$ NMR ($CDCl_3$) δ 59.7; ^1H NMR ($CDCl_3$) δ 7.85 (m, 4H, Ar), 7.39 (m, 7H, Ar), 6.98 (m, 1H, Ar), 6.88 (m, 1H, Ar), 6.71 (m, 2H, Ar), 6.59 (m, 2H, Ar), 6.42 (m, 1H, Ar), 6.30 (d, 1H, ^2J(H,P) 8 Hz, NH), 3.94 (d, 2H, ^4J(H,P) 2 Hz, CH_2N (dmba)), 3.81 (s, 3H, CH_3O), 2.77 (d, 6H, ^4J(H,P) 3 Hz, CH_3N). IR (KBr, cm^{-1}): 3197 [w, ν(NH)].

[Pt(dmba)Cl(L^1)] (22): as for **18** using [Pt(dmba)(μ-Cl)]$_2$ (0.141 g, 0.19 mmol) and L^1 (0.100 g, 0.39 mmol). Recrystallisation from dichloromethane-diethyl ether gave colourless crystals. (Found: C, 45.9; H, 4.85; N, 4.34. $C_{24}H_{30}ClN_2OPPt$ requires C, 46.2; H, 4.85; N, 4.49%); $^{31}P\{^1H\}$ NMR ($CDCl_3$) δ 42.1 [^1J(P,Pt) 4460 Hz]; ^1H NMR ($CDCl_3$) δ 7.86 (m, Ar), 7.40 (m, Ar), 6.98 (m, Ar), 6.86 (m, Ar), 6.75 (m, Ar), 6.52

(m, Ar), 4.23 (dt, ^{2}J(H,P) 11 Hz, NH), 3.95 (m, CH_2N (dmba)), 3.28 (t, ^{3}J(H,H) 6 Hz, CH_2O), 3.25 (s, CH_3O), 2.89 (m, ^{3}J(H,Pt) 24 Hz, ^{4}J(H,P) 3 Hz, CH_3N), 2.86 (m, CH_2N). IR (KBr, cm^{-1}): 3308 [w (br), ν(NH)]. (Yield 44%)

[Pt(dmba)Cl(L^3)] (23): as for **18** using [Pt(dmba)(μ-Cl)]$_2$ (0.189 g, 0.26 mmol) and L^3 (0.150 g, 0.52 mmol). Recrystallisation from dichloromethane-hexane gave a pale yellow powder. (Found: C, 46.0; H, 5.06; N, 4.21. $C_{25}H_{31}ClN_2O_2PPt$ requires C, 45.9; H, 4.93; N, 4.28%); $^{31}P\{^1H\}$ NMR ($CDCl_3$) δ 42.3 [^{1}J(P,Pt) 4470 Hz]; ^{1}H NMR ($CDCl_3$) δ 7.88 (m, 4H, Ar), 7.42 (m, 6H, Ar), 7.02 (d, 1H, Ar), 6.89 (t, 1H, Ar), 6.78 (m, 1H, Ar), 6.55 (m, 1H, Ar), 4.24 (dt, 1H, ^{2}J(H,P) 12 Hz, ^{3}J(H,H) 6 Hz, NH), 4.18 (t, 1H, ^{3}J(H,H) 6 Hz, CH), 3.99 (m, 2H, ^{3}J(H,Pt) 28 Hz, ^{4}J(H,P) 3 Hz, CH_2N (dmba)), 3.28 (s, 6H, CH_3O), 2.94 (m, 6H, ^{3}J(H,Pt) 23 Hz, ^{4}J(H,P) 3 Hz, CH_3N), 2.82 (m, 2H, CH_2). IR (KBr, cm^{-1}): 3294 [w (br), ν(NH)].

[Pt(dmba)Cl(L^4)] (24): as for **18** using [Pt(dmba)(μ-Cl)]$_2$ (0.257 g, 0.35 mmol) and L^4 (0.217 g, 0.71 mmol). Recrystallisation from THF-hexane, followed by dichloromethane-hexane gave yellow microcrystals. (Found: C, 46.6; H, 4.40; N, 3.64. $C_{28}H_{30}ClN_2OPPt{\cdot}\frac{3}{4}CH_2Cl_2$ requires C, 46.9; H, 4.32; N, 3.81%); $^{31}P\{^1H\}$ NMR ($CDCl_3$) δ 34.8 [^{1}J(P,Pt) 4464 Hz]; ^{1}H NMR ($CDCl_3$) δ 7.88 (m, 4H, Ar), 7.39 (m, 6H, Ar), 7.27 (m, 1H, Ar), 7.02 (m, 1H, Ar), 6.88 (m, 2H, Ar), 6.71 (m, 2H, Ar), 6.58 (m, 1H, Ar), 6.46 (m, 1H, Ar), 6.37 (d, 1H, ^{2}J(H,P) 8 Hz, NH), 3.96 (m, 2H, ^{3}J(H,Pt) 28 Hz, ^{4}J(H,P) 3 Hz, CH_2N (dmba)), 3.80 (s, 3H, CH_3O), 2.90 (m, 6H, ^{3}J(H,Pt) 23 Hz, ^{4}J(H,P) 3 Hz, CH_3N). IR (KBr, cm^{-1}): 3214 [w (br), ν(NH)]. (Yield 46%).

Reaction of 22 with $AgBF_4$: Synthesis of $[Pt(dmba)(L^1)](BF_4)$ (25)

$AgBF_4$ (0.052 g, 0.27 mmol) was added to a solution of **22** (0.100 g, 0.16 mmol) in dichloromethane (20 cm^3) and the mixture stirred in darkness for 30 minutes. The resulting solution was filtered, the residue washed with dichloromethane, and the filtrate and washings combined. This solvent was then evaporated under reduced pressure to give **25** as an off-white solid. Recrystallisation from dichloromethane-pentane gave colourless crystals. (Found: C, 42.9; H, 4.65; N, 3.96. $C_{24}H_{30}BF_4N_2OPPt$ requires C, 42.7; H, 4.48; N, 4.15%); $^{31}P\{^1H\}$ NMR (CD_2Cl_2) δ 48.8 [^1J(P,Pt) 4396 Hz]; ^1H NMR (CD_2Cl_2) δ 7.83 (m, Ar), 7.48 (m, Ar), 6.92 (d, Ar), 6.77 (t, Ar), 6.32 (t, Ar), 6.15 (m, Ar), 4.11 (m (br), CH_2O), 4.02 (m, ^3J(H,Pt) 28 Hz, ^4J(H,P) 2 Hz, CH_2N (dmba)), 3.52 (s, CH_3O), 3.38 (s (br), CH_2N), 3.15 (m (br), NH), 2.83 (m, ^3J(H,Pt) 20 Hz, ^4J(H,P) 3 Hz, CH_3N).). IR (KBr, cm^{-1}): 3308 [w, ν(NH)], 1060 [vs, ν(BF_4)].

$[Pt(dmba)(L^4)](BF_4)$ (26): as for **25** using $AgBF_4$ (0.030 g, 0.16 mmol) and **22** (0.104 g, 0.16 mmol). $^{31}P\{^1H\}$ NMR (CD_2Cl_2) δ 60.9 [^1J(P,Pt) 4393 Hz]; ^1H NMR (CD_2Cl_2) δ 7.70 (m, Ar), 7.10 (m, Ar), 6.50 (m, Ar), 6.40 (m, Ar), 6.00 (br, NH), 4.17 (s, CH_3O), 4.09 (CH_2), 3.01 (CH_3N). IR (KBr, cm^{-1}): 3390 [w, ν(NH)], 1070 [vs, ν(BF_4)].

$[Pd(dmba)(L^1)](BF_4)$ (27): as for **25** using $AgBF_4$ (0.122 g, 0.63 mmol) and **18** (0.200 g, 0.37 mmol). The resulting solution was evaporated under reduced pressure to give **27** as a pale brown solid. $^{31}P\{^1H\}$ NMR (CD_2Cl_2) δ 75.2; ^1H NMR (CD_2Cl_2) δ 7.79 (m, 4H, Ar), 7.47 (m, 6H, Ar), 6.94 (d, 1H, Ar), 6.84 (t, 1H, Ar), 6.43 (t, 1H, Ar),

6.19 (t, 1H, Ar), 4.01 (s (br), 2H, CH_2N (dmba)), 3.85 (m, 2H, CH_2O), 3.40 (br, 1H, NH), 3.33 (m, 5H, CH_3O/CH_2N), 2.73 (d, 6H, $^4J(H,P)$ 3 Hz, CH_3N).

[Pd(dmba)(L^1)](PF_6) (28): as for **25** using $AgPF_6$ (0.192 g, 0.76 mmol) and **18** (0.200 g, 0.37 mmol). The resulting solution was evaporated under reduced pressure to give **28** as a yellow solid. $^{31}P\{^1H\}$ NMR (CD_2Cl_2) δ 69.5, -143.6 (sep, $^1J(P,F)$ 711 Hz); ^1H NMR (CD_2Cl_2) δ 8.02 (m, 4H, Ar), 7.74 (m, 6H, Ar), 6.87 (d, 1H, Ar), 7.21 (t, 1H, Ar), 6.87 (t, 1H, Ar), 6.36 (t, 1H, Ar), 4.14 (d, 2H, CH_2N (dmba)), 4.01 (t, 2H, $^3J(H,H)$ 4 Hz, CH_2O), 3.56 (m, 1H, NH), 3.50 (s, 3H, CH_3O), 3.42 (m (br), 2H, CH_2N), 2.78 (d, 6H, $^4J(H,P)$ 3 Hz, CH_3N).

Reaction of 25 with CO: Synthesis of [Pt(dmba)(CO)(L^1)](BF_4) (29)

CO was bubbled through a solution of **25** formed *in situ* from $AgBF_4$ (0.052 g, 0.27 mmol) and **22** (0.100 g, 0.16 mmol). Recrystallisation from dichloromethane-diethyl ether gave colourless crystals of **29**. (Found: C, 42.6; H, 4.44; N, 3.95. $C_{25}H_{30}BF_4N_2O_2PPt \cdot {}^3/_2CH_2Cl_2$ requires C, 42.3; H, 4.51; N, 3.80%); $^{31}P\{^1H\}$ NMR (CD_2Cl_2) δ 38.8 [$^1J(P,Pt)$ 3666 Hz]; ^1H NMR (CD_2Cl_2) δ 7.74 (m, Ar), 7.54 (m, Ar), 7.25 (m, Ar), 7.17 (m, Ar), 7.10 (m, Ar), 6.85 (m, Ar), 4.35 (m, $^3J(H,Pt)$ 28 Hz, $^4J(H,P)$ 3 Hz, CH_2N (dmba)), 3.57 (m, NH), 3.48 (t, $^3J(H,H)$ 5 Hz, CH_2O), 3.26 (br, CH_3O/CH_3N) 3.20 (m, CH_2N). IR (KBr, cm^{-1}): 3334 [m, ν(NH)], 2114 [vs, ν(CO)], 1060 [vs (br), ν(BF_4)].

[Pt(dmba)(CO)(L^3)](BF_4) (30): as for **29** using $AgBF_4$ (0.039 g, 0.20 mmol) and **23** (0.110 g, 0.17 mmol). $^{31}P\{^1H\}$ NMR (CD_2Cl_2) δ 39.1 [$^1J(P,Pt)$ 3622 Hz]; ^1H NMR

(CD_2Cl_2) δ 7.80 (m, Ar), 7.65 (m, Ar), 7.34 (d, Ar), 7.17 (m, Ar), 7.00 (t, Ar), 4.46 (t, ^3J(H,H) 4 Hz, CH), 4.39 (d (br), CH_2N (dmba)), 4.12 (m, NH), 3.36 (s, CH_3O), 3.25 (m, ^4J(H,P) 3 Hz, CH_3N), 3.13 (m (br), CH_2N). IR (CH_2Cl_2, cm^{-1}): 2106 [vs, ν(CO)], 1070 [vs (br), ν(BF_4)].

[Pt(dmba)(CO)(L^4)](BF_4) (31): as for **29** using $AgBF_4$ (0.052 g, 0.27 mmol) and **24** (0.100 g, 0.16 mmol). $^{31}P\{^1H\}$ NMR (CD_2Cl_2) δ 35.4 [^1J(P,Pt) 3696 Hz]; ^1H NMR (CD_2Cl_2) δ 7.86 (m, Ar), 7.57 (m, Ar), 7.31 (m, Ar), 7.18 (m, Ar), 6.88 (m, Ar), 6.73 (m, Ar), 5.90 (m, NH), 4.33 (m, CH_2), 3.76 (s, CH_3O), 3.25 (m CH_3N). IR (CH_2Cl_2, cm^{-1}): 2105 [s (br), ν(CO)], 1060 [vs (br), ν(BF_4)].

Reaction of 25 with Acetonitrile: Synthesis of [Pt(dmba)(L^1)($NCCH_3$)](BF_4) (32)

Excess acetonitrile (1 cm^3) was added to a solution of **25**, formed *in situ* from $AgBF_4$ (0.015 g, 0.08 mmol) and **22** (0.050 g, 0.08 mmol). $^{31}P\{^1H\}$ NMR (CD_2Cl_2) δ 44.4 [^1J(P,Pt) 4252 Hz]; ^1H NMR ($CDCl_3$) δ 7.70 (m, Ar), 7.51 (m, Ar), 7.10 (m, Ar), 6.75 (t, Ar), 4.03 (m, ^4J(H,P) 3 Hz, CH_2N (dmba)), 3.42 (t, ^3J(H,H) 5 Hz, CH_2O), 3.28 (s, CH_3), 3.17 (m, CH_2N), 2.96 (m, ^4J(H,P) 3 Hz, CH_3N), 2.02 (s, CH_3CN). IR (KBr, cm^{-1}): 3350 [w, ν(NH)], 1070 [vs (br), ν(BF_4)].

[Pt(dmba)(L^4)($NCCH_3$)](BF_4) (33): as for **32** $AgBF_4$ (0.015 g, 0.08 mmol) and **24** (0.050 g, 0.07 mmol). $^{31}P\{^1H\}$ NMR (CD_2Cl_2) δ 38.5 [^1J(P,Pt) 4256 Hz]; ^1H NMR ($CDCl_3$) δ 7.76 (m, Ar), 7.49 (m, Ar), 7.10 (d, Ar), 7.01 (m, Ar), 6.89 (m, Ar), 6.73 (m, Ar), 5.74 (m, NH), 4.07 (m, ^3J(H,Pt) 30 Hz, ^4J(H,P) 3 Hz, CH_2), 3.77 (s, CH_3O),

2.98 (m, ^{3}J(H,Pt) 26 Hz, ^{4}J(H,P) 3 Hz, CH_3N), 1.83 (s, CH_3CN). IR (KBr, cm^{-1}): 3370 [w, ν(NH)], 1060 [vs (br), ν(BF_4)].

Reaction of 26 with XylNC: Synthesis of [Pt(dmba)(L^4)(CNXyl)](BF_4) 34

CNXyl (0.050 g, 0.38 mmol) was added to a solution of **25**, formed *in situ* from $AgBF_4$ (0.015 g, 0.08 mmol) and **24** (0.050 g, 0.08 mmol). $^{31}P\{^1H\}$ NMR ($CDCl_3$) δ 36.7 [^{1}J(P,Pt) 3897 Hz]; ^{1}H NMR ($CDCl_3$) δ 7.86 (m, Ar), 7.45 (m, Ar), 7.17 (m, Ar), 6.82 (m, Ar), 5.85 (m, NH), 4.37 (d, ^{4}J(H,P) 3 Hz, CH_2), 3.66 (s, CH_3O), 3.24 (d, ^{4}J(H,P) 3 Hz, CH_3N), 2.19 (s, CH_3C). IR (KBr, cm^{-1}): 3376 [w, ν(NH)], 2179 [s, ν(CN)], 1060 [vs (br), ν(BF_4)].

Formation of [Pt(dmba)(PPh_2O)]$_2$ (35)

Recrystallisation of **25** from wet dichloromethane-pentane resulted in decomposition to give a number of compounds, with the minor component **35** isolated as colourless block shaped crystals.

Synthesis of [Mo(CO)$_4$(L^1)$_2$] (36)

[Mo(CO)$_4$(NHC_5H_{10})$_2$] (0.20 g, 0.53 mmol) was added to a solution of L^1 (0.29 g, 1.1 mmol) in dichloromethane (20 cm^3) and the mixture refluxed under nitrogen for 1 hour. The resulting solution was filtered and the solution concentrated under reduced pressure and pentane added to precipitate any unreacted starting material. The solution was then filtered and the solvent evaporated under reduced pressure. Recrystallisation from dichloromethane-methanol at -20°C gave colourless crystals of **36**. (Found: C, 55.9; H, 5.02; N, 3.81. $C_{34}H_{36}N_2O_6P_2Mo$ requires C, 56.2; H, 4.99; N, 3.86%).

$^{31}P\{^1H\}$ NMR ($CDCl_3$) δ 77.2; ^1H NMR ($CDCl_3$) δ 7.59 (m, 4H, Ar), 7.42 (m, 6H, Ar), 3.28 (s, 3H, CH_3). 2.95 (t, 2H, $^3J(H,H)$ 5 Hz, CH_2O), 3.30 (m, 1H, NH), 2.68 (m, CH_2N). FAB-MS *m/z* 726 $[M]^+$, 698 $[M–CO]^+$, 670 $[M–2CO]^+$, 642 $[M-3CO]^+$, 614 $[M–4CO]^+$. IR (KBr, cm^{-1}): 3400, 3380 [w, ν(NH)], 2016 [vs, ν(CO)], 1900 [vs (br), ν(CO)].

$[Mo(CO)_4(L^3)_2]$ (37): as for **36** using $[Mo(CO)_4(NHC_5H_{10})_2]$ (0.100 g, 0.26 mmol) and $\mathbf{L^3}$ (0.161 g, 0.56 mmol). Recrystallised from dichloromethane-diethyl ether. $^{31}P\{^1H\}$ NMR ($CDCl_3$) δ 78.4; ^1H NMR ($CDCl_3$) δ 7.57 - 7.48 (br, Ar), 7.44 - 7.42 (br, Ar), 3.82 (t, $^3J(H,H)$ 5 Hz, CH), 3.20 (s, CH_3), 2.78 (m (br), NH), 2.66 (m (br), CH_2).

$[Mo(CO)_4(L^4)_2]$ (38): as for **36** using $[Mo(CO)_4(NHC_5H_{10})_2]$ (0.217 g, 0.57 mmol) and $\mathbf{L^4}$ (0.353 g, 1.15 mmol). (Found: C, 60.5; H, 4.38; N, 3.28. $C_{42}H_{36}N_2O_6P_2Mo{\cdot}CH_3OH$ requires C, 60.4; H, 4.72; N, 3.28%). NMR ($CDCl_3$): $^{31}P\{^1H\}$ δ 70.9; ^1H NMR ($CDCl_3$) δ 7.65 - 7.55 (m, 4H, Ar), 7.48 - 7.32 (m, 6H, Ar), 6.75 (m, 1H, Ar), 6.67 (m, 1H, Ar), 6.35 (m, 1H, Ar), 6.11 (d, 1H, Ar), 5.88 (m (br), 1H, NH), 3.74 (s, 3H, CH_3). FAB-MS *m/z* 822 $[M]^+$. IR (KBr, cm^{-1}): 3399 [m, ν(NH)], 2022 [vs, ν(CO)], 1900 [vs (br), ν(CO)].

Synthesis of $[Mo(CO)_3(L^3)_3]$ (39)

$[Mo(C_7H_8)(CO)_3]$ (0.083 g, 0.30 mmol) was added with stirring to a solution of $\mathbf{L^3}$ (0.176 g, 0.61 mmol) in toluene (10 cm^3). After 30 minutes, the solvent was evaporated under reduced pressure. Recrystallised from dichloromethane-hexane

followed by dichloromethane-diethyl ether to give colourless crystals. (Found: C, 58.3; H, 5.80; N, 4.06. $C_{51}H_{60}N_3O_9P_3Mo$ requires C, 58.4; H, 5.77; N, 4.01%). $^{31}P\{^1H\}$ NMR ($CDCl_3$) δ 78.7; ^1H NMR ($CDCl_3$) δ 7.33 (m, 2H, Ar), 7.20 (m, 8H, Ar), 3.89 (t, 1H, $^3J(H,H)$ 5 Hz, CH), 3.81 (m (br), 1H, NH), 3.23 (s, 6H, CH_3), 2.68 (m (br), 2H, CH_2). IR (KBr, cm^{-1}): 3297 [m (br), ν(NH)], 1939 [vs, ν(CO)], 1842 [vs (br), ν(CO)].

Synthesis of [RhCl(CO)(L^1)$_2$] (40)

[Rh(μ-Cl)(CO)$_2$]$_2$ (0.075 g, 0.19 mmol) was added with stirring to a solution of L^1 (0.200 g, 0.77 mmol) in dichloromethane (10 cm^3). After 30 minutes, the solution was concentrated under reduced pressure and hexane added to give **40** as an orange powder. Recrystallisation from dichloromethane-diethyl ether gave orange crystals. (Found: C, 53.7; H, 5.31; N, 3.93. $C_{31}H_{36}ClN_2O_3P_2Rh$ requires C, 54.4; H, 5.30; N, 4.09%). $^{31}P\{^1H\}$ NMR ($CDCl_3$) δ 60.0 [$^1J(P,Rh)$ 124 Hz]; ^1H NMR ($CDCl_3$) δ 7.80 (m, Ar), 7.45 (m, Ar), 4.22 (m, NH), 3.34 (m, CH_2O), 3.30 (s, CH_3), 2.93 (m (br), CH_2N). IR (KBr, cm^{-1}): 3330 [w, ν(NH)], 1988 [vs, ν(CO)]; IR (CH_2Cl_2, cm^{-1}): 1977 [vs, ν(CO)].

[RhCl(CO)(L^3)$_2$] (41): as for **40** using [Rh(μ-Cl)(CO)$_2$]$_2$ (0.048 g, 0.12 mmol) and L^3 (0.142 g, 0.49 mmol). (Found: C, 53.1; H, 5.38; N, 3.56. $C_{33}H_{40}ClN_2O_5P_2Rh$ requires C, 53.2; H, 5.41; N, 3.76%). $^{31}P\{^1H\}$ NMR ($CDCl_3$) δ 60.3 [$^1J(P,Rh)$ 127 Hz]; ^1H NMR ($CDCl_3$) δ 7.81 (m (br), 4H, Ar), 7.46 (m (br), 6H, Ar), 4.24 (m, 1H, NH), 4.14 (t (br), 1H, CH), 3.30 (s, 6H, CH_3), 2.89 (m (br), 2H, CH_2). IR (KBr, cm^{-1}): 3423, 3318 [w, ν(NH)], 1958 [vs, ν(CO)]; IR (CH_2Cl_2, cm^{-1}): 1977 [vs, ν(CO)].

[RhCl(CO)(L^4)$_2$] (42): as for **40** using [Rh(μ-Cl)(CO)$_2$]$_2$ (0.050 g, 0.13 mmol) and L^4 (0.158 g, 0.51 mmol). (Found: C, 56.1; H, 4.45; N, 3.18. $C_{37}H_{36}ClN_2O_3P_2Rh{\cdot}CH_2Cl_2$ requires C, 56.0; H, 4.58; N, 3.18%). $^{31}P\{^1H\}$ NMR ($CDCl_3$) δ 53.2 [^1J(P,Rh) 131 Hz]; ^1H NMR ($CDCl_3$) δ 7.85 (m, Ar), 7.42 (m, Ar), 6.78 (m, Ar), 6.52 (m, Ar), 3.89 (s, CH_3/NH). IR (KBr, cm^{-1}): 3402, 3325 [w, ν(NH)], 1965 [vs, ν(CO)]; IR (CH_2Cl_2, cm^{-1}): 1980 [vs, ν(CO)].

Synthesis of [$PtCl_2$(L^7)$_2$] (43)

[$PtCl_2$(cod)] (0.136 g, 0.36 mmol) was added with stirring to a solution of L^7 (0.214 g, 0.75 mmol) in dichloromethane (10 cm^3). After 30 minutes the solution was frozen and allowed to slowly warm up, just after all the dichloromethane had melted, the solution was filtered to remove a small quantity of insoluble material. The solvent was then removed under reduced pressure. Recrystallised from THF-hexane. (Found: C, 49.8; H, 5.99; N, 6.19. $C_{34}H_{46}Cl_2N_4P_2Pt{\cdot}C_4H_8O$ requires C, 50.1; H, 5.98; N, 6.15%). $^{31}P\{^1H\}$ NMR (400 MHz, CD_2Cl_2, +25°C) δ 50.1 [^1J(P,Pt) 3904 Hz], (400 MHz, CD_2Cl_2, -50°C) δ_a 49.6 [$^1J(P_a,Pt)$ 4209 Hz], δ_b 46.9 [$^1J(P_b,Pt)$ 3202 Hz], ^2J(P,P) not determined; ^1H NMR (270 MHz, CD_2Cl_2, +25°C) δ 7.46 - 7.20 (m, Ar), 3.20 (m (br), 2H, CH_2NP), 2.68 (m (br), 2H, CH_2N), 2.51 (d, 3H, ^3J(H,P) 10 Hz, CH_3NP), 2.39 (s (br), 6H, CH_3N).

[$PtCl_2$(L^8)$_2$] (44): as for **43** using [$PtCl_2$(cod)] (0.322 g, 0.86 mmol) and L^8 (0.470 g, 1.73 mmol). Recrystallised from dichloromethane-diethyl ether. (Found: C, 47.1; H, 5.21; N, 6.14. $C_{32}H_{42}Cl_2N_4P_2Pt$ requires C, 47.4; H, 5.22; N, 6.91%). $^{31}P\{^1H\}$ NMR (400 MHz, CD_2Cl_2, +25°C) δ 35.1 [^1J(P,Pt) 3936 Hz], (400 MHz, CD_2Cl_2, -40°C) δ_a

38.4 [^{1}J(P_a,Pt) 3953 Hz], δ_b 29.9 [^{1}J(P_b,Pt) 3601 Hz], ^{2}J(P,P) 18 Hz; ^{31}P{^{1}H} (270 MHz, d^6-acetone) δ 36.8 [^{1}J(P,Pt) 3906 Hz]; ^{1}H (270 MHz, d^6-acetone) δ 7.80 (m, Ar), 7.57 (m, Ar), 7.50 (m, Ar), 4.69 (br, NH), 2.66 (br, CH_2), 2.25 (br, CH_2), 2.12 (br, CH_3). IR (KBr, cm^{-1}): 3370 [m (br), ν(NH)].

Synthesis of [$PtCl_2(L^7)$] (45)

[$PtCl_2$(cod)] (0.228 g, 0.61 mmol) was added with stirring to a solution of $\mathbf{L^7}$ (0.175 g, 0.61 mmol) in dichloromethane (30 cm^3). After 1 hour the solvent was removed under reduced pressure, and the solid washed with diethyl ether (3 × 10 cm^3). Recrystallised from dichloromethane-diethyl ether to give pale yellow crystals. (Found: C, 37.1; H, 4.22; N, 4.85. $C_{17}H_{23}Cl_2N_2PPt$ requires C, 37.0; H, 4.20; N, 5.07%). ^{31}P{^{1}H} NMR ($CDCl_3$) δ 32.8 [^{1}J(P,Pt) 4175 Hz]; ^{1}H NMR ($CDCl_3$) δ 7.83 (m, 4H, Ar), 7.46 (m, 6H, Ar), 3.32 (m (br), 2H, CH_2), 3.27 (s (br), 2H, CH_2), 3.12 (m (br), 6H, CH_3N), 2.38 (d, 3H, ^{3}J(H,P) 8 Hz, CH_3NP).

Synthesis of [$PtCl(L^8$-*P,N*$)(L^8$-*P*$)](PF_6$) (46)

$TlPF_6$ (0.260 g, 0.75 mmol) was added to a solution of **44** (0.200 g, 0.25 mmol) in dichloromethane (20 cm^3) and the mixture stirred for 3 hours. The resulting solution was filtered, the residue washed with dichloromethane (20 cm^3), and the filtrate and washings combined. The solvent was then evaporated under reduced pressure to give a yellow solid. Recrystallised from dichloromethane-pentane followed by methanol-diethyl ether to give a pale yellow crystalline material. (Found: C, 41.6; H, 4.71; N, 5.84. $C_{32}H_{42}ClF_6N_4P_3Pt$ requires C, 41.8; H, 4.60; N, 6.09%). ^{31}P{^{1}H} NMR (CD_2Cl_2) δ_a 40.3 [^{1}J(P_a,Pt) 4038 Hz], δ_b 33.2 [^{1}J(P_b,Pt) 3587 Hz], ^{2}J(P,P) 20 Hz,

-143.5 (sep, ^{1}J(P,F) 714 Hz, PF_6); ^{1}H NMR (CD_2Cl_2) δ 7.73 - 7.58 (m, Ar), 7.47 (m, Ar), 7.34 (m, Ar), 3.47 (br, CH_2), 3.32 (m, NH), 3.07 (m (br), CH_2), 2.99 (m, ^{4}J(H,P) 3 Hz, CH_3NPt), 2.45 (m, CH_2), 2.26 (br, CH_2), 2.06 (s, CH_3N). IR (KBr, cm^{-1}): 3367, 3212 [m, ν(NH)], 840 [vs, ν(PF_6)].

Synthesis of [PtCl(L^8-*P*,*N*)(L^8-*P*)](BF_4) (47)

A solution of $NaBF_4$ (0.236 g, 2.15 mmol) in methanol/water (10 cm^3) was added with stirring to a solution of **44** (0.174 g, 0.22 mmol) in methanol (20 cm^3). After 30 minutes the solvent was removed under reduced pressure, the product was extracted with dichloromethane (3 × 10 cm^3) and recrystallised from dichloromethane-pentane followed by dichloromethane-diethyl ether to give pale yellow crystalline material. $^{31}P\{^1H\}$ NMR (CD_2Cl_2) δ_a 40.2 [$^1J(P_a,Pt)$ 4008 Hz], δ_b 32.8 [$^1J(P_b,Pt)$ 3595 Hz], ^{2}J(P,P) 20 Hz; ^{1}H NMR (CD_2Cl_2) δ 7.72 (m, Ar), 7.58 (m, Ar), 7.45 (m, Ar), 7.32 (m, Ar), 3.45 (br, CH_2), 3.31 (br, NH), 2.96 (br, CH_3/CH_2), 2.41 (br, CH_2), 2.16 (br, CH_2), 1.97 (s, CH_3N). IR (KBr, cm^{-1}): 3436, 3280 [w (br), ν(NH)], 1070 [vs (br), ν(BF_4)].

[Pd(dmba)Cl(L^7)] (48): as for **18** using [Pd(dmba)(μ-Cl)]$_2$ (0.189 g, 0.34 mmol) and L^7 (0.196 g, 0.68 mmol). $^{31}P\{^1H\}$ NMR ($CDCl_3$) δ 93.2; ^{1}H NMR ($CDCl_3$) δ 8.0 - 7.75 (br, 4H, Ar), 7.55 - 7.25 (br, 6H, Ar), 7.06 - 6.94 (m, 3H, Ar), 6.72 (t, 1H, Ar), 4.03 (br, 2H, CH_2N (dmba)), 3.31 (m (br), 2H, CH_2NP), 2.81 (s (br), 6H, CH_3N (dmba)), 2.66 (d, 3H, ^{3}J(H,P) 10 Hz, CH_3NP), 2.46 (br, 2H, CH_2N), 2.15 (s (br), 6H, CH_3N).

[Pt(dmba)Cl(L^7)] (49): as for **18** using [Pt(dmba)(μ-Cl)]$_2$ (0.204 g, 0.28 mmol) and L^7 (0.160 g, 0.56 mmol). Recrystallised from dichloromethane-diethyl ether. (Found: C, 48.1; H, 5.57; N, 5.87. $C_{26}H_{35}ClN_3PPt$ requires C, 48.0; H, 5.42; N, 6.45%). $^{31}P\{^1H\}$ NMR ($CDCl_3$) δ 66.4 [^1J(P,Pt) 4618 Hz]; ^1H δ 7.85 (m, 4H, Ar), 7.38 (m, 6H, Ar), 7.10 (m, Ar), 6.97 (t, Ar), 6.69 (t, Ar), 4.05 (m, 2H, ^4J(H,P) 3 Hz, CH_2N (dmba)), 3.38 (m, 2H, CH_2NP), 2.95 (m, 6H, ^4J(H,P) 3 Hz, CH_3N (dmba)), 2.75 (d, 3H, ^3J(H,P) 11 Hz, CH_3NP), 2.49 (t, 2H, ^3J(H,H) 8 Hz, CH_2N), 2.14 (s, 6H, CH_3N).

Synthesis of [Pt(dmba)(L^7)](PF_6) (50)

$TlPF_6$ (0.072 g, 0.21 mmol) was added to a solution of **49** (0.103 g, 0.16 mmol) in dichloromethane (10 cm^3) and the mixture stirred overnight. The resulting solution was filtered, residue washed with dichloromethane and the filtrate and washings combined. The solvent was then evaporated under reduced pressure to give a yellow solid. Recrystallised from dichloromethane-hexane to give a crystalline material. $^{31}P\{^1H\}$ NMR (CD_2Cl_2) δ 51.2 [^1J(P,Pt) 4880 Hz], -143.6 (sep, ^1J(P,F) 771 Hz, PF_6); ^1H NMR (CD_2Cl_2) δ 7.85 (m, Ar), 7.48 (m, Ar), 6.82 (d, 1H, Ar), 6.63 (t, 1H, Ar), 6.40 (m, 1H, Ar), 6.21 (t, 1H, Ar), 3.99 (m (br), 2H, CH_2N (dmba)), 3.26 (br, 4H, CH_2N/CH_2NP), 2.90 (s, 6H, CH_3N), 2.88 (m, 6H, ^4J(H,P) 3 Hz, CH_3N (dmba)), 2.44 (d, 2H, ^3J(H,P) 9 Hz, CH_3NP).

[Pt(dmba)(L^7)](BF_4) (51): as for **25** using $AgBF_4$ (0.110 g, 0.57 mmol) and **49** (0.337 g, 0.51 mmol). $^{31}P\{^1H\}$ NMR (CD_2Cl_2) δ 51.2 [^1J(P,Pt) 4876 Hz]; ^1H NMR (CD_2Cl_2) δ 7.84 (m, Ar), 7.44 (m, Ar), 6.82 (d, 1H, Ar), 6.61 (t, 1H, Ar), 6.36 (m, 1H, Ar), 6.18 (t, 1H, Ar), 3.99 (m, 2H, CH_2N (dmba)), 3.26 (br, 4H, CH_2N/CH_2NP), 2.92 (s, 6H,

CH_3N), 2.89 (m, 6H, ^4J(H,P) 3 Hz, CH_3N (dmba)), 2.44 (d, 3H, ^3J(H,P) 9 Hz, CH_3NP). IR (KBr, cm^{-1}): 1070 [vs (br), $\nu(BF_4)$]. (Yield 41%)

Synthesis of [Pt(L^7-*P,N*)(μ-L^7)$CoCl_3$] (52)

$CoCl_2.6H_2O$ (0.069 g, 0.29 mmol) was added to a solution of **43** (0.244 g, 0.29 mmol) in acetone (20 cm^3). The solution was stirred 30 minutes, after which the solvent was removed under reduced pressure, the product extracted with dichloromethane (4 × 10 cm^3) and recrystallised from dichloromethane-diethyl ether to give small blue crystals. (Found: C, 40.9; H, 4.76; N, 5.45. $C_{34}H_{46}Cl_4N_4P_2CoPt \cdot \frac{1}{2}CH_2Cl_2$ requires C, 41.0; H, 4.69; N, 5.54%). FAB-MS *m/z* 803, $[PtCl(L^7)_2]^+$.

Synthesis of [Pt(L^7-*P,N*)(μ-L^7)$ZnCl_3$]: as for **52** using $ZnCl_2$ (0.074 g, 0.54 mmol) and **43** (0.455 g, 0.54 mmol). Recrystallised from dichloromethane-diethyl ether to give colourless crystalline material. (Found: C, 40.1; H, 4.60; N, 5.22. $C_{34}H_{46}N_4P_2Cl_3PtZn \cdot {}^3/_2CH_2Cl_2$ requires C, 40.0; H, 4.63; N, 5.25%).

Synthesis of [Pt($O_2C_6H_3{}^tBu$)(L^7)$_2$] (53)

L^7 (0.306 g, 0.82 mmol) was added to a solution of [Pt($O_2C_6H_3{}^tBu$)(cod)] formed *in situ* from [$PtCl_2$(cod)] (0.200 g, 0.53 mmol), t-butyl catechol (0.089 g, 0.53 mmol) and Dbu (0.17 cm^3, 0.173 g, 1.14 mmol). The mixture was stirred for 30 minutes after which the solvent was removed under reduced pressure and the product extracted with hexane (40 cm^3). The solution was then cooled to -78°C to precipitate the product as an orange powder. (Found: C, 56.2; H, 6.34; N, 6.04. $C_{44}H_{58}N_4O_2P_2Pt$ requires C, 56.7; H, 6.27; N, 6.01%). $^{31}P\{^1H\}$ NMR ($CDCl_3$) δ_a 55.4 [$^1J(P_a,Pt)$ 3796 Hz], δ_b 54.5

[$^1J(P_b,Pt)$ 3800 Hz], $^2J(P,P)$ 27 Hz; ^1H NMR ($CDCl_3$) δ 7.60 (m, Ar), 7.38 (m, Ar), 7.22 (m, Ar), 6.85 (m, Ar), 6.71 (m, Ar), 6.56 (m, Ar), 3.34 (m (br), 2H, CH_2NP), 2.83 (m, 3H, CH_3NP), 2.43 (m, 2H, CH_2N), 2.15 and 2.12 (s, 6H, CH_3N), 1.40 (s, 9H, t-Butyl).

Synthesis of [RhCl(CO)(L^8)] (54)

[Rh(μ-Cl)$(CO)_2]_2$ (0.074 g, 0.19 mmol) was added to a stirred solution of L^8 (0.103 g, 0.38 mmol) in dichloromethane (10 cm^3). After 30 minutes the solvent was evaporated under reduced pressure. Recrystallised from dichloromethane-hexane to give a red crystalline material. (Found: C, 45.8; H, 4.64; N, 5.52. $C_{18}H_{20}ClN_2O_2PRh \cdot {}^1/_8CH_2Cl_2$ requires C, 45.6; H, 4.49; N, 5.87%). $^{31}P\{^1H\}$ NMR (CD_2Cl_2) δ 75.7 [$^1J(P,Rh)$ 181 Hz]; ^1H NMR (CD_2Cl_2) δ 7.74 (m, 4H, Ar), 7.42 (m (br), 6H, Ar), 3.41 (m (br), 2H, CH_2NP), 2.96 (m (br), 1H, NH), 2.62 (m (br), 2H, CH_2N), 2.55 (s, 6H, CH_3N). IR (KBr, cm^{-1}): 3256 [w (br), ν(NH)], 1988 [vs, ν(CO)]; IR (CH_2Cl_2, cm^{-1}): 1995 [vs, ν(CO)].

[RhCl(CO)(L^8)$_2$] (55): as for **40** using [Rh(μ-Cl)$(CO)_2]_2$ (0.069 g, 0.18 mmol) and L^8 (0.194 g, 0.71 mmol). Recrystallised from dichloromethane-diethyl ether. $^{31}P\{^1H\}$ NMR (CD_2Cl_2) δ 59.9 [$^1J(P,Rh)$ 128 Hz]; ^1H NMR (CD_2Cl_2) δ 7.84 (m, 4H, Ar), 7.46 (m, 6H, Ar), 4.26 (m (br), 1H, NH), 2.92 (m (br), 2H, CH_2NP), 2.35 (t, 2H, $^3J(H,H)$ 7 Hz, CH_2N), 2.19 (s, 6H, CH_3N). IR (CH_2Cl_2, cm^{-1}): 1976 [vs, ν(CO)].

[$PdCl_2(L^{10})_2$] (56): as for **1** using [$PdCl_2$(cod)] (0.100 g, 0.35 mmol) L^{10} (0.206 g, 0.70 mmol). (Found: C, 54.3; H, 4.27; N, 3.33. $C_{36}H_{32}Cl_2N_2O_2P_2Pd \cdot \frac{1}{2}CH_2Cl_2$ requires C, 54.4; H, 4.12; N, 3.47%). IR (KBr, cm^{-1}): 1644 [s, ν(C=O)].

[$PtCl_2(L^{10})_2$] (57): as for **1** using [$PtCl_2$(cod)] (0.100 g, 0.27 mmol) and L^{10} (0.157 g, 0.54 mmol). (Found: C, 49.0; H, 3.79; N, 3.07. $C_{36}H_{32}Cl_2N_2O_2P_2Pt \cdot \frac{1}{2}CH_2Cl_2$ requires C, 49.0; H, 3.72; N, 3.13%). IR (KBr, cm^{-1}): 1651 [s, ν(C=O)].

[Pd(dmba)Cl(L^{10})] (58): as for **18** using [Pd(dmba)(μ-Cl)]$_2$ (0.100 g, 0.37 mmol) and L^{10} (0.106 g, 0.36 mmol). (Found: C, 54.8; H, 4.48; N, 5.04. $C_{27}H_{28}ClN_2OPPd \cdot \frac{1}{4}CH_2Cl_2$ requires C, 55.4; H, 4.86; N, 4.74%). $^{31}P\{^1H\}$ NMR ($CDCl_3$) δ 88.6; ^1H NMR ($CDCl_3$) δ 7.94 (m, Ar), 7.44 (m, Ar), 7.01 (d, 1H, Ar), 6.95 (s (br), 1H, CH), 6.88 (t, 1H, Ar), 6.51 (s (br), CH), 6.48 (t, Ar), 6.24 (s (br), 1H, CH), 6.10 (t, 1H, Ar), 4.09 (s (br), 2H, CH_2N (dmba)), 2.82 (d, 6H, ^4J(H,P) 3 Hz, CH_3N (dmba)), 2.04 (s, 3H, CH_3). IR (KBr, cm^{-1}): 1649 [s, ν(C=O)].

[Pt(dmba)Cl(L^{10})] (59): as for **18** using [Pt(dmba)(μ-Cl)]$_2$ (0.100 g, 0.14 mmol) and L^{10} (0.080 g, 0.27 mmol). (Found: C, 49.4; H, 4.80; N, 3.95. $C_{27}H_{28}ClN_2OPPt$ requires C, 49.3; H, 4.29; N, 4.26%). $^{31}P\{^1H\}$ NMR ($CDCl_3$) δ 63.3 [^1J(P,Pt) 5097 Hz]; ^1H NMR ($CDCl_3$) δ 7.91 (m, 4H, Ar), 7.40 (m, 6H, Ar), 7.00 (d, 1H, Ar), 6.94 (m, 1H, CH), 6.84 (t, 1H, Ar), 6.40 (m (br), 2H, Ar/CH), 6.17 (m (br), 2H, Ar/CH), 4.02 (m (br), 2H, CH_2N (dmba)), 2.90 (m (br), 6H, ^4J(H,P) 3 Hz, CH_3N (dmba)), 2.06 (s, 3H, CH_3). IR (KBr, cm^{-1}): 1657 [s, ν(C=O)].

[Pd(dmba)(L^{10})](BF_4) (60): as for **25** using $AgBF_4$ (0.038 g, 0.19 mmol) and **58** (0.100 g, 0.18 mmol). (Found: C, 52.1; H, 4.62; N, 4.52. $C_{27}H_{28}BF_4N_2OPPd$ requires C, 52.2; H, 4.55; N, 4.51%). $^{31}P\{^1H\}$ NMR (CD_2Cl_2) δ 87.1; ^1H NMR (CD_2Cl_2) δ 7.79 (m, 1H, CH), 7.71 - 7.55 (m, Ar), 7.07 (d, 1H, Ar), 6.94 (t, 1H, Ar), 6.85 (m (br), 1H, CH), 6.61 (m, 1H, CH), 6.51 (t, 1H, Ar), 6.17 (t, 1H, Ar), 4.16 (m (br), 2H, CH_2N (dmba)), 2.92 (d, 6H, ^4J(H,P) 3 Hz, CH_3N (dmba)), 2.72 (s, CH_3). IR (KBr, cm^{-1}): 1594, 1580 [s, ν(C=O)], 1050 [vs (br), ν(BF_4)].

[Pd(dmba)(L^{10})](PF_6) (61): as for **50** using $TlPF_6$ (0.152 g, 0.44 mmol) and **58** (0.206 g, 0.36 mmol). Recrystallised from dichloromethane-hexane followed by dichloromethane-pentane to give an orange crystalline solid. $^{31}P\{^1H\}$ NMR (CD_2Cl_2) δ 87.4, -143.6 (sep, ^1J(P,F) 711 Hz, PF_6); ^1H NMR (CD_2Cl_2) δ 7.76 - 7.46 (m, Ar/CH), 7.10 (d (br), 1H, Ar), 6.98 (d, 1H, Ar), 6.93 (m, 1H, CH), 6.63 (m, 1H, CH), 6.54 (t, 1H, Ar), 6.24 (t, 1H, Ar), 4.15 (d, 2H, ^4J(H,P) 3 Hz, CH_2N (dmba)), 2.90 (d, 6H, ^4J(H,P) 3 Hz, CH_3N (dmba)), 2.70 (s, 3H, CH_3). IR (KBr, cm^{-1}): 1596 [s, ν(C=O)], 838 [vs, ν(PF_6)].

[Pt(dmba)(L^{10})](BF_4) (62): as for **25** using $AgBF_4$ (0.035 g, 0.18 mmol) and **59** (0.108 g, 0.16 mmol). Recrystallised from dichloromethane-pentane. (Found: C, 45.2; H, 4.02; N, 3.95. $C_{27}H_{28}BF_4N_2OPPt$ requires C, 45.7; H, 3.98; N, 3.95%). $^{31}P\{^1H\}$ NMR (CD_2Cl_2) δ 62.6 [^1J(P,Pt) 4423 Hz]; ^1H NMR (CD_2Cl_2) δ 7.85 (m, 1H, CH) 7.70 (m, 6H, Ar), 7.58 (m, 4H, Ar), 7.12 (d, 1H, Ar), 7.04 (s (br), 1H, CH), 6.93 (t, 1H, Ar), 6.65 (m, 1H, CH), 6.51 (m, 1H, Ar), 6.33 (m, 1H, Ar), 4.22 (m, 2H, ^3J(H,Pt) 33

Hz, ^{4}J(H,P) 3 Hz, CH_2N (dmba)), 3.00 (m, 6H, ^{3}J(H,Pt) 23 Hz, ^{4}J(H,P) 3 Hz, CH_3N (dmba)), 2.73 (s, 3H, CH_3). IR (KBr, cm^{-1}): 1583 [s, ν(C=O)], 1060 [vs (br), ν(BF_4)].

[Pt(dmba)(L^{10})](PF_6) (63): as for **50** using $TlPF_6$ (0.029 g, 0.083 mmol) and **59** (0.050 g, 0.076 mmol). Recrystallised from dichloromethane-hexane followed by dichloromethane-pentane to give colourless crystals. (Found: C, 41.9; H, 3.74; N, 3.61. $C_{27}H_{28}F_6N_2OP_2Pt$ requires C, 42.2; H, 3.68; N, 3.65%). $^{31}P\{^1H\}$ NMR ($CDCl_3$) δ 62.8 [^{1}J(P,Pt) 4437 Hz], -143.6 (sep, ^{1}J(P,F) 711 Hz, PF_6); ^{1}H NMR ($CDCl_3$) δ 7.76 (m, 1H, CH) 7.64 (m, 6H, Ar), 7.54 (m, 4H, Ar), 7.08 (d (br), 1H, Ar), 6.99 (m, 1H, CH), 6.91 (t, 1H, Ar), 6.60 (m, 1H, CH), 6.48 (t, 1H, Ar), 6.28 (m, 1H, Ar), 4.17 (m, 2H, ^{3}J(H,Pt) 34 Hz, ^{4}J(H,P) 3 Hz, CH_2N (dmba)), 2.95 (m, 6H, ^{3}J(H,Pt) 23 Hz, ^{4}J(H,P) 3 Hz, CH_3N (dmba)), 2.68 (s, 3H, CH_3). IR (KBr, cm^{-1}): 1579 [s, ν(C=O)], 838 [vs, ν(PF_6)].

[RhCl(CO)(L^{10})] (64): as for **54** using [Rh(μ-Cl)$(CO)_2]_2$ (0.100 g, 0.26 mmol) and L^{10} (0.151 g, 0.52 mmol). Recrystallisation from dichloromethane-hexane followed by toluene-dichloromethane-hexane gave orange coloured crystals. (Found: C, 49.6; H, 3.60; N, 2.95. $C_{19}H_{17}ClNO_2PRh$ requires C, 49.6; H, 3.51; N, 3.05%). $^{31}P\{^1H\}$ NMR ($CDCl_3$) δ 93.6 [^{1}J(P,Rh) 178 Hz]; ^{1}H NMR ($CDCl_3$) δ 7.65 (m, 1H, CH), 7.58 - 7.47 (m, 10H, Ar), 6.96 (m (br), 1H, CH), 6.60 (m, 1H, CH), 2.60 (s, 3H, CH_3). IR (KBr, cm^{-1}): 1989 [vs, ν(CO)], 1576 [vs, ν(C=O)]; IR (CH_2Cl_2, cm^{-1}): 2007 [vs, ν(CO)], 1587 [vs, ν(C=O)].

Synthesis of [RhCl(CO)(L^{10})$_2$] (65)

[Rh(μ-Cl)(CO)$_2$]$_2$ (0.050 g, 0.13 mmol) was added to a solution of L^{10} (0.151 g, 0.52 mmol) in toluene (10 cm^3) and the mixture stirred for 30 minutes. The resulting solution was filtered, and the yellow precipitate washed with toluene (5 cm^3) followed by hexane (20 cm^3) and dried under reduced pressure. (Found: C, 58.7; H, 4.35; N, 3.66. $C_{37}H_{32}ClN_2O_3P_2Rh$ requires C, 59.0; H, 4.28; N, 3.72%). $^{31}P\{^1H\}$ NMR ($CDCl_3$) δ 84.4 [^1J(P,Rh) 158 Hz]; ^1H NMR ($CDCl_3$) δ 7.80 - 7.60 (m, Ar), 7.54 - 7.32 (m (br), Ar), 7.23 - 7.12 (m (br), Ar/CH), 6.44 (m (br), CH), 6.18 (m (br), CH), 2.40 (s, CH_3). IR (KBr, cm^{-1}): 1963 [vs, ν(CO)], 1650 [vs, ν(C=O)]; (CH_2Cl_2, cm^{-1}): 1981 [vs, ν(CO)], 1650 [s, ν(C=O)].

Formation of [RhCl(CO)(PPh_2OPPh_2)]$_2$ (66)

65 was formed *in situ* using [Rh(μ-Cl)(CO)$_2$]$_2$ (0.050 g, 0.13 mmol) and L^{10} (0.151 g, 0.52 mmol) in dichloromethane (10 cm^3). On standing for a few hours the initial yellow solution changed to give a red solution and red needle shaped crystals. The solvent was removed by filtration to leave the red crystals, these were washed with dichloromethane (2 × 10 cm^3) and dried under reduced pressure. The crystalline material was found to be insoluble in THF, dichloromethane, chloroform, and toluene. (Found: C, 51.1; H, 3.59; N, 0.0. $C_{50}H_{40}Cl_2O_4P_4Rh_2 \cdot CH_2Cl_2$ requires C, 51.5; H, 3.56; N, 0.00%). IR (KBr, cm^{-1}): 1964 [vs, ν(CO)], 1793 [m, ν(μ-CO)].

Synthesis of [Rh(L^{10})$_2$]Cl (67)

L^{10} (0.119 g, 0.41 mmol) was added to a solution of [Rh(μ-Cl)(cod)]$_2$ (0.050 g, 0.10 mmol) in dichloromethane (10 cm^3) and the mixture stirred for 1½ hours. The solvent

was evaporated under reduced pressure, and the solid washed with cold hexane (2 × 10 cm^3) and dried under reduced pressure. $^{31}P\{^1H\}$ NMR ($CDCl_3$) δ 108.0 [^1J(P,Rh) 204 Hz]; ^1H NMR ($CDCl_3$) δ 7.88 (m (br), CH), 7.68 - 6.88 (m (br), Ar), 6.67 (m (br), CH), 6.37 (m (br), CH), 2.63 (s, CH_3). IR (KBr, cm^{-1}): 1574 [vs, ν(C=O)].

Synthesis of $[Rh(L^{10})_2](PF_6)$ (68)

NH_4PF_6 (0.034 g, 0.21 mmol) was added to a solution of **67** formed *in situ* from L^{10} (0.119 g, 0.41 mmol) and $[Rh(\mu\text{-}Cl)(cod)]_2$ (0.050 g, 0.10 mmol) in THF (30 cm^3). The mixture was stirred for 2 hours, after which the solution was filtered to remove NH_4Cl. The resulting solution was evaporated under reduced pressure, and the solid washed with cold diethyl ether (2 × 20 cm^3) and dried under reduced pressure. Recrystallised from dichloromethane-hexane to give orange coloured crystals. (Found: C, 50.9; H, 3.93; N, 3.16. $C_{36}H_{32}F_6N_2O_2P_3Rh{\cdot}¼CH_2Cl_2$ requires C, 50.9; H, 3.83; N, 3.27%). $^{31}P\{^1H\}$ NMR ($CDCl_3$) δ 108.3 [^1J(P,Rh) 205 Hz], -143.5 (sep, ^1J(P,F) 711 Hz, PF_6); ^1H NMR ($CDCl_3$) δ 7.54 (m, 1H, CH), 7.42 (m, 2H, Ar), 7.24 (m, 8H, Ar), 6.73 (m, 1H, CH), 6.42 (m, 1H, CH), 2.71 (s, 3H, CH_3). IR (KBr, cm^{-1}): 1570 [s, ν(C=O)], 837 [vs (br), ν(PF_6)].

Synthesis of $[(c\text{-}C_5H_9)_7Si_7O_9(OSiMe_3)O_2Pt(dppe)]$ (69)

Two methods were used to synthesise **69**:

(**Method 1**): $[(c\text{-}C_5H_9)_7Si_7O_9(OSiMe_3)(OH)_2]$ (S^1) (0.147 g, 0.15 mmol) was added to a solution of $[Pt(CO_3)(dppe)]$ (0.100 g, 0.15 mmol) in dichloromethane (30 cm^3) and the mixture stirred at room temperature (typically 7 days). The solvent was removed under reduced pressure, and the crude product recrystallised from

dichloromethane-diethyl ether to precipitate any unreacted starting materials. The resulting solution was filtered, and the solvent removed under reduced pressure. Recrystallised from toluene-acetonitrile to give colourless crystals of **69**. (Found: C, 49.8; H, 6.25; $C_{62}H_{96}Si_8O_{12}P_2Pt$ requires C, 49.8; H, 6.41 %). $^{31}P\{^1H\}$ NMR (270 MHz, $CDCl_3$) δ 27.3 [^1J(P,Pt) 3773 Hz]; ^1H NMR (400 MHz, $CDCl_3$, 25 °C) δ 8.06 (dq, 8H, Ar), 7.50 (t, 4H, Ar), 7.43 (m, 8H, Ar), 2.14 (m, 4H, $P(CH_2)_2P$), 1.72 (m, 12H, C_5H_9), 1.50 (m, 28H, C_5H_9), 1.27 (m, 4H, C_5H_9), 1.12 (m, 12H, C_5H_9), 0.92 (m, 3H, C_5H_9), 0.81 (m, 2H, C_5H_9), 0.54 (m, 2H, C_5H_9), -0.29 (s, 9H, $SiMe_3$). $^{13}C\{^1H\}$ NMR (100 MHz, $CDCl_3$, 25°C) δ 28.7 (CH_2P), 28.5 - 26.4 (other CH_2), 25.1, 24.2, 23.2, 23.0 (2:3:1:1 for CH), 1.0 ($SiMe_3$). $^{29}Si\{^1H\}$ NMR (79 MHz, CH_2Cl_2, 0.02 M $Cr(acac)_3$, 25 °C) δ 6.0 ($SiMe_3$), -65.1, -66.3, -66.6, -68.7 (1:1:2:3). FAB-MS, *m/z* 1539 $[M + H]^+$.

(**Method 2**): $\mathbf{S^1}$ (0.254 g, 0.27 mmol) and Ag_2O (0.248 g, 1.07 mmol) were added to a solution of $[PtCl_2(dppe)]$ formed *in situ* from $[PtCl_2(cod)]$ (0.100 g, 0.27 mmol) and bis(diphenylphosphino)ethane (dppe) (0.106 g, 0.27 mmol) in dichloromethane (30 cm^3) and the mixture refluxed under nitrogen (typically 7 days). The solution was filtered and the black solid residue washed with dichloromethane (2 × 10 cm^3) and the washings combined with the filtrate. The solvent was removed under reduced pressure, and the crude product recrystallised from dichloromethane-diethyl ether to precipitate any unreacted starting materials. The resulting solution was filtered, and the solvent removed under reduced pressure. Recrystallised from toluene-acetonitrile to give colourless crystals of **69**. $^{31}P\{^1H\}$ NMR ($CDCl_3$) δ 27.3 [^1J(P,Pt) 3769 Hz]. Analysis as for Method 1.

[(c-C_6H_{11})$_7Si_7O_9$(OSiMe$_3$)O_2Pt(dppe)] (70):

As for **69** (Method 1), using [(c-C_6H_{11})$_7Si_7O_9$(OSiMe$_3$)(OH)$_2$] (**S^2**) (0.160 g, 0.15 mmol) and [Pt(CO_3)(dppe)] (0.100 g, 0.15 mmol). Recrystallised from toluene-acetonitrile to give colourless crystals plus a waxy residue. (Found: C, 52.2; H, 6.88; $C_{69}H_{106}Si_8O_{12}P_2Pt$ requires C, 52.1; H, 6.77 %). $^{31}P\{^1H\}$ NMR ($CDCl_3$) δ 27.7 [^1J(P,Pt) 3776 Hz]; ^1H NMR ($CDCl_3$) δ 8.1 (m, Ar), 7.5 (m, Ar), 2.2 (m, br, P(CH_2)$_2$P), 1.73 (br, C_6H_{11}), 1.24 (br, C_6H_{11}), 0.8 (br, C_6H_{11}), -0.24 (s, SiMe$_3$). IR (KBr, cm^{-1}): 1435 [s, ν(PCH_2)], 1100 [vs (br), ν(Si-O-R)]. FAB-MS, *m/z* 1046 [*M - Pt(dppe)*]$^+$.

As for **69** (Method 2), using **S^2** (0.280 g, 0.27 mmol), [$PtCl_2$(dppe)] (0.177 g, 0.27 mmol) and Ag_2O (0.186 g, 0.80 mmol). Recrystallised from toluene-acetonitrile to give colourless block shaped crystals and a waxy residue. $^{31}P\{^1H\}$ NMR ($CDCl_3$) δ 27.5 [^1J(P,Pt) 3773 Hz]. Analysis as for Method 1.

[(c-C_5H_9)$_7Si_7O_9$(OH)O_2Pt(dppe)] (71): as for **69** (Method 1), using (c-C_5H_9)$_7Si_7O_9$(OH)$_3$ (**S^3**) (0.269 g, 0.31 mmol) and [Pt(CO_3)(dppe)] (0.200 g, 0.31 mmol). $^{31}P\{^1H\}$ NMR (270 MHz, $CDCl_3$) δ 27.0 [^1J(P,Pt) 3729 Hz]; ^1H NMR (400 MHz, $CDCl_3$, 25 °C) δ 8.0 (m, 8H, Ar), 7.5 (m, 12H, Ar), 2.2 (m, 4H, P(CH_2)$_2$P), 1.9 - 0.8 (m, 63H, C_5H_9); $^{13}C\{^1H\}$ NMR (100 MHz, $CDCl_3$, 25 °C) δ 29 (CH_2P), 28.6 - 26.7 (other CH_2), 25.10, 23.22, 23.11, 22.69, 22.60 (2:2:1:1:1 for CH).

[(c-C_6H_{11})$_7Si_7O_9$(OSiMe$_3$)O_2Pd(dppe)] (72): as for **69** (Method 2), using **S^1** (0.105 g, 0.19 mmol), Ag_2O (0.180 g, 0.78 mmol) and [$PdCl_2$(dppe)] formed *in situ* from [$PdCl_2$(cod)] (0.055 g, 0.19 mmol) and dppe (0.077 g, 0.19 mmol). Recrystallisation

was attempted from toluene-acetonitrile but formed a waxy solid. $^{31}P\{^1H\}$ NMR ($CDCl_3$) δ 33.7; ^1H NMR ($CDCl_3$) δ 7.75 - 7.62 (m, Ar), 7.55 - 7.40 (m, Ar), 2.40 (m, $P(CH_2)_2P$), 1.7 (br, C_5H_9), 1.5 (br, C_5H_9), 1.0 (m (br), C_5H_9), 0.5 (s, $SiMe_3$).

Synthesis of $[Pd(dppe)(NC_5HCO_2H\text{-}4)_2](BF_4)_2$ (73)

Isonicotinic acid (0.087 g, 0.70 mmol) was added to a stirred dichloromethane/THF solution of $[Pd(dppe)(THF)_2](BF_4)$ formed *in situ* from $[PdCl_2(cod)]$ (0.100 g, 0.35 mmol), dppe (0.140 g, 0.35 mmol), $AgBF_4$ (0.205 g, 1.05 mmol) and THF (20 cm^3). After 2 hours the solution was filtered and the solvent evaporated under reduced pressure, leaving a pale yellow solid. Recrystallised from butanone-hexane. (Found: C, 49.2; H, 4.46; N, 2.74. $C_{38}H_{34}B_2F_8N_2O_4P_2Pd$ requires C, 50.0; H, 3.99; N, 2.92 %). $^{31}P\{^1H\}$ NMR (d^6-acetone) δ 68.3; ^1H δ 9.08 (br, 4H, CH), 8.02 - 7.90 (m, Ar), 7.80 - 7.50 (m, Ar), 3.4 (m (br), 4H, CH_2). IR (KBr, cm^{-1}): 1734 [s, ν(CO_2H)], 1060 [vs (br), ν(BF_4)].

$[Pt(dppe)(NC_5HCO_2H\text{-}4)_2](BF_4)_2$ (74): as for **73** using isonicotinic acid (0.066 g, 0.54 mmol) and $[PtCl_2(dppe)]$ formed *in situ* from $[PtCl_2(cod)]$ (0.100 g, 0.27 mmol), dppe (0.106 g, 0.27 mmol), $AgBF_4$ (0.104 g, 0.53 mmol) and acetone (40 cm^3). $^{31}P\{^1H\}$ NMR (d^6 -acetone) δ 39.2 [^1J(P,Pt) 3233 Hz]; ^1H δ 9.08 (d, 4H, ^3J(H,H) 4 Hz, CH), 8.00 - 7.82 (m, 8H, Ar), 7.84 (d, 4H, ^3J(H,H) 6 Hz, CH), 7.73 - 7.65 (m, 12H, Ar), 3.25 (m, 4H, CH_2). IR (KBr, cm^{-1}): 1733 [s, ν(CO_2H)], 1060 [vs (br), ν(BF_4)].

Synthesis of $[Ag_3(NC_5H_4CO_2\text{-}4)_2]BF_4$ (75)

$AgBF_4$ (0.474 g, 2.44 mmol) was added to a suspension of isonicotinic acid (0.200 g, 1.62 mmol) in acetone (30 cm^3) and the mixture stirred in darkness overnight. The resulting solution was filtered, the residue washed with acetone (2 × 10 cm^3) and the washings and filtrate combined. The solvent was evaporated under reduced pressure to give an off white solid. Recrystallised from acetone-hexane to give colourless crystals of **75**. (Found: C, 22.0; H, 1.25; N, 4.32. $C_{12}H_8Ag_3BF_4N_2O_4$, requires C, 22.0; H, 1.23; N, 4.28 %). ^1H NMR (d^6-acetone) δ 9.24 (d, 4H, $^3J(H,H)$ 7 Hz, CH), 8.65 (d, 4H, $^3J(H,H)$ 7 Hz, CH); $^{13}C\{^1H\}$ δ 208 (s, CO_2^-), 163 (s, Ar $\{C_{ipso}\}$), 146 (s, Ar $\{C_{meta}\}$), 127 (s, Ar $\{C_{ortho}\}$). IR (Nujol); 1580, 1547 [s, $\nu(CO_2)$], 1156, 1092, 1026, 1009 [s, $\nu(BF_4)$.

7.3 References

1 D. Drew and J. R. Doyle, *Inorg. Synth.*, 1972, **13**, 48.

2 J. Chatt, L. M. Vallarino and L. M. Venanzi, *J. Chem. Soc.*, 1957, 3413

3 M. A. Andrews, G. L. Gould, W. T. Klooster, K. S. Koenig and E. J. Voss, *Inorg. Chem.*, 1996, *35*, 5478.

4 A. C. Cope and E. C. Friedrich, *J. Am. Chem. Soc.*, 1968, **90**, 909.

5 D. J. Darensbourg and R. L. Kump, *Inorg. Chem.*, 1978, **17**, 2680.

6 F. A. Cotton, J. A. McCleverty and J. E. White, *Inorg. Synth.*, 1990, **28**, 45.

7 J. A. McCleverty and G. Wilkinson, *Inorg. Synth.*, 1966, **8**, 211.

8 G. Giordano and R. H. Crabtree, *Inorg Synth.*, 1990, **28**, 88.

9 H. C. L. Abbenhuis, Schuit Institute of Catalysis, Eindhoven Univeristy of Technology, The Netherlands.

Appendix 1 - Crystallography

Data for complexes **3**, **16**, **18**, **35**, **38**, **63** and **66** were collected on a CAD4 automatic 4-circle diffractometer, data for **1** and **75** were collected on the EPSRC FAST system, data for **19** was collected on a Brüker SMART 1000 CCD diffractometer, whereas data collection for **69** was carried out at Utrecht University on an Enraf-Nonius CAD4T diffractometer. The crystal structures were solved by Dr. Mary Mahon, with the solution of the structures and their refinement carried out using SHELX86[1] and SHELX93[2] respectively. The figures of the asymmetric units along with their labelling were produced using ORTEX.[3]

Hydrogen atoms were included in calculated positions on carbon centres for all structures. Hydrogens attached to nitrogen atoms were readily located throughout in the penultimate difference Fourier electron density maps, and included in the final stage of refinement with various restraints. In **1**, the hydrogen attached to N(1) was refined at a fixed distance of 0.90 Å from the parent atom. The corresponding hydrogens in compounds **3**, **19** and **38** were treated similarly, whereas the corresponding hydrogens in compounds **16** and **18** were refined at a fixed distance of 0.98 Å from the parent nitrogen atom.

In the structural refinement of complex **16**, the maximum residual electron density peak was noted to be very close to the nitrite moiety, which points to some disorder and librational effects in this region of the electron density map, given the large thermal vibration of the atoms therein. This disorder could not be successfully modelled and in the latter stages of refinement, the N–O distances in the nitrite group were constrained to be similar to each other.

The crystal used for the structural determination of **35** was not a strong diffractor. This is exemplified by the statistics on the data and the larger than desirable ESDs for the geometric parameters associated with this crystal structure. In the final stages of the refinement, the components of the anisotropic displacement parameters for atoms in the phenyl ring containing C(7) were refined subject to 'rigid bond' restraints and the thermal parameters for C(5) and C(6) were also treated similarly using SHELXL.[2]

In the structural refinement of complex **75**, during the final least squares cycles all atoms were allowed to vibrate anisotropically, except N(1), C(3), C(9) and C(12). Anisotropic refinement of these 4 atoms would have given unsatisfactory thermal parameters.

An empirical absorption correction (DIFABS[4]) was applied to the data compounds **16**, **35**, **63** and **75**. The associated maximum and minimum transmission factors for **16**, **35**, **63** and **75** were 1.000, 0.860 for **16**, 1.000, 0.219 for **35**, 1.000, 0.578 for **63** and 1.000, 0.500 for **75**, respectively.

---

1 G. M. Sheldrick, *Acta Cryst.*, 1990, **A46**, 467.

2 G. M. Sheldrick, SHELXL-93, a computer program for crystal structure refinement, University of Göttingen, 1993.

3 P. McArdle, *J. Appl. Cryst.*, 1995, **28**, 65.

4 N. Walker and D. Stuart, *Acta Cryst.*, 1983, **A39**, 158.

Appendix 2 – Crystallographic Data for Complexes **1**, **3**, **16**, **18**, **19**, **35**, **38**, **52**, **63**, **66**, **69** and **75**

Complex	**1**	**3**
Empirical formula	$C_{30}H_{36}Cl_2N_2O_2P_2Pd$	$C_{32}H_{40}Cl_2N_2O_4P_2Pd$
M	695.84	755.90
T/K	150(2)	293(2)
Crystal system	Monoclinic	Triclinic
Space group	$P2_1/c$	$P\bar{1}$
a/Å	10.456(2)	8.396(2)
b/Å	7.553(1)	10.146(2)
c/Å	19.935(2)	10.849(3)
α/°		94.97(2)
β/°	100.641(13)	111.01(2)
γ/°		94.71(2)
U/Å^3	1547.3(4)	853.1(4)
Z	2	1
D_c/g cm^{-3}	1.494	1.471
μ/mm^{-1}	0.906	0.832
F(000)	712	388
Crystal size/mm	0.18 × 0.16 × 0.10	0.3 × 0.3 × 0.3
θ/°	1.98 – 24.95	2.02 – 24.92
Reflections collected	6352	3413
Independent reflections	2395	2973
	[R(int) 0.0904]	[R(int) 0.0537]
Goodness-of-fit on F^2	1.146	1.223
$R1$, $wR2$ [$I > 2\sigma(I)$]	0.0383, 0.1084	0.0518, 0.1298
(all data)	0.0451, 0.1098	0.0620, 0.1458
Largest diff. peak hole / eÅ^{-3}	0.830, –0.907	1.252, –0.758

Complex	**16**	**18**
Empirical formula	$C_{30}H_{36}BrN_3O_4P_2Pt$	$C_{24}H_{30}ClN_2OPPd$
M	839.56	535.32
T/K	293(2)	293(2)
Crystal system	Monoclinic	Orthorhombic
Space group	$P2_1/n$	*P*bca
a/Å	9.576(2)	14.070(2)
b/Å	24.119(5)	17.080(3)
c/Å	14.306(2)	18.899(4)
α/°		
β/°	105.09(2)	
γ/°		
U/Å^3	3190.2(10)	4541.7(14)
Z	4	8
D_c/g cm^{-3}	1.748	1.566
μ/mm^{-1}	5.790	1.024
F(000)	1648	2192
Crystal size/mm	0.2 × 0.2 × 0.2	0.2 × 0.2 × 0.2
θ/°	2.36 – 24.97	2.15 – 25.01
Reflections collected	5596	3785
Independent reflections	5587	3715
	[*R*(int) 0.0329[a]]	[*R*(int) 0.002]
Goodness-of-fit on F^2	1.091	1.104
*R*1, *wR*2 [$I > 2\sigma(I)$]	0.0325, 0.0887	0.0534, 0.1366
(all data)	0.0454, 0.0949	0.0874, 0.1446
Largest diff. peak hole / eÅ^{-3}	2.234, –1.753	1.382, –0.708

[a] Pre DIFABS.

Complex	**19**	**35**
Empirical formula	$C_{25}H_{32}ClN_2OPPd$	$C_{42}H_{44}N_2O_2P_2Pt_2 \cdot CH_2Cl_2$
M	549.35	1145.84
T/K	293(2)	293(2)
Crystal system	Monoclinic	Monoclinic
Space group	$P2_1/c$	$P2_1/c$
a/Å	16.835(2)	13.877(5)
b/Å	8.3350(9)	20.984(7)
c/Å	19.590(2)	15.345(5)
α/°		
β/°	111.922(2)	107.09(3)
γ/°		
U/Å^3	2550.1(5)	4271(3)
Z	4	4
D_c/g cm^{-3}	1.431	1.777
μ/mm^{-1}	0.914	6.781
F(000)	1128	2204
Crystal size/mm	0.45 × 0.25 × 0.15	0.2 × 0.2 × 0.2
θ/°	1.30 – 26.37	2.38 – 23.98
Reflections collected	14866	6620
Independent reflections	5207	6620
	[*R*(int) 0.0385]	[*R*(int) 0.0267[a]]
Goodness-of-fit on F^2	0.909	1.046
*R*1, *wR*2 [$I > 2\sigma(I)$]	0.0392, 0.0942	0.0715, 0.1449
(all data)	0.058, 0.1028	0.1541, 0.1776
Largest diff. peak, hole/eÅ^{-3}	0.846, –0.686	0.982, –1.187

[a] Pre DIFABS.

Complex	**38**	**52**
Empirical formula	$C_{42}H_{36}N_2O_6P_2Mo$	$C_{39}H_{46}Cl_4CoN_4P_2Pt$
M	822.61	1028.56
T/K	293(2)	293(2)
Crystal system	Monoclinic	Monoclinic
Space group	*C*2/c	$P2_1/c$
a/Å	13.182(2)	16.710(3)
b/Å	13.531(2)	12.160(2)
c/Å	22.375(3)	19.666(5))
α/°		
β/°	92.340(10)	104.82(2)
γ/°		
U/Å^3	3987.6(10)	3863.1(14)
Z	4	4
D_c/g cm^{-3}	1.494	1.768
μ/mm^{-1}	1.370	4.442
F(000)	1688	2044
Crystal size/mm	0.3 × 0.2 × 0.2	0.18 × 0.18 × 0.15
θ/°	2.15 – 23.92	2.10 – 24.99
Reflections collected	3319	7270
Independent reflections	3120	6785
	[*R*(int) 0.0180]	[*R*(int) 0.0127]
Goodness-of-fit on F^2	1.019	1.017
*R*1, *wR*2 [$I > 2\sigma(I)$]	0.0731, 0.1621	0.0367, 0.0.838
(all data)	0.1251, 0.1974	0.0570, 0.0886
Largest diff. peak, hole/eÅ^{-3}	0.839, –0.622	1.707, –1.186

Complex	**63**	**66**
Empirical formula	$C_{27}H_{28}F_6N_2OP_2Pt$	$C_{50}H_{40}Cl_2O_2P_4Rh_2 \cdot CH_2Cl_2$
M	767.54	579.17
T/K	170(2)	170(2)
Crystal system	Monoclinic	Monoclinic
Space group	$P2_1/n$	$P2_1/n$
a/Å	11.952(2)	14.394(2)
b/Å	16.342(3)	9.683(2)
c/Å	14.165(2)	17.287(3)
α/°		
β/°	98.93(2)	92.93(2)
γ/°		
U/Å^3	2733.2(8)	2406.3(7)
Z	4	2
D_c/g cm^{-3}	1.865	1.599
μ/mm^{-1}	5.317	1.081
F(000)	1496	1164
Crystal size/mm	0.20 × 0.20 × 0.15	0.15 × 0.2 × 0.2
θ/°	2.13 – 24.97	2.36 – 24.97
Reflections collected	4787	4539
Independent reflections	4778	4230
		[*R*(int) 0.0167]
Goodness-of-fit	0.973	0.870
*R*1, *wR*2 [$I > 2\sigma(I)$]	0.0340, 0.0860	0.0475, 0.1165
(all data)	0.0463, 0.0992	0.0682, 0.1278
Largest diff. peak, hole/eÅ^{-3}	1.956, –1.361	1.451, –1.970

Complex	**69**	**75**
Empirical formula	$C_{64}H_{96}Si_8P_2O_{12}Pt \cdot C_2H_3N$	$C_{12}H_8Ag_3BF_4N_2O_4$
M	1580.22	654.62
T/K	153	150(2)
Crystal system	Orthorhombic	Triclinic
Space group	$Pccn$	$P\bar{1}$
a/Å	47.997(4)	8.328(6)
b/Å	13.9845(11)	10.43(2)
c/Å	21.803(2)	10.618(3)
α/°		61.49(9)
β/°		71.48(9)
γ/°		81.66(10)
U/Å^3	14634(2)	769(2)
Z	8	2
D_c/g cm^{-3}	1.434	2.828
μ/mm^{-1}	2.15	3.852
F(000)	6544	616
Crystal size/mm	0.5 × 0.4 × 0.2	0.24 × 0.18 × 0.10
θ/°	1.0 – 25.00	2.22 – 24.66
Reflections collected	13789	2146
Independent reflections	12902	1381
	[R(int) 0.0267]	[R(int) 0.0809[a]]
Goodness-of-fit	1.111	0.643
$R1$, $wR2$ [$I > 2\sigma(I)$]	0.0525, 0.1071	0.0325, 0.0617
(all data)	0.1172, 0.1439	0.0577, 0.0878
Largest diff. peak, hole/eÅ^{-3}	1.973, -1.570	0.747, –0.751

[a] Pre DIFABS.